Structural setting and petrogenesis of Silurian granites in the Caledonides of northern Scotland

Henning Kocks

A thesis submitted in partial fulfilment of the requirements of Oxford Brookes University for the degree of Doctor of Philosophy

August 2002

FIGURES ON FOLOWING PAGES HAVE NOT BEEN SCANNED ON INSTRUCTION FROM THE UNIVERSITY

12,16,24,31,33,39,55, and 134

CONTAINS

PULLOUTS

Abstract

In the Ordovician-Silurian Caledonian orogenic belt of northern Scotland, two major thrust nappes, the Moine and Naver nappes, contain a series of granitic plutons. The Rogart, Strath Halladale and Helmsdale granites have been studied using field and microstructural fabric analysis. Their emplacement mechanisms and pre, syn or post-tectonic status with respect to phases of Caledonian ductile deformation have been detailed. The petrogenesis of the Strath Halladale and Helmsdale granites has been examined within the framework of a regional geochemical study involving nine Caledonian high Ba-Sr granitoids.

The foliated Strath Halladale Granite comprises a series of easterly-dipping sheets that were intruded into structurally high parts of the Naver Nappe in northeastern Sutherland. The granite contains magmatic-state shear zones that consistently show top-to-the-W-to-NW sense of movement; it was emplaced during Caledonian (D2) west-directed thrusting. The Rogart Granite was emplaced into the footwall of the Naver Thrust in southeastern Sutherland. It comprises early, sheeted quartz diorites that carry magmatic to solid-state fabrics formed by thrust-related, west-directed ductile deformation and a central igneous quartz monzodiorite-granodiorite-granite complex that ballooned into a tectonically created void formed along the Strath Fleet Lineament after D2 thrusting. The emplacement of the Rogart Granite encompassed the switchover from west-directed thrusting to strike-slip tectonics in this area. The Helmsdale Granite was emplaced into the highest parts of the Naver Nappe in eastern Sutherland. It does not contain any emplacement-related or tectonically-induced fabrics and is post-tectonic with respect to Caledonian deformation. Its emplacement mechanism and hence the Caledonian significance of the adjacent Helmsdale Fault remain speculative.

Geochemistry confirms that the Strath Halladale and Helmsdale granites are part of the Caledonian high Ba-Sr granites (*sensu* Tarney & Jones 1994) and indicates melt evolution by assimilation fractional crystallization (AFC) involving Moine metasediment. Associated mafic rocks do not form parents to the granites but represent a variety of genetically-related cumulates. Nine Caledonian high Ba-Sr plutons in northern Scotland show a systematic isotopic variability. Plutons with the highest $^{87}Sr/^{86}Sr_{(i)}$ have the lowest $\varepsilon Nd_{(i)}$ and the highest $\delta^{18}O$, whereas plutons with lower $^{87}Sr/^{86}Sr_{(i)}$ have complementary higher $\varepsilon Nd_{(i)}$ and lower $\delta^{18}O$. Syenite-dominated complexes evolved by *assimilation fractional crystallization* (AFC) involving depleted granulite-facies basement whereas the granites assimilated Moine metasediment. Combining available age data with the observed isotope systematics suggests, that the syenites recorded progressive (source) enrichment over *c.* 30 Ma followed by a short-lived, isotopically-diverse, magmatic pulse at *c.* 425 Ma.

Acknowledgements

My motivation to study for a Ph.D. in the Scottish Highlands originated in 1995 when I first met Rob Strachan who then led two field trips to the Moine Thrust Zone and the Knapdale peninsula that were eye-opening landmarks to me during my undergraduate studies. I am indebted to Rob for providing me with the opportunity to do this Ph.D., for his continuous support, excellent supervision and incredible patience! I also thank my co-supervisors Mike Fowler and Richard D'Lemos for all their efforts in guiding me through this project.

I have been extremely lucky to have met, discussed and worked with Fiona Darbyshire, Pete Greenwood and Jane Evans at NIGL and Anton Kearsely, Kevin Jones, Jonathan Redfern and Clark Friend at Brookes University. Dirk Liss and Craig Storey are further thanked for analytical work at Birmingham and Leicester Universities. I also thank Jon Wells for numerous thin sections and am grateful to Mike, Hellen, Jill, John and Phil of the school of BMS for their support.

I owe much to my friends in Oxford, who have made the past three years some of the most enjoyable of my life. The remote research facility crew, Dave Burnett and Jez Inglis, secured that my social life got off to a fantastic start. Since then, the following people have gone to great lengths in keeping these standards high: Ruth Underdown, James, Anna, Tarek, Ruth Connelly, Pippa, Ian, Gianluca, Jude, Richard, Dirk, Marc, Hendrik, Stefan and Nadine.

Back home, continuous support has been forthcoming from Nickl, Tina, Claudi and Stefan, Martin, Katja and Dietmar, Volker, Vati (Jessi's dad) and Inge, Rainer and Marlene and my parents, Regina and Jürgen – without you, this would have been impossible, thank you! Sadly, Rolf Hendriks, who first encouraged me to poke my nose into Oxford's air perished last year and is greatly missed.

Finally, and most importantly, a huge thanks to Jessi for her patience, support and total encouragement over the past three years, and it is to her, I dedicate this thesis.

Structural setting and petrogenesis of Silurian granites in the Caledonides of northern Scotland

Chapter 2 - Approach and methodology

Part B - Field, microstructural and geochemical analysis

Chapter 3 - Structural geology, fabric development and emplacement of the Rogart Granite

List of Figures

List of Tables

Part A

Introduction

Chapter 1

Introduction and regional overview

1 Introduction and Regional Overview

1.1 Aims and scope of the study

1.1.1 Significance of granite plutons

Granitic rocks make up about two-thirds of the continental crust and granitic magmatism is now believed to be the most important mechanism by which crustal growth has occurred (e.g. see reviews by Reymer & Schubert 1984, 1986; Taylor & McLennan 1985; Tarney & Jones 1994). However, there is still considerable debate regarding the origin of granitic melts and the relative importance of processes which govern their subsequent magmatic evolution prior to final emplacement (e.g. Chappell & White 1974, 1992; White & Chappell 1977; McCulloch & Chappell 1982; Gray 1984; Stephens & Halliday 1984; Harmon *et al.* 1984; Frost & O'Nions 1985; Thompson & Fowler 1986; Eby 1990; Thirlwall & Burnard 1990; Collins & Sawyer 1996; Collins 1996; Keay *et al.* 1997; Fowler *et al.* 2001). To date, petrologists recognise many different groups of granite. For example I- and S-type granites are thought to derive from igneous and sedimentary protoliths respectively (Chappell & White 1974), A-type granites are anorogenic (or alkaline) and have several possible sources (Eby 1990) and M-type granites are mantle-derived via extended crystal fractionation in regions otherwise dominated by basalt (Pitcher 1993). More recently, a distinctive suite of mantle-derived high Ba-Sr granitoids has been delineated in the Highlands of Scotland (Tarney & Jones 1994).

Close temporal and spatial links between the emplacement of granite plutons and the sites of active deformation have been demonstrated from various orogenic belts (e.g. Hutton 1988; Hutton & Reavy 1992; D'Lemos *et al.* 1992; Jacques & Reavy 1994; Ingram & Hutton 1994; Karlstrom & Williams 1995; Vigneresse 1995; Schofield *et al.* 1996; Schofield & D'Lemos 1998; Grocott *et al.* 1999; McCaffrey *et al.* 1999; Musumeci 1999; Paterson & Schmidt 1999; Steenken *et al.* 2000; Stewart *et al.* 2001; Strachan *et al.* 2001). An important means by which it is possible to establish a chronology of tectonothermal events in the high-grade cores of orogenic belts is based upon the accurate and precise isotopic dating of igneous rocks with structurally-defined relationships (Rogers & Pankhurst 1993). Of crucial significance is therefore the relative timing of pluton emplacement with respect to the deformation of the country rocks. Syn-tectonic plutons (i.e. plutons emplaced contemporaneously with the deformation of their host rocks) are

obviously of greatest value in calibrating regional deformation histories. Detailed comparison of fabrics and structures developed within plutons with those in their host rocks can be used to establish whether the pluton was emplaced pre, syn, or post-tectonically (e.g. see reviews by Paterson & Tobisch 1988; Paterson *et al.* 1989a, 1989b, 1991, 1998; and also Vernon *et al.* 1989; Karlstrom & Williams 1995; Tribe & D'Lemos 1996). Pluton emplacement takes place over a relatively short time of *c.* < 1Ma (Paterson & Tobish 1992; Tribe & D'Lemos 1996) compared to orogenic processes of *c.* 10 Ma (Paterson & Tobish 1992; Tribe & D'Lemos 1996; McCaffrey *et al.* 1999; Petford *et al.* 2000). As such, a precisely dated syn-tectonic pluton may mark a single discrete event within a period of regional tectonism; a suite of syn-tectonic plutons, however, has the potential to identify tectonic events within an orogeny and thus constrain crustal scale tectonic processes (e.g. Samson & D'Lemos 1999).

1.1.2 The Scottish Highlands

The Scottish Highlands form part of the early Palaeozoic Caledonian-Appalachian Orogen (Fig. 1.1). The region records protracted deformation, metamorphism and plutonism closely linked to the closure of the Iapetus Ocean and the consequent collision of three crustal blocks, Laurentia, Baltica and Avalonia (e.g. Pickering *et al.* 1988; Soper *et al.* 1992). The Scottish Caledonides have traditionally been of great importance in the development of geological ideas regarding the tectonometamorphic and tectonomagmatic evolution of mountain belts. Giletti *et al.* (1961) produced the first integrated regional structural and isotopic study addressing the timing of deformation and fabric development in a mountain belt, in this case the Northern Highlands of Scotland. Major advances in the understanding the complex, polyphase structures in the metamorphic rocks of the Northern Highlands followed the structural studies of Ramsay (1956, 1958) and Ramsay & Spring (1962). Dewey (1969) was the first to propose a plate tectonic reconstruction of the development and destruction of the Iapetus Ocean. Subsequently, significant early geochronological studies detailing the tectonometamorphic and tectonomagmatic history of the Scottish Caledonides were carried out by Dewey & Pankhurst (1970), van Breemen *et al.* (1974, 1979a, 1979b), Pidgeon & Aftalion (1978), Halliday *et al.* (1987) and Rogers & Dunning (1991). Based mainly on structural criteria, Read (1961) divided the Scottish granites into 'Older granites' and 'Newer granites' and the study of Stephens & Halliday (1984) provided the groundbreaking chemical classification of the Caledonian granites, which is still used today. Soper (1963) was amongst the first to investigate pluton

emplacement in the Northern Highlands and recognition of the temporal relationships between active deformation and pluton emplacement sparked a series of influential case studies throughout the 1980's and 1990's (e.g. Hutton 1988, 1988b; Hutton & McErlean 1991; Hutton & Reavy 1992; Jacques & Reavy 1994; Holdsworth *et al.* 1999). The continued development of isotopic techniques (e.g. Rogers & Pankhurst 1993) has considerably refined the understanding of tectonic events affecting the Scottish Caledonides but also shown a wide geochemical variety within the plutonic suites. Elemental and isotopic geochemistry has been contributing to the understanding of magmatic processes and granite petrogenesis has been much debated within a framework of mantle and crustal contributions (e.g. Stephens & Halliday 1984; Harmon *et al.* 1984; Frost & O'Nions 1985, Thompson & Fowler 1986; Fowler 1992; Thirlwall & Burnard 1990; Fowler *et al.* 2001).

1.1.3 Aims of this study

Recent integrated structural, metamorphic and geochronological studies have lead to major advances in understanding the tectonothermal evolution of the Caledonian Orogen in northern Scotland (Kinny *et al.* 1999; Friend *et al.* 2000; Kinny *et al.* in press). Elemental and isotopic geochemical studies of Caledonian plutons have further clarified fundamental processes governing granitoid petrogenesis in this part of the orogen (e.g. Pankhurst 1979; Fowler 1988a&b, 1992; Thirlwall & Burnard 1990; Tarney & Jones 1994; Fowler & Henney 1996; Fowler *et al.* 2001). This thesis focuses initially on the structural setting and emplacement of three 'Newer Granites', the Rogart, Strath Halladale and Helmsdale granites that are exposed in a relatively poorly known part of the Scottish Caledonides in east Sutherland (Fig. 1.1). It establishes the relative timing of pluton emplacement and fabric development with respect to the deformation of the country rocks and considers how it might be possible to use this information to date tectonic events during the Caledonian Orogeny. Using elemental and isotope geochemistry the thesis further considers the detailed magma genesis of the Strath Halladale and Helmsdale intrusions. Isotopic age data for the Rogart, Strath Halladale and Helmsdale granites are currently being generated in relation to this study by Dr. Jane Evans via a collaborative project with the NERC Isotope Geosciences Laboratory (NIGL). At the date of submission of this thesis, the U-Pb TIMS data for the three plutons under investigation has not been finalized and is quoted as preliminary data with the expressed consent of Dr. J. Evans (NIGL). A related, regional elemental and isotopic study of granitoid complexes from the Northern Highlands

investigates the spatial and temporal variation of isotopic signatures of nine Caledonian plutons. Analysis for six plutons were carried out in collaboration with Dr. Mike Fowler (OBU), Mrs. Fiona Darbyshire (NIGL) and Mr. Peter Greenwood (NIGL), and published data was incorporated as appropriate. All new data are quoted with the expressed consent of my co-workers.

1.2 Regional Overview

1.2.1 Introduction

The closure of the Iapetus Ocean led to widespread deformation and regional metamorphism throughout the north Atlantic Region during the lower Palaeozoic Caledonian Orogeny (e.g. Soper & Hutton 1984; Pickering *et al.* 1988; Soper *et al.* 1992; Fig. 1.1). Continental collision occurred between Laurentia, Avalonia and Baltica during the late Silurian-Devonian and was preceded by the accretion of various volcanic arcs onto the Laurentian and Baltican margins during the Ordovician. The Caledonian Orogeny was accompanied by significant igneous activity and most granitic plutons – the 'Newer Granites' of Read (1961) - were intruded during and after the final stages of continental collision (e.g. Soper 1986).

1.2.2 Terrane Architecture

The Caledonian orogenic belt of the British Isles can be divided into five major geological provinces that are bounded by crustal scale faults (Fig. 1.1; e.g. Gibbons & Gayer 1985; Hutton 1987). As the amount of movement along these mostly strike-slip faults is not precisely known and the correlation of stratigraphy, structure and deformational events across them is difficult, a terrane concept was proposed by Gibbons & Gayer (1985) and is accepted for the following discussion (see Fig. 1.1).

The Hebridean Terrane

The Hebridean Terrane comprises an Archaean to Palaeoproterozoic gneiss complex that is unconformably overlain by Neoproterozoic sediments that are, in turn, unconformably overlain by Cambro-Ordovician sediments (Park *et al.* 1994). The Hebridean Terrane is part of the Laurentian margin and represents the Caledonian foreland (e.g. Friend & Kinny 2001). It is bounded against the adjacent Northern Highland Terrane by the Moine Thrust.

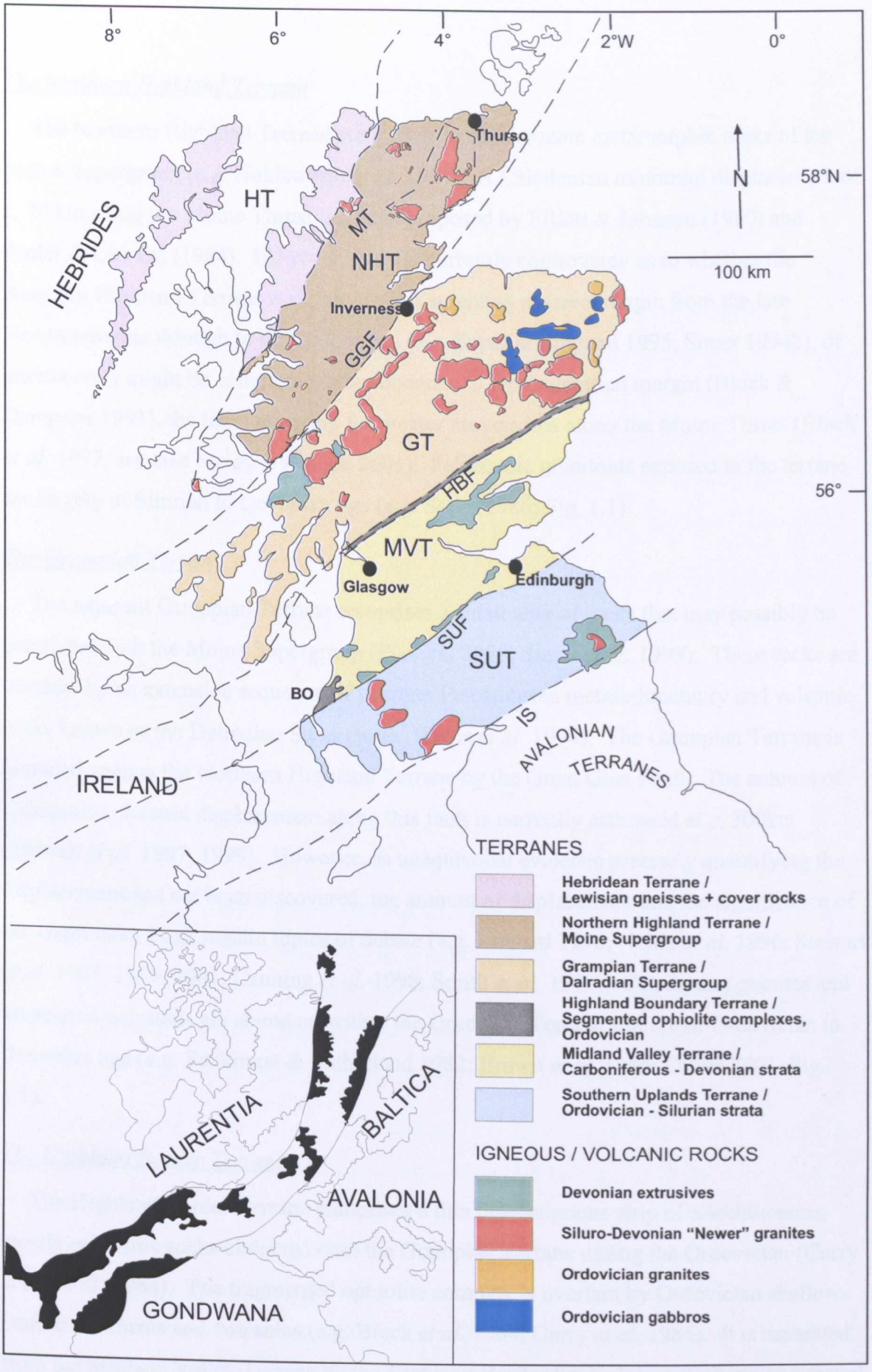

Fig.1.1 Overview of the Scottish Caledonian terranes. HT = Hebridean Terrane, NHT = Northern Highland Terrane, GT = Grampian Terrane, MVT= Midland Valley Terrane, SUT = Southern Uplands Terrane, MT = Moine Thrust, GGF = Great Glen Fault, HBF= Highland Boundary Fault, SUF = Southern Uplands Fault, IS = Iapetus suture. Also shown is the location of the study area (dashed box). Inset shows the extent of the Caledonian-Appalachian Orogen during the Palaeozoic.

The Northern Highland Terrane

The Northern Highland Terrane comprises Neoproterozoic metamorphic rocks of the Moine Supergroup (e.g. Holdsworth *et al.* 1994). A Caledonian minimum displacement of *c.* 70 km along the Moine Thrust has been proposed by Elliott & Johnson (1980) and Butler & Coward (1984). However, there is currently controversy as to whether the Northern Highland Terrane was part of the Laurentian passive margin from the late Neoproterozoic through to the Ordovician (e.g. Soper & England 1995; Soper 1994b), or alternatively might be completely allochthonous to the Laurentian margin (Bluck & Dempster 1991), the latter allowing for greater movements along the Moine Thrust (Bluck *et al.* 1997; see also review by Bluck 2001). Palaeozoic granitoids exposed in the terrane are largely of Silurian to Devonian age (e.g. Soper 1986; Fig. 1.1).

The Grampian Terrane

The adjacent Grampian Terrane comprises a small area of rocks that may possibly be correlated with the Moine Supergroup (Piasecki 1980, Smith *et al.* 1999). These rocks are overlain by an extensive sequence of younger Precambrian metasedimentary and volcanic rocks known as the Dalradian Supergroup (Harris *et al.* 1994). The Grampian Terrane is bounded against the Northern Highland Terrane by the Great Glen Fault. The amount of Caledonian sinistral displacement along this fault is currently estimated at *c.* 300km (Stewart *et al.* 1997, 1999). However, as unequivocal evidence precisely quantifying the displacement has not been discovered, the amount of displacement and the significance of the Great Glen Fault remain topics of debate (e.g. Coward 1990; Noble *et al.* 1996; Stewart *et al.* 1997, 1999, 2001; Canning *et al.* 1998; Smith *et al.* 1999). Caledonian granites and associated volcanics are abundant within the Grampian Terrane and are of Ordovician to Devonian age (e.g. Pankhurst & Sutherland 1982; Brown *et al.* 1985; Oliver 2001, Fig. 1.1).

The Highland Border Terrane

The Highland Border Terrane comprises a thin discontinuous strip of allochthonous, mostly ophiolitic rocks obducted onto the Grampian Terrane during the Ordovician (Curry *et al.* 1982, 1984). The fragmented ophiolite complex is overlain by Ordovician shallow-marine sediments and volcanics (e.g. Bluck *et al.* 1984; Curry *et al.* 1984). It is separated from the Midland Valley Terrane by the Highland Border Fault along which major sinistral

Caledonian displacements have occurred (Bluck 1983, 1985; Curry *et al.* 1982, 1984; Bluck & Leake 1986).

The Midland Valley Terrane

The Midland Valley Terrane mostly comprises sedimentary rocks of Devonian to Carboniferous age that are thought to conceal an underlying Ordovician volcanic arc (e.g. Longman *et al.* 1979; Bluck 1983, 1984). The presence of Proterozoic basement within the terrane is indicated by xenoliths obtained from late Palaeozoic basalts (e.g. Aftalion *et al.* 1984; Upton *et al.* 1984) with Sm-Nd model ages varying from 0.6-1.8 Ga and an average of *c.* 1.2 Ga (Halliday *et al.* 1993). The Ballantrae ophiolite complex in the southwest forms an allochthonous unit that is overlain by an Ordovician cover sequence (e.g. Bluck *et al.* 1980). Devonian volcanics occur in the northeast and along the southern boundary of the terrane (e.g. Thirlwall 1988, Fig. 1.1)

The Southern Uplands Terrane

The Southern Uplands Terrane is separated from the Midland Valley Terrane by the Southern Uplands Fault. It comprises three major fault-bounded tectono-stratigraphic belts that contain strongly folded Ordovician-Silurian marine sediments and rare volcanics (e.g. Bluck 1985; Hutton 1987; Needham 1993). The most widely believed tectonic interpretation of the Southern Uplands Terrane is that of an accretionary prism which developed above a northerly dipping Iapetus subduction zone as proposed by Leggett *et al.* (1979) and Leggett (1987). This is, however, controversial and alternative models have been proposed by, for example, Hutton & Murphy (1987), Morris (1987), Stone *et al.* (1987), Armstrong *et al.* (1996) and Owen *et al.* (1999). The southern boundary of the Southern Uplands Terrane along the Solway Line is commonly interpreted to mark the Iapetus Suture (e.g. McKerrow & Soper 1989; Soper *et al.* 1992 b).

In summary, the Caledonides of Scotland are divided into five terranes that are bounded by important faults along which terranes were juxtaposed during the Caledonian Orogeny. The Hebridean Terrane forms the Caledonian foreland and is separated from the Scottish Caledonides by the Moine Thrust. The Northern Highland and Grampian terranes comprise broadly similar lithologies and are separated by the Great Glen Fault. Caledonian sinistral displacements along this fault are currently estimated at *c.* 300km (e.g. Stewart et al. 1997, 1999, 2001). The Midland Valley Terrane is interpreted to represent a concealed, Ordovician volcanic arc onto which the Highland Border and Ballantrae

ophiolite complexes were obducted during the early stages of the Caledonian Orogeny (Bluck 1983, 1984; Curry *et al.* 1984). The most widely accepted interpretation of the Southern Uplands Terrane is that of an accretionary prism developed above a northerly-dipping subduction zone during the closure of the Iapetus Ocean (e.g. Leggett *et al.* 1979). Most of the terrane boundaries can be traced into Ireland (Fig. 1.1; e.g. Hutton 1987) where similar lithologies exist and comparable tectonometamorphic and tectonomagmatic histories have been reported (e.g. compare Friedrich *et al.* 1999a & b with Oliver 2001, see also Armstrong & Owen 2001). The following overview focuses largely on the Grampian and Northern Highland terranes.

1.2.3 Orogenic events

The Caledonian Orogeny affected all terranes north of the Iapetus Suture, but only the Northern Highland and Grampian terranes record polyphase deformation and regional metamorphism. Within these terranes, two distinct Caledonian orogenic phases are now recognised: a middle Ordovician arc-continent collision called the Grampian event and a Silurian continent-continent collision called the Scandian event (*sensu* McKerrow *et al.* 2000). Recently, isotopic studies have indicated a Neoproterozoic Knoydartian *c.* 820-790 Ma orogenic event that affected parts of the Grampian and Northern Highland terranes (e.g. Vance *et al.* 1998; Noble *et al.* 1996; Highton *et al.* 1999). The nature, timing and extent of an even earlier tectonothermal event affecting the Northern Highlands Terrane at *c.* 870 Ma is still debated (e.g. Friend *et al.* 1997; Millar 1999; Dalziel & Soper 2001). The Caledonian belt of Scotland is unaffected by any post Caledonian orogenic activity apart from late Palaeozoic to Mesozoic reactivation of faults (Roberts & Holdsworth 1999).

1.2.4 Caledonian Plutonism

The closure of the Iapetus Ocean was associated with widespread calc-alkaline and minor associated alkaline magmatism throughout the Scottish Highlands between the early Ordovician and the early Devonian (e.g. Thirlwall 1981, 1982, 1988; Pankhurst & Sutherland 1982; Soper 1986; Fowler 1992; Tarney & Jones 1994; Stephenson *et al.* 1999; Fig. 1.1). In Aberdeenshire, a suite of syn-tectonic granites and gabbros was intruded during the Grampian arc-continent collision (Fig. 1.1; e.g. Rogers *et al.* 1994; Oliver 2001). The bulk of the plutons exposed in the Grampian and Northern Highland terranes, however, are the 'Newer Granites' of Read (1961) which were emplaced either during or

shortly after the Scandian continental collision event and are late Silurian to early Devonian in age (Fig. 1.1; e.g. Soper 1986). In the Grampian Terrane and the terranes to the south, these mostly calc-alkaline plutons are in part thought to be associated and contemporaneous with large volumes of Devonian calc-alkaline lavas (Fig. 1.1; e.g. Bailey 1960; Thirlwall 1988).

1.3 The Northern Highland Terrane

1.3.1 Introduction

The Moine Supergroup is a thick sequence of metamorphosed, arenaeceous and argillaceous sediments that dominates the geology of the Northern Highland Terrane between the Great Glen Fault and the Moine Thrust (Fig. 1.2; e.g. Holdsworth *et al.* 1994). It comprises mainly psammites, semi-pelites and pelites that occur as thick formations and also as banded units. Sedimentary structures are preserved in areas of low tectonic strain and calc-silicate dominated horizons and heavy mineral laminae locally define marker horizons (e.g. Johnstone *et al.* 1969). Amphibolites are abundant throughout the Moine Supergroup, the majority of which were emplaced as basic igneous sheets early in the geological history (e.g. Moorhouse & Moorhouse 1979; Winchester 1985; Rock *et al.* 1985). Basement inliers in various structural settings are common throughout the terrane (Fig 1.2; e.g. Barr *et al.* 1986; Holdsworth 1989a). The Moine Supergroup is unconformably overlain by undeformed continental sediments of Devonian age (e.g. Mykura 1991 and references therein).

1.3.2 Tectonostratigraphy

Due to the lack of laterally extensive marker horizons and the heterogeneous deformation and metamorphism affecting the Moine rocks, early studies were only able to establish local tectonostratigraphies within the Moine (e.g. Johnstone *et al.* 1969; Tobisch *et al.* 1970; Brown *et al.* 1970). Major advances in understanding the Moine rocks of Western Inverness-shire were made after basement inliers were recognised in Glenelg (Ramsay 1958) and the Sgurr Beag Thrust was identified (Tanner *et al.* 1970). A regional framework for the entire Northern Highlands was established after basement-cover relationships and the thrust sheet configuration of major Caledonian structures was identified (Holdsworth *et al.* 1994).

Fig. 1.2 Tectono-stratigraphy of the Northern Highlands Terrane (modified after Strachan & Holdsworth 1988). SHG = Strath Halladale Granite, HD = Helmsdale Granite, RG = Rogart Granite, GF= Glenfinnan, BK=Ben Klibreck, AGG= Ardgour granite gneiss, FAGG= Fort Augustus granite gneiss, GGF=Great Glen Fault, SBT=Sgurr Beag Thrust, KT=Knoydart Thrust, BHT=Ben Hope Thrust, KH=Kinloch Hourn, F=Fannich, SR=Strontian, *GD*=Glen Doe, *LE*=Loch Eil, *Ag*=Ardgour area.

1.3.2.1 Tectonostratigraphy of Western Inverness-shire / southern Moine

The Moine Supergroup of Inverness-shire comprises three tectonically bounded units, the Morar (oldest), Glenfinnan and Loch Eil groups (youngest) (Fig. 1.2; Holdsworth *et al.* 1994). In its type area in Western Inverness-shire, the Morar Group stratigraphy is characterised by a *c.* 5km thick succession of psammites-pelites-psammites (Johnstone *et al.* 1969; Brown *et al.* 1970). Basement inliers that occupy major early isoclinal fold cores are exposed in the lower parts of the sequence (Powell 1974). The sequence is disrupted by the Knoydart Thrust which thrusts mid-amphibolite facies rocks over upper-greenschist facies rocks although a common metasedimentary succession is recognised below and above the thrust (Powell & Glendinning 1988). In large areas of low tectonic strain, sedimentary structures are abundant. The Sgurr Beag Thrust carries the characteristically striped units of interbanded psammites, semi-pelites, quarzites and pelites of the Glenfinnan Group (Roberts *et al.* 1987). North of Kinloch Hourn, basement rocks occur in the hanging wall of the Sgurr Beag Thrust and are inferred to be unconformably overlain by Glenfinnan Group rocks (Tanner *et al.* 1970). High levels of ductile strain coupled with mid to upper amphibolite facies metamorphism have largely obliterated sedimentary structures, and estimates of the original stratigraphic thickness range from 1 to 4 km (Holdsworth *et al.* 1994). Structurally above the Glenfinnan Group follows the Loch Eil Group, a monotonous sequence of psammites with occasional discontinuous quartzite and striped formations in the Loch Eil and Ardgour areas (Strachan 1985). Sedimentary structures are locally preserved and the original stratigraphic thickness is estimated at *c.* 5 km (Strachan 1985).

1.3.2.2 Tectonostratigraphy of Ross-shire

Extending the type stratigraphy northwards was possible after major Caledonian structures were recognised in Ross-shire (Wilson & Shepherd 1979; Kelley & Powell 1985). Western Ross-shire is dominated by psammitic Moine facies that are correlated with the Morar Group, and Glenfinnan-type rocks occur in the hanging wall of the Sgurr Beag Thrust around Fannich (Fig. 1.2; Holdsworth *et al.* 1994). Eastern Ross-shire is characterised by Glenfinnan-type pelitic and psammitic gneisses that occur in the hanging wall of the northern extension of the Sgurr Beag Thrust (e.g. Tanner et al 1970; Wilson 1975; Kelley & Powell 1985; Barr *et al.* 1986) and pass southeastwards into psammitic rocks of Loch Eil Group affinity.

1.3.2.3 Tectonostratigraphy of Sutherland and Caithness

Poor exposure and extensive post-Caledonian cover make it impossible to directly trace either the lithologies or the major thrusts exposed in eastern Ross-shire into Sutherland. The Sutherland Moine rocks comprise two major thrust sheets: the Moine Nappe, which is floored by the Moine Thrust, and the structurally higher Naver Nappe that is floored by the Naver Thrust (Fig. 1.2 e.g. Barr *et al.* 1986; Moorhouse & Moorhouse 1988). Both nappes are imbricated internally by subordinate ductile thrusts (e.g. Ben Hope Thrust, Swordly Thrust). The Moine Nappe comprises a monotonous sequence of psammites at the base (Holdsworth 1989a) which grade into finer-grained, micaceous varieties and subordinate garnet-mica pelite with minor calc-silicate horizons towards the top (Burns 1994). These have been correlated with the Morar Group rocks to the south, although their total stratigraphic thickness in west Sutherland does not exceed *c.* 500m, once the effects of deformation are removed (Holdsworth 1989a). Sedimentary structures are generally preserved. Numerous inliers of interbanded basic, intermediate and acidic basement gneisses have been recognised throughout the Moine and Naver nappes (Fig. 1.2; e.g. Moorhouse & Moorhouse 1977; Barr *et al.* 1986; Holdsworth 1989a). These are either located above Caledonian ductile thrusts or occupy major anticlinal fold cores, or occur as combinations of the two (Holdsworth 1989a; Burns 1994).

The stratigraphy directly above the Naver Thrust comprises a psammite-dominated sequence in the area around Ben Klibreck and a series of semi-pelitic banded gneisses of mid-amphibolite facies that incorporates large proportions of varied orthogneiss along the north coast. There, strong deformation and intense segregation melting has obliterated any earlier sedimentary structures. The rocks in the hanging wall of the Swordly Thrust are mostly sillimanite grade pelitic and semi-pelitic migmatites with subordinate psammites (Moorhouse & Moorhouse 1983, 1988; Moorhouse *et al.* 1988; Burns 1994; Watt *et al.* 1996). The Strathy Complex comprises a suite of siliceous gneisses and amphibolites which Burns (1994) interpreted as metamorphosed, hydrothermally-altered, bimodal calc-alkaline volcanics. The Strathy complex has yielded a Sm-Nd model age of *c.* 1150 Ma (M. Whitehouse, pers. comm.) and is thought to represent parts of the basement that underlies the Moine. The highest parts of the Naver Nappe exposed in northeastern Sutherland and Caithness are dominated by variably migmatitic, grey, psammitic gneisses of uncertain metamorphic grade. To the east of the Strath Halladale Granite (Fig. 1.2), a series of semi-pelitic gneisses of sillimanite grade disappear underneath the Old Red

Sandstone. In southeastern Sutherland, these semi-pelitic gneisses are overlain by psammites that preserve sedimentary structures and pelites with interbedded quarzite (Strachan 1988). The lithologies in the hanging wall of the Naver Thrust which carry a strong metamorphic segregation fabric have been correlated with the lower parts of the Glenfinnan Group in Ross-shire and Inverness-shire (Burns 1994) and the unmigmatitic rocks exposed in the higher part of the Naver Nappe may correspond to the Loch Eil Group (Strachan 1988).

1.3.3 Age and deposition of the Moine Supergroup

Detrital and inherited zircon grains obtained from Moine metasediments, migmatites and crust-derived granites range in age from *c.* 1800 Ma to *c.* 1000 Ma (Friend *et al.* 1997; Kinny *et al.* 1999; Friend *et al.* in press) and thus provide an upper age limit for Moine sedimentation. A lower age limit is provided by the West Highland granite gneiss that intrudes the Moine rocks between Strontian and Glen Doe. Early Rb-Sr whole rock ages for this complex of 1028 ± 43 Ma (Brook *et al.* 1976) have been superseded by new single grain TIMS and SHRIMP data which give protolith ages of 873± 7 Ma for the Ardgour gneiss (Friend *et al.* 1997) and 870± 30 Ma for the Fort Augustus gneiss (Fig. 1.2; Rogers *et al.* 2001). The Moine rocks of Western Inverness-shire have been interpreted as the fill of two major rift basins, each of half-graben type controlled by east-facing normal faults and sourced from the south (e.g. Glendinning 1988; Soper *et al.* 1998; Fig. 1.3). The Morar Group was deposited under shallow-marine conditions in the western half-graben (Glendinning 1988). The Glenfinnan Group probably represents its distal equivalent and the Loch Eil Group was deposited on top of Glenfinnan strata in the eastern half-graben (Soper *et al.* 1998). Isotopic dating of detrital grains has identified the Rhinns basement complex on Islay and the Annagh gneiss complex of northwest Ireland as possible source regions (Menuge & Daly 1994; Muir *et al.* 1994). The Archaean Lewisian rocks exposed on the Caledonian foreland were clearly not a major source (Friend *et al.* in press); this supports arguments for considerable movements along major thrust and faults during the Caledonian terrane assembly (Kinny *et al.* 1999; Friend *et al.* in press).

Fig. 1.3 Original stratigraphic relations of the sedimentary units in the Moine Supergroup according to Soper *et al.* 1998.

1.3.4 Orogenies and tectonothermal events in the Northern Highland Terrane

Major tectonothermal events occurred within the Northern Highland Terrane during the Neoproterozoic, the early Ordovician and the Silurian.

1.3.4.1 Neoproterozoic events

Bowes (1968) suggested the existence of a "Knoydartian" event affecting the Morar Group in Western Inverness-shire between *c.* 800 Ma and *c.* 700 Ma (van Breemen *et al.* 1974). Friend *et al.* (1997) argued for the formation of the West Highland granite gneiss (WHGG; Fig. 1.2) during an orogenic event at *c.* 870 Ma and Vance *et al.* (1998) and Rogers *et al.* (1998) recognised metamorphic assemblages that record prograde garnet growth during 'Knoydartian' crustal thickening at *c.* 830 – 790 Ma. Other workers, however, favour a prolonged episode of Neoproterozoic – early Ordovician crustal extension of *c.* 400 million years in the Northern Highland and Grampian terranes during which the Moine and Dalradian successions were deposited (Soper 1994a; Soper & Harris 1997; Dalziel & Soper 2001; Ryan & Soper 2001). These authors argue that the formation of WHGG at *c.* 870 Ma was induced by basalt injection into the lower crust and reject the age for evidence of crustal thickening at 830 –790 Ma (Dalziel & Soper 2001). Millar (1999) suggested that early extension-related magmatism at *c.* 870 Ma was followed by the onset of an orogeny at *c.* 830 Ma. In Sutherland, neither the rocks of the Moine nor the Naver Nappe seem to possess any isotopic record of the 870 Ma-event and evidence for crustal thickening at 830-780 Ma has also yet to be reported.

1.3.4.2 Palaeozoic events – the Caledonian Orogeny

Grampian Orogeny

A high-pressure metamorphic event has been demonstrated in the Naver Nappe in Sutherland (Friend *et al.* 2000) where syn-deformational melting and migmatization have been dated at 467 ± 10 Ma and 461 ± 13 Ma (Kinny *et al.* 1999). Evidence for possible Grampian-age metamorphism in southwestern Inverness-shire is provided by concordant U-Pb monazite ages of 455 ±3 Ma obtained from the Ardgour granite gneiss and host psammites at Glenfinnan (Aftalion & van Breemen 1980) and a Rb-Sr whole rock age of 467 ± 20 Ma obtained from the Morar Pelite (Brewer *et al.* 1979). A U-Pb titanite age of 470 ± 2 Ma obtained from the Fort Augustus granite gneiss is thought to date Grampian

age amphibolite facies metamorphism in the Loch Eil Group (Rogers *et al.* 2001). The Glen Dessarry Syenite postdates two phases of regional deformation and is dated at 456 ± 5 Ma (van Breemen *et al.* 1979a; Roberts *et al.* 1984).

Scandian orogeny

Syn-tectonic metagranite sheets dated at *c.* 429 – 420 Ma (Kinny *et al.* in press) were emplaced during the late stages of the main ductile thrusting event in central Sutherland. The pervasive fabrics and dominant structures produced during this event are thought to have resulted from the final collision of Laurentia and Baltica during the Silurian Scandian orogeny (Kinny *et al.* in press). This is compatible with movements in the Moine Thrust Zone dated at 437-408 Ma (Freeman *et al.* 1998) and supports the idea that the ductile Naver and Moine thrusts and the brittle Moine Thrust Zone are part of the same kinematically-linked, foreland-propagating thrust belt as proposed by Barr *et al.* (1986). Predominantly sinistral strike-slip faulting along major NE-trending faults, notably the Great Glen-Walls Boundary Fault system, followed the Scandian ductile thrusting in the Northern Highland Terrane between *c.*430 and 410 Ma (e.g. Watson 1984; Stewart *et al.* 1999). Post-Caledonian normal faulting and associated brittle folding resulting from gravity-driven collapse of the Scandian nappe pile has been demonstrated in Sutherland (Holdsworth 1989b) and in the Moine Thrust Zone (Coward 1983, 1985).

1.3.5 Regional Structure and deformation

The Moine rocks of the Northern Highland Terrane are characterised by complex patterns of up to 6 sequences of polyphase deformation which are usually placed in relative chronological order (i.e. D1, D2, D3...) based on structural, metamorphic and recently isotopic criteria (e.g. Ramsay 1963; Brown *et al.* 1970; Barber & May 1976; Holdsworth 1989a; Kinny *et al.* 1999). It is possible to distinguish domains of coherent structural style and deformational and metamorphic histories. Lateral correlation of individual events across the domains is sometimes difficult and in the following discussion any described individual event is restricted to its designated domain.

1.3.5.1 Regional structure and timing of deformation in the northern Moine

The Moine rocks of Sutherland are divisible into two major metamorphic thrust sheets, the Moine Nappe and the Naver Nappe (Moorhouse & Moorhouse 1983, Barr *et al.* 1986, Moorhouse *et al.* 1988; Holdsworth 1989a). They are bounded by major WNW- to NW-

directed Caledonian ductile thrusts, the Moine Thrust and the Naver Thrust (Moorhouse & Moorhouse 1988; Holdsworth 1990; Alsop *et al.* 1996; Holdsworth *et al.* 2001). Recently, combined structural, metamorphic and isotopic studies have succeeded in assigning locally pervasive fabrics formed during the Caledonian orogeny to the Scandian event and the Grampian event respectively (e.g. Kinny *et al.* 1999; Friend *et al.* 2000; Kinny *et al.* in press). It is possible to identify four domains which record coherent structural histories (Fig. 1.4). The Moine Nappe (1) records dominantly Scandian fabrics and forms the largest domain. The Naver Nappe comprises three additional domains, a '*western belt*' (2) bracketed by the Naver and Swordly thrusts where Grampian fabrics have been intensely reworked and are overprinted by Scandian fabrics; a '*central belt*' (3) above the Swordly thrust which is dominated by Grampian fabrics and an '*eastern belt*' (4) east of the Strath Halladale river where fabric patterns are of unknown age (see below and chapter 4). The 'Torrisdale steep belt' on the north coast forms another domain (Moorhouse & Moorhouse 1988; Burns 1994) that records a post-D2 phase of dextral transpression. Its effects, however, die out *c.* 5-6 km inland (Burns 1994; Kinny *et al.* 1999) and it is therefore omitted from the present discussion.

1.3.5.1.1 The Moine Nappe

In the Moine Nappe pre-D2 structures such as planar fabrics (S_0/S_1) and a weak N- to NNE trending mineral lineation (L_1) are associated with metamorphism of at least garnet grade (Barr *et al.*1986; Holdsworth 1989a). Throughout the Moine Nappe the dominant tight-to-isoclinal, reclined folds, ductile thrusts and associated fabrics are generally related to a local D2 phase of deformation (e.g. Soper & Brown 1971; Soper & Wilkinson 1975; Barr *et al.* 1986; Moorhouse & Moorhouse 1988; Moorhouse *et al.* 1988; Strachan & Holdsworth 1988). During D2 thrusting, a composite SE to E dipping $S_0/S_1/S_2$ foliation and a SSE to ESE plunging mineral lineation (L_2) were developed (e.g. Barr *et al.* 1986; Strachan & Holdsworth 1988). Thrusting was generally top-to-the-WNW-to-NW (Holdsworth 1990; Holdsworth *et al.* 2001) and resulted in the tectonic interleaving of Moine psammites and basement gneisses (Strachan & Holdsworth 1988). Progressive thrusting and shearing produced the dominant tight-to-isoclinal recumbent F2 folds which often display sheath fold geometries with curvilinear hinge lines that have been rotated into parallelism with the L_2 mineral lineation. In the vicinity of the Moine Thrust, the L_2 lineation plunges to the ESE, however, in the vicinity of the Naver Thrust it swings round and plunges SSE (Barr *et al.* 1986; Alsop *et al.* 1996). A similar pattern is observed in late

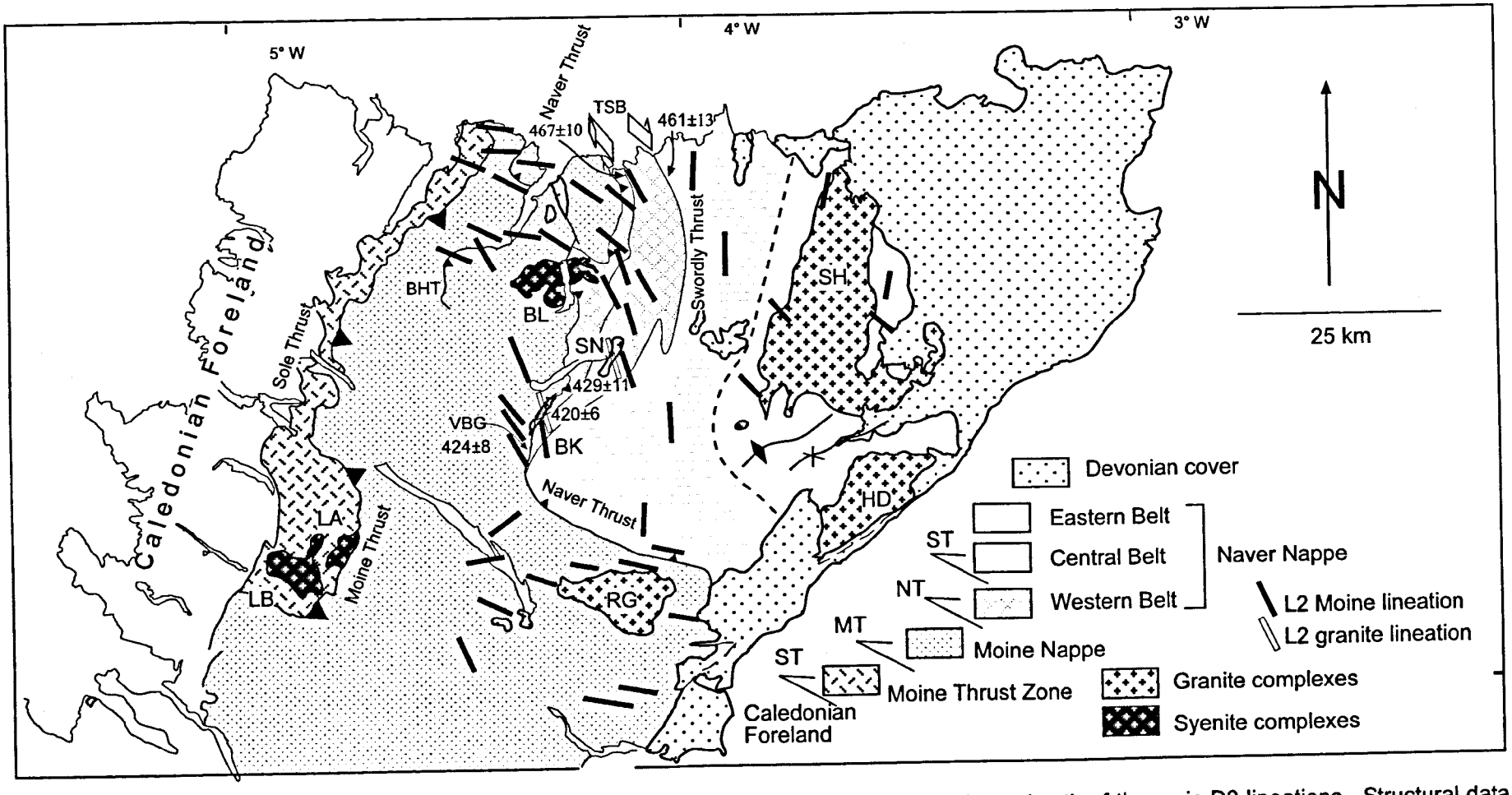

Fig. 1.4 Structural domains of Sutherland. Note the thrust sheet configuration and the changing azimuth of the main D2 lineations. Structural data compiled from Strachan & Holdsworth 1988, Holdsworth & Strachan 1988, Holdsworth 1990, Alsop et al. 1996, and Strachan & Kocks (unpublished data). Isotopic age data (SHRIMP) from Kinny et al. 1999 and Kinny et al in press. LB= Borallan syenite, LA= Loch Ailsh syenite, BL= Ben Loyal syenite, RG= Rogart granite, VBG= Vagastie Bridge granite, SN= Strath Naver granite, SH= Strath Halladale granite, HD= Helmsdale granite, BK= Ben Klibreck, TSB= Torrisdale Steep Belt, BHT= Ben Hope Thrust, filled circles= location of dated migmatites, further explanation see text.

open (F3) cross folds that deform early ductile D2 thrusts and the regional S_2 foliation (Alsop & Holdsworth 1993). The Caledonian D2 thrust transport direction therefore changed progressively from early (Naver Thrust) NNW-directed to later (Moine Thrust) WNW-directed thrusting (Strachan & Holdsworth 1988; Alsop *et al.* 1996). Metagranite sheets (Strath Vagastie, Ben Klibreck and Strathnaver granites, Fig. 1.4) that were emplaced at a high structural level in the Moine Nappe in the vicinity of the Naver Thrust clearly post date the early D2 folding but do carry a significant late D2 L-S fabric and are hence syn-tectonic with the late D2 deformation (Strachan & Holdsworth 1988; Kinny *et al.* in press). They have recently been dated at *c.* 429-420 Ma (U-Pb zircon SHRIMP, Kinny *et al.* in press) and therefore constrain D2 deformation in the Moine Nappe to the late Silurian. The presence of syn-D2 garnet and staurolite within Moine pelites, the widespread parallelism of hornblende with L_2 in mafic rocks and the identification of post-D2 kyanite within basement rocks of the Meadie inlier indicate that D2 was accompanied by amphibolite facies metamorphism at temperatures greater than *c.* 550-600°C (Strachan & Holdsworth 1988; Holdsworth 1989a; Burns 1994; Holdsworth *et al.* 2001). D2 fabrics in southern Sutherland are warped around the gently eastward plunging Assynt culmination (e.g. Strachan & Holdsworth 1988). Brittle folds in the Moine Nappe and associated low angle faults of various orientations show a late Caledonian post D2 ESE-directed extension (Holdsworth 1989b). They relate to the extensional collapse of the nappe pile (Holdsworth 1989b) and are possibly contemporaneous with the emplacement of the Loch Loyal Syenites (Holdsworth *et al.* 1999).

1.3.5.1.2 The Naver Nappe

The regional foliation throughout the Naver Nappe is parallel to the gross lithological banding and gneissosity within the paragneisses, orthogneisses and amphibolites (Burns 1994). In the migmatitic rocks the fabric is generally parallel to the prominent stromatic layering characteristic of the metatexites, and throughout the nappe the fabric is deformed by common, tight to close D2 folds on all scales (Kinny *et al.* 1999).

The western belt

Between the Swordly and Naver thrusts, Scandian fabrics intensely overprint pre-existing migmatitic layering and relict high-pressure granulite facies assemblages (Friend *et al.* 2000). Migmatization has been dated at 467 ±10 Ma (Fig 1.4; Kinny *et al.* 1999). The dominant D2 structures are tight-to-isoclinal, reclined F2 folds which often display

sheath fold geometries and composite easterly-dipping foliations. Mostly ESE-SE plunging mineral lineations are pervasive throughout this domain where they have not been affected by later Torrisdale steep belt deformation. Late D3, open SE to ESE plunging cross folds slightly warp all early planar fabrics (Alsop *et al.* 1996). Both D2 and D3 related structures are equivalent to the D2 and D3 related structures in the Moine Nappe and D2 in this domain is constrained by the intrusion age of the late syn-tectonic Strathnaver Granite of 429 ± 11 Ma (U-Pb, zircon SHRIMP, Kinny *et al.* in press).

The central belt

Throughout the higher parts of the Naver Nappe above the Swordly Thrust, the dominant planar fabric is a composite $S_0/S_1/S_2$ foliation. It is associated with a N-S trending lineation that occurs throughout the central belt from the north coast to southeast of Loch Coire in central Sutherland (Burns 1994; R. A. Strachan pers. comm.). Leucosomes within the Kirtomy Migmatites both crosscut local F2 folds and are themselves folded, indicating that migmatization was contemporaneous with folding (Kinny *et al.* 1999). A U-Pb zircon SHRIMP age of 461 ± 13 Ma (Kinny *et al.* 1999) dates the migmatization, and constrains the associated local deformation and sillimanite grade metamorphism (Friend & Strachan pers. comm. 10/2001) to be of Ordovician, i.e. Grampian age. The D2 deformation in the central belt is therefore of different age to the Scandian D2 deformation observed further west. However, a monazite age of 431 ±10 Ma (U-Pb SHRIMP, Kinny *et al.* 1999) possibly reflects reheating during the Scandian event (Kinny *et al.* 1999).

The eastern belt

The third structural domain in the upper Naver Nappe corresponds to the area east of the Strath Halladale river and the north of the Strath of Kildonan. To the west of the Strath Halladale Granite, the Moine rocks are strongly migmatitic whereas on its eastern side widespread regional migmatisation is absent. A pervasive foliation locally crenulates the segregation fabric and is commonly attributed to D2 deformation (e.g. McCourt 1980; Strachan 1988); it strikes *c.* 020-040° and dips moderately to the east in the north of the eastern belt. The southern part of the domain is largely dominated by late NNE trending F3 folds that refold D2 fabrics (Strachan 1988). Two sets of linear fabrics, one trending N-S and a second trending NW-SE are observed in areas unaffected by D3 deformation (R. A. Strachan pers. comm.; this study). A fourth phase of deformation is indicated by the

kinking of F3 fold axis (e.g. McCourt 1980). Isotopic constraints on the timing of migmatization and D1-D4 deformation are limited and will be discussed in more detail in chapter 4.

1.3.5.2 Regional structure and timing of deformation in the southern Moine

The southern Moine rocks comprise a stack of three major thrust nappes, the Moine, Knoydart and Sgurr Beag Nappes which are bounded by major Caledonian ductile thrusts, the Moine, Knoydart and Sgurr Beag thrusts, respectively (Figs. 1.2 & 1.5; e.g. Barr *et al.* 1986; Soper *et al.* 1998). Caledonian ductile thrusting in the southern Moine occurred during the D2 phase of a local D1 to D4 deformation sequence (Kelley & Powell 1985) and was followed by subsequent upright folding (D3). The D2 structures in Western Ross-shire clearly overprint pre-existing coarse migmatitic layering, fold hinges and metamorphic assemblages (e.g. Rathbone & Harris 1979; Kelley & Powell 1985; Barr *et al.* 1986). As the lateral extent of the D3 deformation varies throughout the southern Moine it is convenient to distinguish three structurally coherent domains.

The steep belt of Western Inverness-shire

In southwestern Inverness-shire D2 ductile deformation is assigned to movements along the Sgurr Beag and Knoydart thrusts, the latter of which tectonically thickens the Moine Nappe (Fig. 1.2). Kelley & Powell (1985) suggested a combined minimum displacement along both structures of *c.* 50 km. A suite of pegmatites that cut presumed D2 folds at Glenfinnan (Fig. 1.2) has been dated at 445 ± 10 Ma (Rb-Sr muscovite) and 450 ± 10 Ma (U-Pb monazite, bulk fractions) by van Breemen *et al.* (1974) and the Glen Dessarry Syenite, dated at 456 ± 5 Ma (van Breemen *et al.* 1979a), has also been interpreted to post-date two phases of regional deformation. A Rb-Sr whole rock age of 467 ± 20 Ma obtained from the Morar pelite (Brewer *et al.* 1979) and a U-Pb monazite age of 455±3 Ma obtained from the Ardgour granite gneiss (Aftalion & van Breemen 1980) are thought to reflect (syn D2) peak metamorphism in the Morar and Glenfinnan groups (e.g. Kelley & Powell 1985). D2 deformation and associated metamorphism affecting the Moine rocks in Western Inverness-shire are therefore currently interpreted to be of Ordovician age. However, the geology of Western Inverness-shire is dominated by tight, upright, NNE-SSW trending, steeply-plunging F3 folds known as the *steep belt* (Fig. 1.5) which clearly fold the Sgurr Beag and Knoydart thrusts (Fig 1.5; e.g. Powell & Phillips 1985; Barr *et al.* 1986).

Fig. 1.5 Semi-schematic x-section of the southwestern Moine (modified after Barr *et al.* 1986; Powell & Glendinning 1988). For profile line see Fig. 1.2, explanation see text. MT=Moine Thrust, KT=Knoydarrt Thrust, SBT=Sgurr Beag Thrust, LQL= Loch Quoich Line, GGF= Great Glen Fault, ma=Morar anticline, gs= Glenshian synform, lea = Loch Eilt antiform, sms= Sgurr A Muidhe synform, le= Loch Eilt.

D3 upright folding led to a post D2 shortening of *c.* 50% (Holdsworth & Roberts 1984) that occurred above an easterly-dipping detachment, possibly the Moine Thrust Zone (Barr *et al.* 1986). D3 open folding and the formation of the *steep belt* in SW Inverness-shire must be younger than the Glen Dessarry Syenite (456 ± 5 Ma van Breemen *et al.* 1979a) which is located in the core of a major F3 synform (Fig. 1.5; van Breemen *et al.* 1979a; Roberts *et al.* 1984).

The flat Belt of Eastern Inverness-shire

The Loch Quoich Line (Fig. 1.5) separates the steep belt from an area that is largely unaffected by D3 open folding to the east, known as the flat belt (Clifford 1957; Roberts & Harris 1983; Barr *et al.* 1986). Recumbent, tight-to-isoclinal sheath folds dominate the area, which were developed by heterogeneous low-angle simple shear parallel to a N-S trending lineation (Holdsworth & Roberts 1984). Rare S-C and shear fabrics indicate top-to-the-N movements parallel to that lineation (R. A. Strachan pers. comm.). A U-Pb titanite age of 470 ± 2 Ma (Rogers *et al.* 2001) obtained from the Fort Augustus granite gneiss (Fig. 1.2) has been interpreted to date syn-D2 amphibolite facies metamorphism in the Glenfinnan and Loch Eil groups (Rogers *et al.* 2001).

Western Ross-shire

In western Ross-shire, D3 upright folding is also of limited significance (e.g. Kelley & Powell 1985). D2-related, tight-to-isoclinal, reclined F2 folds and a pervasive L_2 mineral and extension lineation that generally trends towards 130-140° are dominant (Wilson & Shepherd 1979; Kelly & Powell 1985; May *et al.* 1993). These structures are clearly related to NW-directed movements on the Sgurr Beag Slide during D2 deformation and are identical to the D2 structures described in the Moine and lower Naver nappes in central and northwestern Sutherland (Fig 1.4; Kinny *et al.* in press).

1.3.5.3 Correlation of deformation events between the southern and northern Moine

Problems in isotopically dating D2 deformation and correlating deformation events between Inverness-shire and Sutherland (table 1.1) largely result from the absence of suitable, syn-tectonic intrusions with well-defined structural relationships. Arguably, the D2 structures and fabrics that are traceable throughout the Moine Nappe from Inverness-shire to Sutherland should be related to the same deformational event. At present, the currently accepted Ordovician age for D2 in the southern Moine of Western Inverness-

shire therefore conflicts with the recently established timing of D2 deformation in the Moine Nappe in Sutherland (Kinny *et al.* in press). A summary of deformational phases and currently available isotopic age data in the Northern Highlands Terrane (table 1.1) highlights the problems encountered in the correlation of events between the south and the north.

Table 1.1 Deformational phases in the Northern Highland Terrane. Grey background = uncertain age, green background = Knoydartian event, blue background = Grampian event, yellow background = Scandian event, red frame = directly dated deformation fabric. Note: D2 has been assigned different ages throughout the terrane. The background colours reflect the currently accepted timing of deformational events, only the data in red frames shows fabrics that have been dated using syn-tectonic intrusions, syn-tectonically recrystallized minerals, and syn-deformational leucosomes.

North

Moine Nappe	Naver Nappe		
	Western belt	Central belt	Eastern belt
D1: • Local S_0/S_1 refolded by D2, • associated with Grt-grade metamorphism – 1), 2)	D1: • Fabrics reworked during D2 • Migmatization dated at 467±10Ma (U-Pb, zircon SHRIMP – 9))	D1: • Locally D1 fabrics are reworked by D2 – 6), 10)	D1: • Lit-par-lit migmatites, crenulated by D2 – 12) • High pressure melting (Grt in leucosome) – 13) • Interpreted to correspond to the 461±13 Ma event observed further W - 10) page 1150)
D2: • Tight to isoclinal F2-folds, sheath folds, ductile thrusts – 1), 2), 3) • L2-lineation indicates changing transport direction from early NNW to late WNW – 5) • Syn D2 Grt-St-grade metamorphism – 2), 4), 6) • Late syn-D2 metagranites date fabric to *c.*429±11 Ma (U-Pb, zircon, SHRIMP) – 7)	D2: • Tight to isoclinal F2-folds, sheath folds, ductile thrusts – 1), 2), 3) • L2 plunges ESE – SE – 6) • Late syn-D2 metagranites date fabric to *c.*429±11 Ma (U-Pb, zircon, SHRIMP – 7)	D2: • S0/S1/S2 foliation, N-S trending lineations – 6), 11) • Tight to isoclinal F2-folding, sillimanite grade metamorphism contemporaneous with migmatization at 461±13 Ma (U-Pb zircon SHRIMP –10) • Interpreted to result from high-pressure, crustal thickening – 9), 10)	D2: • Composite $S_0S_1S_2$ foliation, N-S trending L2 – 12) • Tight to isoclinal folds – 14) • S-C fabrics, NW trending L2, top-to-NW shear, sillimanite grade metamorphism – 13)
Post D2: • Brittle imbrication in Moine Thrust footwall => Assynt culmination • Brittle folds show ESE-extension – 8)		Post D2: • 431±10Ma monazite age (U-Pb SHRIMP) may reflect heating during renewed crustal thickening – 10)	D3: • Large scale open F3-folds, trending NE-SW, no pervasive fabric associated – 12), 14) D4: • Kinking of F3-folds – 12), 14)
	D3: • F3-cross folds – 5) • Torrisdale steep belt, sinistral transpression –6)		

South

Ross-shire	Inverness-shire	
D1: • Local S0/S1 commonly crenulated by D2 – 15 • Prograde garnet growth at c. 820 Ma - 26	D1: • Migmatitic lit-par-lit layering, commonly reworked by D2 – 15), 11)	
D2: • Isoclinal & reclined F2-folds, associated NW-trending L2 – 15), 16) • NW-directed thrusting along the Sgurr Beag Thrust – 11)	D2 in the Moine Thrust Zone • Interpreted to be the youngest part of the kinematically linked, foreland-propagating Scandian thrust system – 1) • Thrust movements dated at c.437 – 408 Ma – 24), 25)	D2 in the Morar Group below the Sgurr Beag Thrust: • Tight-to-isoclinal D2 folding during NW-directed ductile thrusting, NW-trending L2 lineation – 11) 22), 23) 24) • Amphibolite facies metamorphism reflected by a Rb-Sr whole rock age of 467±20 Ma obtained from the Morar Pelite – 28).
	D2 in the Glenfinnan group of the "steep belt" (W of the Loch Quoich Line): • Structures & fabrics that are thought to be of a D2 age are traceable from the flat belt into the steep belt where they pre-date the Glen Dessarry Syenite dated at 456±5Ma – 19), 20) • Structures & fabrics that are thought to be of a D2 age are cut by a suite of pegmatites at Glenfinnan, dated at 445±10 Ma (Rb-Sr muscovite – 21) and 450±10 Ma (U-Pb bulk zircon – 21) • Metamorphism reflected by a 455±3 Ma U-Pb monazite age (27) obtained from the Ardgour granite gneiss.	D2 in the Loch Eil group of the "flat belt" (E of Loch Quoich Line): • Recumbent tigh-to-isoclinal sheath folds developed by low angle simple shear parallel to a N-S trending lineation – 17) • S-C-fabrics indicating top-to-N sense of shear parallel a N-S trending lineation – 11) • Amphibolite facies metamorphism reflected by a 470±2Ma U-Pb titanite age obtained from the Fort Augustus granite gneiss (– 18)
	D3: • Widespread upright folding to the W of the Loch Quoich Line, formation of the Northern Highland Steep Belt. F3 folds trend N-S to NNE-SSW. Post-dates the emplacement of the Glen Dessarry Syenite (456±5 Ma – 19) that occupies the core of an F3 syncline and carries a solid-state fabric (-11).	

1) Barr *et al.* 1986, 2) Holdsworth 1989a, 3) Moorhouse & Moorhouse 1988, 4) Strachan & Holdsworth 1988, 5) Alsop *et al.* 1996, 6) Burns 1994, 7) Kinny *et al.* in press, 8) Holdsworth 1989b, 9) Friend *et al.* 2000, 10) Kinny *et al.* 1999, 11) Strachan pers. comm., 12) McCourt 1980, 13) this study, 14) Strachan 1988, 15) Kelley & Powell 1985, 16) Wilson & Sheperd 1979, 17) Holdsworth & Roberts 1984, 18) Rogers *et al.* 2001, 19) Van Breeman *et al.* 1979a, 20) Roberts *et al.* 1984, 21) Van Breemen *et al.* 1974, 22) May *et al.* 1993, 23) Ramsay 1958, 24) Powell 1966, Van Breemen *et al.* 1979b, 25) Freeman *et al.* 1998, 26) Vance *et al.* 1998, 27) Aftalion & van Breemen 1980, 28) Brewer *et al.* 1979

1.3.6 Caledonian plutonism in the Northern Highland Terrane

Caledonian igneous activity in the Northern Highland Terrane spans from the Glen Dessarry Syenite at 456 ± 5 Ma (van Breemen *et al.* 1979a) to the "Newer Granites" (Read 1961) which were emplaced between *c.* 435- 420 Ma (e.g. Halliday *et al.* 1987; Rogers & Dunning 1991; Stewart *et al.* 2001). The peak of igneous activity appears to lie at around 425 Ma and is thus syn-tectonic with the Scandian Orogeny (e.g. Rogers & Dunning 1991, Kinny *et al.* in press). Proposed pluton emplacement mechanisms in the terrane vary from emplacement into extensional shear zones in strike-slip regimes (e.g. Strontian, Hutton 1988b; Clunes Tonalite, Stewart *et al.* 2001) to emplacement into active thrust zones (e.g. the sheeted granites in central Sutherland, Kinny *et al.* in press) and forceful diapiric emplacement into Moine country rocks (e.g. Rogart, Soper 1963, 1999). The Caledonian igneous complexes exposed in the Northern Highland Terrane can be divided petrographically into two groups: a western belt of syenites (Glen Dessarry, Loch Borralan, Loch Ailsh, Loch Loyal) and a central to eastern belt of granitic complexes (Strontian, Cluanie, Rogart, Helmsdale, Strath Halladale) (Fig. 1.6). Petrographically the alkaline complexes are dominated by leuco- to mela-syenites with minor monzodiorite. The calc-alkaline granite complexes are dominated by granodiorites but also comprise quartz diorites, tonalites and granites (e.g. Fowler & Henney 1996, Highton 1999). Appendix 1 provides currently accepted classifications of igneous rocks and a glossary that explains scotland-specific igneous terminology. The localities, currently accepted isotopic age data, previous emplacement studies and the tectonic significance of individual plutons exposed in the Northern Highlands Terrane are summarised in Fig. 1.6 and table 1.2.

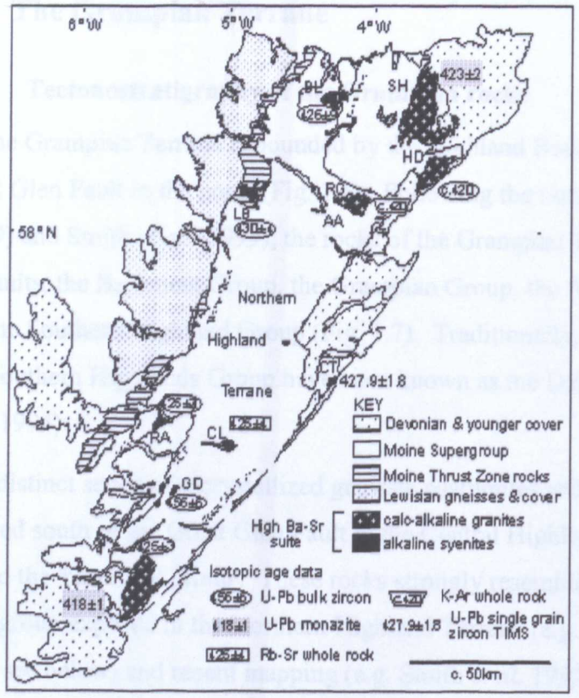

Fig. 1.6 Caledonian plutons in the Northern Highland Terrane (AA = Ach' Uaine hybrids). All other locality abbreviations, details of available isotopic age data and pluton significance are given in table 1.2.

Table 1.2 Summary of currently available isotopic age data and previous emplacement studies of Caledonian plutons in the Northern Highland Terrane.

Pluton	Age [Ma]	Method / Author	Significance – Interpretation
Glen Dessarry Syenite (GD)	456±5	U-Pb bulk zircon – Van Breemen et al. 1979b	Crystallization age (complete cooling history published by Cliff 1985). Emplaced into Glenfinnan group of Inverness-shire, post-dating local D2 but prior to D3 steep belt formation (Roberts et al. 1984)
Loch Ailsh Syenite	439±4	^{207}Pb-^{206}Pb zircon – Halliday et al. 1987	Crystallization age. Pluton is located in the Moine Thrust Zone but currently believed pre-tectonic with respect to Moine Thrust Zone movements (Halliday et al. 1987; Butler 1986).
Loch Borallan Syenite (LL)	430±4	U-Pb bulk zircon – Pidgeon & Aftalion 1978	Crystallization age. Pluton is located in the Moine Thrust Zone, significance controversial due to poor exposure (Coward 1985; Butler 1986).
Loch Loyal Syenite (BL)	426±9	U-Pb bulk zircon – Halliday et al. 1987	Crystallization age. Emplacement into Morrar Group rocks in Sutherland was controlled by pre-existing host rock architecture and may have been facilitated by extensional collapse of the Moine & Naver nappes (Holdsworth et al.1999).
Clunes Tonalite (CT)	427.8±1.9	U-Pb single zircon TIMS – Stewart et al. 2001	Crystallization age. Interpreted to date earliest sinistral movements along the Great Glen Fault.
Strontian granodiorite (SR)	425±3	U-Pb bulk zircon – Rogers & Dunning 1991	Crystallization age. The inner granodiorite was emplaced into an extensional shear zone developed in response to dextral movements along the Great Glen Fault (Hutton 1988b).
Ratagain complex (Px-mica-diorite) (RA)	425±3	U-Pb bulk zircon – Rogers & Dunning 1991	Crystallization age. Internal high-T, sigmoidal deformation fabrics are interpreted by Hutton & McErlean (1991) to reflect (and date) sinistral movements along the Strathconan Fault.
Cluanie granite (CL)	425±4	Rb-Sr whole rock – quoted in Brown et al. 1985	Crystallization age. Ballooning and country rock deformation proposed by Leedal (1952) but disputed by Peacock et al. (1992).
Strath Halladale Granite (SH)	423±2	U-Pb titanite – G. Rogers pers. comm.	Post emplacement cooling age through the closure T of titanite for U (c.550°C) interpreted to closely date intrusion (Rogers, G. pers comm). Age is believed more reliable than an earlier Rb-Sr whole rock age of 649±30 Ma (M. Brook quoted in Pankhurst 1982); small fractions of zircon and monazite are currently analyzed (Dr. J. Evans, NIGL; this study) to identify a crystallization age. Previously the pluton was interpreted to be post-tectonic to local D2 (McCourt 1980) but is now considered syn-tectonic with D2 thrusting (this study).
Reay Diorite	424±3	^{39}Ar-^{40}Ar (Hbl) – Dallmeyer et al 2001	Interpreted as a cooling age through the blocking T of Hbl possibly closely dating pluton emplacement (Dallmeyer et al. 2001). Note that this agrees well with the titanite age of the Strath Halladale Granite which is part of the same magmatic pulse (Storey & Lintern 1981; this study).
Helmsdale Granite (HD)	c. 420	U-Pb bulk zircon – Pidgeon & Aftalion 1978	Imprecisely constrained lower concordia intercept, no error given. Possibly dates emplacement and is currently under re-investigation (Dr. J. Evans, NIGL; this study).
Rogart Granite (RG)	c. 420	K-Ar whole rock – Brown et al. 1968 quoted by Brown, P. E. 1991	Sample locality not known. Interpreted here as regional cooling age, giving a minimum pluton age. Pluton was previously interpreted as a hot stokes diapir that actively deformed its host rocks (Soper 1963, 1999). Emplacement may however relate to ductile deformation in the footwall of the Naver Thrust and dextral movements along the Strath Fleet lineament (this study). Currently being dated by Dr. J. Evans (NIGL).

1.4 The Grampian Terrane

1.4.1 Tectonostratigraphy of the Grampian rocks

The Grampian Terrane is bounded by the Highland Boundary fault in the south and the Great Glen Fault in the north (Fig. 1.1). Following the nomenclature of Tanner & Bluck (1999) and Smith *et al.* (1999), the rocks of the Grampian Terrane can be subdivided into five units, the Basement Group, the Grampian Group, the Appin Group, the Argyll Group and the Southern Highland Group (Fig. 1.7). Traditionally, the Grampian, Appin, Argyll and Southern Highlands Group have been known as the Dalradian Supergroup (e.g. Harris *et al.* 1994).

A distinct series of recrystallized gneissic psammites and migmatitic psammites is exposed south of the Great Glen Fault in the Central Highlands that Smith *et al.* (1999) termed the 'basement group'. These rocks strongly resemble parts of the Moine Supergroup exposed in the Northern Highland Terrane (e.g. Piasecki 1980; Harris *et al.* 1994; see below) and recent mapping (e.g. Smith *et al.* 1999; Robertson & Smith 1999) has identified two distinct units, the Glen Banchor and Dava successions. The Glen Banchor succession consists of banded quartzofeldspathic psammites, striped garnetiferous semi-pelite and psammite and migmatitic quarzites. The Dava succession comprises an association of migmatitic psammites with subordinate semi-pelites. The Grampian Group rests unconformably above rocks of the Basement Group, however, the original contact relationships are tectonically reworked throughout much of the Central Highlands (Smith *et al.* 1999; Robertson & Smith 1999). The Grampian Group is the lowermost unit assigned to the Dalradian Supergroup and comprises *c.* 8 km of monotonous quartzofeldspathic psammite and pelite to semi-pelite (Harris *et al.* 1994). Rocks of the Appin Group overstep the Grampian Group and the Dava and Glen Banchor divisions in the central and southwestern Highlands and are separated from the Grampian Group throughout the eastern Highlands by the Boundary slide; contacts between the Appin Group and younger rocks are conformable (e.g. Smith *et al.* 1999). The Appin and Argyll groups comprise rocks that document initial shallow shelf conditions which give way to a series of marine turbidite basins and the development of intense volcanicity (e.g. Harris *et al.* 1978; Anderton 1985; Harris *et al.* 1994).

Fig. 1.7 Dalradian tectonostratigraphy of the Grampian Terrane (after Harris *et al.* 1994; Smith *et al.* 1999; Stephenson & Gould 1995). A = Aberdeen, BS = Boundary Slide, TF = Tay Fault, TDF = Tyndrum Fault.

This was followed by deposition of coarse grained turbidites of continental provenance and volcanic rocks that form the Southern Highland Group (e.g. Harris *et al.* 1994).

1.4.2 Age and deposition of Grampian rocks

The age of the Grampian Group and the Basement Group (*sensu* Smith *et al.* 1999) is not known, however, the deposition of the Grampian Group must post-date a *c.* 840 Ma metamorphic event identified in the Basement Group by Noble *et al.* (1996) and Highton *et al.* (1999). The age of the Dalradian Supergroup is better constrained as the Port Askaig Tillite at the base of the Argyll Group is currently correlated with the Sturtian glacial event at *c.* 720 Ma (Prave 1999; Condon & Prave 2000) and volcanic rocks near the base of the Southern Highland Group have been dated at *c.* 595±4 Ma (U-Pb zircon, Halliday *et al.* 1989) and 601±4 Ma (U-Pb zircon, Dempster *et al.* 2002). Uppermost parts of the group have been biostratigraphically dated to be of Lower Cambrian age (Cowie *et al.* 1972; Molyneux 1998). There is wide agreement that the Dalradian Supergroup represents a succession of metasedimentary and volcanic rocks that were deposited during continental extension, i.e. the break up of Rodinia which culminated in the formation of the Iapetus Ocean (e.g. Anderton 1982, 1985; Harris *et al.* 1994; Soper 1994 a; Soper & England 1995).

1.4.3 Caledonian orogenic events within the Grampian Terrane

The Grampian Orogeny is the most significant tectonometamorphic event recorded in the Grampian Terrane (e.g. Lambert & McKerrow 1976; Soper *et al.* 1999; Oliver *et al.* 2000; Oliver 2001). It was a short lived arc-accretion event associated with regional ductile deformation leading to several distinct deformational phases and Barrovian and Buchan type metamorphism between *c.* 480-465 Ma followed by rapid exhumation (Oliver *et al.* 2000; Oliver 2001). The Grampian Terrane is unaffected by the Scandian Orogeny which led to intense reworking of Grampian and earlier fabrics in the Northern Highland Terrane.

1.4.4 Structure of the Grampian Terrane

The rocks exposed in the Grampian Terrane display a complex fold and thrust pattern that is the result of regional deformation during the Grampian Orogeny (Fig. 1.8; e.g. Johnson 1991). The number of deformation phases recognized throughout the terrane

Fig. 1.8 Block diagram of major structures in the Grampian Terrane (Stephenson & Gould 1995, Fig. 19). Note that the Central Highland Migmatite Complex is now referred to as the Glen Banchor and Dava successions after Smith *et al.* (1999).

varies but in most areas the structural development has traditionally be explained in four major episodes of deformation (Stephenson & Gould 1995 and references therein). Early NW-directed thrusting (D1) led to the formation major thrust nappes and initiated large-scale folds such as the Tay Nappe. Continued deformation resulted in the progressive flattening of the early structures during D2 and D3 (e.g. Stephenson & Gould 1995) and the main deformation (D3) was associated with peak Barrovian metamorphism and the emplacement of syn-tectonic plutons (e.g. Johnson 1991). Later underthrusting of a volcanic arc and Midland Valley basement along the Highland Boundary Fault (D4) led to the development of southeast verging structures (e.g. Johnson 1991). A block diagram illustrating the general structure is shown in figure 1.8.

1.4.5 Caledonian plutonism in the Grampian Terrane

Several suites of plutonic rocks were intruded into the Dalradian rocks of the northeastern Grampians during the late stages of the Grampian Orogeny (e.g. Pankhurst & Sutherland 1982; Brown 1991). The gabbros of Aberdeenshire were emplaced along major N-S and E-W trending crustal shear zones such as the Portsoy shear zone during Grampian D3 deformation (Fig. 1.9; e.g. Brown 1991). The syn-tectonic gabbros are dated at 468 ± 8 Ma (U-Pb zircon, Rogers *et al.* 1994) and 470 ± 9 Ma (Dempster *et al.* 2002). A group of associated granites post-dates the gabroic suite but still records D3 deformation (Kneller & Leslie 1984; Harrison 1987). U-Pb monazite cooling ages for the Aberdeen and Strichen granites of 470 ± 1 Ma (Kneller & Aftalion 1987) and 476 ± 5 (Pidgeon & Aftalion 1978) respectively are thought to date the development of the D3-related solid-state fabrics within these granites. A second suite of granites is spatially associated with the gabbros in the northeastern Grampian Mountains but post-dates the D3 deformation. An Ordovician Rb-Sr whole rock isochron of 453 ± 3 Ma was obtained from the Kennethmont intrusion of this suite by Pankhurst (1974) which is supported by a U-Pb zircon evaporation age of 458 ± 1 Ma quoted by Oliver (2001). Similar granites crop out in the northwestern Grampians but are as yet imprecisely dated (e.g. Ardlach Granite, Moy Granite, see Fig.1.9). Whilst the elemental and isotopic chemistry of the gabbros is compatible with their generation in the roots of a calc-alkaline arc (e.g. Pankhurst 1970, Pankhurst & Sutherland 1982; Thompson 1985) the associated granites clearly show crustal components within their isotopic array (e.g. Pankhurst 1974; Stephens 1988; Haughton *et al.* 1990; Stephenson & Gould 1995).

The Newer Granites (Read 1961) exposed in the Grampian Terrane are of middle Silurian to early Devonian age (e.g. Rogers & Dunning 1991) and contemporaneous igneous and volcanic activity is evident at Glen Coe and Ben Nevis (e.g. Thirlwall 1988). The Newer Granite plutons are aligned in gross NE-trending linear arrays along major strike-slip faults or lineaments that formed during the terminal stages of the Caledonian Orogeny (e.g. Soper 1986; Leake 1990a; Jacques & Reavy 1994). There is a clear temporal and spatial relationship between strike-slip faulting and pluton emplacement (e.g. Watson 1984; Leake 1990 a & b; Hutton & Reavy 1992; Jacques & Reavy 1994). Jacques & Reavy (1994) suggested that most of the Newer Granites are sited at intersections of shear zones and lineaments that may project down into the lower crust (Fettes *et al.* 1986). They further argued that these structures facilitated ascent of magma as a series of steep sheets in transtensional zones that developed in response to crustal scale block rotations at these intersections.

1.5 The Newer Granites

1.5.1 Magma generation

The calc-alkaline nature of most granitoids belonging to the Newer Granite suite and in particular the chemical characteristics of their Devonian volcanic counterparts (e.g. the Glen Coe and Lorne Lavas) are most readily explained if the lavas and granitoids were generated in a subduction-related volcanic arc above a northwesterly dipping subduction zone as first proposed by Dewey (1971), and endorsed by Brown (1979), Van Breeman & Bluck (1981) and Thirlwall (1981, 1982, 1983, 1988). This interpretation clearly hinges on the timing of continental collision and the consequent cessation of active subduction (e.g. Watson 1984; Soper 1986). However, Thirlwall (1988) argued that the nature and timing of plutonism north of the Southern Uplands Fault is compatible with active subduction whereas calc-alkaline plutons to its south are too close to the suture to be explained by this mechanism. Von Blankenburg & Davies (1995), in a study from the Alps, proposed that although once active subduction had ceased slab break-off could provide a heat influx capable of generating syn-tectonic collisional magmatism, and recently Atherton (1999) and Atherton & Ghani (2002) suggested that this may be applicable to generation of the Newer Granites. However, elemental and isotopic signatures clearly identify crustally-derived granites within the suite which are not

genetically linked to subduction (Stephens & Halliday 1984). Models for generating these types of melts in mountain belts involve syn-metamorphic melting during crustal thickening, decompression melting during uplift and erosion (e.g. England & Thompson 1986; Pitcher 1987) and post-collisional mantle delamination. Clearly, the variety of geochemical signatures present in the Newer Granite suite (Stephens & Halliday 1984) suggests that more than one magma generating process is responsible for the generation of the suite and the relative contributions have to be assessed carefully.

1.5.2 Geochemistry of the Newer Granites

Based on elemental and isotopic data Stephens & Halliday (1984) divided the late Caledonian granites of the Northern Highland and Grampian terranes into the Cairngorm and Argyll suites which are separated by the Mid Grampian Line (Halliday 1984, Fig. 1.10). This classification was re-iterated by Tarney & Jones (1994) who included the Northern Highland plutons in the Argyll suite and renamed both suites as the West Highland and East Highland granites (aka Cairngorm suite) (Fig. 1.10). Subsequently, further subdivisions were proposed by Stephenson & Gould (1995) and Highton (1999). Geochemically, the East Highland suite is characterised by low Ba, Sr, Ti and P with relatively high levels of U, Th, and Rb (leading to low K/Rb), and moderately high HREE and Y relative to Ti (Tarney & Jones 1994). Further, its initial εNd is more radiogenic than the West Highland suite (Halliday *et al.* 1985) and its overall characteristics are similar to Palaeozoic I-type granites (*sensu* Chapel & White 1992) of the Lachlan Fold belt (Tarney & Jones 1994). The West Highland suite, however, is distinguished by very high Ba and Sr contents and consistently has about ten trace element characteristics, such as low U, Th and Rb (leading to high K/Rb), marked negative Nb and very low HREE and Y, that are contrasting in nature to the East Highland suite or indeed any I-, S- or A-type granite (Tarney & Jones 1994). Thompson & Fowler (1986) noticed the shoshonitic nature of the alkaline suite and suggested that these magmas could be generated from melting of subduction-related, enriched asthenospheric mantle therefore linking them to the calc-alkaline granitoids. Other authors preferred a magma source within the subcontinental lithospheric mantle (e.g. Varne 1985; Halliday *et al.* 1985; Stephens & Halliday 1984) or emphasized the dominant importance of intracrustal recycling for the granitoid generation as supported by the presence of inherited zircons (e.g. Frost & O'Nions 1985; Harmon *et al.* 1984). However, Fowler (1988b, 1992) and

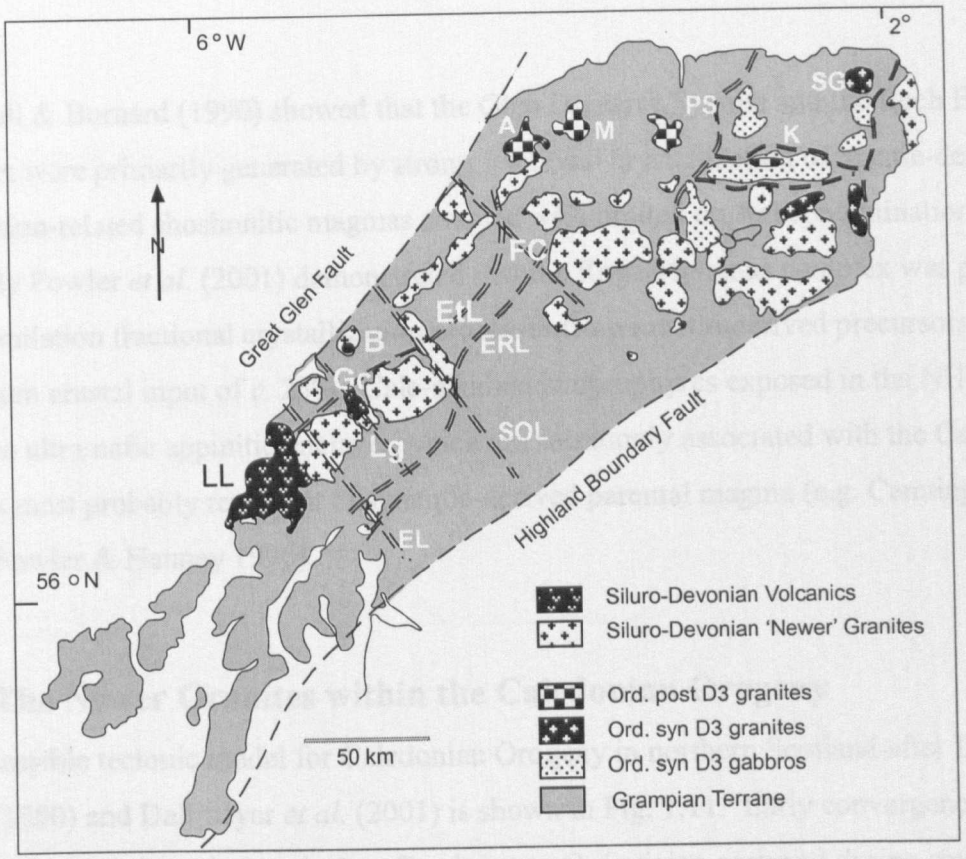

Fig. 1.9 Caledonian igneous complexes and crustal lineaments in the Grampian Terrane (compiled from Harris 1985; Thirlwall 1988; Rogers & Dunning 1991; Jacques & Reavy 1994; Smith *et al.* 1999; Oliver 2001). EtL= Etive Lagan Lineament, LCR= Cruachan Lineament, Lg= Glencoe Line, SOL= Strath Ossian Lineament, FC= Foyers Cairngorm Lineament, PS= Portsoy Shear Zone, Gc= Glen Coe igneous complex, LL = Lorne Lavas, B= Ben Nevis igneous complex, A= Ardlach Granite, M= Moy Granite, K= Kennethmont Granite, Ab= Aberdeen Granite, SG= Strichen Granite.

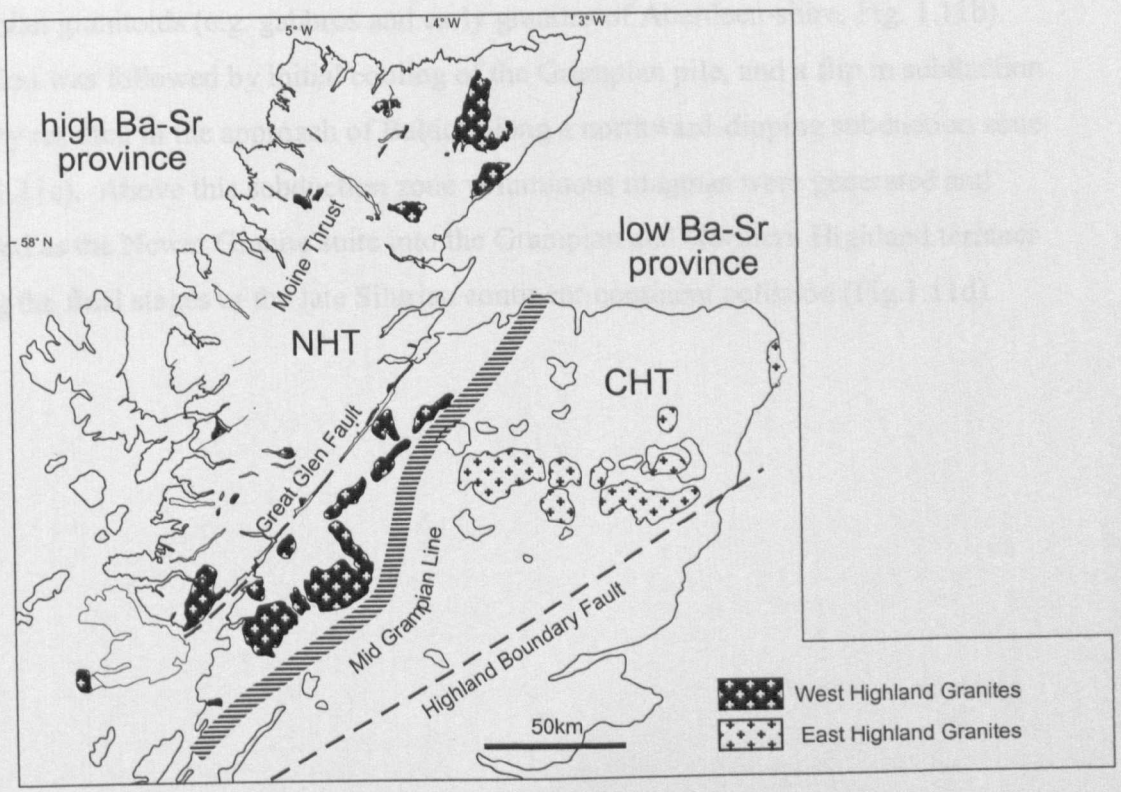

Fig. 1.10 Currently accepted geochemical classification of the late Caledonian granitoids after Stephens & Halliday (1984); Tarney & Jones (1994), Stephenson & Gould (1995) and Highton (1999).

Thirlwall & Burnard (1990) showed that the Glen Dessarry Syenite and the Loch Borralan complex were primarily generated by strong fractional crystallization of mantle-derived, subduction-related shoshonitic magmas coupled with limited crustal contamination. Recently Fowler *et al.* (2001) demonstrated that the Rogart igneous complex was produced by assimilation fractional crystallization processes from mantle-derived precursors with a maximum crustal input of *c.* 25%. Calc-alkaline lamprophyres exposed in the NHT and mafic to ultramafic appinitic enclaves which are commonly associated with the Caledonian plutons most probably represent this mantle-derived parental magma (e.g. Canning *et al.* 1996; Fowler & Henney 1996).

1.6 The Newer Granites within the Caledonian Orogeny

A possible tectonic model for Caledonian Orogeny in northern Scotland after Dewey & Ryan (1990) and Dallmeyer *et al.* (2001) is shown in Fig. 1.11. Early convergence of Laurentia and Baltica during the late Cambrian to Ordovician occurred during southward-directed subduction underneath the Midland Valley arc (Fig. 1.11a). Arc-continent collision during the early Ordovician Grampian event lead to widespread ductile deformation and metamorphism in the Grampian and Northern Highland terranes, the obduction of the Highland Border Ophiolite and the intrusion of the early syn-tectonic Grampian granitoids (e.g. gabbros and early granites of Aberdeen-shire, Fig. 1.11b). Collision was followed by initial cooling of the Grampian pile, and a flip in subduction polarity resulted in the approach of Baltica along a northward-dipping subduction zone (Fig. 1.11c). Above this subduction zone voluminous magmas were generated and intruded as the Newer Granite suite into the Grampian and Northern Highland terranes during the final stages of the late Silurian continent-continent collision (Fig.1.11d).

Fig. 1.11 Possible tectonic model for the Caledonian Orogeny in Scotland based within the Laurentia-Baltica collision zone (modified after Dewey & Ryan 1990; Dallmeyer et al. 2001). a) Convergence of Laurentia and Baltica during S-ward directed subduction underneath an island arc (e.g. Midland Valley arc= MVA). b) Grampian arc-continent collision leading to widespread ductile deformation and metamorphism in the Grampian (GT) and Northern Highland terranes (NHT), to the obduction of the Highland Border Complex (HBC), and a flip in subduction polarity. c) Continuous subduction underneath the island arc, initial cooling of the Grampian metamorphic pile, and formation of intraoceanic accretionary prisms. d) Scandian continent-continent collision leading to final amalgamation, renewed ductile deformation, nappe stacking and metamorphism in the NHT and ophiolite obduction and nappe stacking in Scandinavia. Final juxtaposition of terranes occured along major sinistral strike-slip faults. Also indicated is the emplacement of the Newer Granites associated with crustal-scale ductile thrusts (MT= Moine Thrust, NT= Naver Thrust), shear zones (dashes) and strike-slip faults (GGF= Great Glen Fault). Note that throughout a) to c) the GT and the NHT form lateral equivalents which have only been juxtaposed in d).

1.7 Aims of this study – Newer Granites of the Northern Highland Terrane

1.7.1 Pluton emplacement

In the northern Grampian Terrane the emplacement of the majority of the Newer Granites is thought to have been controlled by strike-slip movements along important lineaments (Jacques & Reavy 1994). Clearly, this emplacement mechanism was also important in Western Inverness-shire and has been widely used to calibrate deformation along major strike-slip faults in the Northern Highland Terrane (e.g. Hutton & McErlean 1991; Stewart *et al.* 2001). However, in Sutherland Scandian nappe stacking was contemporaneous with renewed thrusting, regional D2 deformation and the emplacement of granitic sheets (Dallmeyer *et al.* 2001; Kinny *et al.* in press). The Rogart and Strath Halladale granites carry pervasive textures (Soper 1963; McCourt 1980) which have prior to this study not been investigated in the light of Scandian-related fabric development and thrust sheet development in Sutherland. Understanding the emplacement mechanism and the structural setting of these plutons with respect to regional deformation events is hence critical for calibrating reported Scandian deformation events above and below the Naver Thrust. The Helmsdale pluton has not been reported to carry pervasive deformation textures. However, it is located next to an important lineament which is thought to have been active prior to the Mesozoic (Stewart *et al.* 1997, 1999) and as such might be comparable in its emplacement setting to the Newer Granites of the Grampian Terrane.

1.7.2 Geochemistry

Geochemically, the syenitic and granitic plutons of the Northern Highland Terrane form part of the definitive high Ba-Sr class of Tarney & Jones (1994) and the Rogart pluton has lately been confirmed to represent the first granitic member of this class in Sutherland (Fowler *et al.* 2001). Based on previous descriptions, the Strath Halladale and Helmsdale granites (e.g. Storey & Lintern 1981) are most likely part of this suite, too, however their magmatic evolution has not been investigated and discussed with respect to their possible subduction-related genesis and the relevance of contributing sources is also undetermined. Further, the Caledonian granitoids display a regional isotopic diversity which is evident by comparison between the Glen Dessarry Syenite (Fowler 1992), the Borralan Syenites

(Thirlwall & Burnard 1990), the Ach'Uaine Hybrids (Fowler & Henney 1996) and the Rogart granite (Fowler *et al.* 2001). This variation is thought to be a function of the Caledonian subduction system (Fowler *et al.* 2001), however a comprehensive regional elemental and isotopic study to disentangle the complexities of this variation has not been attempted prior to this study.

1.7.3 Specific targets

- To study, describe and present the field relationships, regional tectonic structures and fabrics of the Rogart, Strath Halladale and Helmsdale granites and their host rocks.
- To define paths of down-temperature fabric development in the granites and understand the true nature of the pluton fabric (emplacement related vs. deformation related)
- To develop emplacement models for the plutons that satisfy observed regional and microstructural fabric patterns.
- To critically assess the tectonic status of the pluton fabric (pre, syn, post tectonic) with respect to regional deformation.
- To investigate in detail the petrogenesis of the Strath Halladale and Helmsdale granites using whole rock major, trace element and isotope analysis.
- To define the extend of the high Ba-Sr granitoids in the Northern Highland Terrane by investigating the geochemistry of six previously less well studied or neglected Newer Granites.
- To define and explain the spatial and temporal variations observed in the elemental and isotopic record of the Northern Highland high Ba-Sr granitoids using new and published whole rock major element, trace element and isotopic data.
- To integrate the above with newly derived isotopic age data (produced in association with this study) to test currently accepted/proposed tectonomagmatic models for the Scottish Caledonides.

Chapter 2

Approach and methodology

2 Approach and methodology

2.1 Introduction

Granite intrusions that have well-defined structural relationships with their hosts are important because they can be dated isotopically and thus help to place absolute constraints on specific events within a period of regional tectonism (e.g. Samson & D'Lemos 1999). Their geochemistry may also detail fundamental melt evolution processes operating within a specific tectonic environment (e.g. Thirlwall & Burnard 1990; Keay *et al.* 1997). If, therefore, the tectonomagmatic history of a particular piece of crust is to be investigated, three critical issues have to be addressed. In order to establish the significance of isotopic age data, the style of pluton emplacement must be detailed (1) and the fabric development in the pluton must be related to the timing of deformation, fabric development and metamorphism in the country rocks (2). Further, the petrogenesis of individual plutons needs to be investigated (3), in order to evaluate melt generation, contributing sources and melt evolution until final crystallization and emplacement. Also, temporal and spatial variations in the elemental and isotope systematics throughout the plutonic suite need to be investigated as these may provide information on the regional composition and structure of the unexposed lower crust and mantle.

2.2 Structural approach

2.2.1 Granite emplacement mechanisms

Geological observations around granite plutons will provide information about final emplacement, regional deformation and pluton assembly, but generally do not elucidate magma generation, segregation and ascend mechanisms unless contrasting crustal sections are exposed (Clemens & Mawer 1992; Strachan *et al.* 2001). Consequently, a wide variety of magma transport mechanisms have been competing in the literature, including diapirism and stoping (e.g. Bateman 1984; Ramsay 1989; Paterson & Vernon 1995; Miller & Paterson 1999), diking and conduit-fed in-situ ballooning (e.g. Clemens & Mawer 1992; Petford *et al.* 1993; Grocott *et al.* 1999; Rubin 1995; Petford *et al.* 2000; Molyneux & Hutton 2000) and syn-tectonic pervasive flow of of small batches of magma enhanced by actively deforming crust (Brown 1994; Collins & Sawyer 1996; Brown & Solar 1998b;

Weinberg & Searle 1999). Whereas there is considerable disagreement regarding these magma transfer processes, numerous case studies have successfully investigated and elucidated the emplacement of granites in contractional (e.g. Ingram & Hutton 1994; Brown & Solar 1998a; Solar *et al.* 1998; Musumeci 1999; Miller & Paterson 2001), strike-slip (e.g. Hutton 1982, 1988; Glazner 1991; McCaffrey 1992; D'Lemos *et al.* 1992, 1997; Tikoff & Tessier 1992; Tommasi *et al.* 1994; Stewart *et al.* 2001) and extensional (e.g. Hutton *et al.* 1990; Hodges *et al.* 1992; Grocott *et al.* 1994; Searle 1999; Strachan *et al.* 2001) tectonic settings. Identifying pluton emplacement mechanisms is commonly based on field mapping, microstructural analysis (e.g. Miller & Paterson 1994; Tribe & D'Lemos 1996; Paterson *et al.* 1998), interpretation of mineralogical and geochemical zoning (e.g. Paterson & Vernon 1995; Castro & Fernández 1998; Molyneux & Hutton 2000), analogue and numerical models (e.g. Marsh 1982; Roman-Berdiel *et al.* 1997; Cruden 1988; Weinberg & Podlachikov 1994) and geophysical data (e.g. De Saint Blankquat & Tikoff 1997; Ferré *et al.* 1997; Gleizes *et al.* 1998).

2.2.2 Identifying syn-tectonic plutons

Identifying whether a pluton was emplaced prior to, during, or after a particular tectonic episode mainly centres around the understanding of the fabrics developed in the pluton and its host rocks (Paterson *et al.* 1991). Syn-tectonic intrusions have the greatest potential to unravel deformational histories (e.g. Paterson & Tobisch 1988; Paterson *et al.* 1989a, 1998; Vernon *et al.* 1989; Miller & Paterson 1994; Karlstrom & Williams 1995; Tribe & D'Lemos 1996; McCaffrey *et al.* 1999). The structures observed in and around plutons are the result of the superposition of emplacement-related deformation and regional deformation (Paterson *et al.* 1991). The development of microstructures and pervasive fabrics depends on three main variables, a) the rates at which emplacement-related and regional scale tectonic processes operate, b) the mineralogy of the pluton, and c) the rate at which the pluton cools (e.g. Paterson *et al.* 1991; Paterson & Tobisch 1992; Karlstrom & Williams 1995; Tribe & D'Lemos 1996).

The available estimates for the duration of pluton-related and orogen-related processes are summarised in table 2.1. Overall, the data suggest that pluton-related processes occur over comparably short time intervals of *c.* 1 Ma whereas regional deformation takes place over tens of millions of years (e.g. Paterson & Tobisch 1992; Karlstrom & Williams 1995; Tribe & D'Lemos 1996). Therefore, isotopic dating of syn-tectonic granites holds the key

Table 2.1 Average rates of plutonic, metamorphic and orogenic processes

Process		timescale / rate	References
Long term magma supply		10^{-2} km^3/a	1
Short term peak magma supply		350 km^3/a	1, 2
Diapiric pluton ascent rate		1 to 3 m/a	1, 2
Diapiric rise		10^5 to 10^9 a	10
Dyke/conduit flow		10^{-1} to 10^2 a	10
Pervasive flow		$\leq 10^6$ a	10
Emplacement of sheeted granitic complexes		10^3 to 10^5 a	7
Pluton emplacement and crystallisation in active arc regions		< 1Ma	9
General (dike/conduit-fed) pluton emplacement		10^2 to 10^4 a	10
Post-emplacement pluton cooling to ambient host rock temperatures at low heat flow, or high crustal levels		10^5 to 1 Ma	1, 2, 7
Post-emplacement pluton cooling to/ at ambient host rock temperatures at upper greenschist- to lower amphibolite facies		5 to 15 Ma	9
Crystal growth rate in magmas		3 x 10^{-4} cm/a	1
Lithospheric plate collision		1 Ma to 100 Ma	7
Collision of arcs, seamounts, or oceanic plateaus		1 Ma to 10 Ma	8
Orogenic strain rates		10^{-13}/s to 10^{-14}/s	1, 5
Average fault displacements (brittle?)		3 cm/a	1
Regional cleavage development at orogenic strain rates		~ 1 Ma	1, 7
Growth rates of metamorphic porphyroblasts	Regional	10^{-5} cm/a	1, 3, 4
	Aureole	10^{-2} cm/a	1, 3, 4
Prograde path of metamorphism		1 to 10 Ma	6
Duration of regional metamorphism at high heat flow		> 10 Ma	9
Retrograde path of metamorphism, slow cooling		100 Ma	6

References: 1) Paterson & Tobisch 1992; 2) Paterson *et al.* 1991; 3)Bell & Cuff 1989; 4) Williams 1994; 5) Pfiffner & Ramsay 1982; 6) Hodges *et al.* 1994; 7) Karlstrom & Williams 1995; 8) Hamilton 1988; 9) Samson & D'Lemos 1999, 10) Petford *et al.* 2000.

Note: 3,4,5,6 and 8 are all quoted in 7.

to identifying (and separating) orogenic (and regional tectonic) events provided the errors on the isotopic dates are considerably smaller than the estimates for the duration of orogenic processes. However, because of the differences between the rates of pluton emplacement and regional deformation (two orders of magnitude), very accurately and precisely dated syn-tectonic plutons may only mark important points within a progressive regional tectonic episode (Samson & D'Lemos 1999). Constraints on the duration of regional tectonic events and the timing of kinematic changes throughout them can be gained by dating successively intruded syn-tectonic plutons (Tribe & D'Lemos 1996; Miller *et al.* 2001).

As soon as a magma contains crystals and is placed under directed stress, a fabric (defined by the shape, orientation and spatial distribution of minerals) forms and evolves through crystallization and cooling (De Saint Blanquat & Tikoff 1997) often forming a foliation and/or lineation. The fabric within a syn-tectonic pluton will record kinematic information related to both emplacement induced and tectonically induced strain (e.g. Hutton 1988, Paterson & Tobisch 1988; Paterson *et al.* 1989, 1991; Vernon *et al.* 1989; Miller & Paterson 1994; De Saint Blanquat & Tikoff 1997). The type of kinematic information a fabric records mainly depends upon the pluton petrography, the rate of cooling and the regional strain rate during emplacement (e.g. Bouchez *et al.* 1992; Miller & Paterson 1994; Tribe & D'Lemos 1996). Ideally, a truly syn-tectonic pluton will show a continuous history of fabrics developed from magmatic flow through high-temperature solid-state to low-temperature solid-state deformation (Paterson & Tobisch 1988; Paterson *et al.* 1989, 1991, 1998; Vernon *et al.* 1989). However, Miller & Paterson (1994) and Tribe & D'Lemos (1996) note that this is rarely the case and that gaps often exist within the down-temperature fabric history. The fabric patterns displayed by any pluton are therefore often complex and sometimes ambiguous, leading to misinterpretations regarding the timing of pluton emplacement and fabric development (see reviews by Paterson *et al.* 1991, 1998; Karlstrom & Williams 1995).

2.2.3 Timing of pluton emplacement

Much debate in the literature has focused on which structural criteria can be used to identify the pre, syn, or post-tectonic nature of any pluton with respect to regional fabrics and/or metamorphic assemblages in its host rock (Paterson & Tobisch 1988; Paterson *et al.* 1989,1991; Vernon *et al.* 1989; Miller & Paterson 1994; Ingram & Hutton 1994; Karlstrom

& Williams 1995; Tribe & D'Lemos 1996; De Saint Blanquat & Tikoff 1997; Schofield & D'Lemos 1998; McCaffrey *et al.* 1999; Paterson & Schmid 1999). Although pertinent structural features are numerous (table 2.2), the basic approach to delineating the tectonic status of any pluton, outlined by Paterson *et al.* (1989 and 1991, p. 695), has remained more or less unchanged: (1) to determine the nature of the structures and fabrics developed within the pluton, (2) to relate fabrics and kinematic markers developed within the pluton to structural and metamorphic features in the wall rock, (3) to determine how emplacement mechanisms have caused or affected these structures, (4) to examine the relationships between wall rock structures and porphyroblasts developed in the metamorphic aureole, and (5) to isotopically date both igneous and metamorphic minerals. Criteria commonly used to establish the tectonic status of any given intrusion are summarized in table 2.2. It is clear that the applicability of characteristic features to specific cases has to be carefully investigated as most of them depend on pluton size, level of emplacement in the crust, strain rates, ambient temperature of the host rocks, and contrasting rates of granite emplacement, cooling and regional fabric (cleavage) development (e.g. Paterson *et al.* 1991; Paterson & Tobisch 1992; Karlstrom & Williams 1995; Miller & Paterson 1994; Tribe & D'Lemos 1996).

2.2.4 Timing of fabric development

As outlined in section 2.2, the type of fabric that develops within a pluton during and after emplacement critically depends on mineralogy, mineral to melt ratio, strain rate and cooling rate. One of the main aims of emplacement studies is to establish the relative time during which the pluton fabric developed within the crystallization and deformation sequence. Further, the temperature range during which the fabric was developed characterises the nature of the fabric (i.e. magmatic-state or solid-state) and thus places constraints on the significance of isotopic age data (crystallization ages of solid-state deformed plutons only provide a minimum age for the deformation of the surrounding host rocks). It is therefore of particular importance to be able to assign microstructures to rheological and temperature intervals encountered/encompassed during progressive pluton cooling, thus to establish the precise record of down-temperature deformation. As a first-order division, the temperature interval between a (liquid) crystallizing melt and a solid igneous body may be divided rheologically into an interval of magmatic flow and solid-state deformation (e.g. Paterson *et al.* 1989, 1991).

Table 2.2: Commonly used criteria for the identification of 'tectonic' pluton status

Criteria	References
Pre-tectonic plutons	
Low to moderate temperature solid-state foliations cross-cut pluton boundaries	1, 2
Pluton is wrapped by regional cleavage and possesses strain-shadows	1
Regional cleavage cuts emplacement-related structures in the host rocks	1
Heterogeneous strain pattern to foliation within the pluton	1
No alignment of igneous minerals	2
Pluton fabric defined by metamorphic minerals	2
Syn-tectonic plutons	
Concordance of pluton shape and regional structure	1, 2, 3
Continuous record of down-temperature fabric development	1, 2, 3
Parallelism and continuity of magmatic and high T solid-state pluton fabrics with regionally developed foliations and lineations	1, 2, 3
Gradation between pluton related strain fields and tectonic fields with a maximum at the pluton / wall rock interface	2
Presence of cleavage / foliation triple points near the pluton ends	2
Magmatic shear criteria consistent with regional kinematics	1
Syn-tectonic porphyroblasts in the contact aureole	1
Similar age of igneous minerals and porphyroblasts in the aureole	2
Similar U-Pb crystallisation and $^{40}Ar/^{39}Ar$ cooling ages	1
Post-tectonic plutons	
Pluton cuts regionally developed fabrics	1
Pluton emplacement structures defelect regionally developed fabrics	1
Intense flattening strains in and around the pluton, decreasing within a few km of the pluton / wall rock boundary	2
Irregular or rounded shape of plutons	1
Forceful post-tectonic intrusions	
Internal, possibly oblique, heterogeneous foliation defined by flattened enclaves	2
Syn- to post-kinematic growth of porphyroblasts in the aureole	2
Permitted post-tectonic intrusions	
No foliations or evidence for significant deformation	2
No deformation in the wall rocks related to the pluton	2
Only post-kinematic growth of porphyroblasts in the aureole	2

References: 1) Paterson *et al.* 1991; 2) Paterson & Tobisch 1988; 3) Paterson *et al.* 1989, 1998

Whereas solid-state fabrics can be described in terms of the processes by which they form and the particular temperature (range) at which they develop (e.g. Passchier & Trouw 1996; Tribe & D'Lemos 1996), there are different approaches to rheological classification of partly-molten systems (e.g. Hutton 1988; Ingram & Hutton 1994; Tribe & D'Lemos 1996; Vigneresse & Tikoff 1999). This is because "solid-state" crystal-plastic deformation can occur in *partially* crystallized magma. In this study the approach and classification of Tribe & D'Lemos (1996) has been adopted. It is based on rheological criteria and emphasises the importance of the transition from a melt-dominated system with suspended solids to a solid with intervening melt. The point at which the transition of this rheological behaviour occurs and the magma viscosity rapidly increases is termed the rheological critical melt percentage (RCMP) (e.g. Arzi 1978, Tribe & D'Lemos 1996; Steenken *et al.* 2000). It marks the point during pluton cooling where suspended crystals can no longer rotate freely and strain is transmitted across grain boundaries which is thought to occur at 50% to 70% crystal density (Van der Molen & Paterson 1979; Bryon *et al.* 1994; Tribe & D'Lemos 1996). The exact percentage will differ between magmas depending on a wide variety of factors including grain size and shape, pre-existing fabric development and strain rate. This approach, based on rheological divide, is useful as fabrics formed prior to the RCMP (i.e. pre-RCMP fabrics) can be distinguished in handspecimen and thin section from fabrics formed after the RCMP (i.e. post-RCMP fabrics, see Fig. 2.1). As such, this classification is more precise and robust than earlier concepts of 'magmatic vs. sub-solidus fabrics' (Paterson *et al.* 1989, 1991) and 'pre-full crystallization vs. crystal plastic strain fabrics' (Hutton 1988; Ingram & Hutton 1994), which were misleading as although solid minerals were being deformed the system was still in the magmatic state (i.e. above the petrological solidus). Recent studies have developed the concept of 'classification based on rheological divide' even further (e.g. Vigneresse & Tikoff 1999) and identified several rheological threshholds within a crystallizing magma. However, with respect to timing regional deformation this approach does not necessarily provide a more detailed constraint as analytical errors in isotopic age dating presently are too large compared to the estimates for pluton-cooling. The microstructural criteria for timing fabric development used in this study are summarised in Figure 2.1. Detailed reviews of the grain-scale processes of strain accommodation and their associated microstructures depicted in figure 2.1 (brittle fracturing, dislocation glide, dislocation climb, dynamic recrystallization) have been given by Schmid & Handy (1991) and Paschier & Trouw (1996) and their terminology is followed (but not reviewed) in this study. It is worth pointing out, however, that granites

are essentially aggregates of different minerals and hence their (down-temperature) deformation characteristics are governed by the interaction of the different rheological behaviours of the various minerals (Fig. 2.1) during strain. Further, the grain-scale deformation processes for each mineral phase and the associated microstructures indicated on Fig. 2.1 are, next to temperature, strongly dependant on strain rate and fluid content (e.g. Hirth & Tullis 1992, Passchier & Trouw 1996). Also, it should be noted that the absolute and precise calibration of microfabric development against P-T conditions, strain rates and fluid content is still far from resolved. The temperature ranges indicated on figure 2.1 that are used throughout this study should therefore only be viewed as guiding estimates.

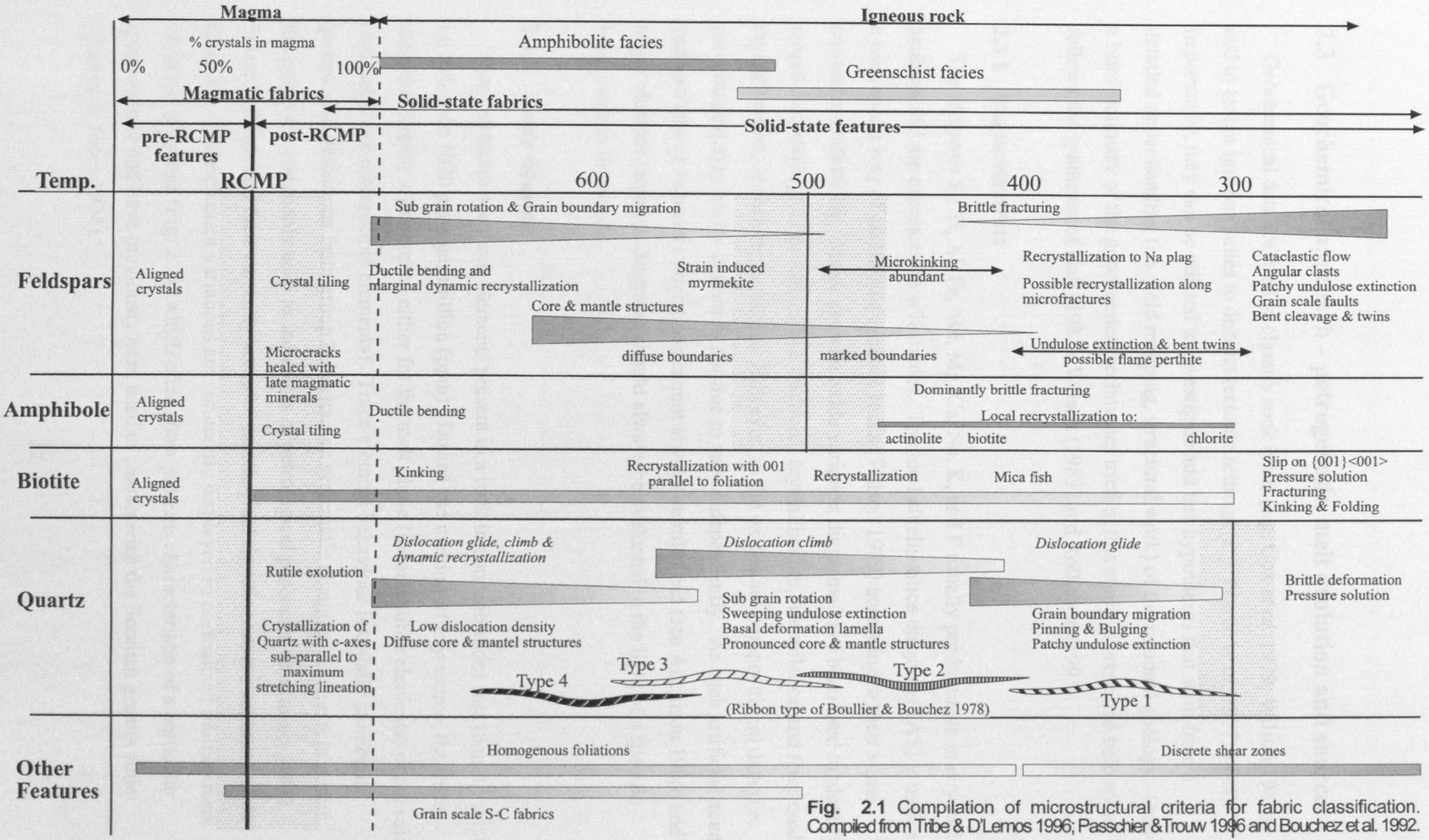

Fig. 2.1 Compilation of microstructural criteria for fabric classification. Compiled from Tribe & D'Lemos 1996; Passchier &Trouw 1996 and Bouchez et al. 1992.

2.3 Geochemical approach – petrogenesis, melt evolution and sources

Geochemical data are used to classify rock types (e.g. Cox *et al.* 1979; Wilson 1989) and to assign igneous suites to distinct tectonic settings (e.g. Pearce *et al.* 1977, 1984). Importantly, they can be utilized to investigate and test hypotheses that stem from a detailed understanding (i.e. field mapping, structural work) of the regional geology. Only a brief summary of the geochemical techniques used in this study is presented below and follows the syntheses of Hall (1987), Wilson (1989) and Rollinson (1993).

2.3.1 Major elements

The elements Si, Ti, Al, Fe, Mn, Mg, Ca, Na, K, and P usually predominate in any rock analysis and are expressed in w% oxides. The total alkalis-silica diagram (TAS) is used as a convenient way of classifying igneous rocks (Wilson 1989) according to their silica content and alkalinity. Major element oxide variation diagrams have been used to identify magmatic/petrological processes like fractional crystallization, assimilation and fractional crystallization, or melting processes. However, as the oxides are compositional data (i.e. percentages) they are by definition not free to vary independently. As such artificial trends and spurious or induced correlations cannot always be ruled out (see Aitchison 1986) and major element variation diagrams should always be evaluated in the light of a specific hypothesis to be tested.

2.3.2 Trace elements

Trace elements are those elements present in a rock in concentrations less than 0.1 wt%, i.e. less than 1000 parts per million (ppm). During the melting of any source, the trace elements display a preference either for the melt phase (incompatible elements) or the solid residual phase (compatible elements). Trace element behaviour is usually studied in groups, and deviations from group behaviour or systematic changes in behaviour within the group are commonly used as indicators of petrological processes (Rollinson 1993). Trace elements and their currently accepted petrological significance are summarized in table 2.3. Trace element variations are commonly displayed in normalized multielement variation diagrams (Fig. 2.2a) which often show patterns characteristic of a particular igneous suite and have previously been used to characterize the Scottish granite suite (Tarney & Jones 1994).

Table 2.3: Petrogenetic significance of selected major and trace elements after Wilson (1987) and Rollinson (1993)

Element	Interpretation
Ba, Rb	Substitute for K in K-feldspar, hornblende and biotite.
Sr	Substitutes for Ca in plagioclase and K in K-feldspar. Incompatible under mantle conditions.
P	Monitors apatite fractionation.
Ni, Cr	High values (e.g. Ni = 250-300ppm; Cr = 500-600 ppm) indicate derivation of parental magmas from a (peridotite) mantle source. Partition into olivine during partial melting (pm) and fractional crystallization (fc).
Sc, Cr, V	Partition into clinopyroxene during fc and pm.
V, Ti	Contemporaneous, parallel decrease indicates ilmenite or titanomagnetite fractionation (Fe-Mn oxides). Divergent behaviour indicates Ti incorporation into accessory phases.
HFSE	Generally immobile, element concentrations are controlled by source chemistry and subsequent crystal/melt evolution. HFSE ratios monitor fc and crustal contamination.
Zr/Hf	Incompatible HFSE, substitute for Ti in titanite and rutile.
Zr	Monitors zircon fractionation.
REE	Fractionate into garnet, hornblende, clinopyroxene, titanite and zircon
Eu^{2+}	Compatible in feldspar at low oxygen fugacities.
Y	Generally incompatible with similar behaviour as HREE. May fractionate into accessory zircon, titanite, or apatite.
Nb, Ta	Compatible in ilmenite, rutile and titanite.

Rare earth element (REE) behaviour during magmatic processes is very well researched and the REE are largely unaffected by subsequent weathering and hydrothermal effects (Michard 1989; Rollinson 1993). REE patterns of the Northern Highland high Ba-Sr granites are very characteristic and have been used previously to distinguish them from other intracrustal granites, to monitor depletion and enrichment (La/Yb ratios) and to identify distinct petrogenetic processes, such as plagioclase fractionation (Eu), amphibole fractionation (HREE) and fractionation of accessory phases (LREE) (e.g. Thirlwall & Burnard 1990; Fowler 1992; Fowler & Henney 1996; Fowler *et al.* 2001).

2.3.3 Isotopes

Isotope studies not only serve dating purposes (see summaries in Faure 1986, and Dickin 1995) but are also widely used as petrogenetic tracers in evaluating the evolution of magmas (Wilson 1989) or even mapping mantle reservoirs (e.g. Zindler & Hart 1986; see also review by Hofman 1997). Radiogenic isotopes of a particular element are not separated from each other during melting or crystal fractionation and thus will copy the initial isotopic composition of their source which will remain constant throughout melt evolution, provided that no contamination occurs. As crustal and mantle reservoirs have very different isotopic ratios (Fig. 2.2c), radiogenic isotopes are a powerful tool in constraining source components and contamination which undoubtedly occurs during granitoid petrogenesis (e.g. Collins 1996; Keay *et al.* 1997; Fowler *et al.* 2001). Stable isotopes, however, may become fractionated by crystal-liquid differentiation processes but these effects are small compared to the profound difference in isotopic composition between crustal and mantle reservoirs (Fig. 2.2d; Harmon *et al.* 1984). Stable isotopes, like $\delta^{18}O$, have previously been successfully used to monitor assimilation of metasedimentary components during melt evolution (e.g. Chivas *et al.* 1982; Fowler 1992). In this study, the radiogenic $^{147}Sm/^{143}Nd$ and $^{87}Rb/^{87}Sr$ isotope systems, and stable $\delta^{18}O/^{16}O$ ratios have been used to investigate granite petrogenesis in the light of parental magmas, contributing sources and contamination processes.

Fig. 2.2
a) Multielement variation diagram(PRIMA normalized) showing the contrasting patterns of intracrustal and high Ba-Sr granites (additional data from Taylor & McLennan 1985).
b) Chondrite-normalized Rare Earth Element plot showing contrasting patterns of I-, S-type granites and members of the Northern Highland high Ba-Sr suite (data from Taylor & McLennan 1985; Fowler et al. 2001).

c & d) Radiogenic and stable isotope plots showing isotopic variability of rocks occurring in the Scottish Highlands and other possible contributing sources towards Caledonian granitoid genesis (adapted from Fowler et al.2001 and Harmon et al. 1984). All initial isotopic ratios are quoted at *c.* 400 Ma. DM= depleted mantle, Lg= Lewisian granulite facies, La= Lewisian amphibolite facies, M= Moine psammites/pelites, D= Dalradian psammites/pelites, Su= Southern Uplands sediments, PS= Pelagic sediments, UC= Upper crustal (meta)sediments, C/L= cherts & limestones.

2.4 General Techniques used in this study

2.4.1 Field mapping

Fieldwork was undertaken during three major field seasons totalling 24 weeks. Lithological variation and geological structure of the three igneous complexes and their country rocks were mapped onto Ordnance Survey base maps on 1:12.500 and 1:25.000 scales.

2.4.2 Sampling and analysis

In addition to the *c.* 220 thin sections of the Strath Halladale granite and its host rocks which were provided by the BGS, a further *c.* 300 structural samples were collected for general thin section work and, in particular, fabric analysis.

Over 75 large and fresh samples were collected for geochemical purposes, carefully selected to represent the full range of rock types exposed. Samples were subsequently reduced to fine powder, in a tungsten carbide tema barrel.

Major elements were determined by ICPAES at Oxford Brookes University by fusion dissolution followed by analysis against calibrations defined with international standard rock materials (SRM's). Accuracy and precision are estimated to be better than 2-3% RSD. Rare earth elements were also analysed by ICPAES at Oxford Brookes University using natural rock standards, following cation-exchange pre-concentration. Rb, Sr, Ba, Y, Zr, Nb, V, Cr, Co, Ni, Cu, Zn, Sc, As, Mo, Hf, U & Pb were analysed by XRF at the University of Leicester. Accuracy and precision of all the trace element analysis are better than 5% RSD. Radiogenic (Nd-Sr) and stable oxygen ($\delta^{18}O/^{16}O$) isotope analysis of a subset of 26 samples was conducted at the NERC Isotope Geosciences Laboratory (NIGL) under the supervision of Mrs. D. P. F. Darbyshire, and in collaboration with Mr. P. E. Greenwood and Dr. M. B. Fowler (Oxford Brookes University) using standard dissolution and fluorination techniques followed by mass spectrometry (e.g. see Fowler *et al.* 2001 for analytical details).

Three fresh samples (each exceeding 50 kg) of granite, granodiorite and quartz diorite were collected for isotopic dating which is being carried out at NIGL by Dr. J. Evans in collaboration with Dr. R. A. Strachan (Oxford Brookes University).

Part B

Field, microstructural and geochemical analysis

Chapter 3

Structural geology, fabric development and emplacement of the Rogart Granite

3 Structural geology, fabric development and emplacement of the Rogart Granite

3.1 Introduction

The Rogart igneous complex is located in southeast Sutherland around the village of Rogart, east of Lairg between Strath Fleet and Strath Brora where it is moderately to well exposed on hilly ground over an area of *c.* 115km^2 (Fig. 3.1). It was originally surveyed by H. Miller in 1890-1894 and has been described subsequently by Read *et al.* (1925; 1926), Soper (1963, 1999) and Fowler *et al.* (2001). The igneous complex comprises a zoned quartz monzodiorite-granodiorite-granite pluton. It was emplaced into Moine metasediments of the Morar Group that are locally migmatitic adjacent to the igneous complex (Soper 1963, 1999). The main pluton is flanked by smaller quartz monzodiorite stocks and sheets and mafic to ultramafic, appinitic enclaves of the Ach'Uaine type are abundant throughout (e.g. Fowler *et al.* 2001). The Naver Thrust is traceable from Ben Klibreck in the northwest into the study area (Strachan pers. comm. 2000). In central Sutherland, the Naver Thrust juxtaposes regionally migmatitic gneisses against non-migmatitic Morar Group Moine. It is exposed in the northwest of the study area south of the Brora River, and juxtaposes banded, semi-pelitic gneisses and metatexites of the Naver Nappe against non-migmatitic psammites of the Moine Nappe. Further east, the thrust is more difficult to trace as the Morar Group psammites in the footwall contain abundant biotite-leucogranites and are strongly migmatitic. The Rogart igneous complex and its host rocks are unconformably overlain by Devonian sedimentary rocks. The igneous complex is bounded to the south by the Strath Fleet Fault.

3.2 Previous work and aims of this study

Read (1925; 1926) published the first petrographic and structural descriptions of the "Central Granodiorite" and the adjacent "Migmatite Complex". The structure, petrography and emplacement of the Rogart complex were investigated by Soper (1963) who interpreted the pluton as a granite diapir that forcefully deformed its Moine host rocks by horizontal expansion.

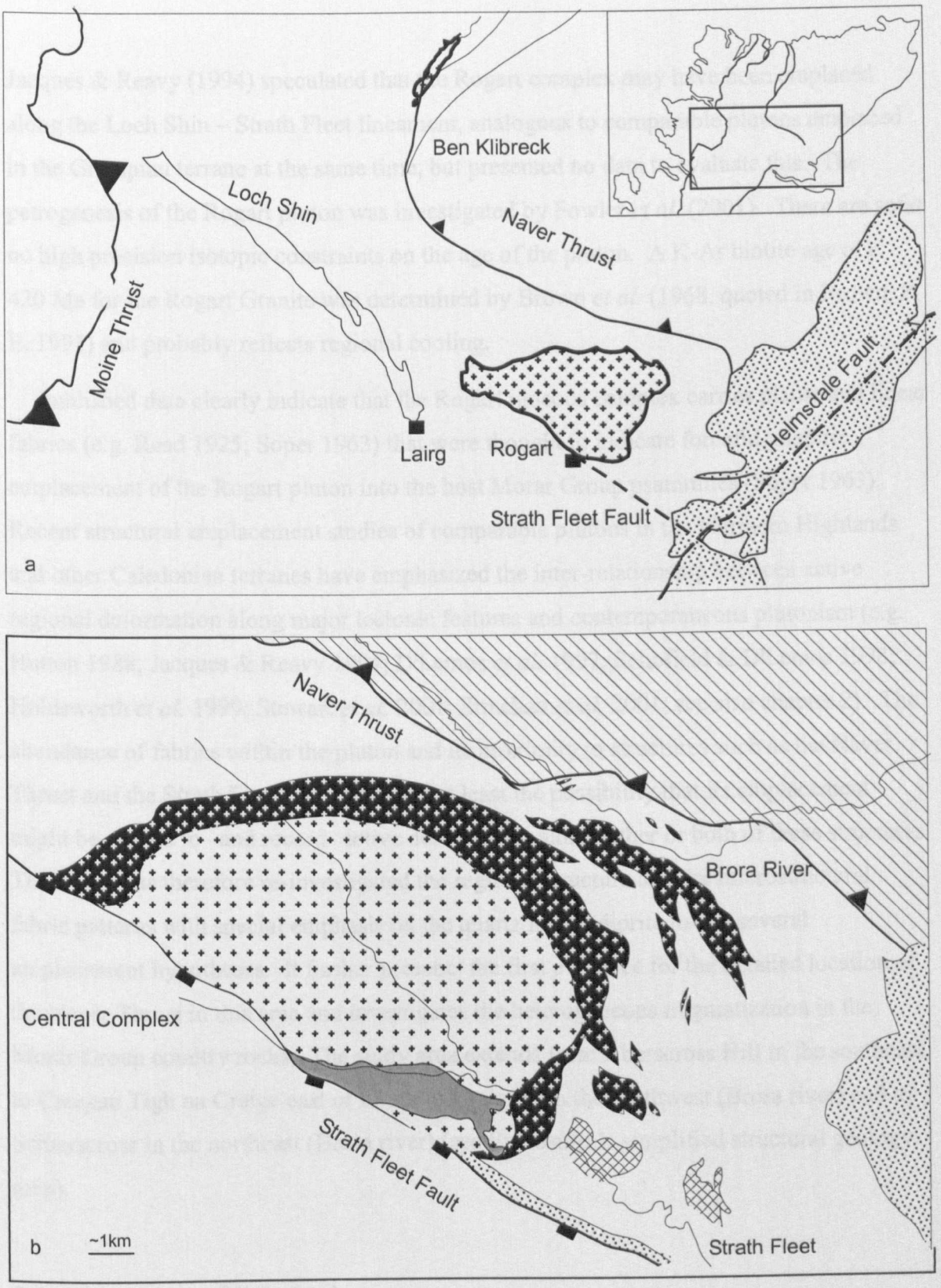

Fig. 3.1 Location map (a) and geological overview (b) of the Rogart igneous complex.

Jacques & Reavy (1994) speculated that the Rogart complex may have been emplaced along the Loch Shin – Strath Fleet lineament, analogous to comparable plutons emplaced in the Grampian terrane at the same time, but presented no data to evaluate this. The petrogenesis of the Rogart pluton was investigated by Fowler *et al.* (2001). There are sofar no high precision isotopic constraints on the age of the pluton. A K-Ar biotite age of *c.* 420 Ma for the Rogart Granite was determined by Brown *et al.* (1968, quoted in Brown, P. E. 1991) and probably reflects regional cooling.

Published data clearly indicate that the Rogart igneous complex carries planar and linear fabrics (e.g. Read 1925; Soper 1963) that were thought to indicate forceful, diapiric emplacement of the Rogart pluton into the host Morar Group psammites (Soper 1963). Recent structural emplacement studies of comparable plutons in the Northern Highlands and other Caledonian terranes have emphasized the inter-relationship between active regional deformation along major tectonic features and contemporaneous plutonism (e.g. Hutton 1988; Jacques & Reavy 1994; D'Lemos *et al.* 1997; Schofield & D'Lemos 1998; Holdsworth *et al.* 1999; Stewart *et al.* 2001; Strachan *et al.* 2001; see also chapter 2). The abundance of fabrics within the pluton and its proximity to structures such as the Naver Thrust and the Strath Fleet Fault suggests at least the possibility that its emplacement might be related to –and record- active deformation along either or both of these structures. This study has therefore re-investigated the regional structure and the microstructural fabric patterns with special emphasis on the quartz monzodiorite to test several emplacement hypotheses. It further presents the first evidence for the detailed location of the Naver Thrust in this area and investigates the heterogeneous migmatization in the Morar Group country rocks. The study area extends from Aberscross Hill in the southeast to Creagan Tigh na Creige east of Lairg, to Craigton in the northwest (Brora river) and to Sciberscross in the northeast (Brora river) (see Enclosure 1: simplified structural geology map).

3.3 Overview of lithologies

The Moine rocks exposed in the study area are the Naver gneisses above the Naver Thrust and the Morar Group psammites below it. The latter are host to the Rogart igneous complex and in its vicinity are locally migmatitic (e.g. Soper 1963, 1999; Fowler *et al.* 2001). The Rogart igneous complex comprises a main, composite quartz monzodiorite-

granodiorite-granite pluton (in the following referred to as 'central complex') that is flanked on the northern and eastern side by several smaller outcrops of quartz monzodiorite and two leucogranite-dominated igneous complexes.

3.3.1 Naver Nappe lithologies

The rocks above the Naver Thrust comprise a variety of fine to medium grained, variably banded and foliated gneisses of predominantly metasedimentary origin that are traditionally referred to as Naver gneisses (e.g. Holdsworth *et al.* 1994) (Fig. 3.2). In the study area, the Naver gneisses are commonly migmatitic and form a diverse sequence of metatexites and diatexites (*sensu* Brown 1973), semi-pelitic gneisses and subordinate othogneisses. Mineralogies of the variably migmatitic, semi-pelitic rocks are simple and consistent over the spectrum of textures observed and comprise biotite + quartz + plagioclase + K-feldspar ± muscovite ± garnet.

In the northeastern part of the study area, fine grained, semi-pelitic to psammitic lithologies of gneissic appearance are dominant. In hand specimen they show a strong, laterally consistent, thin and regularly alternating compositional layering of biotite-rich and quartzofeldspathic layers (Fig. 3.2 a). In thin section, the quartzofeldspathic layers show abundant igneous plagioclase and K-feldspar which suggests that the rocks were partially molten. The feldspars within these leucosomes form small, subhedral grains and are often sericitised and altered to secondary muscovite. Fine grained recrystallized quartz shows lobate grain boundaries and rare garnets are small and of an- to subhedral habit. The melanosomes predominantly contain coarse grained, brown biotite that is occasionally retrogressed to chlorite.

Towards the northwest and along the base of the nappe, the gneisses are slightly coarser grained, more pelitic and show more evidence for segregation melting (Fig 3.2 b, d & e). The migmatites range from regularly layered, stromatic types showing foliation-parallel segregation melting to disrupted, diatexitic lithologies. The degree of partial melting is variable and leucosomes may proportionally increase and coalesce to form distinctly white-coloured, leucocratic granite sheets. Locally, these granite sheets display intrusive and cross-cutting relationships with the migmatitic layering and lead to the formation of schlieric diatexites. Within the more homogenous, regularly banded varieties, *c.* 2mm thick bands of melanocratic biotite-rich layers alternate with 2mm thick, leucocratic bands of essentially granitic composition (microcline + quartz + plagioclase).

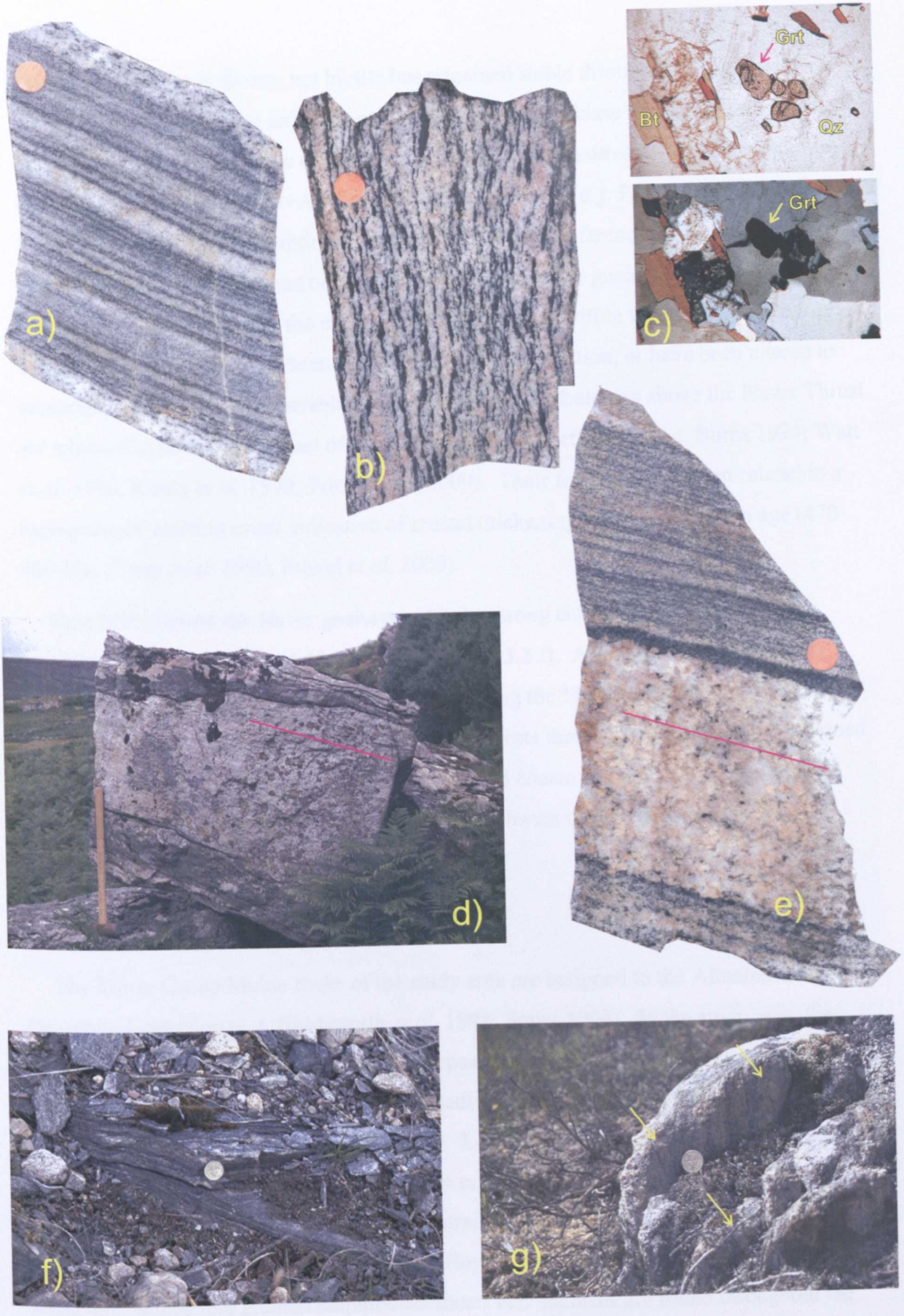

Fig 3.2 Naver Nappe lithologies. a) Banded grey gneisses . b) Stromatic metatexite with slightly disrupted migmatitic layering. c) Thin section photographs showing small anhedral garnets in leucosomes (ppl & xpl). d & e) Subconcordant biotite leucogranite sheets with foliation co-planar to the migmatitic layering. f) Amphibole orthogneiss at NC 7657-0969. g) Augen granite gneiss showing a solid-state fabric at Craig Dailfuessaig. Orange circle on handspecimen is 5mm across. Thin section field of view is *c.* 2mm across.

Primary muscovite is absent, but biotite has remained stable throughout melting and occasionally small, sub- to anhedral garnets with rare plagioclase rims are present in the leucosome. This is indicative of melt generation at high pressures (8-10kbar) by biotite dehydration according to: Bt+Als+Pl+Qtz = Grt+Kfs+melt (e.g. Patino Douce & Beard 1995; Miller *et al.* 1997; Whittington & Treloar 2002 and references therein). Sillimanite and fibrolite are of widespread occurrence in the semi-pelitic gneisses of the Naver Nappe (e.g. Burns 1994), however, the absence of alumosilicates within the metatexites at Rogart suggests that they may have been consumed during the reaction, or have been altered to secondary muscovite. Comparable variably migmatitic lithologies above the Naver Thrust are exposed at Kirtomy and east of Strath Naver on the north coast (e.g. Burns 1994; Watt *et al.* 1996; Kinny *et al.* 1999; Friend *et al.* 2000). Their formation has been related to a high-pressure melting event indicative of crustal thickening of late Ordovician age (470-460 Ma, Kinny *et al.* 1999; Friend *et al.* 2000).

Near Sciberscross the Naver gneisses exhibit a strong compositional banding of amphibole-rich and quartzo-feldspathic layers (Fig 3.2 f). Although they superficially resemble the Lewisianoid basement rocks underlying the Moine (e.g. Burns 1994; Friend pers. comm. 2002), their shallow REE-pattern suggests that they are rather highly strained hornblendic Moine orthogneiss. Strongly deformed coarse grained augen granites, carrying a solid-state fabric, are exposed in the northwest of the study area at Craig Dailfuessiag (Fig. 3.2 g).

3.3.2 Moine Nappe lithologies

The Morar Group Moine rocks of the study area are assigned to the Altnaharra Psammite Formation (e.g. Holdsworth *et al.* 1994; Soper 1999). In the study area, they form a monotonous sequence of dominantly psammitic lithologies with subordinate pelitic horizons. The psammites vary from grey, medium to coarse grained rocks to medium-to-fine grained, brown varieties (Fig. 3.3a & b). Locally, the psammites are very siliceous and in areas of high strain, the psammites are mylonitic, displaying asymmetrically deformed detrital feldspar grains. In lower strain areas, alternating lighter and darker bands may correspond to original bedding. However, way-up criteria have not been observed. Minor fine grained amphibolite sheets and enclaves are found throughout the psammites, and fine grained biotite-leucogranites form locally abundant sheets and stocks.

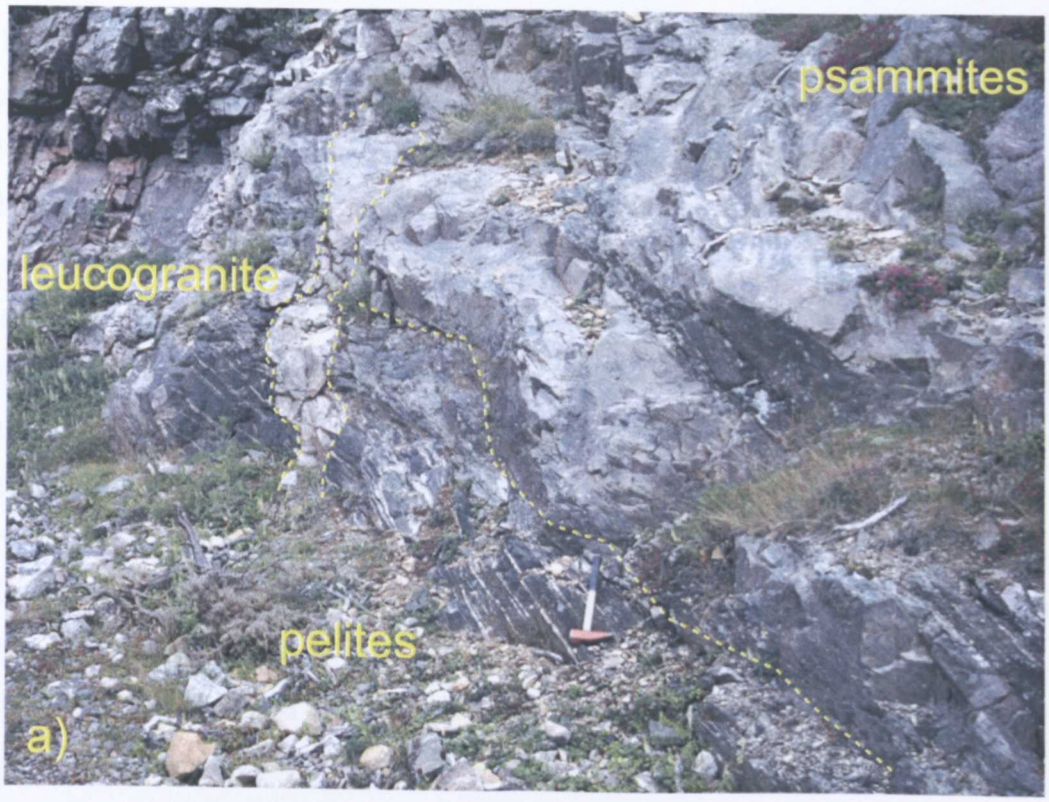

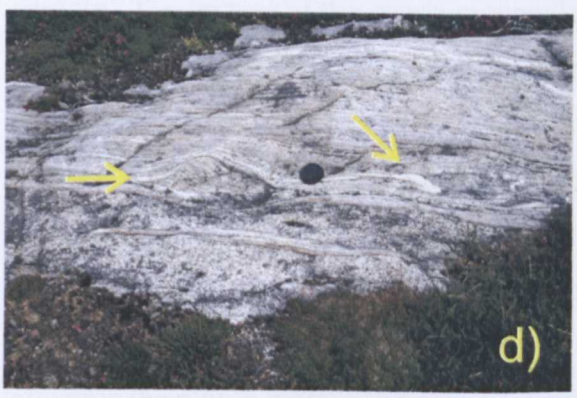

Fig. 3.3 a) Morar Group psammites and pelites cut by leucogranite (East Kinauld quarry). b) Detail of grey psammites cut by granite veins. c) Discordant m-scale biotite leucogranites cutting the compositional S2-fabric of Morar Group psammites. d) Morar Group injection migmatites with increased amounts of S2-parallel leucogranites, note the melt-engulfed psammite raft e) Morar Group injection migmatites, with increased granite proportion leading to disrupted psammitic layering (arrow).

To the north, northeast and east of the Rogart igneous complex the Morar Group psammites are variably migmatitic and show two distinct features. Locally, the semi-pelitic units display a thin, migmatitic layering of leucosomes and melanosomes and the rocks could be described as metatexites (sensu Brown 1973). However, predominantly, the migmatites comprise alternating layers of leucogranites (see below) and psammitic Morar Group rocks. The leucogranites are clearly intruded into the Morar Group rocks as they cross-cut the segregation banding in the semi-pelitic units and the S2 fabric of the psammites. The volume of injected leucogranites varies throughout the Morar Group migmatites and the migmatitic textures developed range from laterally continuous to disrupted (Fig. 3.3 d & e). The Morar Group migmatites are predominantly formed by the injection of leucogranites into Morar Group rocks and cannot sensibly be described in the traditional concept of anatexis and diatexis (sensu Brown 1973). Throughout this study, the term "migmatitic" used in context with Morar Group rocks therefore implies injection migmatites and strictly does not imply any form of in-situ partial melting.

3.3.3 Igneous rocks

Quartz monzodiorites

The composition and texture of the quartz-monzodiorite varies throughout the study area. Within the main plutonic complex, its most common variety is a medium coarse grained, often foliated rock of a distinctly grey colour (Fig. 3.4a). It consists of sodic plagioclase (c. 50%, An_{20} to An_{25}), quartz (c. 18-20%), biotite and hornblendic amphibole (both *c.* 10%) with varying amounts of K-feldspar (less than *c.* 8%) and subordinate, euhedral titanite. Accessory phases are apatite, magnetite, zircon, allanite, rutile and rarely epidote. The texture of the quartz monzodiorite is dominated by aligned, subhedral plagioclase laths of commonly 1 cm length that are often zoned and sericitised. Hornblende forms prismatic crystals of *c.* 0.5 cm length that are usually aligned parallel with the plagioclase. Biotite laths wrap the plagioclase and hornblende, to form a coarse foliation. Depending on the degree of strain, quartz occurs as interstitial multi grain pools or elongate quartz ribbons and myrmekitic intergrowth with plagioclase is common. K-feldspar forms subhedral crystals of 1 to 1.5 cm length with occasional perthite exsolution. Towards the pluton margin the grain size commonly decreases and the texture records varying degrees of strain (see below). Towards the centre of the pluton the quartz monzodiorite grades into the granodiorite over *c.* 50m in the southeast but rather more

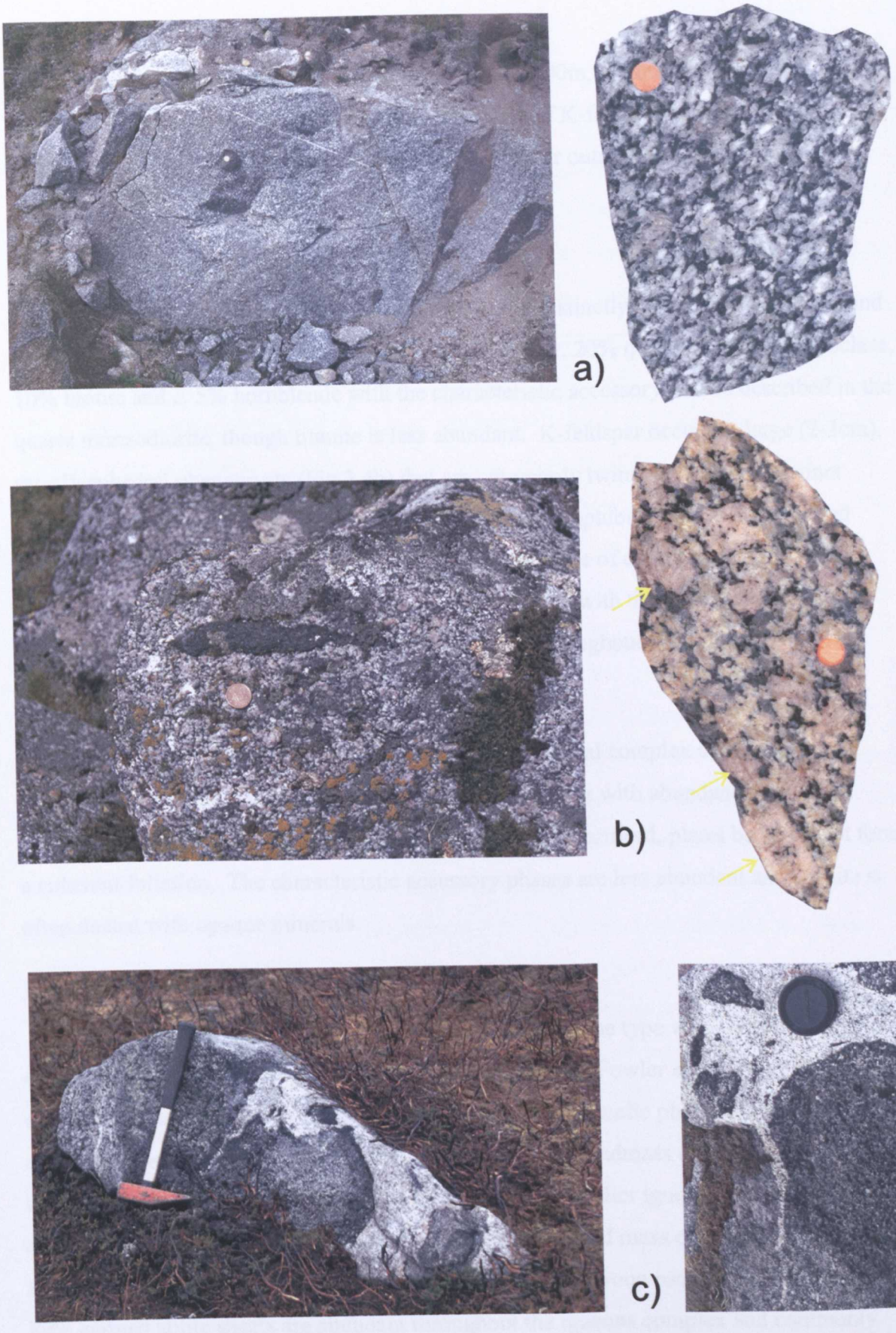

Fig. 3.4 Field photographs and polished handspecimen of igneous rocks of the Rogart complex. a) Quartz monzodiorite, note the pre-RCMP alignment of Hbl and Pl (right). b) Porphyritic granodiorite, note flattened mafic enclave parallel to the foliation (left) and euhedral K-feldspar megacrysts (right). c) Appinitic enclaves cut by leucogranites. Orange circle on handspecimen is 5mm across.

gradually in the northern parts of the complex (c. 100-300m, but limited exposure). This transition is characterised by an increasing abundance of K-feldspar and a significant decrease in hornblende. Quartz monzodiorites that occur outside the central complex are locally poor in K-feldspar megacrysts.

Porphyritic granodiorite (central complex)

The coarse grained, porphyritic granodiorite is of a distinctly orange to pink colour and has an average modal composition of *c.* 18 % K-feldspar, 20% quartz, 45-50% plagioclase, 10% biotite and *c.* 5% hornblende with the characteristic accessory phases described in the quartz monzodiorite, though titanite is less abundant. K-feldspar occurs as large (2-3cm), mostly euhedral phenocrysts (Fig 3.4b) that are commonly twinned and show distinct perthite exsolution. They comprise inclusions of small amphibole, biotite, titanite and plagioclase. Plagioclase, quartz, biotite and hornblende are of comparable habit to the quartz monzodiorite again forming a coarse foliation. As with the quartz monzodiorite, there are minor compositional and textural variations throughout the complex.

Biotite granite (central complex)

The unfoliated, cross-cutting biotite granite of the central complex comprises predominantly subhedral K-feldspar megacrysts and quartz with abundant small plagioclase feldspars. Biotite is present as large, often chloritised, plates but does not form a coherent foliation. The characteristic accessory phases are less abundant and titanite is often dusted with opaque minerals.

Ultramafic to mafic igneous rocks

Ultramafic to mafic rocks form enclaves of the Ach'Uaine type within the central complex and its associated plutons (Fig. 3.4c, Soper 1963, Fowler *et al.* 2001). They are extremely heterogeneous in composition and texture. The mafic phases comprise clinopyroxene, hornblende and biotite that are set in a groundmass of K-feldspar and subordinate plagioclase. Mafic amphibolite sheets and smaller igneous stocks and sheets of appinitic affinity (i.e. hornblende in a fine grained ground mass of equal proportions of K-feldspar and plagioclase) are also present in the Morar Group rocks of the study area. Fine grained aplite sheets are abundant throughout the igneous complex and commonly cross-cut the main pluton fabrics.

Leucogranites

Within the study area there is a widespread occurrence of leucogranitic igneous rocks that are petrographically homogenous and generally contain two feldspars, quartz and varying amounts of brown biotite and minor muscovite. In the north and northeast, leucogranites occur predominantly as sheets in various structural settings above and below the Naver Thrust. Within the Morar Group rocks, they are found as sheets and stocks within the migmatitic areas. In the east and southeast, leucogranitic sheets volumetrically increase and coalesce to form larger igneous complexes (see also Soper 1963, p. 458) which have been named the Rogart Station and Marian's Rock leucogranite complexes. They are characterized by a gradual, heterogeneous increase of leucogranites along strike to the host rock foliation and retain variable amounts of remnant psammitic to semi-pelitic schlieren and rafts. Within these complexes, the leucogranites may occasionally grade into medium grained granodiorites that comprise plagioclase feldspars, biotite, quartz and small hornblende. Field relationships suggest that there are several generations of leucogranites exposed within the study area (see sub-area studies below) but it has been impossible to devise an unequivocal field-based classification of sub-suites of these granites. Geochemically, the leucogranites exposed throughout the study area form a coherent group of peraluminous granites. The leucogranites which occur as 5-10m thick sheets in various structural settings show coherent REE patterns characterized by moderate light REE over heavy REE enrichment (La/Yb of ~ 15-20) and a small, but consistently developed, negative Eu-anomaly (Fig. 3.5b). Leucogranites from the two leucogranite complexes locally show a slightly different, overall less enriched REE-pattern. It is characterized by slightly higher La/Yb-ratios, dish-shaped heavy REE-patterns and variably developed Eu-anomalies (Fig. 3.5c), suggesting that magmatic processes such as crystal fractionation of possibly amphiboles and feldspars were operating during or after emplacement. Migmatization and the origin and significance of the leucogranites exposed in the Rogart igneous complex are discussed below in more detail.

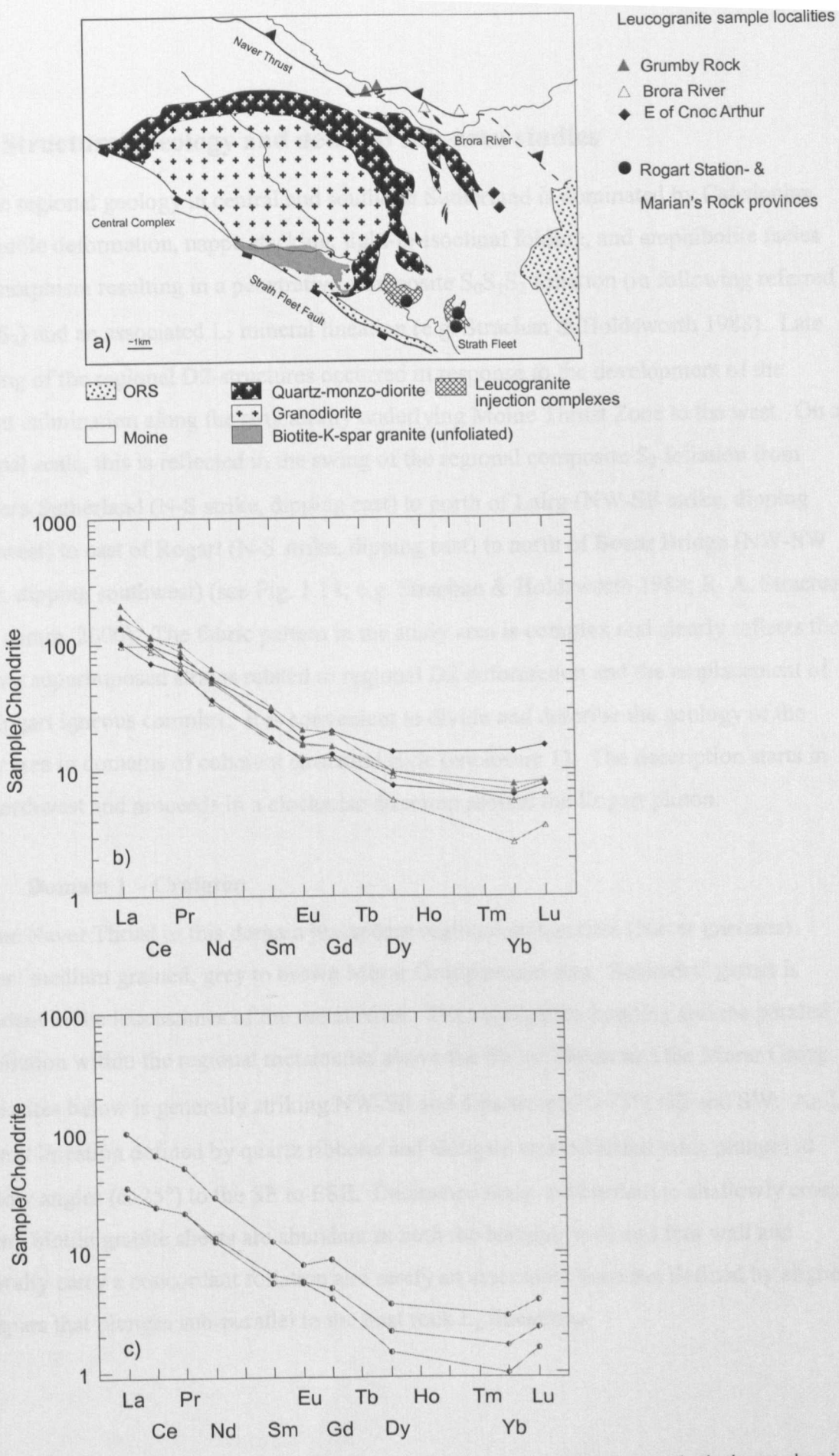

Fig. 3.5. REE-geochemistry of leucogranites in the Rogart area. a) Simplified geological map showing sample localities. b) REE-plot of 5-10m thick leucogranite sheets showing gentle lREE over hREE enrichment with consistently developed, negative, Eu-anomalies. c) REE-plot of leucogranites from the Leucogranite complexes showing an overall similar pattern with dish-shaped hREE and variably developed Eu-anomalies indicating in-situ fractionation processes.

3.4 Structural Geology and detailed sub-area studies

The regional geology in central and southeast Sutherland is dominated by Caledonian D2 ductile deformation, nappe stacking, tight-to-isoclinal folding, and amphibolite facies metamorphism resulting in a penetrative, composite $S_0S_1S_2$ foliation (in following referred to as S_2) and an associated L_2 mineral lineation (e.g. Strachan & Holdsworth 1988). Late warping of the regional D2-structures occurred in response to the development of the Assynt culmination along the structurally underlying Moine Thrust Zone to the west. On a regional scale, this is reflected in the swing of the regional composite S_2 foliation from northern Sutherland (N-S strike, dipping east) to north of Lairg (NW-SE strike, dipping northwest) to east of Rogart (N-S strike, dipping east) to north of Bonar Bridge (NW-SW strike, dipping southwest) (see Fig. 1.14; e.g. Strachan & Holdsworth 1988; R. A. Strachan pers. comm. 2000). The fabric pattern in the study area is complex and clearly reflects the varying superimposed strains related to regional D2 deformation and the emplacement of the Rogart igneous complex. It is convenient to divide and describe the geology of the study area in domains of coherent structural style (enclosure 1). The description starts in the northwest and proceeds in a clockwise direction around the Rogart pluton.

3.4.1 Domain 1 – Craigton

The Naver Thrust in this domain juxtaposes regional metatexites (Naver gneisses) against medium grained, grey to brown Morar Group psammites. Subhedral garnet is abundant in the leucosomes of the metatexites. The segregation banding and the parallel S_2 foliation within the regional metatexites above the Naver Thrust and the Morar Group psammites below is generally striking NW-SE and dips steeply (>75°) NE and SW. An L_2 mineral lineation defined by quartz ribbons and elongate recrystallized mica plunges at shallow angles (c. 25°) to the SE to ESE. Decimetre-scale, concordant to shallowly cross-cutting biotite granite sheets are abundant in both the hanging wall and foot wall and generally carry a concordant foliation and rarely an associated lineation defined by aligned feldspars that plunges sub-parallel to the host rock L_2 lineations.

3.4.2 Domain 2 – Grumby Rock – Brora Gorge

The Moine rocks of this domain (enclosure 1; Fig. 3.6a) comprise migmatitic Naver gneisses, and Morar Group rocks which are locally difficult to distinguish using field criteria. Variably foliated biotite-leucogranite sheets are injected into the Moine rocks throughout the domain and preclude a clear-cut definition of the thrust surface. The Naver Nappe gneisses are rather psammitic *c.* 200m above the thrust and become progressively more pelitic towards lower structural levels where they show abundant migmatitic segregations that locally contain garnets. The Morar Group injection migmatites are comparatively light in colour and comprise laterally discontinuous layers of psammites and leucogranites. No garnets have been observed in the Morar Group injection migmatites anywhere in the study area and this criterion has been used to infer the location of the Naver Thrust. In this domain, the thrust has been inferred at the base of an intensely folded, dark, semi-pelitic metatexite unit which contains the last observed garnets in the leucosomes (going structurally down the Naver Nappe) and is laterally traceable to the east and into domain 3. The composite S_2 foliation of the Moine rocks strikes E-W and dips steeply (>80°) NW to SE (Fig. 3.6). L_2 lineations plunge generally towards the east at shallow angles (c. 20-30°). Small-scale folds have S_2-parallel fold axial planes and hinges that plunge E to NE, subparallel to the L_2 lineation.

Several *c.* 5 to 20m thick quartz monzodiorite sheets have been identified in the footwall of the thrust (Fig. 3.6a). The quartz monzodiorite sheet exposed on the western slope of Grumby Rock (NC 7056|0999) is intruded into migmatitic Morar Group psammites almost immediately beneath the basal metatexite unit of the Naver nappe, i.e. closely beneath the thrust (Fig. 3.6 a). Although it cannot be demonstrated that the sheet cuts the thrust plane, it can be shown that the intrusive contact is steep to the host rock and the earlier leucogranite sheets (Fig 3.6 b). However, the quartz monzodiorite sheet and the granite sheets carry coplanar foliations, that display both solid-state and magmatic-state microstructures (see below, Figs. 3.6 d-g). Kinematic indicators in thin sections cut parallel to the easterly plunging hornblende lineation of the quartz diorite sheet show top-to-the-W sense of shear. Hornblende occurs as 2-4mm long, sometimes longitudinally twinned, prisms and together with subhedral plagioclase, K-feldspar and small biotite forms the pre-RCMP fabric (Figs. 3.6 d & f). In low strain zones, the grain contacts are sharp and are interpreted to represent the original magmatic fabric. In higher strain zones, the feldspar and hornblende crystals are occasionally bent which indicates post-RCMP

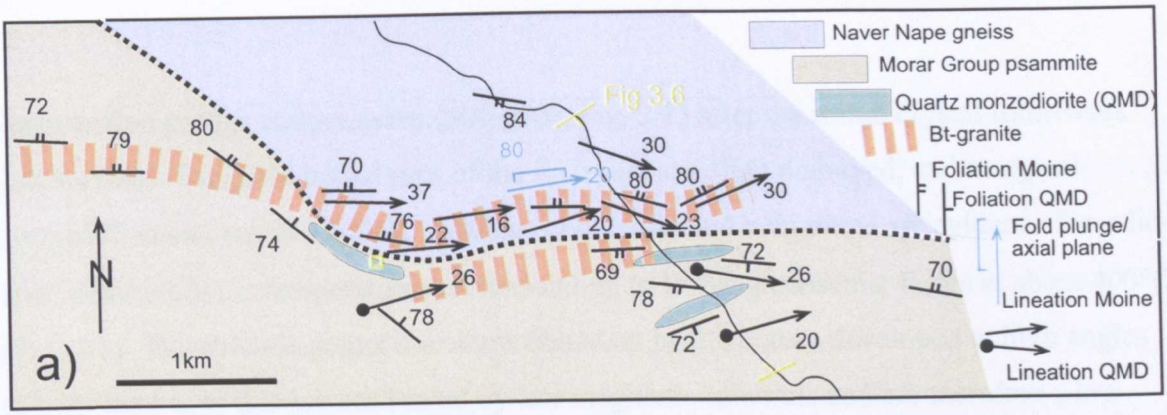

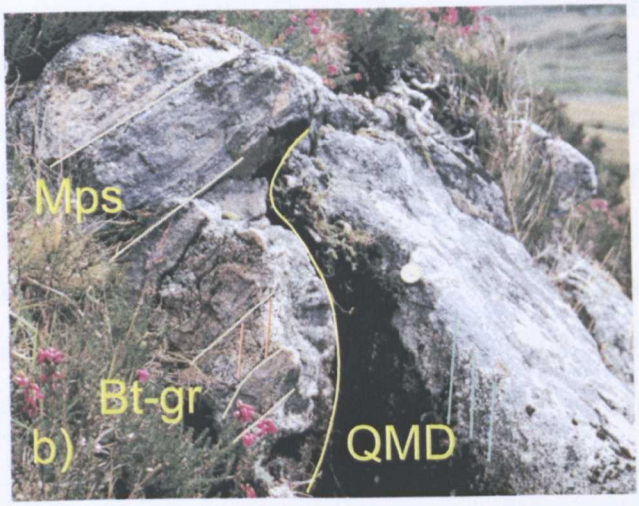

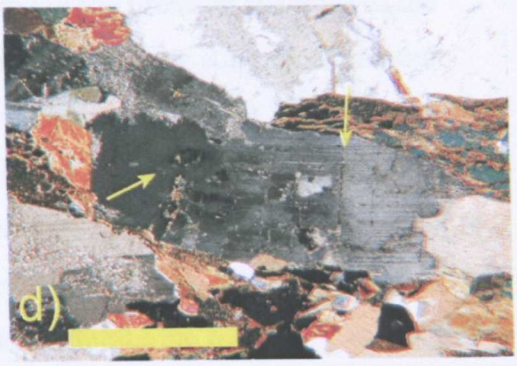

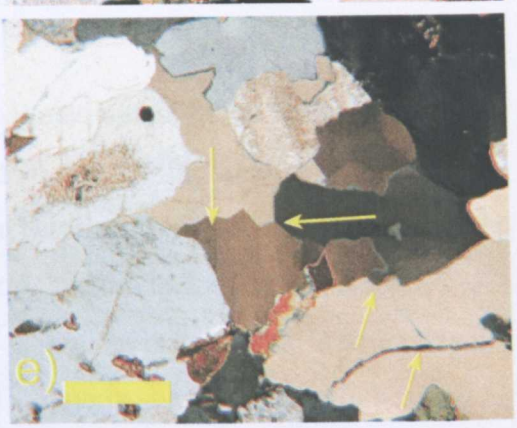

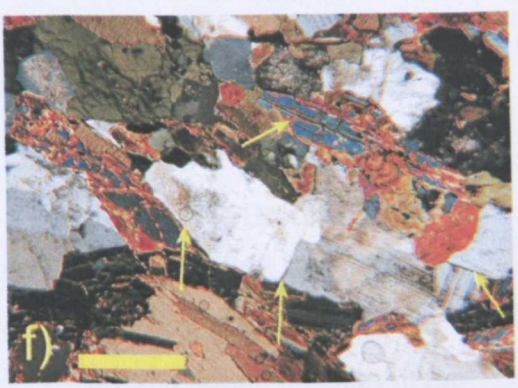

Fig. 3.6 Evidence for high-T fabrics in the quartz monzodiorite (QMD) sheet at Grumby Rock (domain2).

a) Geological sketch map, yellow box shows location of b). b) Field photograph of the cross-cutting relationships (looking E), note the steep cross-cutting contact, and the parallel foliations in QMD and BT-granite. c) Polished slab, orange circle = 5mm, arrows (clockwise) show subhedral K-spar with Qtz growing in P-shadow, elongate Qtz-ribbon, and small euhedral Hbl. Evidence for high-T and solid-state deformation in thin sections of the QMD (d to g); XPL, yellow line = 1mm. d) Tiled, subhorizontal pre-RCMP alignment of subhedral Plag and euhedral Hbl with sharp / straight grain boundaries (bottom left to top right). Note kinking, subgrain formation, and grain boundary migration (gbm) in the P-shadow of the central Plag (arrows) indicating weak solid-state overprint. e) Weakly deformed, multigrain Qtz pool in the P-shadow of K-spar. Note deformation bands, 120° internal grain boundary, gbm, and brittle crack. f) Tiled, subhedral Hbl and Plag laths. Note sharp grain boundaries and cracks in the Hbl (arrows). g) Elongate Qtz ribbon (type 3 of Boullier & Bouchez 1978) in P-shadow of K-spar. Note prismatic subgrains and deformation bands in the Qtz, also note subhedral Hbl with irregular/ embayed grain boundaries, both indicating diffusive mass transfer at moderate to low T (bottom right).

deformation at high temperatures (800-650°, Fig. 2.1) after the initial crystal framework had formed. The grain boundaries of the feldspars are often embayed, and marginal recrystallization, micro kinking, undulose extinction, and bent twins are evidence for solid-state deformation at temperatures corresponding to lower greenschist facies at about 400°C (Fig. 2.1). Hornblende grains also show abundant brittle cracks developed at high angles to their long axes that are not healed by late magmatic minerals and are therefore a low temperature feature. Quartz is occasionally preserved in the pressure shadows of the feldspars where it forms recrystallized multigrain pools that show subgrain formation, prismatic deformation bands and grain boundary migration (Fig. 3.6 e). More commonly, quartz is recrystallized into thin ribbons that show internal prismatic subgrains and deformation bands (Fig. 3.6g). These correspond to type-3 quartz ribbons of Boullier & Bouchez (1978) that are thought to form by diffusive mass transfer (dislocation slide and/or climb) at temperatures corresponding to lower amphibolite to upper greenschist facies, i.e. 450-550°C.

Overall, the microfabrics contain evidence for magmatic-state fabric formation and dynamic recrystallization at temperatures between 550-400°C. Initial alignment of plagioclase and hornblende was followed by ductile bending at high temperatures after the framework had locked up, but these main crystallizing phases lack microstructures indicative of strain accommodation from 650-550° C (e.g. no core & mantle structures in the feldspars, no type-4 quartz ribbons, see Fig. 2.1). Quartz shows features indicating recrystallization and deformation at temperatures of possibly as high as 550°C, but recrystallized feldspars and dominantly grain boundary migration of quartz suggest even lower temperatures (c. 400° C).

A detailed traverse across the Naver Thrust was taken through the Brora Gorge (Fig. 3.7). The composite S_2 foliation of the Moine rocks consistently strikes W-E and dips almost subvertically to the N and S. Going northwest to southeast through the gorge, i.e. towards lower structural levels, gradual changes in lithology and abrupt changes in the volumes of granitic material are evident. The structurally higher parts in the northwest are dominated by banded and rather psammitic gneisses that change into thinly banded metatexitic units which show a consistent and homogenous stromatic layering that is locally cut by small, subconcordant biotite-granite sheets (Fig. 3.7 a). Towards the southeast, the proportion of leucosomes increases rather abruptly (between 3.7 b & c) and foliation-parallel segregation melts are more abundant. However, clearly discordant

leucogranites locally disrupt the stromatic layering (Fig. 3.7 b), contrasting with thicker (50-80cm) leucogranitic sheets that remain almost concordant with the migmatitic layering (Fig. 3.7 c). Throughout the lower part of the gorge, leucogranite sheets remain very abundant. The structurally lowest unit of the Naver gneisses is again the dark, metapelitic metatexite that shows intense folding of the stromatic layering (Fig. 3.7 d) and contains garnet in the leucosomes (Figs. 3.7 e-f). The Naver Thrust has been inferred to the southeast of this basal unit which is structurally underlain by rather grey, banded, psammitic gneisses that locally form injection migmatites. Three quartz diorite sheets occur within the migmatitic Morar Group psammites, shallowly cross-cutting the foliation (Fig. 3.7 h). The quartz diorite sheets carry a coarse foliation that roughly parallels the host rock foliations and hornblende and plagioclase define a shallowly eastward plunging lineation (Fig. 3.7). Microstructures show evidence that these fabrics were initially formed in the magmatic-state and record a limited, low-temperature solid-state overprint but no continuum of down-temperature deformation (Figs. 3.7 k-j). Aligned hornblende and plagioclase laths are generally euhedral in shape and show straight grain contacts with adjacent biotites (Fig. 3.7 i & j) which are interpreted to represent primary igneous features. Quartz is present as thin, elongate ribbons showing subgrain formation and prismatic deformation bands (Fig. 3.7 j) that correspond to type-3 to type-2 ribbons of Boullier & Bouchez (1978) and form at temperatures of 400-550° C (compare table 2.1). Further evidence for low-temperature deformation is preserved within K-feldspar megacrysts that show evidence for brittle cracking and abundant undulose extinction. However, there is no evidence for a continuous development of down-temperature microstructures (such as brittle cracks healed with late magmatic minerals, core-mantle structures, or recrystallization and subgrain formation at intersecting feldspar grains, see table 2.1). This indicates that the small sheets probably cooled quickly and by-passed prolonged residence at high temperatures, thus developing only lower-temperature microstructures that overprint initial magmatic-state features (e.g. Tribe & D'Lemos 1996).

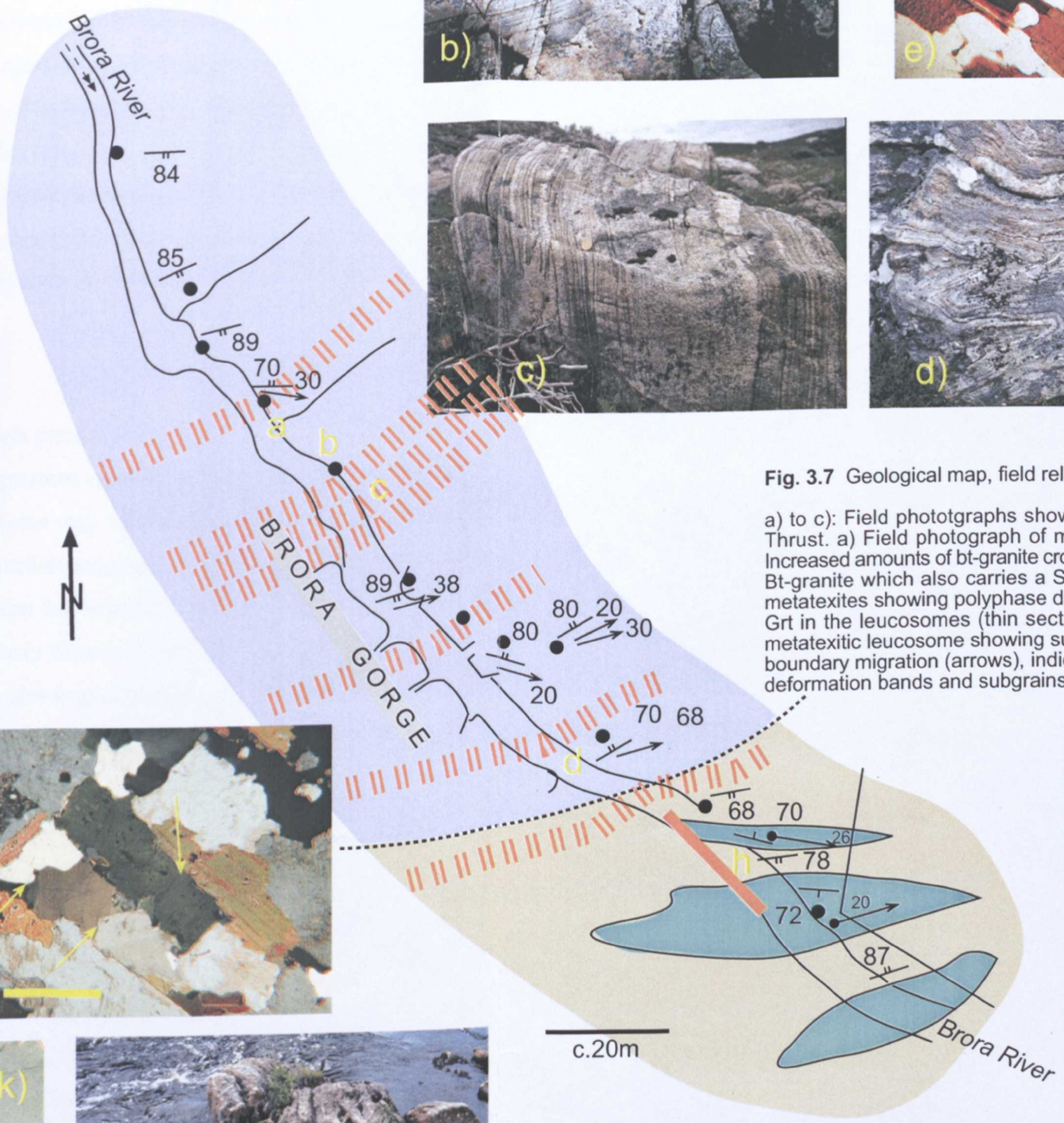

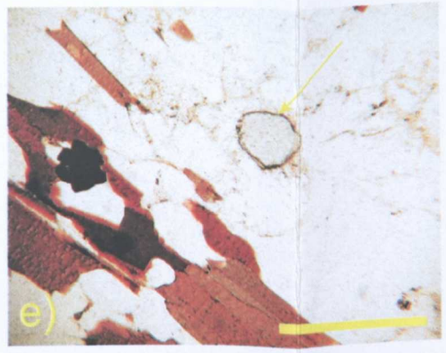

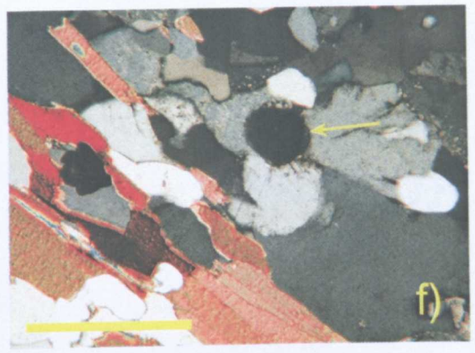

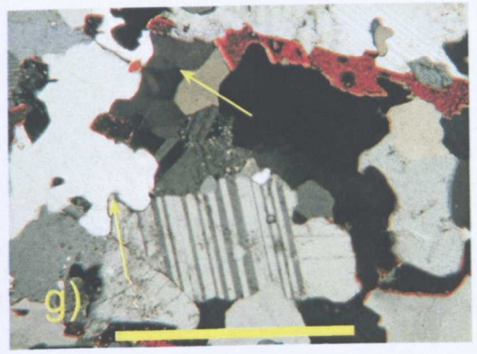

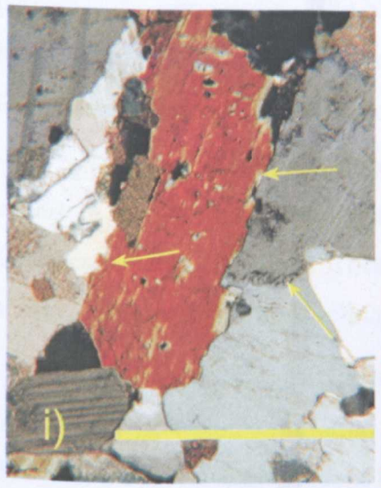

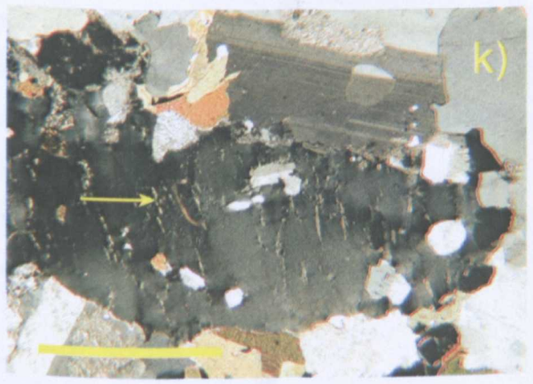

Naver Nappe gneisses
Morar Group psammites
Quartz monzodiorite (QMD)
Bt-leucogranite
X-cutting aplite sheet
Foliation Moine
Foliation QMD
Lineation Moine
Lineation QMD

Fig. 3.7 Geological map, field relationships and microfabrics across the Naver Thrust in the Brora Gorge.

a) to c): Field phototgraphs showing the increasing volume of leucogranites on approach of the Naver Thrust. a) Field photograph of metatexitic Naver gneisses cut by the first small Bt-granite sheets. b) Increased amounts of bt-granite cross-cutting and disrupting the banding. c) Large amounts of subconcordant Bt-granite which also carries a S2 co-planar foliation (compare also fig. 3.2 d & e). d) Pelitic stromatic metatexites showing polyphase ductile folding at the base of the Naver Nappe. Note the small, subhedral Grt in the leucosomes (thin sections: e [PPL] and f [XPL], yellow line = 1mm). g) Thin section of the metatexitic leucosome showing subhedral, magmatic plagioclase and multigrain Qtz pools. Note the grain boundary migration (arrows), indicative of moderate-T deformation and recovery. Qtz also shows internal deformation bands and subgrains that intersect at 120° angles.

h) Field photograph showing the contact between a quartz monzodiorite sheet and the host psammites in the Brora River below the gorge, looking W. i) to k) : Thin section photographs [XPL] providing evidence for high-T and solid-state deformation in the QMD, yellow line = 1mm. i) Euhedral Hbl in sharp contact with subhedral Fsp to its right, representing a primary igneous fabric. Embayed grain boundaries at the interface of Hbl and anhedral Qtz, and grain boundary migration at the grain boundaries of two Fsp's (arrows) indicate moderate-T diffusive mass transfer during solid-state deformation. j) Elongate recrystallized Qtz-ribbon with straight internal subgrain boundaries (type 3 ribbon of Boullier & Bouchez 1978), indicating deformation and recrystallisation at moderate T, note also the sharp grain boundaries between euhedral Hbl and Bt probably representing original igneous features. k) Subhedral K-spar showing undulose extinction indicating high dislocation density, and micro cracks providing evidence for brittle deformation . Note there is little to no grain boundary migration at intersecting Fsp grain boundaries.

3.4.3 Domain 3 – Creag Mhor

The Morar Group psammites within this domain are variably migmatitic and several quartz diorite sheets are present that are poor in K-feldspar megacrysts. Their thickness varies from *c.*10 to 30 metres north of the Brora River. South of the Brora River, several outcrops of quartz monzodiorite occur in sparsely exposed grounds. They are interleaved with abundant Morar Group rocks ("zone of inclusions" of Soper 1963) and as such do not necessarily link up with the central complex (cf. Soper 1963). They further carry distinct microstructures that are different to the central complex (see below) and thus have been interpreted to form a *c.* 500m thick set of sheets that extend eastwards into domain 4 (enclosure 1) and form a separate intrusive body, in the following referred to as the Creag Mhór sheet.

North of the Brora River

The amount of biotite-leucogranite sheets present in the Morar psammites north of the Brora River is very high and injection migmatites are common. Very large amounts of leucogranites are present throughout all Moine rock lithologies and it has not been possible to separate Naver gneisses from Morar injection migmatites based on the presence of garnets in the leucosomes. The Naver Thrust has been inferred at the base of a pelitic horizon that may correspond to the previously described basal unit in the Grumby Rock/ Brora Gorge domain. The S_2 fabric of the Naver gneisses strikes NW to SE, dipping *c.* 50° - 60° NE with an associated mineral lineation plunging *c.* 35° to the E to SE (Fig. 3.8; enclosure 1). Biotite-leucogranites occur in various structural settings within the Morar Group injection migmatites. These range from concordant to shallowly cross-cutting sheets to sheets folded by isoclinal F2 folds which locally show axial planar foliations.

Four small quartz monzodiorite sheets occur in a strongly migmatitic zone structurally below the pelitic horizon inferred to represent the base of the Naver Nappe (Fig 3.8 a). They show host rock-concordant foliations and subparallel aligned hornblende and plagioclase laths define a generally eastward plunging lineation. The four quartz diorite sheets north of the Brora River are fine grained and the fabric is characterized by solid-state microstructures that strongly overprint the initial pre-RCMP alignment of subhedral plagioclase and hornblende that is preserved in low strain zones (Fig. 3.8 b-g). Brittle microcracks in hornblende and titanite are healed by late magmatic minerals (Fig. 3.8 c), which indicates post-RCMP deformation in the magmatic-state, i.e. above *c.* 750°C.

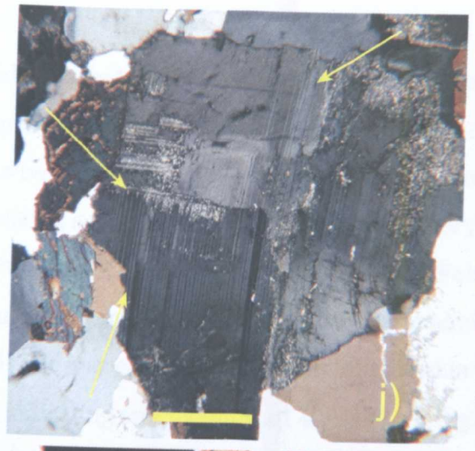

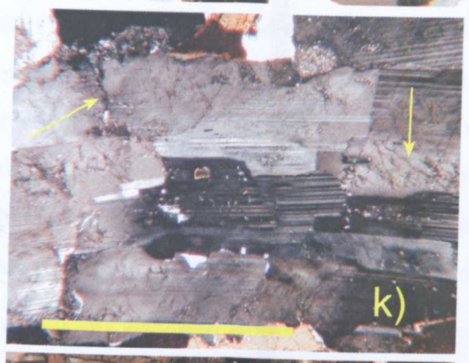

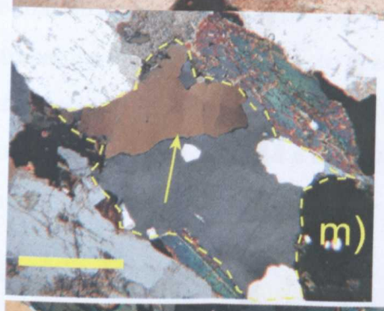

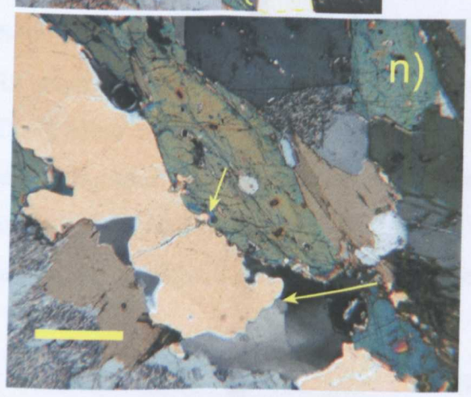

h) & i): Polished Quartz monzodiorite slabs from the Creag Mhor sheet, showing pre-RCMP alignment of euhedral Plag and Hbl with subordinate Bt and interstitial Qtz. Note the rarity of K-spar phenocrysts and the tiled Hbl crystals in i). Orange circle and square = 5mm.

j) to n): Thin section photographs [XPL], yellow line = 1mm.
j) Subhedral Plag with bent twins, undulose extinction and kink band (arrows) indicating high-T solid-state deformation. k) Subhedral Plag comprising distinct subgrains which show bent twins and undulose extinction - high to moderate-T dislocation creep , also note brittle crack (top left corner). l) Brittle fracturing of early titanite healed by late magmatic Plag. m) Rectangular, multigrain Qtz-pool, interstitial between early crystallising Fsp and Hbl hence showing little evidence for deformation. Note, however, Qtz ribbon showing deformation bands with internal prismatic subgrains: moderate-T recovery process. n) Qtz-ribbons recrystallized parallel to foliation defined by Hbl, Plag and Bt. Note the low to moderate-T grain boundary migration between the two Qtz-grains: the low dislocation density grain (orange) grows into and at the expense of the high dislocation density grain (grey, patchy undulose extinction) thereby reducing the overall dislocation density of the aggregate (eg. Jessel 1987). Also note the embayed Hbl crystal at the contact to orange Qtz ribbon, suggesting non-isochemical diffusive mass transfer (arrows).

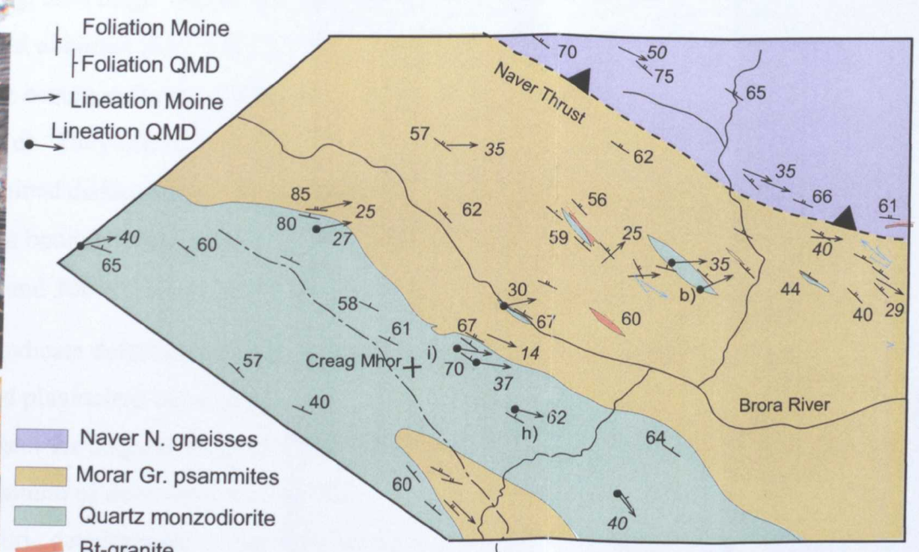

Fig. 3.8 Geology and igneous fabrics of Domain 3 - Creag Mhor.
a) Geological map. Note the parallelism of pluton and host rock fabrics. Abundant Bt-granites north of the Brora River are not shown for clarity. The Naver Thrust has been inferred at the base of the distinct pelitic metatexite unit described in Fig. 3.7.

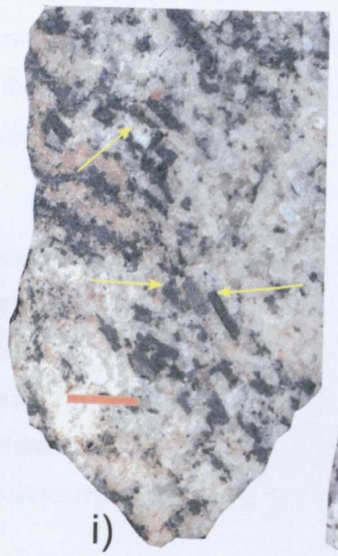

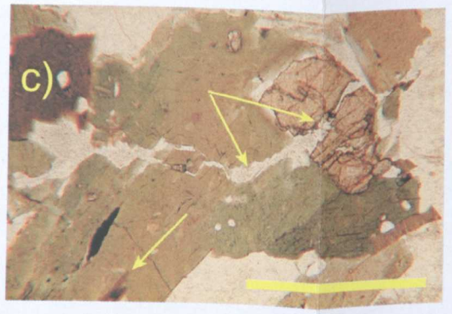

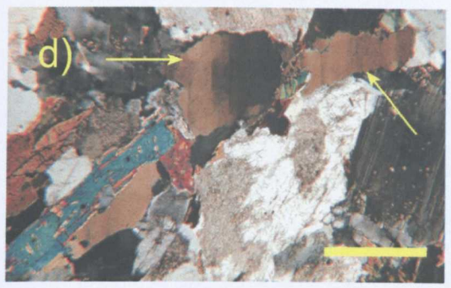

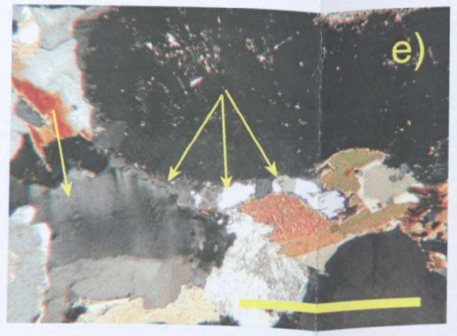

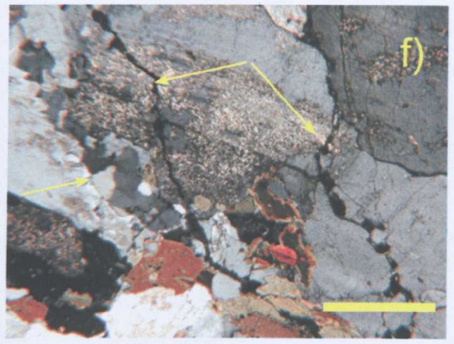

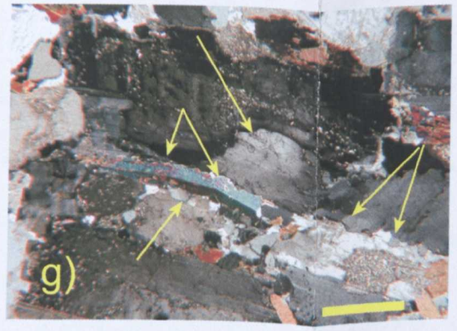

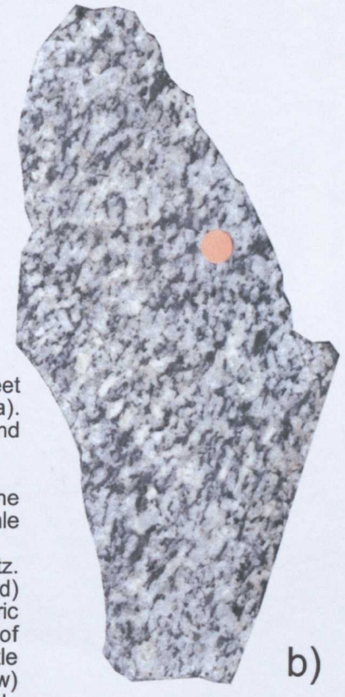

b) Polished slab of the largest quartz monzodiorite sheet exposed north of the Brora River (for location see a). Orange circle=5mm. Note the overall small grain size and the oval shaped Plag laths.

c) to g): Thin section photographs taken parallel to the mineral lineation of the QMD, [XPL] except c), yellow scale bar = 1mm.
c) Brittle crack in Hbl and Ti healed by late magmatic Qtz. Note also the recrystallization of Hbl to Bt (arrows). d) Elongate Qtz-ribbon, recrystallized parallel to original fabric defined by Hbl and Fsp. Note strong development of prsimatic subgrains. e) Weakly developed core-mantle structure in Plag. Note small recrystallized grains (arrow) below the (dark) core. Indicates dislocation climb (possibly combined with dislocation slide) and marks the onset of subgrain rotation (e.g. Paschier & Trouw 1996). Note also the strongly developed deformation bands in the Qtz grain, bottom left.

f) Recrystallization and subgrain development at the interface of two Fsp grains (arrow). Note also the brittle cracks transecting the upper crystal which do not offset and hence predate the sericitisation. g) Down-T deformation behaviour of Plag, Hbl and Qtz. Original pre-RCMP aligned Plag laths, now showing undulose extinction, kinking and internal subgrain development indicating solid-state deformation. Also note the subgrain formation at their crystal margins which is interpreted to represent dynamic recrystallization at progressively lower T. The Hbl crystal is broken twice perpendicular to its long axis and small Qtz ribbons comprising several prismatic subgrains have recrystallized inbetween the Plag laths.

Solid-state features indicate deformation and recrystallization at greenschist facies temperatures (550-350° C): Feldspars show marginal recrystallization along intersecting grain boundaries and sporadically developed core-mantle structures (Fig. 3.8 e, f & g) indicating subgrain rotation and grain boundary migration at temperatures of about 550-500° C (Fig. 2.1, Paschier & Trouw 1996). Feldspars further show bent twins and undulose extinction which indicates high internal dislocation densities. Occasionally, small feldspar grains have recrystallized within brittle microcracks transecting larger grains thus indicating temperatures of 400-300°C (Fig. 3.8 f & g). Small, prismatic hornblende crystals are often broken and also recrystallized to biotite (Fig. 3.8c & g) indicating brittle deformation at about 400° C (Fig 2.1). Quartz occurs as flattened ribbons that show strong prismatic subgrain development (Fig. 3.8 d & e). They correspond to type-3 ribbons of Boullier & Bouchez (1978) that form by combined dislocation climb and glide at temperatures of *c.* 500-550°C. Abundant grain boundary migration of quartz indicates further recovery at temperatures between 400 and 300°C.

Overall, the microstructures (Fig. 3.8 c-h) indicate deformation at greenschist facies temperatures. Locally, aligned hornblende and plagioclase laths with straight grain contacts are observed and interpreted to represent the original magmatic-state fabric. Larger sheets may locally preserve some continuum of down-temperature fabric development. Post-RCMP, magmatic-state fabric development is indicated by cracks within early crystallized minerals that are healed with late magmatic minerals. Diffuse core-mantle structures and type-3 quartz ribbons mark deformation and recrystallization at the transition from amphibolite- to greenschist facies temperatures (~ 550°C). All other microstructures (e.g. undulose extinction, microcracking and incipient recrystallization of hornblende to biotite, Fig. 3.8 e & d) indicate that deformation, recrystallization and recovery occurred at temperatures of ~400°C (compare Fig. 2.1).

South of the Brora River

South of the Brora River, biotite leucogranites are less abundant and the Morar Group rocks occur as unmigmatized, grey to brown psammites. On the steep northwestern flank of Creag Mhor at NC 7311|0876, the contact between the Creag Mhór quartz monzodiorite sheet and the Morar Group psammites is exposed. It is concordant, and foliations and lineations in the host rocks are sub-parallel to those in the Creag Mhór sheet. The foliations strike NW-SE and dip 50-70° northeastwards, and lineations plunge at 25-40° E-

to SE (Fig. 3.8 a). The intrusive contact is traceable to the northwest, where the quartz diorite cuts across the composite S_2 fabric developed in the Morar Group psammites. However, the quartz monzodiorite sheet also carries a magmatic-state foliation that parallels the foliation in its country rocks, indicating that it was emplaced late during the deformation responsible for the development of the planar fabric. Importantly, the lineations developed in the sheet and its host rocks in this area, plunge generally eastward and are consistent with fabric development during W-directed, ductile deformation and thrusting along the Naver Thrust. Within the sheet exposed at Creag Mhór a continuum of high-temperature to low-temperature solid-state fabrics can be demonstrated (Fig. 3.8 h-n). In low strain zones, pre-RCMP alignment of prismatic crystals and tiling of hornblende indicates magmatic flow was directed towards the west (Fig. 3.8h & i). There, quartz occurs largely as interstitial phase between the feldspars and hornblende and is only weakly deformed (Fig. 3.8 m). Microcracks affecting early crystallized titanite and hornblende are healed with late magmatic feldspar (Fig. 3.8 l) showing that early-crystallized phases behaved brittle during post-RCMP deformation whilst the rock was still strictly in the magmatic state. In zones of higher low-temperature strain, mafic enclaves are elongated and aligned parallel with the prismatic minerals. Plagioclase displays weak undulose extinction, bent twins and subgrain formation (Fig 3.8j & k) that indicate a weak low temperature overprint at about 400°C. Quartz occurs as recrystallized ribbons showing prismatic and equant subgrains within widely developed deformation bands that correspond to type-3 and type-2 ribbons of Boullier & Bouchez (1978), indicating temperatures of 550-400°C (Fig. 2.1). Abundant quartz grain boundary migration embays the crystal faces of neighbouring hornblende and feldspar grains. In between quartz grains, low dislocation density grains grow into high dislocation density grains and thus provide evidence for low temperature dislocation glide (Fig. 3.8 n; Jessel 1987). In areas of high solid-state strain, centimetre-scale C-S fabrics are common that are also characteristic of the quartz diorite sheets north of the Brora River and a prominent feature of the Creag Mhór sheet in domain four (Fig. 3.9).

3.4.4 Domain 4 – Cnoc Arthur

From domain three towards Cnoc Arthur, several quartz monzodiorite outcrops occur that show dominantly solid-state microfabrics (Fig. 3.9) but locally preserve original magmatic fabrics. As such, they are comparable to the microstructures present in the

Creag Mhór sheet and have been interpreted as its eastward continuation. Throughout the domain, a solid-state foliation is developed in the quartz monzodiorites and strikes NNW to SSE, dipping at *c.* 45-50° NE and a lineation defined by hornblende and plagioclase plunges generally ENE to E. The Morar Group rocks are strongly migmatitic throughout the domain and biotite-leucogranite is abundant. In the north, close to the Naver Thrust, the S_2 foliation strikes NW-SE dipping steeply NE and an L_2 mineral lineation plunges to the ESE to SE (Appendix 3A). Various small scale folds have S_2 planar axial surfaces and hinge lines that plunge at 20 to 60° to the SE and NW, i.e. perpendicular to the lineation. To the southeast, the structural trend is constant to the east of Acorch (enclosure 1).

Microstructures of the Creag Mhór sheet

The south flank of Cnoc Arthur exposes fine grained quartz monzodiorite showing solid-state foliations and weak C-S fabrics (Fig 3.9 a). Plagioclase and K-feldspar are well aligned and oval. Hornblende crystals either retain euhedral shape, or, together with biotite wrap around the feldspar laths to form a strong foliation. Locally, C-S fabrics indicate top-to-the-W movement (Fig. 3.9 a). The microstructures occasionally preserve evidence for pre-RCMP, magmatic-state fabrics, such as euhedral hornblende and subordinate plagioclase crystals with straight grain boundary contacts, but are mostly consistent with ductile deformation and recrystallization at temperatures of 400-500°C (Fig. 3.9 b to f). Plagioclase and hornblende are commonly kinked and broken with local, incipient recrystallization of plagioclase (Fig. 3.9 b & c). K-feldspar megacrysts are subhedral, showing undulose extinction, microcracks, and intense recrystallization and exolution predominate at grain boundaries (Fig 3.9d), which indicates temperatures of about 400°C (compare Fig. 2.1). Quartz is drawn out into the foliation within the pressure shadows of K-feldspar, or occurs as flattened ribbons that display both, equant, and prismatic subgrains within deformation bands (Fig. 3.9 e & f). They correspond to type 2-3 ribbons of Boullier & Bouchez (1978) and indicate recrystallization at temperatures of 400-550°C (Fig. 2.1). However, as grain boundary migration of quartz is dominant, temperatures may have been closer to 400° C. Both, ribbons and wings show a consistent shear sense of top-to-the-W movements during recrystallization (Fig. 3.9.e & f). Occasionally developed mica fish, and recrystallization of hornblende to biotite further indicate temperatures corresponding to lower to mid-greenschist facies. C-S fabrics are widespread within the quartz monzodiorite outcrops of domain 4.

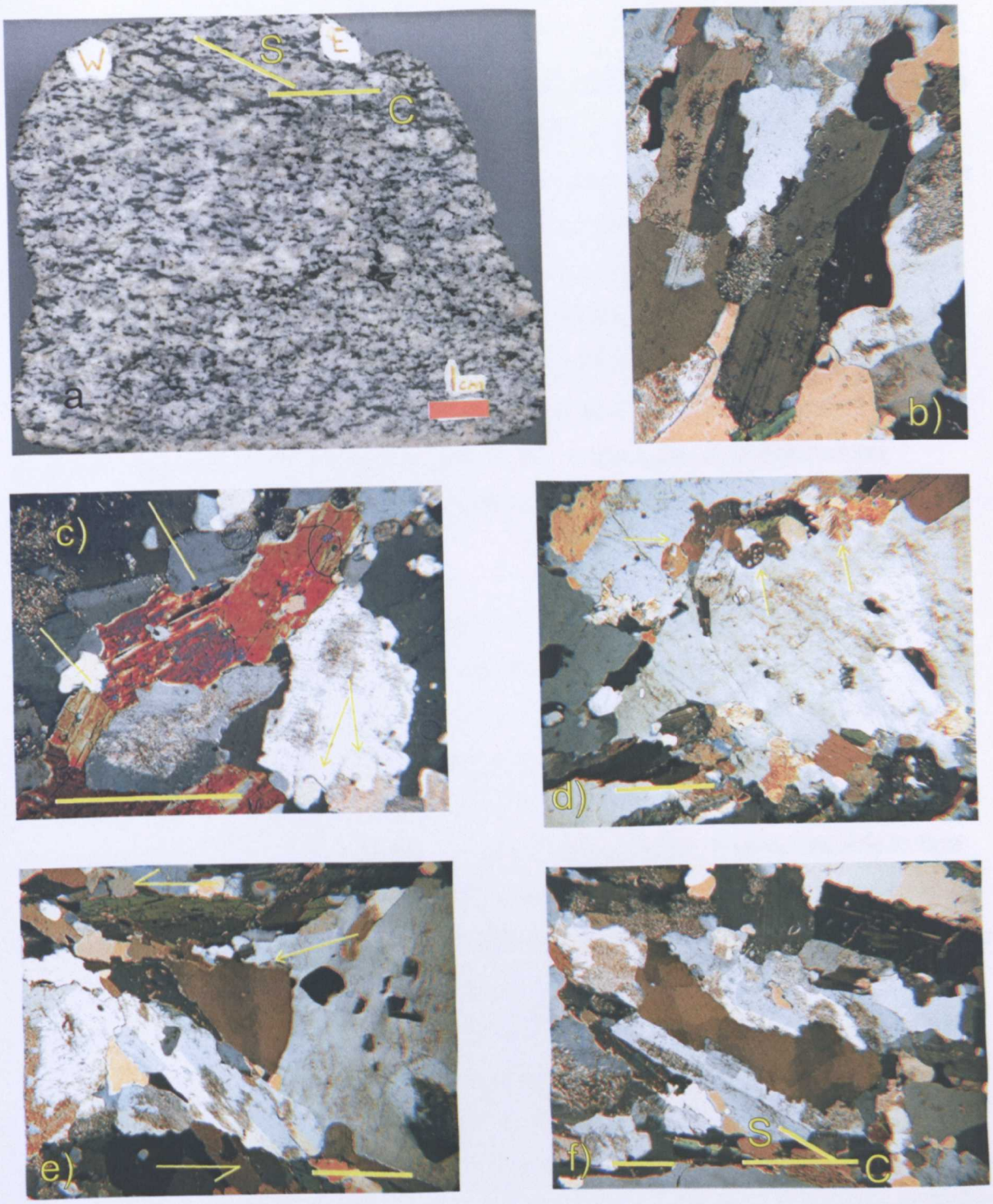

Fig. 3.9 S-C fabrics and solid-state microstructures of domain 4, Cnoc Arthur.

a) Polished slab, cut parallel to mineral lineation (surface strikes west-east). Mafic minerals define grain scale S-C fabrics consistent with top-to-the-W deformation during down-temperature deformation.

b) to f): Thin sections cut parallel to the lineation, [XPL], yellow scale bar = 1mm.
b) Subhedral plagioclase with irregular, embayed grain boundaries. c) Kinked and broken up hornblende crystal, also note the small left-over grains and irregular grain boundaries in feldspar (arrows). d) Subhedral K-feldspar phenocrysts showing marginal recrystallization and exolution at intersecting K-feldspar grain boundaries (arrows). e) Recrystallized quartz in pressure shadow, drawn out into foliation and giving top-to-the-W sense of shear. f) Quartz ribbon, recrystallized parallel to the "s"-fabric defined by earlier crystalized plagioclase.

They are observed on a centimetre to decimetre scale and do not appear to be focussed into discrete high strain zones, nor are they entirely pervasive, indicating syntectonic intrusion and heterogeneous cooling (e.g. Gapais 1989). In domain 4, there is also little evidence for high-temperature solid-state deformation features (550-800°C) such as extreme ductile bending and marginal recrystallization of hornblende and plagioclase (e.g. Paterson *et al.* 1989, Miller & Paterson 1994), or microcracks in hornblende and plagioclase which are healed with late magmatic minerals (e.g. Bouchez *et al.* 1992). Overall, the microfabrics of the quartz monzodiorite exposed in domain 4 only show early magmatic-state and moderate temperature (~400°C) deformation with a distinct gap of microstructures characteristic of deformation in the intervening temperature range.

Migmatites E of Cnoc Arthur

East of Cnoc Arthur, the Morar Group injection migmatites are well exposed in a few, small outcrops (Fig. 3.10 a & b). They comprise laterally discontinuous bands of psammites and semi-pelites that alternate with subconcordant sheets and lenses of biotite-leucogranites (Fig. 3.10 c). The leucogranites show pinch and swell structures and are commonly infolded with their host rocks into isoclinal folds. Within these folds, they show thickness variations in the limbs and cores, indicating that magma was able to flow during folding (Fig 3.10 d). Locally, the injected granites are volumetrically dominant but retain biotite-dominated schlieren or host rock rafts (Fig. 3.10 e). Semi-pelitic Morar rocks locally contain granitic leucosomes and biotite-dominated melanososmes forming a metatexitic banding that is locally clearly folded (Fig. 3.10 f). The contact between the (locally metatexitic) host rocks and the biotite-leucogranites is clearly intrusive (Fig 3.10 g) and the migmatites are predominantly of the injection-type. They carry a strong, composite S_2 foliation. L_2 lineations in the Morar Group rocks are defined by recrystallized mica and quartz and parallel a magmatic-state lineation in the leucogranites that is defined by euhedral plagioclase (Fig. 3.10 h & j). On surfaces parallel to the L_2 lineation and perpendicular to the S_2 foliation, kinematic indicators within psammite-dominated horizons show top-to-the-W movements (Fig 3.10 i). Within semi-pelitic, metatexitic units, mineral lineations in the melanosomes are parallel to small scale fold hinges exposed in the leucosomes (Fig. 3.10 f) and no refolded lineations or folds which relate to the earlier melting event, have been observed. The hinge lines and lineations in the semi-pelites are also subparallel (but not 100% coaxial) to the magmatic-state lineation within the biotite-leucogranites (Fig. 3.10 f).

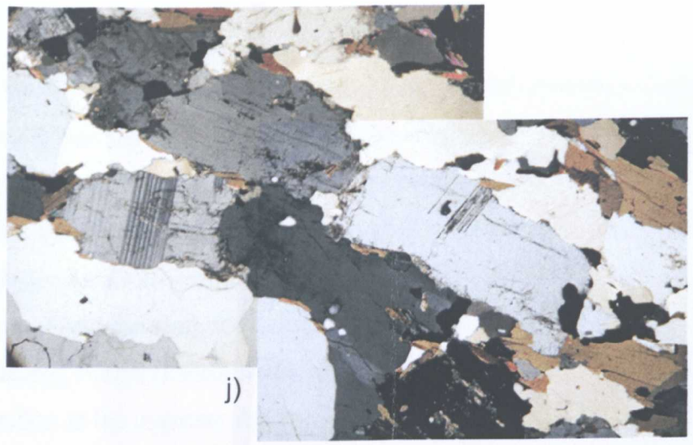

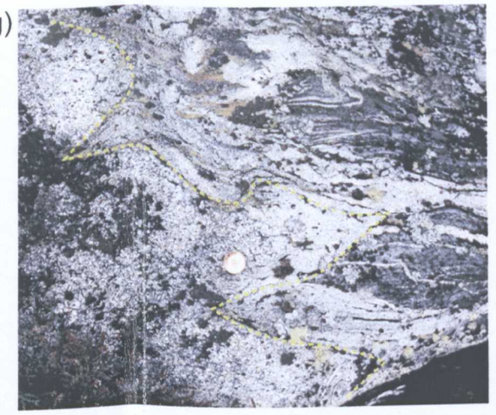

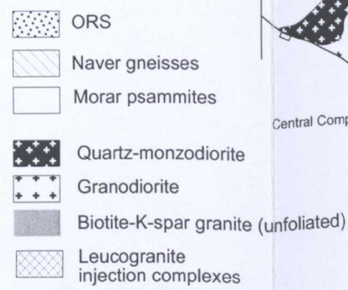

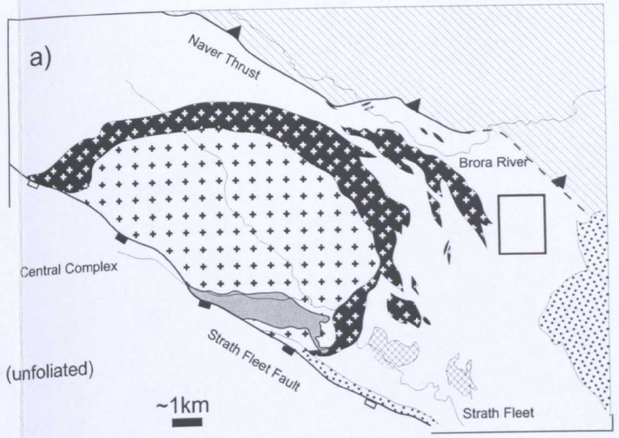

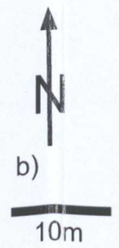

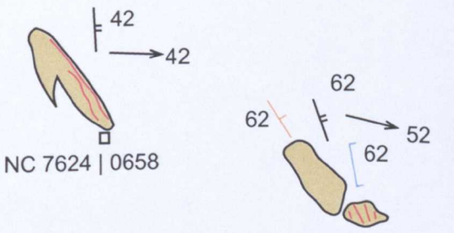

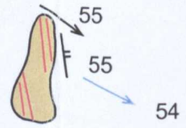

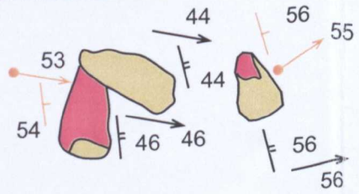

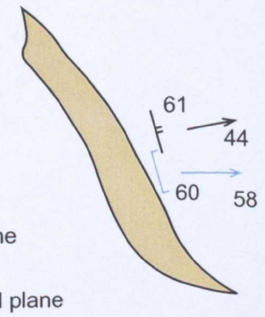

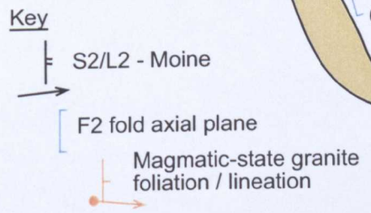

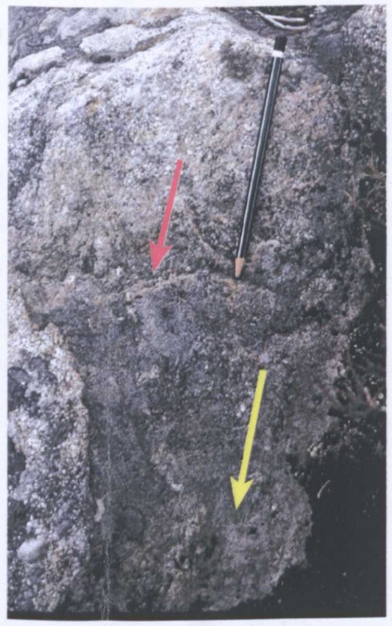

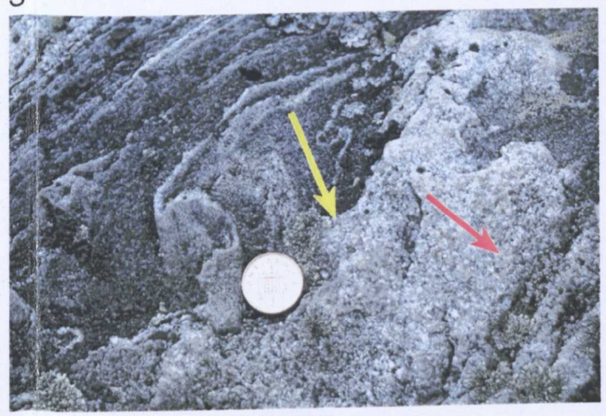

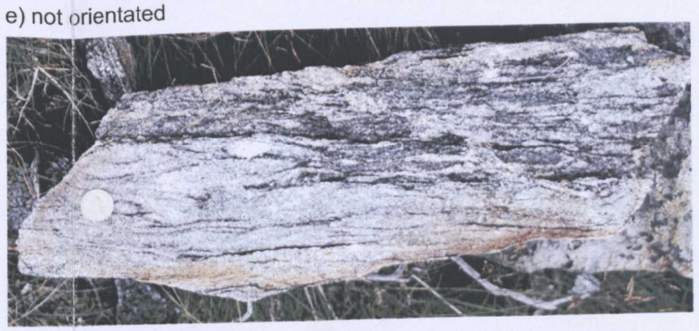

Fig. 3.10 Injection migmatites east of Cnoc Arthur.

a) Location map. b) Detailed field sketch (granite = red), note the parallelism of granite and host rock fabrics. c) Laterally discontinuous granite sheets and host rock psammites. d) Isoclinal F2 fold, note the thickness variations in the granite. e) High granite content leading to schlieric appearance. f) Small-scale fold, folding a metatexitic segregation fabric. g) Intrusive contact of leucogranite and Morar Group rocks. h) Parallel, eastward-plunging L2 lineations. i) Asymmetrically sheared K-feldspar indicating top-to-the-W movements. j) Aligned plagioclase laths defining the magmatic-state fabric in the leucogranites (c. 5mm long). Further explanation, see text.

The fabrics of the leucogranites are defined by mostly euhedral plagioclase laths of 2-3mm length that are wrapped by small, brown biotite that itself is occasionally retrogressed to chlorite (Fig. 3.10 j). The grain contacts between these early-crystallized phases are generally straight and well defined, indicating magmatic-state mineral alignment. The plagioclase crystals are rarely slightly bent, or show minute undulose extinction or marginal recrystallization, indicating that solid-state deformation was negligible. Occasionally, euhedral titanite and subhedral K-feldspar grow within the foliation. Quartz occurs either in the pressure shadows of early crystallizing phases, or as recrystallized thin ribbons between them (Fig. 3.10 j). These dominantly type-2 (to type-3) quartz ribbons (Boullier & Bouchez 1978) show prismatic and equant deformation bands, as well as undulose extinction, and grain boundary migration that occasionally leads to subgrain formation and are the only evidence for recrystallization at temperatures corresponding to lower greenschist facies (c. 400 C). The fabric developed in the leucogranites is therefore predominantly magmatic.

Field relationships suggest, that the Morar Group migmatites are predominantly injection migmatites, although locally, an earlier formed segregation fabric is present. The parallelism of pervasive planar and linear fabrics in the Morar Group rocks and the leucogranites suggests contemporaneous fabric development. Fabric development is most likely of D2 age, as a locally present segregation fabric (D1) is clearly folded by the D2 deformation. The ESE plunging lineations developed in the migmatites and top-to-the-W kinematic indicators are consistent with ductile deformation in the footwall during D2 W-directed thrusting along the Naver Thrust (e.g. Strachan & Holdsworth 1988). The leucogranite sheets display predominantly magmatic-state fabrics suggesting that granite injection, D2 deformation and fabric development was contemporaneous. The lack of evidence for continued down-temperature, or strong solid-state deformation further suggests that the granites were partially molten during their entire deformation. This requires either, that subsequent deformation was channelled away from these areas allowing the injection migmatites (Morar Group rocks + leucogranites) to cool slowly in a low strain domain, or that the assemblage remained at high temperatures throughout subsequent deformation until deformation terminated.

3.4.5 Domain 5 – Sciberscross

This domain comprises para and orthogneisses assigned to the Naver Nappe that show varying degrees of partial melting and metatexitic banding. Foliations dominantly strike N-S and dip eastwards but are not as consistent as in other areas and several foliations deviate considerably from this general trend (enclosure 1). Lineations generally plunge eastwards with a few exceptions plunging north or south. Several refolded folds have been observed on outcrop scale (Fig. 3.11 a) and unexposed large-scale analogues may provide an explanation for the observed deviations.

3.4.6 Domain 6 – Glen Cottage

This domain comprises extensive peat and drift cover with only two areas of moderate exposure. In the north, occasional outcrops expose migmatitic Morar psammites that show evidence for small scale folding and structural data do not form a coherent pattern. In the east, towards Glen Cottage the psammites are not migmatitic but show a strong mylonitic fabric in the footwall of the Naver Thrust (Fig. 3.11 b). In thin section, the mylonites show a strongly recrystallized fabric that is principally defined by quartz ribbons of 2-4 mm length and 0.2-0.4mm thickness which are bounded by small, platy mica that is strongly chloritized. The quartz ribbons show subgrain formation which show straight extinction, patchy undulose extinction, or prismatic deformation bands with sweeping undulose extinction. Occasionally, these larger ribbons are bordered by smaller, dynamically recrystallized quartz grains that were most probably formed by subgrain rotation, as grain boundary migration is largely absent. Overall, the quartz ribbons correspond largely to type-2 quartz ribbons of Boullier & Bouchez (1978) with some ribbons of type-3 affinity, whereas some grains still show evidence for high internal dislocation densities and may not have recrystallized. The mylonitic fabric is interpreted to have formed at upper greenschist facies temperatures of less than 500° C, as lower-temperature quartz microstructures are abundant. In the vicinity of the Naver Thrust, west of Glen Cottage, the strike of foliations again varies around N-S, and dips generally E. A strong lineation consistently plunges east and kinematic indicators indicate top-to-the-W movements, which is consistent with generally west-directed movements on the Naver Thrust.

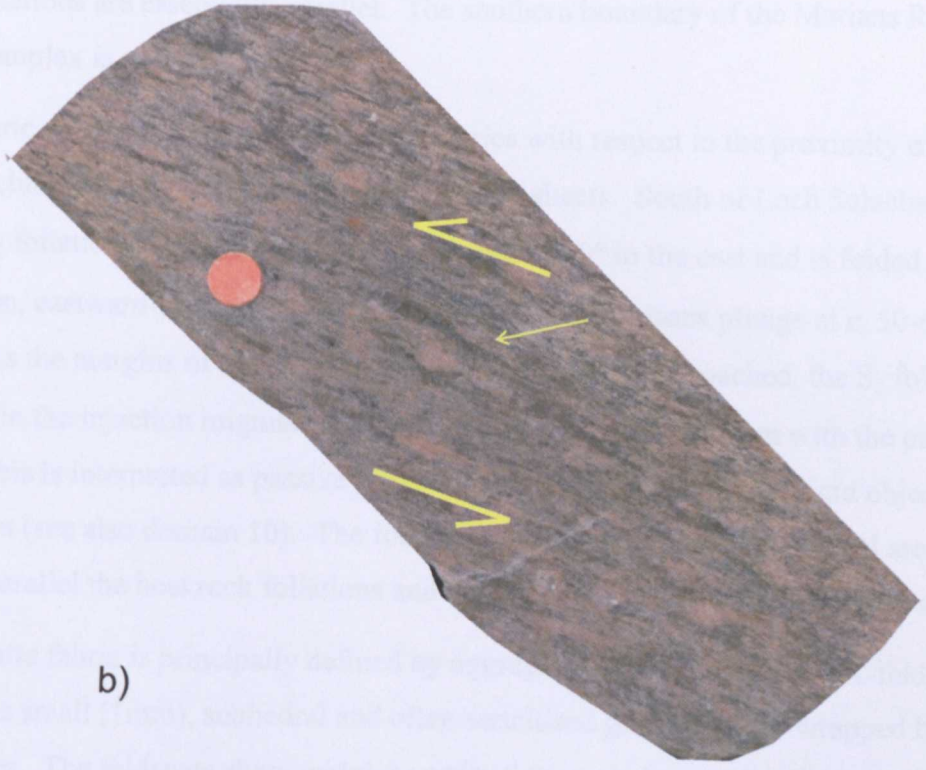

Fig. 3.11 a) Refolded F1 fold in metatexites above the Naver Thrust in domain 5 [NC7613|0912]. Photo is upright but not orientated. b) Mylonitic Morar psammite exposed west of Glen Cottage [NC7783|0500] in domain 6. Section cut parallel to L2 (59°=>106), looking north. Sheared K-feldspar grains indicate top-to-the-W sense of shear. Orange circle = 5mm. See text.

3.4.7 Domain 7 – Aberscross Hill to Ben Lundi

Occasional outcrops of Morar psammites consistently strike NW-SE, dipping at *c.*40° to the NE. A quartz lineation plunges consistently SE and the fabric is occasionally mylonitic.

3.4.8 Domain 8 – Loch Salachaidh to Marians Rock

The northern part of this domain is dominated by migmatitic Morar Group psammites that comprise mafic sheets and bosses, with subordinate unmigmatized psammites. Towards the south, the leucogranites become dominant and form the Marians Rock igneous complex. This transition from injection migmatites into the granite-dominated domain occurs gradually along the strike of the regional foliation and as such, the mapped boundary does not represent a primary igneous contact that cross-cuts regional fabrics, but rather the boundary where granite forms the bulk of the rock. However, locally, unmigmatized psammites are also in contact with the granite, but regional S_2 foliations and granite foliations are essentially parallel. The southern boundary of the Marians Rock igneous complex is not exposed.

The fabric pattern throughout the domain varies with respect to the proximity of igneous bodies, excluding the abundant biotite-leucogranite sheets. South of Loch Salachaidh, the regional S_2 foliation of the Morar Group rocks dips at 60° to the east and is folded into a gentle, open, eastward-closing antiform (enclosure 1). Lineations plunge at *c.* 50-60° to the east. As the margins of the smaller, mafic intrusions are approached, the S_2 foliation developed in the injection migmatites generally swings into parallelism with the pluton contact. This is interpreted as passive host rock fabric rotation around a rigid object during deformation (see also domain 10). The foliations within the granite-dominated areas generally parallel the host rock foliations and both appear to be folded on a larger scale.

The granite fabric is principally defined by aggregates of plagioclase and K-feldspar that occur as small (1mm), subhedral and often sericitised grains and are wrapped by small biotite flakes. The feldspars show undulose extinction, grain boundary migration and marginal recrystallization and exolution, indicative of temperatures corresponding to lower greenschist facies (*c.* 400°C). Rarely they are preserved as phenocrysts (3mm) that show marginal recrystallization at intersecting feldspar boundaries but are in straight contact with small biotite grains, possibly preserving original magmatic contacts. Quartz is either

associated with the feldspar aggregates and forms flattened, oval multigrain pools, or occurs as 2 to 3 mm wide quartz ribbons. These are generally recrystallized parallel to the foliation and show strong, prismatic deformation bands and undulose extinction (type2-3 ribbons of Boullier & Bouchez 1978), indicating temperatures of about 400-500°C. Abundant grain boundary migration of quartz indicates deformation and recrystallization by predominantly dislocation glide at about 400°C. In contrast to the leucogranites exposed within the injection migmatites to the east of Cnoc Arthur, the leucogranites in the Marians Rock province carry features indicating limited solid state deformation and recovery postdating their emplacement. Petrographically, the "Marians Rock granites" are similar to the leucogranite sheets observed throughout the domain and can not be distinguished using field or thin section studies. However, field relationships and microstructures indicate that emplacement of the granite may have initially occurred along planes of weakness (e.g. S_2 foliation planes) leading to coalescence of the melt, followed by cooling and down-temperature deformation of host rock and granite. However, this down-temperature deformation is not well developed and the solid-state overprint is only weak.

3.4.9 Domain 9 – Garvoult Bridge

This domain comprises the typical variably-migmatitic Morar Group lithologies and is structurally characterized by a subvertical S_2 fabric that strikes broadly N-S. Lineations plunge towards the northeast as do small scale fold hinges. The fabric pattern of this province is considerably steeper than fabrics of adjacent domains, and lineations plunge NNE, i.e. different to the regional trend that is plunging E-ESE. The rocks and fabrics have therefore probably undergone substantial steepening and rotation (rotated lineations) which is possibly related to the emplacement of the nearby central complex. However, the domain contains a key outcrop in which the contemporaneous nature of leucogranite emplacement and thrusting can be observed (NC7418¦0483). In the W-E striking surface (Fig. 3.12 a) it can be demonstrated that mafic sheets were emplaced early into the Morar Group psammites that were subsequently affected by thrust movements and leucogranites were channelled up the thrust planes (Fig. 3.12 a & b). Granites also form small stocks in the hanging-wall of local thrusts (Fig. 3.12 b). The leucogranite sheets cross-cut the S_2 foliation in the psammites but at the same time carry co-planar foliations, and are also incorporated in small scale folds locally showing axial planar foliations (Fig 3.12 c),

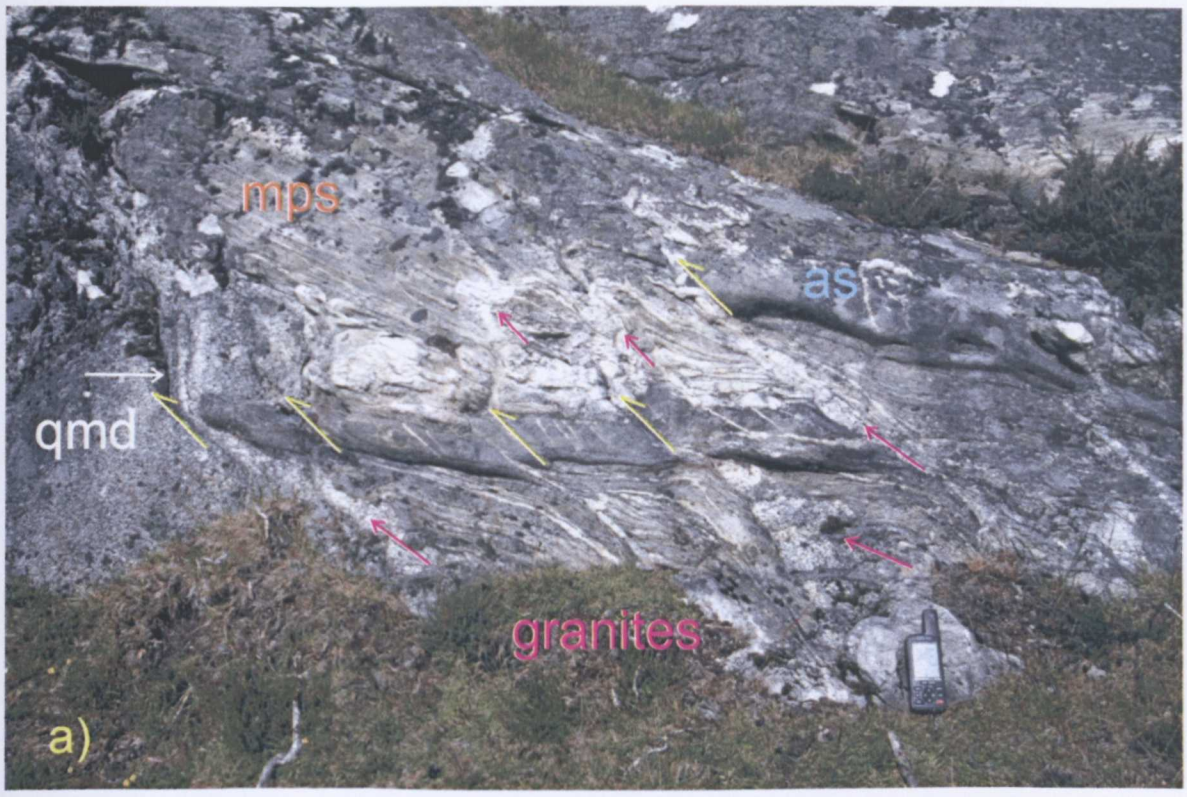

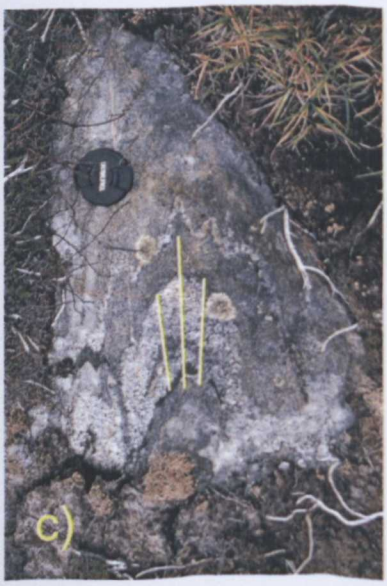

Fig. 3.12 Syn-deformational emplacement of biotite-leucogranite sheets along thrust planes displayed in a 3x2m east-west striking outcrop at NC 0732|0945, east of Garvoult Bridge.

a) Outcrop view, note the amphibolite sheet defining the thrust offsets (thrusts shown in yellow), the main lithologies (qmd = quartz monzodiorite, mps = Morar psammite, as = amphibolite sheet) and granites (indicated by red arrows). b) Detail of the central part. Thrusts and associated folds are shown in yellow, granites are indicated by red arrows. Note the granitic sheets emplaced along thrust planes (1) and the granite ponds in the hangingwall (2). c) Detail of small-scale folds incorporating biotite granite which shows axial planar, high-T foliation (shown in yellow) indicating syn-deformational emplacement.

defined by small feldspar laths and platy brown biotite. The feldspars are locally recrystallized but generally retain euhedral shape and straight grain boundary contacts indicating magmatic-state fabric development. Quartz is generally recrystallized and shows strong grain boundary migration but little subgrain formation, indicating predominantly dislocation glide at lower- to mid-greenschist facies temperatures (c. 400°C, see Fig. 2.1). Although the fabric is clearly recrystallized, there is no evidence for a pervasive, high-strain overprint in the solid-state at low temperatures. In this outcrop, the quartz monzodiorite occurs immediately below the structurally lowest thrust (Fig. 3.12 a), but its structural relationship with the thrust is not known. Nonetheless, this particular outcrop provides good evidence for syn-tectonic granite emplacement during regional D2 deformation associated with thrusting.

3.4.10 Domain 10 – Rogart Station

The Rogart Station complex (enclosure 1) is located on the southeastern side of the central complex, immediately to the north of the Strath Fleet Fault. Variably migmatitic Morar Group psammites are host to several igneous bodies, such as the Reidchalmei quartz monzodiorite and mafic igneous sheets (enclosure 1, Fig. 3.13). To the south of Creag Bhata, leucogranites become progressively more abundant and form the Rogart Station igneous complex in comparable style to the Marian's Rock igneous complex.

The simplified geological map (enclosure 1) shows the overall foliation trend of the Morar migmatites that defines an open, eastward-plunging, eastward-closing antiform. The hinge of this antiform is exposed at NC7375|0180 where it plunges *c.*60° towards the SE. The S_2 foliation of the northern limb strikes roughly NNW-SSE and dips at *c.*65-70° NE whereas on the southwestern limb it strikes WNW-ESE and dips SE at *c.*70°. In the west and northwest of the domain, the planar fabrics of Morar Group rocks, granites and quartz diorites are subvertical and may have been steepened by the expanding central complex. A detailed structural map of this area (Fig 3.13) demonstrates how the S_2 foliations of the country rocks locally swing into parallelism with the pluton boundaries of the Reidchalmei quartz monzodiorite and several smaller mafic sheets.

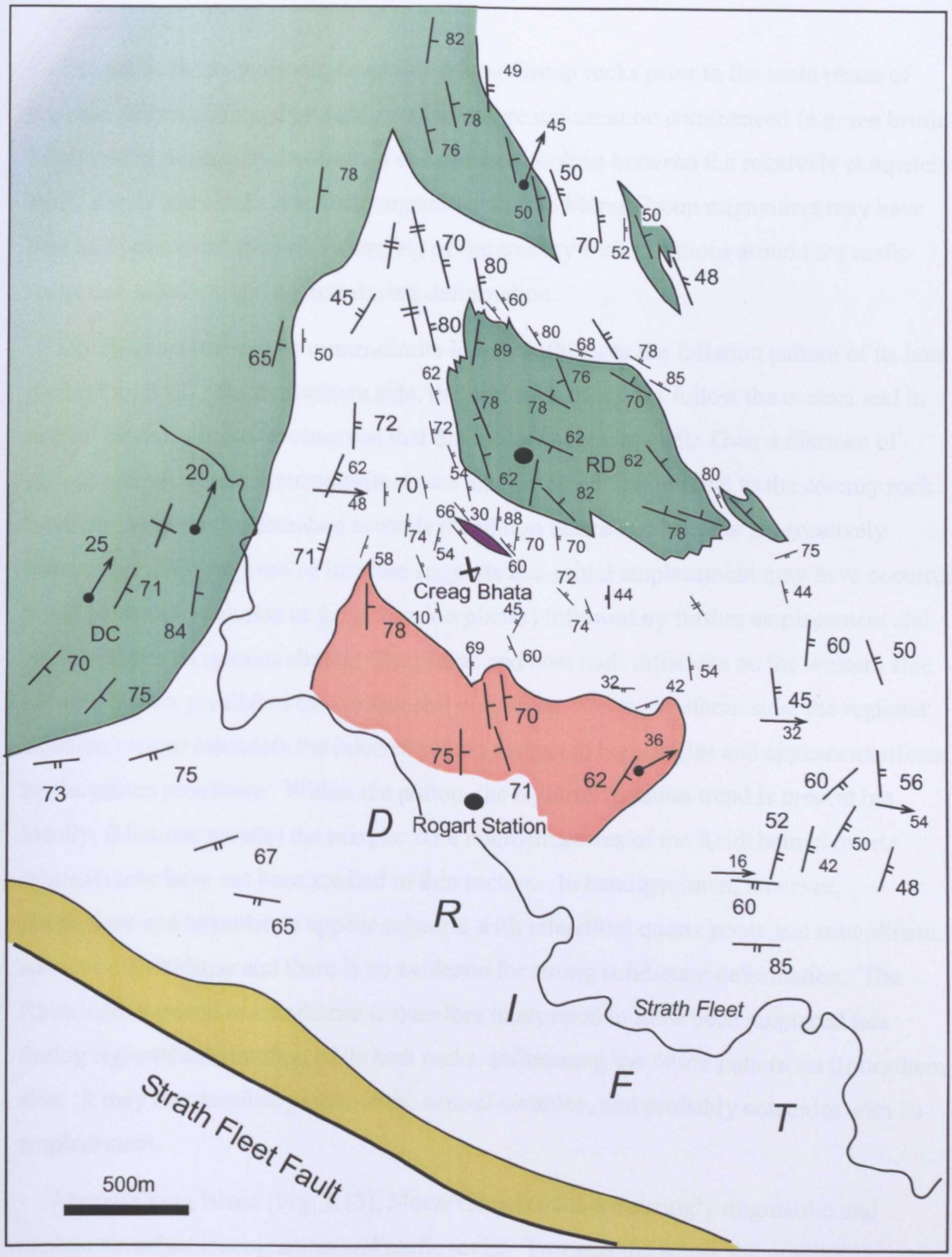

Fig. 3.13 Geological map of Creag Bhata and Rogart Station (domain 10).

Note the clockwise swing of Moine foliations towards the Strath Fleet Fault and the general parallelism of magmatic-state pluton and (solid-state) host rock fabrics. Note also that the quartz monzodiorite of the central complex grades westwards into the central granodiorite. See text.

The mafic sheets were emplaced into Morar Group rocks prior to the main phase of regional deformation and probably cooled before deformation commenced (e.g. see brittle behaviour in domain 9). As such, a competence contrast between the relatively competent, mafic sheets and stocks, and the comparably ductile Morar Group migmatites may have lead to a passive rotation and wrapping of the country rock foliations around the mafic rocks that acted as rigid objects during deformation.

The Reidchalmei quartz monzodiorite locally influences the foliation pattern of its host rocks (Fig. 3.13). On its northern side, the host rock foliations follow the contact and in several outcrops it can be observed that the contact is gradational. Over a distance of several metres, quartz monzodiorite sheets are emplaced first parallel to the country rock foliation but get more abundant towards the pluton centre and become progressively discordant. This progressive increase suggests that initial emplacement may have occurred along planes of weakness (e.g. S_2 foliation planes) followed by further emplacement and amalgamation of igneous sheets. The pluton and host rock foliations on the western side are concordant, parallel to the contact and very steep. On the southern side, the regional foliation pattern intersects the inferred pluton contact at high angles and appears unaffected by the pluton proximity. Within the pluton, the regional foliation trend is present but locally, foliations parallel the margin. The microstructures of the Reidchalmei quartz monzodiorite have not been studied in thin section. In handspecimen, however, plagioclase and hornblende appear euhedral with interstitial quartz pools and subordinate, subhedral K-feldspar and there is no evidence for strong solid-state deformation. The Reidchalmei quartz monzodiorite is therefore interpreted to have been emplaced late during regional deformation of its host rocks, influencing the fabric pattern on its northern side. It may be a satellite pluton of the central complex, and probably coincides with its emplacement.

Around Creag Bhata (Fig. 3.13), Morar Group rocks are strongly migmatitic and contain abundant leucogranites and mafic rocks. Towards the south, the granites become the dominant lithology but commonly retain schlieren or host rock rafts. The change of lithology occurs along strike of the country rock foliation and the mapped boundary does not constitute an igneous contact, but rather defines the area where the leucogranites make up the bulk of the rock (>80%). In this study, the province has been termed the Rogart Station injection complex that in part corresponds to Soper's (1963) " inner migmatite zone with a dominantly igneous portion". The southern boundary of the granite-dominated

domain is covered by drift. Petrographically, the granites are closely comparable to the leucogranite sheets observed in adjacent areas. However, locally, fine grained granodiorites contain rare, euhedral hornblende and titanite that grow within a primary igneous foliation. South of Creag Bhata, several transitions from non-migmatitic Morar Group psammites into injection migmatites into granite have been observed. Although this appears to be a common transition, non-migmatitic grey psammites are also in contact with the granite.

The migmatites contain high but varying amounts of biotite-leucogranite, and the fabric patterns and rock textures vary, depending on granite volume present (Figs. 3.3 & 3.14). At low granite portions, the migmatites locally display a metatexite banding that is laterally continuous, with only occasional, granite-engulfed host rock rafts (see Fig. 3.3 d). At these low granite contents, the contacts between granite and psammite are sharp and both rocks carry foliations that parallel the contact (Fig. 3.14 b). As observed in other domains (2,3,4) the fabric in the granite sheets is typically defined by plagioclase with subordinate, rounded feldspars and ribbon quartz, which shows widespread grain boundary migration. Again this indicates recrystallization and recovery at greenschist facies temperatures. In low-strain zones, however, euhedral crystals and straight grain contacts, indicating magmatic-state fabric development, are preserved. At higher proportions of granite, only the most siliceous psammites retain some lateral continuity whilst less siliceous, and semi-pelitic host rocks have been replaced by granite sheets (Fig. 3.14 c). Occasionally, the granites comprise mafic enclaves that are either undeformed (Fig. 3.14 c & d) and show evidence for hybridisation with the granite (Fig. 3.14 c), or are foliated and flattened parallel to the host rock and granite foliations (Fig. 3.14 b). In intensely deformed areas, where granite is abundant even the most siliceous bands are laterally discontinuous (compare Fig. 3.3 e). In intensely deformed areas with less-abundant granite, leucogranite sheets are concordant to shallowly discordant to the host rock foliation, or are infolded with the Morar Group migmatites (Fig. 3.14 a & e). In the latter case, the granite foliation and the host rock foliation are folded around the same fold hinges, indicating that some granitic sheets must have been emplaced prior to, or early during the deformation. However, cross-cutting relationships of early and late granite sheets have not been observed. Recrystallized quartz provides evidence for low-temperature recovery without high solid-state strain and the granite foliation is therefore interpreted to be predominantly magmatic.

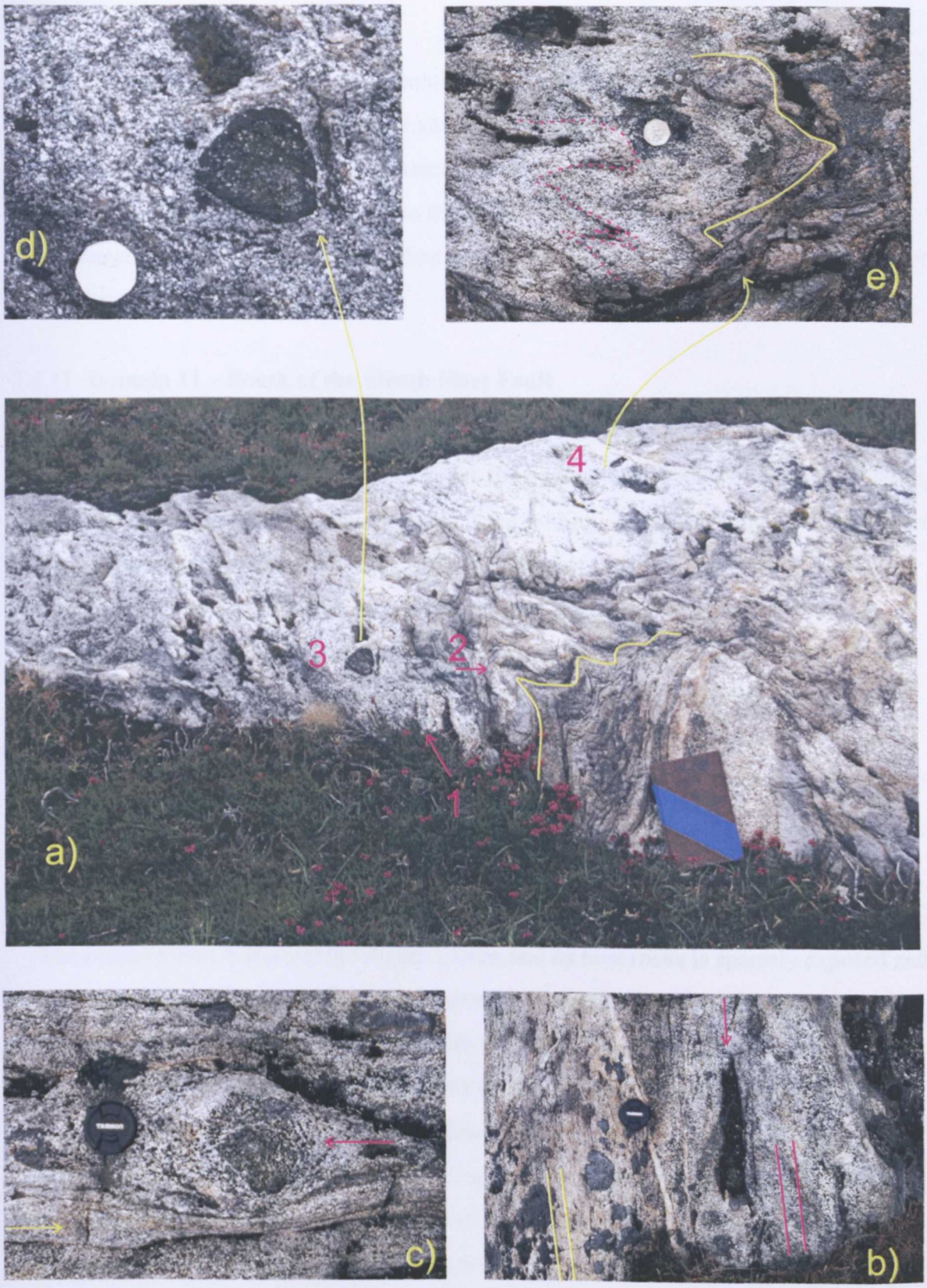

Fig 3.14 Injection migmatites exposed at Creag Bhata.

a) Outcrop view, 1= discordant foliated granite sheet, 2= concordant folded granite vein, 3= mafic enclave, 4= domain of intense small-scale folding. b) Contact of migmatitic psammites and biotite granites, note the parallel foliations (red and yellow lines) and the flattened mafic enclave (red arrow). c) Injection migmatite with high granite content, note the pinch and swell structures (yellow arrow) and the mafic enclave with hybridisation of the surrounding granite (red arrow). d) Detail of mafic enclave within the biotite granite, note the biotite selvedge. e) Detail of the small-scale folds (4), note the parallel fold traces. See text.

The textural style and lateral fabric continuity of the migmatites is controlled by the volume of granitic sheets and there is as such clear evidence for melt-enhanced and melt-controlled deformation. Again, the absence of widespread, solid-state fabrics and the lack of down-temperature deformation within the syn-tectonic sheets suggests that post-emplacement deformation was either taken up elsewhere, or that deformation finished prior to cooling.

3.4.11 Domain 11 – South of the Strath Fleet Fault

The Morar Group psammites to the south of the Strath Fleet Fault have been mapped to the west of Rhaoine towards Meall Dola where the S_2 foliation strikes NE-SW and dips at 40-60° NW or SE indicating kilometre-scale, open folding. Lineations plunge shallowly to the east. Immediately west of Rhaoine, the orientation of the foliation changes and becomes subparallel to the fault with associated lineations plunging to the southeast. Further to the southeast, published data indicates large-scale, open, steeply eastward-plunging, eastward-closing antiforms; the cores of these F2 isoclines locally contain Lewisianoid basement rocks (Strachan & Holdsworth 1988, Soper 1963). Directly south of the fault, the general trend of the foliation strikes NNW-SSE and intersects the trace of the fault at high angles (enclosure 1; Fig. 3.13).

3.4.12 Domain 12 – Creagan Tigh na Creige

The northwestern margin of the Rogart pluton and its host rocks is sparsely exposed and stream sections provide almost the only exposure. Morar Group psammites are occasionally migmatitic and within the stream sections pelitic horizons occur. At Creagan Tigh na Creige (enclosure 1), the S_2 foliations of Morar psammites strike NW-SE and L_2 lineations plunge at *c.*35° to the SE. In the lower parts of the stream sections north of Achatomlinie the orientation of the fabrics change, as S_2 foliations of migmatized psammites strike NE-SW, to E-W and dip NW and SE, to N and S. There, the strike of the foliation generally parallels the overall margin of the central igneous complex. Fold hinges, derived from stereonet analysis, plunge ESE and are also parallel to the pluton margin. This local deviation of foliations from the regional trend, close to the pluton, may relate to the emplacement of the central complex and pluton-induced deformation may also have caused the margin-parallel folding.

3.4.13 Domain 13 – West Langwell to East Langwell

The domain comprises the coarse grained quartz monzodiorite of the central complex that grades over a distance of several 100 metres inwards into the porphyritic granodiorite. Both rock types are essentially foliated. Preferred linear orientations of hornblende and plagioclase are generally absent, except in the east where the quartz monzodiorite occasionally contains a N-NE plunging lineation. Foliations consistently trend NW and dip NE at 60-70°, i.e. away from the pluton centre. In low-strain areas (i.e. inwards of the pluton margin), the fabric of the quartz monzodiorite is defined by euhedral plagioclase and hornblende that together with minor by biotite and interstitial quartz form a magmatic, pre-RCMP fabric (Fig 3.15). In local zones of higher strain, bent feldspars and hornblende indicate some high-temperature, post-RCMP, solid-state deformation and undulose extinction in feldspars indicates a weak low-temperature overprint. Towards the pluton margin, crystals become smaller and subhedral, and the foliation intensifies and is closer spaced (Fig. 3.15). In the east, the magmatic-state foliation is generally very steep and mafic enclaves occur within the foliation planes. They are flattened within the foliation planes and are of oblate shape within foliation planes (Fig. 3.15d). This is interpreted to indicate a mainly flattening strain that may have resulted from the emplacement and ballooning of the central complex.

3.4.14 Domain 14 – Lettie's grave to Dalmore quarry to Muie

The western and central part of this domain comprises porphyritic granodiorite. It is coarse grained and contains a wide-spaced foliation that consistently strikes N-S and dips at 70-85° E and W. It is defined by large (1-2cm) K-feldspar and smaller plagioclase phenocrysts that are often sericitised. The phenocrysts are wrapped by biotite, and quartz forms interstitial multigrain pools. The crystals are generally euhedral and show straight grain contacts indicating original magmatic relationships. Fractures and cracks that occasionally transect K-feldspar phenocrysts perpendicular to its c-axis indicate some brittle deformation (compare Fig. 3.4 b), but overall, the fabric is predominantly magmatic. Towards the east, the granodiorite grades into the quartz monzodiorite over a short distance of commonly less than 100 metres. The foliation developed there in the granodiorite and quartz monzodiorite is still very steep and parallels the pluton margin (enclosure 1). Mafic enclaves that are flattened parallel to the foliation are present throughout this region.

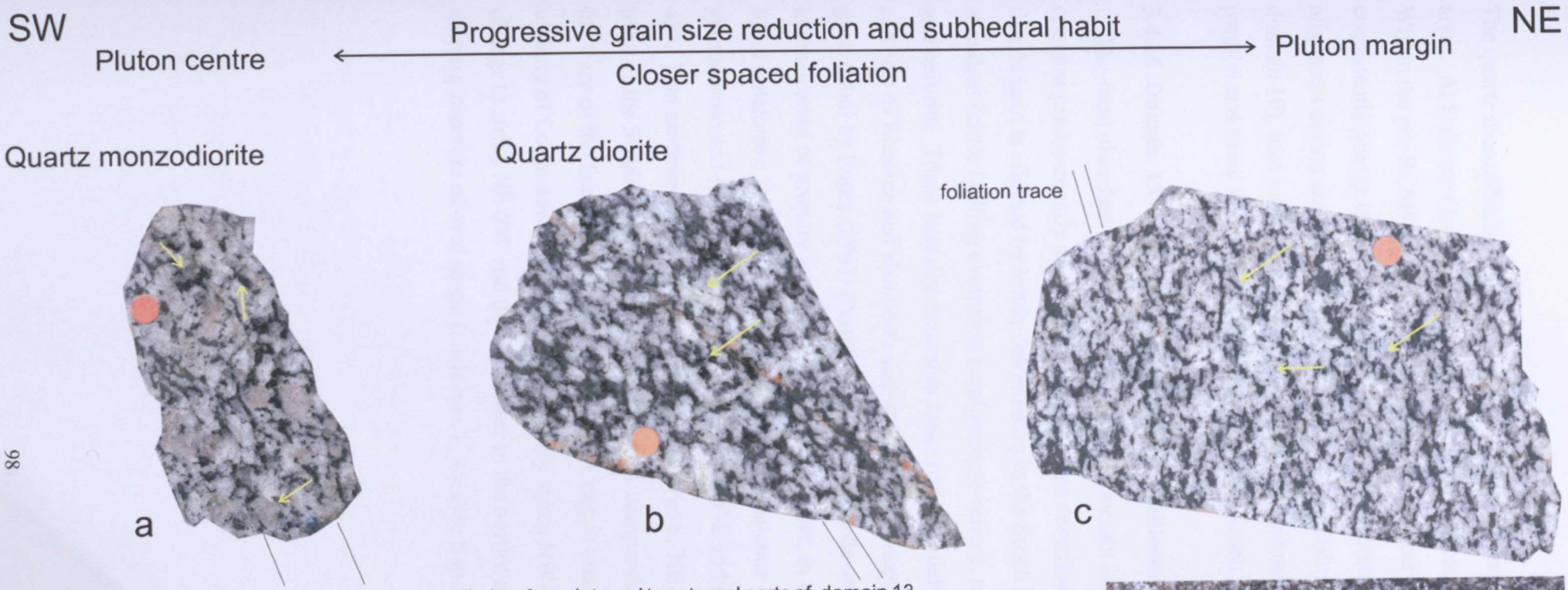

Fig. 3.15 Fabric development in the quartz monzo diorites from internal to external parts of domain 13.

a) Polished slab of quartz monzodiorite, showing the pre-RCMP alignment of euhedral and subhedral K-feldspar, subhedral plagioclase and euhedral hornblende. Note the weakly deformed, circular shaped, interstitial quartz pools (top arrow).

b) Polished slab of quartz diorite comprising small, euhedral hornblende and subhedral plagioclase (pre-RCMP fabric), interstitial quartz pools are oval-shaped. Note the absence of K-feldspar phenocrysts.

c) Polished slab of quartz diorite form the pluton margin. Note the rarity of euhedral plagioclase and the dominant oval-shaped aggregates of plagioclase and quartz inbetween small but still euhedral hornblende.

d) Field photograph showing a close up of a mafic enclave looking down onto a foliation plane within the quartz diorite (at the pluton margin). Note the circular shape of the enclave suggesting flattening strain.

The quartz monzodiorite is heterogeneously deformed and comprises high and low strain areas. At Dalmore Quarry (enclosure 1; Fig. 3.13), it preserves magmatic-state fabrics. Within the pre-RCMP foliation, euhedral hornblende and plagioclase (compare Fig. 3.4 a) consistently plunge towards the N to NE and are interpreted to represent magmatic flow-alignment during emplacement. To the southeast of Dalmore Quarry (overlapping with domain 10), host rock foliations and magmatic-state pluton foliations are essentially parallel and show a clockwise rotation towards the Strath Fleet Fault.

3.4.15 Domain 15 – Muie to Loch Craggie to Collinstown

The most abundant rock type exposed in this domain is the porphyritic granodiorite that contains predominantly magmatic-state fabrics as described above. The southern part of this domain is affected by brittle deformation in the Strath Fleet fault zone and, in places, abundant brittle faulting overprints emplacement-related, magmatic-state fabrics of the granodiorite. These laterally-extensive zones of brittle deformation are well exposed north and east of Rhaoine and also north and east of Loch Craggie and have been mapped in great detail by Soper (1963) ("crush lines"). The brittle overprint locally inhibits the identification of primary igneous foliations. However, in unaffected areas to the west of Muie (enclosure 1), emplacement-related, magmatic-state foliations present within the granodiorite and mafic enclaves strike generally W-E and dip N at shallow angles of *c.*30-45°. 1km northwest of Rhaoine, this foliation turns to NE-SW strike and intersects the trace of the Strath Fleet Fault at a high angle. A comparable swing of foliations towards the trace of the fault is observed around Loch Craggie (enclosure 1). Foliations in the vicinity of Collinstown (enclosure 1) generally strike NW-SE and dip at 50° NE but change to strike NE-SW and dip SE further to the northwest, indicating an overall inward dipping structure of oval shape (enclosure 1, see also Soper 1963).

3.5 Summary of key features

3.5.1 Moine country rocks

The Moine rocks in the study area comprise Naver gneisses and Morar Group psammites and subordinate pelites that are separated by the Naver Thrust (Fig. 3.16). The Naver gneisses comprise dominantly semi-pelitic, strongly-banded gneisses, stromatic metatexites and diatexites. The Morar Group rocks comprise predominantly psammites that are locally injected by abundant leucogranites and thus strongly migmatitic. The Naver Thrust traverses the study area from the northwest to the southeast. Locally abundant leucogranite sheets were emplaced in the vicinity of the thrust and the Moine rocks are strongly migmatized; thus, the identification of a discrete thrust plane is locally difficult. However, the migmatitic Naver gneisses contain garnet in the leucosomes indicating that they were generated by biotite dehydration at high pressures, probably exceeding 10 kbars (e.g. Miller et al. 1997). As comparable garnets are absent in the migmatitic Morar Group rocks, this criterion has been used to infer the location of the Naver Thrust.

On the north and east side of the central complex, the Morar Group psammites and semi-pelites are interleaved with large amounts of biotite-leucogranites and form injection migmatites (Fig. 3.16). Cross-cutting relationships and microstructures indicate that the Morar Group injection migmatites contain different generations of biotite-leucogranites all of which are broadly contemporaneous with D2 deformation. On outcrop scale it is evident that the leucogranites were emplaced along ductile thrusts (domain 9), and that magma was able to flow during folding (domains 4, 10). The texture of the injection migmatites is strongly controlled by the volume of syn-deformationally injected leucogranites (e.g. domain 10). It varies from laterally continuous migmatites to disrupted, alternating bands and lenses of psammites and granites. Granite-dominated areas are developed at Rogart Station and Marians Rock (domains 8 and 10) where leucogranite complexes only locally retain schlieren and rafts of Morar Group rocks. These igneous complexes appear to form areas where leucogranite sheets were able to amalgamate and coalesce during deformation.

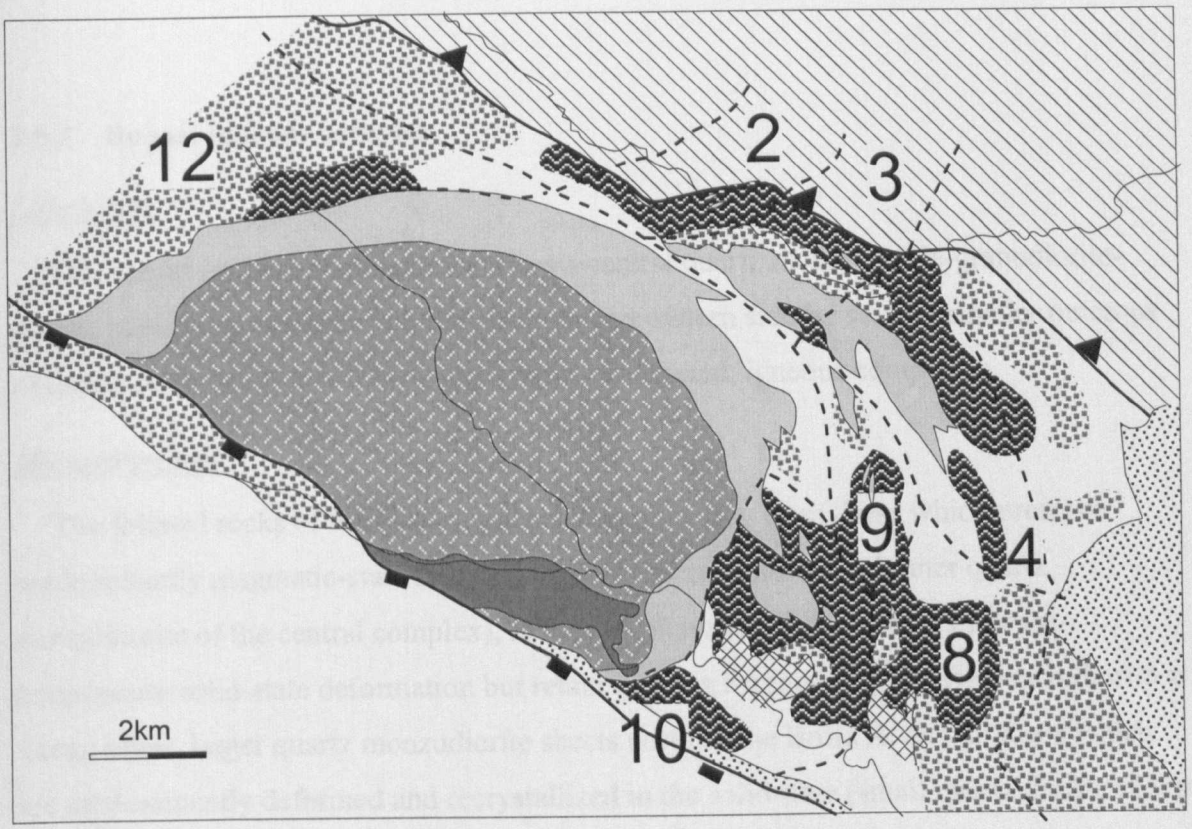

ORS

Moine rocks

Naver gneisses (metatexites & diatexites)

Morar Group injection-migmatites

Morar Group psammites

No data

Leucogranite complexes

Rogart igneous complex

Quartz monzodiorite

Granodiorite

Biotite-K-spar granite

Fig. 3.16 Distribution of Naver gneisses, Morar Group psammites and injection migmatites, leucogranite provinces and rocks assigned to the Rogart igneous complex. Note that although regionally the injection migmatites are spatially associated with the Rogart pluton, they are not part of this magmatic suite. The Rogart igneous complex may have provided heat at deeper crustal levels to generate leucogranites but it did not cause large-scale in situ melting of its host rocks.

3.5.2 Rogart igneous complex

Lithologies

The Rogart igneous complex comprises a central quartz monzodiorite-granodiorite-granite pluton that is flanked on the northern and eastern side by several smaller outcrops of quartz monzodiorite and two leucogranite-dominated, igneous complexes.

Microstructures

The foliated rocks of the Rogart igneous complex vary from those which preserve predominantly magmatic-state fabrics (porphyritic granodiorite and inner quartz monzodiorite of the central complex), to those which show a continuum of down-temperature solid-state deformation but retain igneous features (e.g. quartz monzodiorite at Creag Mhór, larger quartz monzodiorite sheets north of the Brora River), to those which are predominantly deformed and recrystallized in the solid state (small quartz diorite sheets north of the Brora River and Creag Mhór sheet at Cnoc Arthur) (Fig. 3.17 a). The microfabrics indicate that the Rogart pluton comprises the following igneous bodies (excluding the leucogranite-complexes): a central quartz monzodiorite-granodiorite-granite complex (possibly including the Reidchalmei quartz monzodiorite), the Creag Mhór quartz monzodiorite sheet, and several smaller quartz (monzo)diorite sheets to the north which are in the following referred to as the "Brora River sheets" (Fig. 3.17 b).

The porphyritic granodiorite of the central complex comprises microstructures that demonstrate predominantly magmatic-state, pre-RCMP alignment of early crystallizing feldspars and plagioclase that are wrapped by biotite, with quartz being mostly interstitial. The quartz monzodiorite shows similar magmatic-state fabrics, but in local high strain zones and at the pluton margin there is evidence for ductile, solid-state deformation and recrystallization at temperatures corresponding to lower amphibolite to greenschist facies (see table 3.1). Brittle deformation occurs in all rock types of the central complex along the Strath Fleet Fault in the south. The central complex shows no evidence for down-temperature deformation, or intense recrystallization and deformation in the solid-state, instead magmatic-state fabrics are dominant.

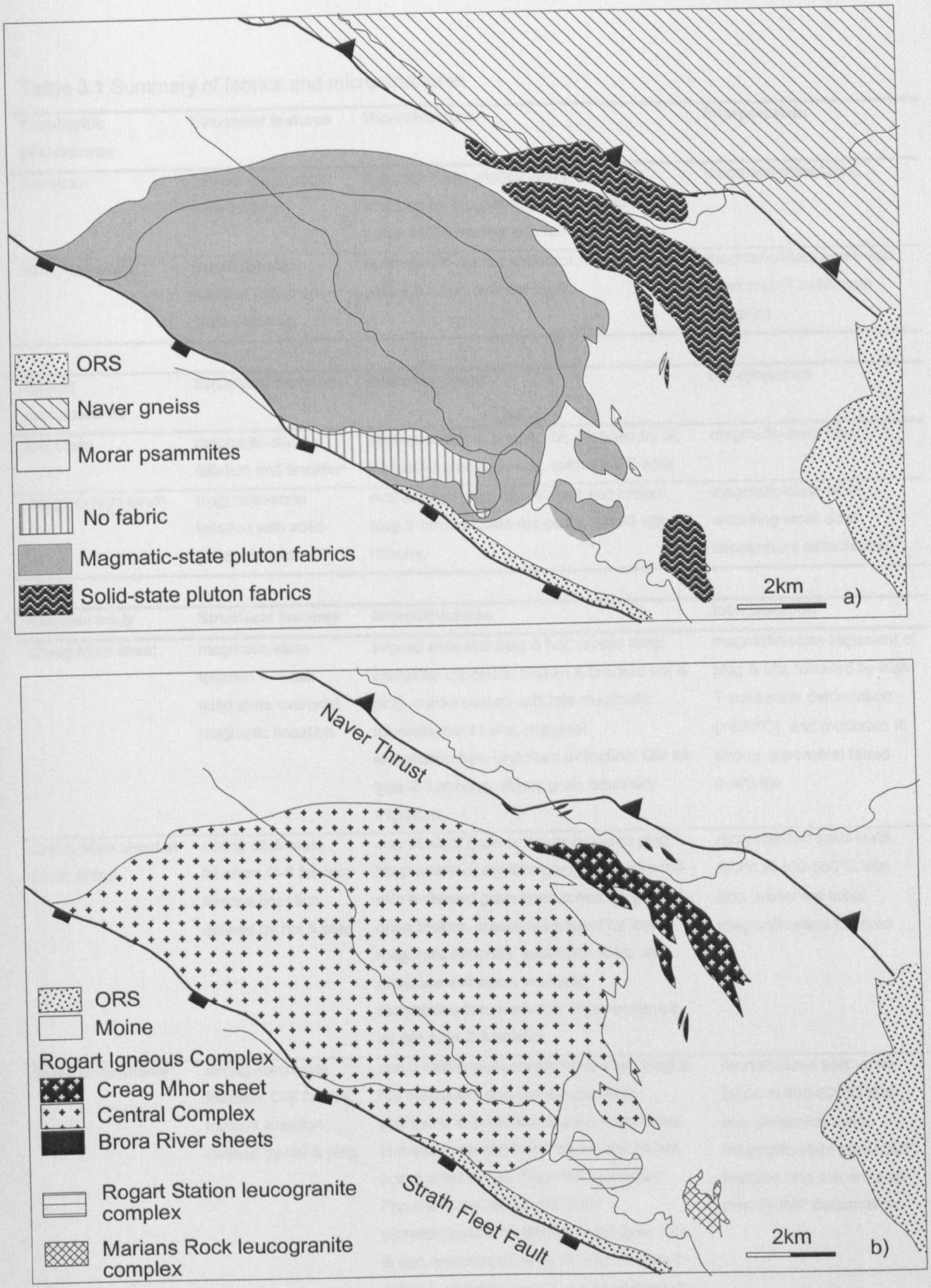

Fig. 3.17 a) Distribution of magmatic-state and solid-state microstructures of the Rogart igneous rocks. b) Proposed igneous bodies contained within the Rogart igneous complex.

Table 3.1 Summary of fabrics and microstructures

Porphyritic granodiorite	Structural features	Microstructures	Interpretation
low strain	coarse, magmatic-state foliation	euhedral K-fsp aligned with plag laths; wrapped by bt; undeformed interstitial qtz pools. brittle fracturing & faulting in S	magmatic-state fabric
local high strain	magmatic-state foliation with solid-state overprint	subhedral K-fsp but euhedral plag; occ. bent plag & K-spar, oval qtz-pools	magmatic-state fabric with weak high-T solid-state overprint

Quartz monzodiorite	Structural features	Microstructures	Interpretation
low strain	magmatic-state foliation and lineation	aligned euhedral plag & hbl; wrapped by bt; interstitial qtz-pools; occ. subhedral K-spar	magmatic-state fabric
marginal high strain	magmatic-state foliation with solid-state overprint	oval shaped plag; occ. kinked and broken plag & hbl; elongate qtz-pools, type-3 qtz-ribbons	magmatic-state fabric recording weak down temperature deformation

Plutonic body	Structural features	Microstructures	Interpretation
Creag Mhór sheet	magmatic-state foliation + weak solid-state overprint magmatic lineation	aligned euhedral plag & hbl; crystal tiling; interstitial qtz-pools; broken & cracked hbl & plag, cracks healed with late magmatic minerals, bent twins, marginal recrystallization; undulose extinction; Qtz as type 2-3 ribbons, strong grain boundary migration	magmatic-state alignment of plag & hbl, followed by high T solid-state deformation (>650°C), and moderate to strong greenshist facies overprint
Creag Mhór sheet at Cnoc Arthur	strong soldi-state foliation; C-S fabrics; mineral lineation defined by hbl & plag	occ. straight grain contacts between plag & hbl preserved; crystals generally subhedral with embayed grain boundaries; plag & hbl often broken, cracks not healed by late magmatic minerals; subhedral K-fsp with undulose extinction, marginal recrystallization, exolution, myrmekite; qtz as flat, type 2-3 ribbons	recrystallized solid-state fabric at 400-500°C that occ. preserves initial magmatic-state features
Brora River sheets	strong solid-state foliation; C-S fabrics; mineral lineation defined by hbl & plag	occ. straight grain contacts between plag & hbl preserved, crystals are generally subhedral with embayed grain boundaries and often cracked and broken, cracks are occ. healed by late magmatic minerals; Fsp show bent twins, marginal recrystallization, undulose exctinction; Hbl is occ. recrystazllized by bt; Qtz as type-3 ribbons, showing abundant grain boundary migration	recrystallized solid-state fabric at 400-500°C that occ. preserves initial magmatic-state pre-RCMP features and evidence for post-RCMP deformation

The Creag Mhór sheet shows a continuum of down-temperature deformation from the magmatic to the solid-state at *c.* 400°C. Within the Creag Mhór sheet, magmatic-state alignment and tiling of euhedral plagioclase and hornblende is preserved in a low strain area at Creag Mhór, and brittle cracks in hornblende are healed with late magmatic minerals. Quartz monzodiorite outcrops towards Cnoc Arthur are characterized by microstructures indicating dominantly ductile deformation and recrystallization at temperatures corresponding to lower amphibolite – to greenschist facies. The small Brora River quartz monzodiorite sheets show dominantly solid-state fabrics, and only occasionally preserve initial magmatic-state features. They rarely contain evidence for high-temperature solid-state deformation and instead show distinct solid-state microstructures formed at temperatures between *c.* 400-500°C. The larger Brora River sheets locally contain microstructures indicating a continuum of down-temperature fabric development. Overall, the Brora River- and Creag Mhór sheets show distinct solid-state fabrics that are absent from the other parts of the Rogart igneous complex (table 3.1).

3.5.3 Cross-cutting relationships of the Rogart igneous complex and its host rocks

Creag Mhór- and Brora River sheets

At Creag Mhór, the contacts are concordant and magmatic-state pluton foliations parallel S_2 host rock foliations, suggesting broadly contemporaneous fabric development. In adjacent areas, the magmatic to solid-state pluton fabrics are parallel to the host rock fabrics although the quartz monzodiorite shallowly cuts across the S_2 host rock foliation. Together, this suggests that the Creag Mhór sheet was emplaced after the initial fabric had formed but prior to the end of regional ductile deformation. Southeast of the Brora Gorge, the Brora River sheets gently cross-cut the composite S_2 foliation of the Morar Group rocks but solid-state pluton fabrics generally parallel the S_2 host rock fabrics, again indicating that emplacement preceded the deformation. To the east and over large areas of domains 3 and 4 (enclosure 1), the contacts between the Brora River sheets and their host rocks are not exposed. Two quartz monzodiorite sheets which are steeply discordant to the Moine rock foliation and biotite-leucogranites have been observed (at Grumby Rock and in domain 3), where they carry thrust-related solid-state fabrics.

Central Complex

On a regional scale, the central complex is discordant to the composite S_2 foliation of the Moine country rocks and re-orientates and steepens the host rock fabrics especially to

its north and east (e.g. domains 1, 2, 3, 9, 10, 13, Fig. 3.18 a, see also Soper 1963). However, in the southeast, the quartz monzodiorite is intruded parallel to the S_2 foliation of the Moine rocks, and magmatic–state foliations of the quartz monzodiorite are generally parallel to the host rock foliations.

3.5.4 Large-scale host rock and pluton fabric patterns

Host rocks

The composite foliation of the Moine rocks swings around the central Rogart igneous complex, and is very steep on its northern side. On the western side, the country rock foliation is locally parallel to the pluton contact. To the eastern side of the central complex, a triangular zone exists in between the Naver Thrust, the Strath Fleet Fault, and the central complex. In general, the fabric patterns away from the central complex (i.e. domains 4, 6, and 7) dip gently to the east and appear little affected by pluton-related deformation. In contrast, a significant steepening of planar structures and lineations that deviate from the regional E-ESE plunging trend are observed in domains 9 and 10. In domains 8 and 10, the presence of smaller quartz monzodiorite bodies, mafic sheets and leucogranites locally further complicates the host rock fabric patterns, as host rock S_2 fabrics are rotated into parallelism with the respective pluton margins. In domain 10, a significant swing of planar fabrics in both, the central complex and the host rocks is observed, as the fabrics are turning clockwise towards the Strath Fleet Fault.

Plutons

Magmatic-state foliations of the central complex generally parallel the pluton margin and are subvertical on the eastern pluton side (Fig. 3.18 b). Foliations in the northern part of the central complex dip at *c.* 60° outwards, away from the pluton centre (domain 14). Within the central- to western part of the porphyritic granodiorite (domains 13 & 15), foliations form a kidney-shaped, inward dipping funnel structure, which has been previously described as an asymmetrically centred funnel structure (Soper 1963, 1999). Linear and planar, solid-state fabrics developed in the Creag Mhór-, Brora River sheets generally parallel the respective local D2 host rock fabrics (e.g. Creag Mhór, domain 3, Cnoc Arthur).

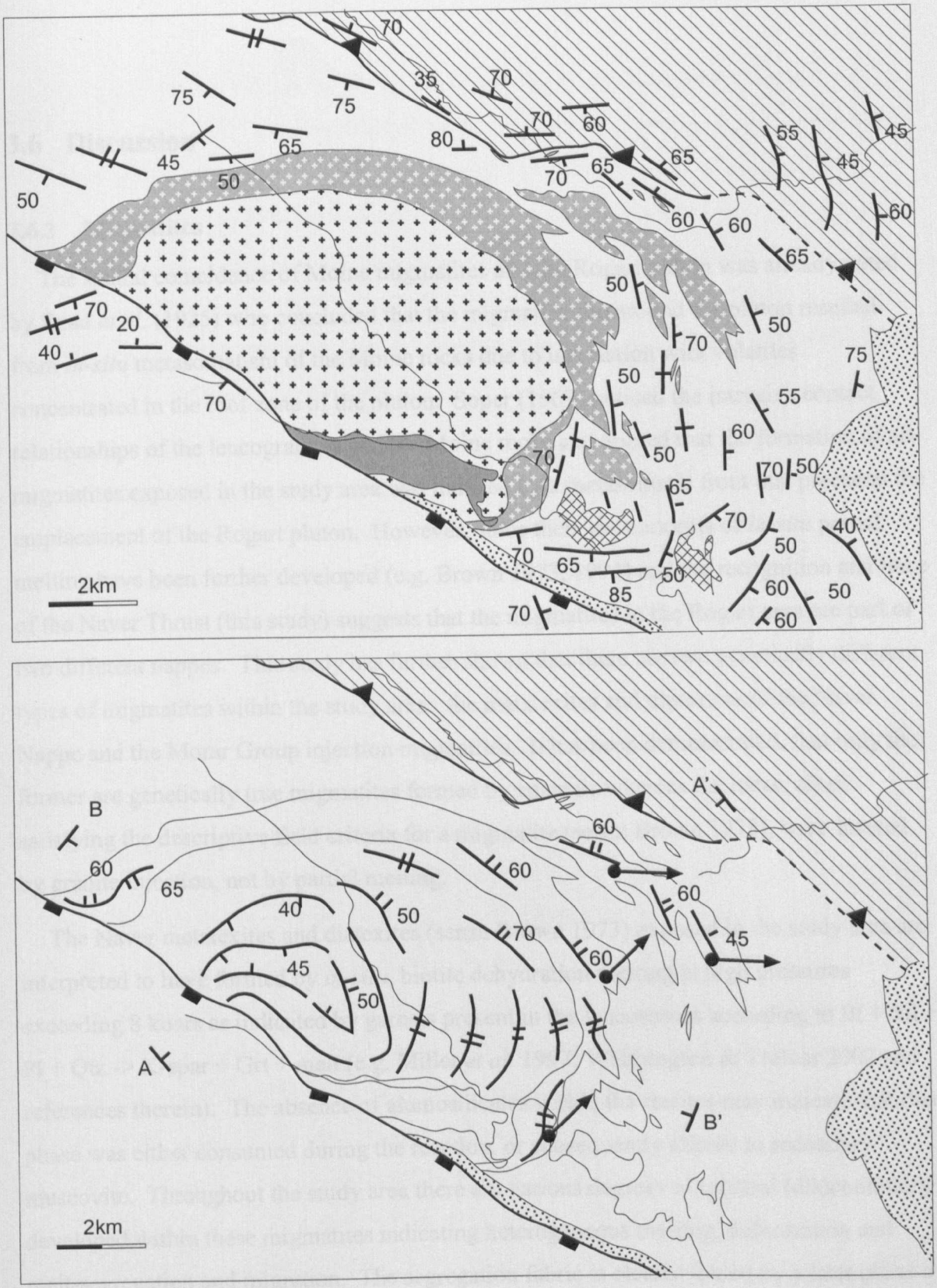

Fig. 3.18 Simplified pluton and host rock fabric patterns of the Rogart area.

a) Large-scale S_2 foliation pattern of the Moine country rocks. Note the clockwise swing of S_2 foliations towards the trace of the Strath Fleet Fault in the southeast indicating fabric development during dextral shear.

b) Pluton foliation patterns. Note the kidney-shaped funnel structure in the central complex, the subvertical foliations to its east and the outward dipping foliations in the northeast. Also note easterly plunging lineations in the Creag Mhor sheet and the northerly plunging lineations on the eastern side of the central complex.

3.6 Discussion

3.6.1 Migmatites

The spatial coincidence of Moine migmatites and the Rogart pluton was already noted by Read *et al.* (1925) who concluded that the migmatization around the pluton resulted from *in-situ* metasomatism of the Moine rocks due to interaction with volatiles concentrated in the roof zone of the pluton. Soper (1963) noticed the intrusive contact relationships of the leucogranites and the Moine rocks and argued that the formation of all migmatites exposed in the study area was induced by a metasomatic front that preceded the emplacement of the Rogart pluton. However, since then, the concepts of *in-situ* partial melting have been further developed (e.g. Brown 1973, 1994) and the recognition and trace of the Naver Thrust (this study) suggests that the migmatites in the Rogart area are part of two different nappes. This study has further shown that there are two genetically different types of migmatites within the study area: the metatexites and diatexites of the Naver Nappe and the Morar Group injection migmatites. It has been demonstrated, that only the former are genetically true migmatites formed by anatexis whereas the latter, albeit satisfying the descriptive field criteria for a migmatite (sensu Brown 1973), were formed by granite injection, not by partial melting.

The Naver metatexites and diatexites (sensu Brown 1973) exposed in the study area are interpreted to have formed by *in-situ*, biotite dehydration melting at high pressures exceeding 8 kbars as indicated by garnets present in the leucosomes according to Bt + Sil + Pl + Qtz -> K-spar + Grt + melt (e.g. Miller *et al.* 1997; Whithington & Treloar 2002 and references therein). The absence of alumosilicates within the restites may indicate that this phase was either consumed during the reaction, or subsequently altered to secondary muscovite. Throughout the study area there are various degrees of textural (dis)continuity developed within these migmatites indicating heterogeneous melting, deformation and melt-segregation and migration. The segregation fabric is clearly folded by a later phase of deformation, indicating that this partial melting event occurred early within the geological history of the study area. At present, the absence of a detailed geochemical, P-T, metamorphic and age data for these migmatites precludes the detailed evaluation of their formation. However, comparable migmatites have been identified above the Naver Thrust on the north coast where they formed during a high-pressure melting event during crustal

thickening at *c.* 470 - 460 Ma (U-Pb SHRIMP zircon, Kinny *et al.* 1999, Friend *et al.* 2000). The metatexites and diatexites of the Naver Nappe exposed at Rogart share a common petrology, relative deformational history, migmatitic textures and structural settings with the comparatively well understood migmatites exposed to the north. It is therefore tentatively proposed that the Naver metatexites exposed at Rogart relate to the same, early Ordovician high-pressure melting event discovered further north. However, this requires rigorous testing by high-precision age dating of leucosomes with well-defined structural and metamorphic relationships.

In contrast to earlier views, the injection migmatites on the north and east side of the central complex have demonstrably been formed by the syn-tectonic injection of biotite-leucogranites into Morar Group rocks (e.g. domains 2, 3, 4, 9 & 10, Figs. 3.3 & 3.14) and not by *in-situ* partial melting or metasomatism. On outcrop scale, it can be shown that the intrusion of leucogranites was broadly contemporaneous with the main phase of ductile folding and thrusting effecting the host rocks (e.g. domains 4, 9 & 10, Fig 3.12), although their diverse structural settings indicate various early-to-late syn-D2 granite generations. Although possible mechanisms of leucogranite emplacement can be observed in the study area, evidence for the onset of melt generation, melt source, segregation, and migration are not exposed. The spatial coincidence of the injection migmatites and the Rogart pluton suggests some form of genetic relationship (e.g. Read *et al.* 1925; Soper 1963) and it needs to be evaluated whether the leucogranites may belong to the Rogart igneous suite, or are crustal melts. The Rogart pluton has been established as a member of the mantle-derived Caledonian high Ba-Sr suite (Fowler *et al.* 2001). Crustal melting and migmatization have been the subject of intense isotope-based geochemical research which highlights that parameters such as the protolith, the melting processes, the degree of partial melting and stable mineral phases at the time of partial fusion may lead to very heterogeneous granitic melts (e.g. Brown 1973, 1994; Patino Douce & Beard 1995; Pressley & Brown 1999; Withington & Treloar 2002; and references therein). This study does not possess the necessary detailed isotopic data to evaluate melt generation processes. However, available whole rock major and in particular REE data permit a tentative comparison of the leucogranites, the Rogart pluton and possible alternative crustal protoliths (Moine) (Fig. 3.19).

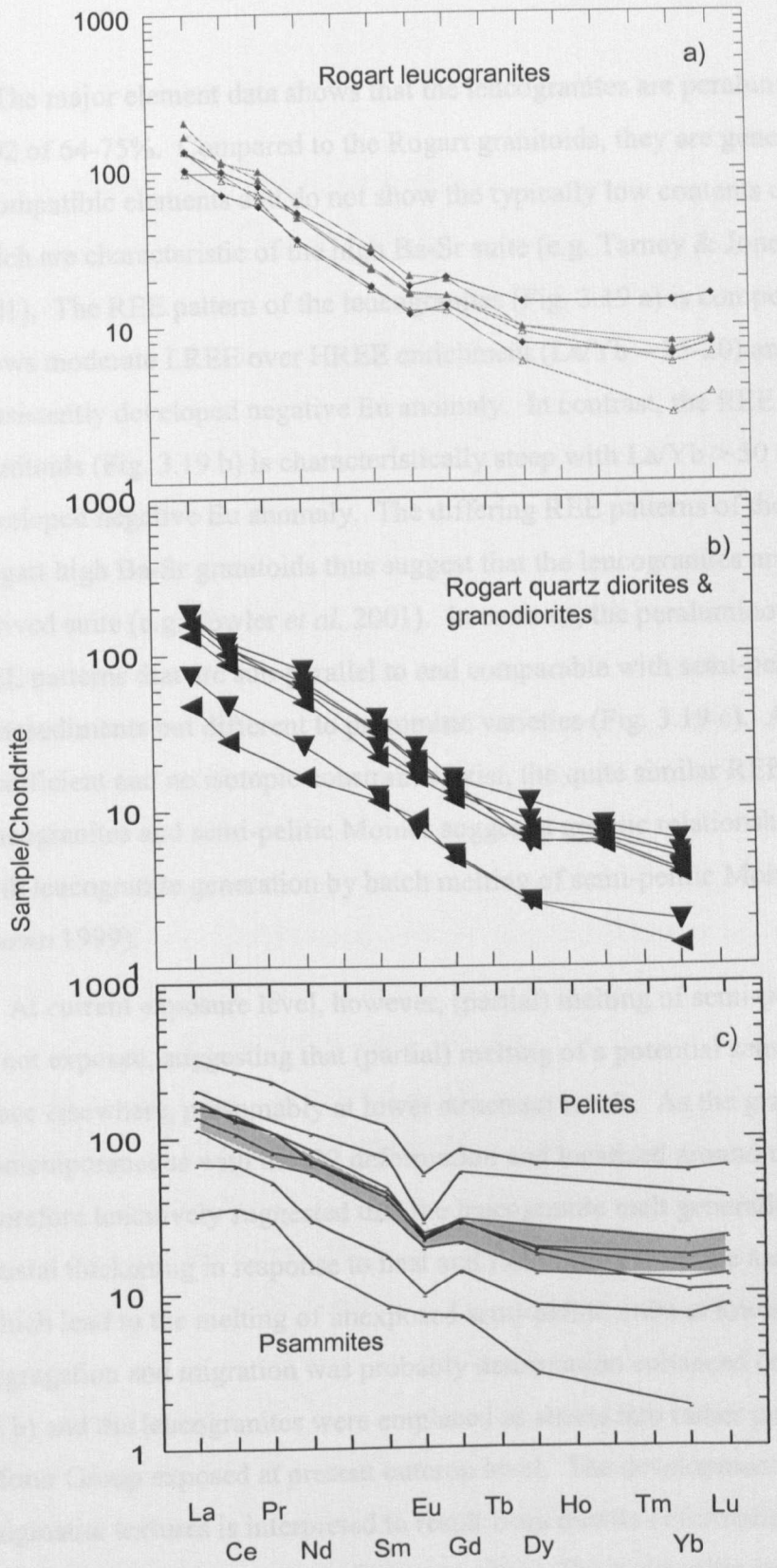

Fig. 3.19 REE patterns of the Rogart leucogranites (a) compared to the Rogart central complex (b) and Moine metasediments (c). Note the small but consistently developed, negative Eu anomaly in the leucogranites that is absent from the quartzdiorites and granodiorites. Overall, the REE pattern of the leucogranites is comparable to semi-pelitic Moine metasediments (grey field in b) consistent with leucogranite melt generation by fusion of Moine meta-pelites at depth. See text. Diagrams b) and c) were kindly provided by Dr. M. Fowler.

The major element data shows that the leucogranites are peraluminous granites with SiO2 of 64-75%. Compared to the Rogart granitoids, they are generally less enriched in incompatible elements and do not show the typically low contents of Y and heavy REE which are characteristic of the high Ba-Sr suite (e.g. Tarney & Jones 1994; Fowler *et al.* 2001). The REE pattern of the leucogranites (Fig. 3.19 a) is comperably shallow and shows moderate LREE over HREE enrichment (La/Yb ~ 15-20) and has a small, but consistently developed negative Eu anomaly. In contrast, the REE pattern of the Rogart granitoids (Fig. 3.19 b) is characteristically steep with La/Yb > 50 and lacks a widely developed negative Eu anomaly. The differing REE patterns of the leucogranites and the Rogart high Ba-Sr granitoids thus suggest that the leucogranites are not part of this mantle-derived suite (e.g. Fowler *et al.* 2001). In contrast, the peraluminous leucogranites show REE patterns that are sub-parallel to and comparable with semi-pelitic Moine metasediments but different to psammitic varieties (Fig. 3.19 c). Although the data set is insufficient and no isotopic constraints exist, the quite similar REE patterns of leucogranites and semi-pelitic Moines suggest a genetic relationship and are consistent with leucogranite generation by batch melting of semi-pelitic Moine rocks (e.g. Pressley & Brown 1999).

At current exposure level, however, (partial) melting of semi-pelitic Morar Group units is not exposed, suggesting that (partial) melting of a potential semi-pelitic protolith took place elsewhere, presumably at lower structural levels. As the granite injection is contemporaneous with the D2 deformation and localized around the Rogart pluton it is therefore tentatively suggested that the leucogranite melt generation occurred during D2 crustal thickening in response to heat and fluid influx from the ascending Rogart magma which lead to the melting of unexposed semi-pelitic units at lower crustal levels. Melt segregation and migration was probably deformation enhanced (e.g. Brown & Solar 1998 a & b) and the leucogranites were emplaced as sheets into rather psammitic units of the Morar Group exposed at present outcrop level. The development of the variably disrupted migmatite textures is interpreted to result from ductile deformation of injection migmatites containing variable amounts of leucogranites. The metatexitic layering observed locally in semi-pelitic Morar Group rocks, at present, remains enigmatic. It could relate to a separate, earlier migmatization event which may coincide with the formation of the Naver migmatites. However, the degree of injection-induced anatexis in the Morar Group host rocks exposed at present day level is unknown.

3.6.2 Pluton emplacement

3.6.2.1 Pluton shape and fabric patterns

In 2D map view, the shape of the central complex can be described as a teardrop-shaped, fault-bound intrusion that is flanked by several, smaller quartz monzodiorite plutons of possibly sheet geometry (Fig. 3.18). The surface data allows several 3D pluton geometries to be inferred (Fig. 3.20). Three of the hypothetical cross-sections (3.20 a to c) are drawn NE-SW along the same line of section using the same surface data, whereas the fourth (3.20 d) strikes NW-SE. All sections are shown pre-normal faulting. Fig. 3.20a shows the central complex interpreted as a large-scale shear body in the footwall of the Naver Thrust with the Creag Mhór sheet forming an individual duplex to the north. This geometry is entirely consistent with the steep, outward dipping foliations at the N margin which shallow out towards the centre and is further supported by the proximity of the Naver Thrust, the observed thrust-related emplacement of leucogranites (see below) and the C-S shear fabrics, developed in the Creag Mhór sheet. However, the concentric petrological zoning and the absence of C-S fabrics within the central complex make this 3D pluton geometry, as a whole, unlikely. Fig. 3.20b shows the complex as a ballooned sheet in the footwall of the Naver Thrust, comparable to pluton geometries inferred for high Himalayan granite sheets (Searle *et al.* 1997). Although all the surface data are satisfied, explaining the concentric nature of the central complex is again problematic. Fig. 3.20c (drawn along the same line of section) shows a diapir that has experienced post-emplacement deformation. The Creag Mhór sheet is now drawn as an apophysis of the central complex and weak deformation whilst the pluton is still in the magmatic-state could account for the changes in foliation attenuation. Although this satisfies the concentric petrological zoning of the central complex, it neglects the sheet-like nature of the northern quartz monzodiorites, the Naver Thrust, and the distribution of the microfabrics.
Fig. 3.20d shows a model based on Soper's "ballooning diapir" (1963) and satisfies all surface data in the line of section. It shows host rock deformation that may be induced by the emplacement of the central complex but neglects the Strath Fleet Fault and the Naver Thrust as the section runs parallel to these structures.

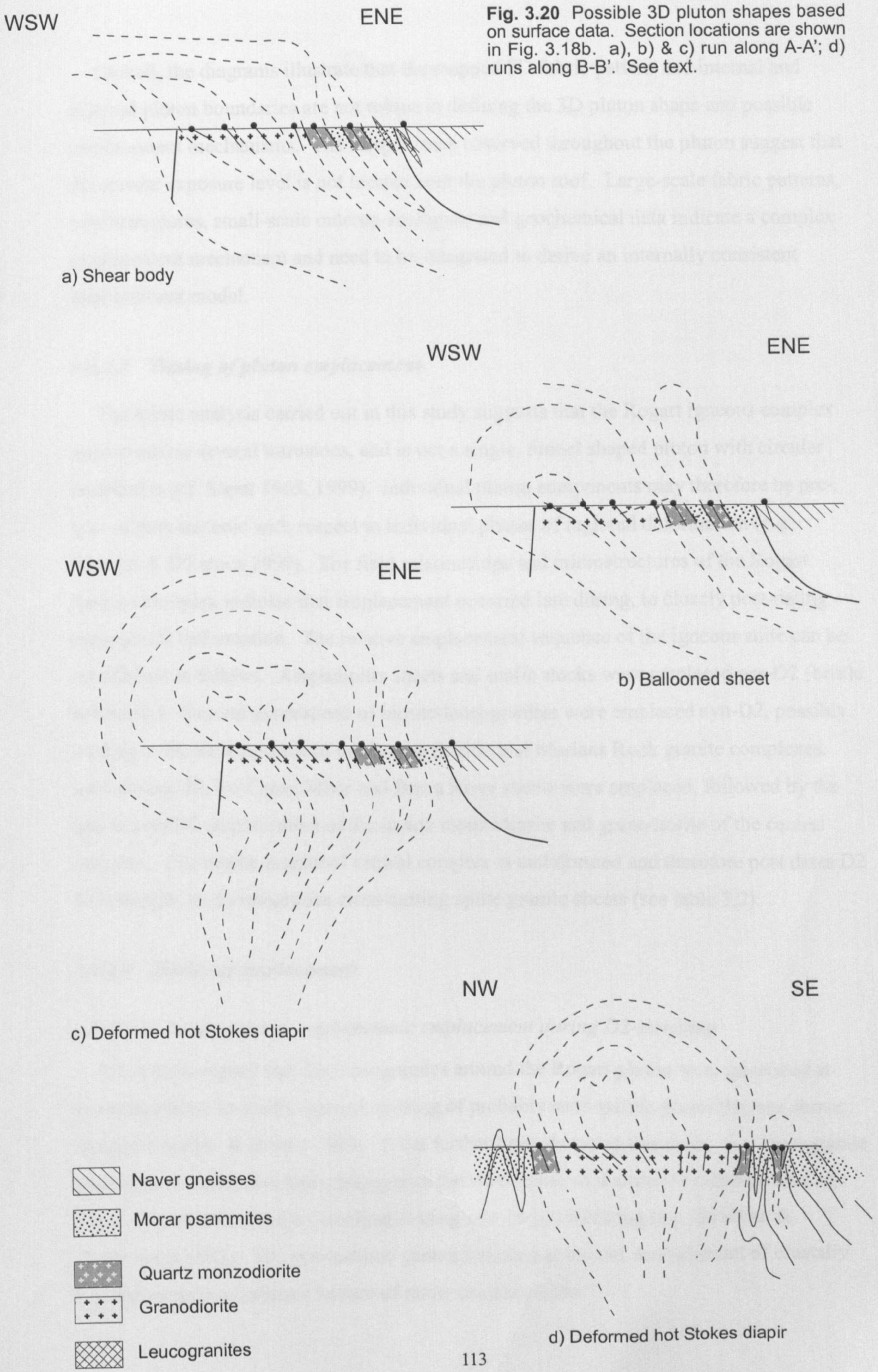

Fig. 3.20 Possible 3D pluton shapes based on surface data. Section locations are shown in Fig. 3.18b. a), b) & c) run along A-A'; d) runs along B-B'. See text.

Overall, the diagrams illustrate that the mapped 2D fabric pattern and internal and external pluton boundaries are not robust in defining the 3D pluton shape and possible emplacement mechanisms. The steep fabrics observed throughout the pluton suggest that the current exposure level is not located near the pluton roof. Large-scale fabric patterns, microstructures, small-scale outcrop analogues and geochemical data indicate a complex emplacement mechanism and need to be integrated to derive an internally consistent emplacement model.

3.6.2.2 Timing of pluton emplacement

The fabric analysis carried out in this study suggests that the Rogart igneous complex may comprise several intrusions, and is not a single, funnel shaped pluton with circular boundaries (cf. Soper 1963, 1999). Individual pluton components may therefore be pre-, syn- or post-tectonic with respect to individual phases of regional deformation (e.g. Samson & D'Lemos 1999). The field relationships and microstructures of the Rogart igneous complex indicate that emplacement occurred late during, to closely post-dating regional D2 deformation. The relative emplacement sequence of the igneous suite can be established as follows. Amphibolite sheets and mafic stocks were emplaced pre-D2 (brittle behaviour). Several generations of biotite-leucogranites were emplaced syn-D2, possibly leading to the development of the Rogart Station and Marians Rock granite complexes. Late during D2, the Creag Mhór and Brora River sheets were emplaced, followed by the late to post D2 emplacement of the quartz monzodiorite and granodiorite of the central complex. The biotite granite of central complex is undeformed and therefore post dates D2 deformation, as do ubiquitous cross-cutting aplite granite sheets (see table 3.2).

3.6.2.3 Modes of emplacement

3.6.2.3.1 Leucogranites – syn-tectonic emplacement during D2-thrusting

It has been argued that the leucogranites around the Rogart pluton were generated at lower structural levels by (partial) melting of probably semi-pelitic protoliths (see above; see also Pressley & Brown 1999). It has further been shown in this study, that leucogranite emplacement was contemporaneous with the main phase of ductile D2 deformation (e.g. Fig. 3.14), characterized by isoclinal folding and ductile thrusting (e.g. Strachan & Holdsworth 1988). The syn-tectonic generation, migration and emplacement of crustally derived melts is a common feature of many orogenic belts

Table 3.2 Timing of emplacement of individual igneous bodies assigned to the Rogart igneous complex (old to young from bottom to top).

Igneous body / timing / mode	Evidence	Locality	Other
Aplite granite sheets	Cross-cut pluton host rock boundaries and are undeformed.	Throughout.	
Central Complex emplaced post-D2 thrusting, possibly during right lateral movements along the Strath Fleet Fault.	No D2 thrust-related pluton fabrics; steepening of D2-thrust fabrics in host rocks.	Domains 13, 14, 15; N & NE margins of pluton.	Itself composite with outer quartz monzodiorite, porphyritic granodiorite and biotite granite forming consecutive igneous pulses. Reidchalmei quartz monzodiorite possibly coincides with emplacement of central complex.
Creag Mhór & Brora River sheets emplaced into Naver Thrust footwall after initial formation of D2-fabrics in host rocks but prior to termination of W-directed D2 deformation.	Locally cross-cutting the composite S2-foliation but containing foliations and lineations which parallel D2 host rock fabrics; also W-directed shear sense indicators & C-S fabrics and therefore D2-related fabrics.	Creag Mhór, Cnoc Arthur, Brora River, Grumby Rock - (domains 2, 3 & 4)	Down-temperature deformation, occ. preserving magmatic-state fabrics but dominant solid-state overprint. Possibly confined to footwall due to density barrier generated by leucogranites focussed into the thrust plane.
Leucogranite sheets emplaced broadly contemporaneous with D2, several pre-, syn- and post-tectonic suites.	In outcrop syn-thrusting (D2), syn-D2 folding, but also cross-cutting S2 fabrics and discordant.	e.g. domains3, 4, 8, 9, 10 see Figs. 3.11 & 3.13	Formation of Morar Group injection-migmatites. Possibly coalescing to form Rogart Station- and Marian's Rock leucogranite provinces. Possibly focused into Naver Thrust leading to large granite volumes obscuring thrust plane.
Mafic sheets & stocks emplaced into Morar Group prior to D2 deformation.	Brittle behaviour during D2 deformation (outcrop).	e.g. domain 9, see Fig. 3.11	May influence host rock fabrics due to "rigid object" behaviour during D2.

(e.g. Appalachians, Solar *et al.* 1998; Himalayas, Weinberg & Searle 1999; East Greenland Caledonides, Strachan *et al.* 2001) and tectonically induced melt extraction and migration by pervasive flow through ductily-deforming crust is currently viewed as a very important ascent and emplacement mechanism (e.g. Collins & Sawyer 1996; Brown & Rushmer 1997; Brown & Solar 1998b; Weinberg & Searle 1999; Strachan *et al.* 2001). The Rogart leucogranites show many features compatible with these processes (Fig. 3.21): sub-concordant, centimetre to metre- scale melt sheets were emplaced along previously formed foliation planes and thin melt sheets were focussed upwards along local ductile thrusts (Fig. 3.12). Granites also pooled in the hangingwall wedges of small-scale thrust (Fig. 3.12) and granites widely 'invade' host rocks along pre-existing foliations or migmatitic layering, locally only preserving relict host rock rafts and biotite schlieren (Figs. 3.3, 3.10 & 3.14). Locally, granitic sheets are folded by ductile D2 folds on all scales (Fig. 3.10).

The large volume of leucogranite injected in the vicinity of the Naver Thrust suggests that this surface represented a preferred catchment and ascent path for leucogranite melts which in turn may have facilitated thrusting (e.g. Hollister & Crawford 1986; Brown & Solar 1998a). North of the study area, the sheeted granite complexes of Ben Klibreck, Strath Vagastie and Strath Naver were emplaced into the footwalls of regionally important ductile thrusts (Strachan & Holdsworth 1988, Kinny *et al.* in press.) indicating that the channelling of granitic melts into actively deforming crustal-scale ductile thrusts is a widespread and regionally-important process elsewhere in Sutherland.

3.6.2.3.2 Creag Mhór & Brora River sheets – late syn-D2 emplacement

On outcrop scale, the Creag Mhór, Brora River and other individual quartz monzodiorite sheets cannot be shown to be incorporated into D2 isoclinal folds, or channelled upwards along thrust planes. However, within domain 9 they occur directly underneath the lowest exposed ductile thrusts (Fig. 3.12), and appear to be focussed into the footwall of the Naver Thrust in domains 2 and 3. Structural settings of quartz monzodiorite sheets emplaced in the footwall of the Naver Thrust vary from concordant to S_2, to shallowly-discordant, to steeply-discordant, indicating that emplacement may have occurred by different mechanisms. The Creag Mhór and Brora River sheets locally show preferred linear mineral alignment that is parallel to D2 thrust related lineations developed in the host rocks (Fig. 3.8 & enclusre 1) which implies contemporanity of fabric development.

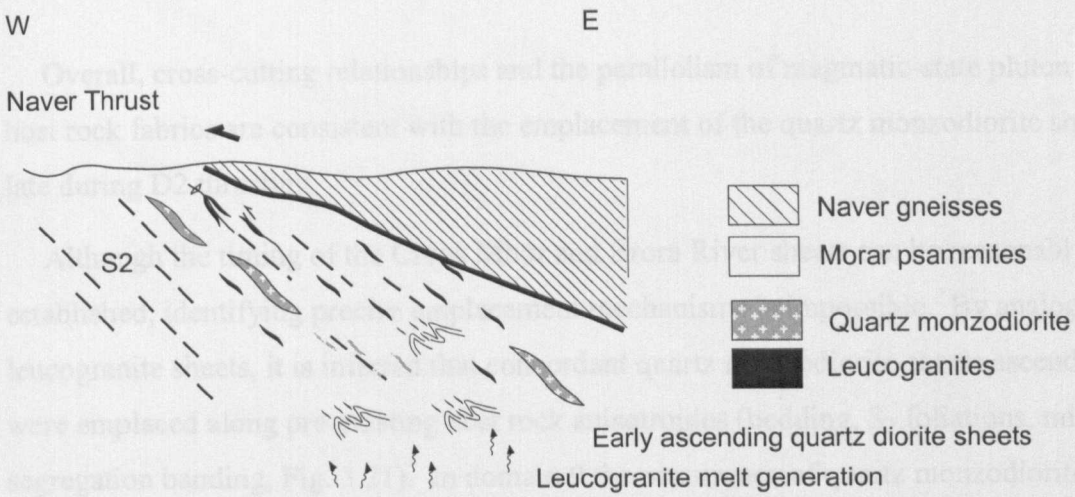

Fig. 3.21 D2 thrust-related granite emplacement leading to early, isoclinally-folded leucogranite sheets (e.g. domains 2 & 3), leucogranites that are emplaced along small scale thrusts (e.g. domain 9) and small, quartz diorite sheets containing top-to-the-NW/W, solid-state C-S fabrics.

Overall, cross-cutting relationships and the parallelism of magmatic-state pluton and host rock fabrics are consistent with the emplacement of the quartz monzodiorite sheets late during D2 thrusting.

Although the timing of the Creag Mhór and Brora River sheets can be reasonably well established, identifying precise emplacement mechanisms is impossible. By analogy to the leucogranite sheets, it is inferred that concordant quartz monzodiorite sheets ascended and were emplaced along pre-existing host rock anisotropies (bedding, S_2 foliations, migmatitic segregation banding, Fig. 3.21). In domain 9 the occurrence of quartz monzodiorite below the lowest exposed thrust indicates that its emplacement may have been facilitated by and occurred along ductile thrusts. In contrast, the steeply cross-cutting sheets (domains 2 & 3, see Fig. 3.6) must have pierced the pre-existing host rock anisotropies although their elongate, sheet-like nature argues against diapiric ascent. The absence of quartz monzodiorite sheets above the Naver Thrust may be explained in terms of negligible buoyancy contrasts between intruding quartz monzodiorites and the previously emplaced leucogranites which may have formed a physical barrier to ascent.

3.6.2.3.3 Post D2 thrusting, syn-tectonic emplacement of the central complex during dextral shear along the Strath Fleet lineament

Contemporaneous host rock deformation and plutonism largely obviate the "space problem" (Read 1948) as even large plutons can be emplaced passively into local dilatational jogs, extensional joints, step-overs or pull apart structures during compressional and transpressional deformation (e.g. Hutton 1988; D'Lemos *et al.* 1992, 1997; Tikoff & Tessier 1992; Karlstrom & Williams 1995). The British Caledonides were undergoing major sinistral transpression during the late Caledonian Orogeny (Soper *et al.* 1992) and pluton emplacement into dilatational structures related to major late Caledonian shear zones is abundant (e.g. Hutton 1988; Hutton & Reavy 1992; Jacques & Reavy 1994; Stewart *et al.* 2001; see also Chapter 1). In Rogart, the large-scale, clockwise swing of host rock foliations to the southeast of the central complex indicates that ductile host rock deformation may have occurred during dextral shear along the Strath Fleet lineament (Fig. 3.22 a). Space creation and pluton emplacement during dextral shear is further consistent with the flattened tear-drop 2D pluton shape (Fig. 3.22 a), with the magmatic-state foliations of the central granodiorite that parallel the host rock fabrics, with the steepening of magmatic-state fabrics in the east of the central complex and the asymmetry of the 'kidney shaped' central funnel defined by magmatic-state foliations.

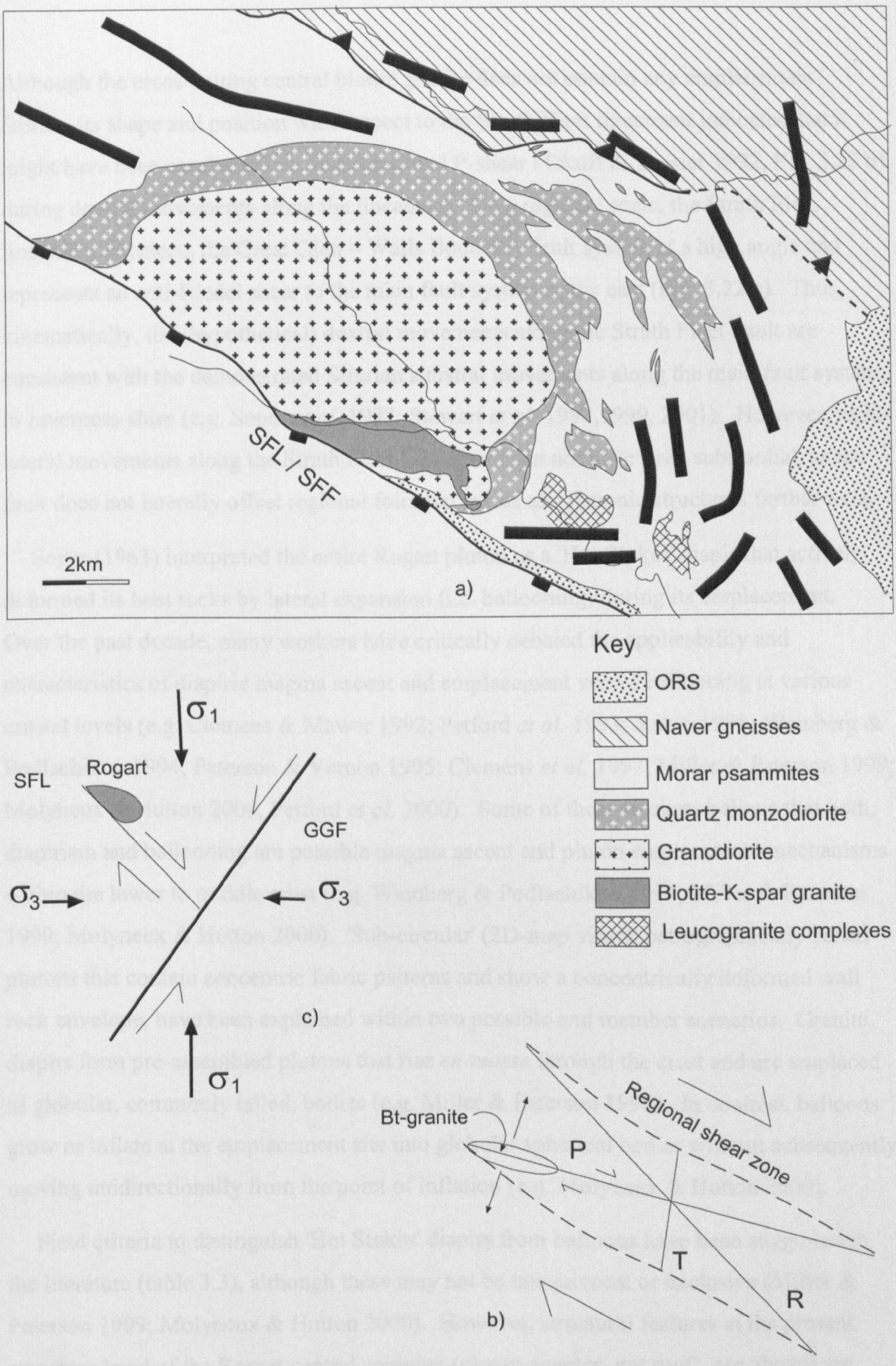

Fig. 3.22 Emplacement of the central complex into a void formed by dextral movements along the Strath Fleet Lineament (SFL /SFF)as an alternative mechanism to diapirism. Local ballooning and steepening of D2 thrust-related fabrics may occur. a) Map showing simplified foliation trends. b) Schematic P-shear model after Tikoff & Tessier (1992) that possibly explains the emplacement of the biotite granite of the central complex c) The Strath Fleet Fault (SFF) as an anti-Riedel-shear within the Great Glen-Walls Boundary Fault system (GGF).

Although the cross-cutting central biotite granite does not contain any emplacement fabrics, its shape and position with respect to the Strath Fleet lineament indicates that it might have been emplaced into an extensional P-shear (Tikoff & Tessier 1992, Fig. 3.22 b) during dextral movements along the lineament. On a regional scale, the Strath Fleet lineament intersects the Great Glen – Walls Boundary fault system at a high angle and represents an anti-Riedel shear to the main fault system in the east (Fig. 3.22 c). Thus, kinematically, the (hypothetical) dextral movements along the Strath Fleet Fault are consistent with the demonstrated Silurian sinistral movements along the main fault system in Inverness-shire (e.g. Soper *et al.* 1992; Stewart *et al.* 1997,1999, 2001). However, right-lateral movements along the Strath Fleet Lineament can not have been substantial, as the fault does not laterally offset regional foliation trends and tectonic structures further west.

Soper (1963) interpreted the entire Rogart pluton as a 'Hot Stokes' diapir that actively deformed its host rocks by lateral expansion (i.e. ballooning) during its emplacement. Over the past decade, many workers have critically debated the applicability and characteristics of diapiric magma ascent and emplacement versus ballooning at various crustal levels (e.g. Clemens & Mawer 1992; Petford *et al.* 1993; Rubin 1995; Weinberg & Podlachikov 1994; Paterson & Vernon 1995; Clemens *et al.* 1997; Miller & Paterson 1999; Molyneux & Hutton 2000, Petford *et al.* 2000). Some of these workers believe that both, diapirism and ballooning are possible magma ascent and pluton emplacement mechanisms within the lower to middle crust (e.g. Weinberg & Podlachikov 1994; Miller & Paterson 1999; Molyneux & Hutton 2000). 'Sub-circular' (2D-map view), petrographically zoned plutons that contain concentric fabric patterns and show a concentrically deformed wall rock envelope, have been explained within two possible end member scenarios. Granite diapirs form pre-assembled plutons that rise *en-masse* through the crust and are emplaced as globular, commonly tailed, bodies (e.g. Miller & Paterson 1999). In contrast, balloons grow or inflate at the emplacement site into globular spherical bodies without subsequently moving unidirectionally from the point of inflation (e.g. Molyneux & Hutton 2000).

Field criteria to distinguish 'Hot Stokes' diapirs from balloons have been suggested in the literature (table 3.3), although these may not be unequivocal or exclusive (Miller & Paterson 1999; Molyneux & Hutton 2000). However, structural features at the present exposure level of the Rogart central complex (pluton equator, not roof!, see above) are inconsistent with a 'standard Hot Stokes' diapir (Fig. 3.23 a) as critical features such as steeply plunging mineral lineations in an unfoliated pluton centre, distinct margin-parallel

Table 3.3 Characteristics of hot Stokes diapirs after Clemens et al. (1997), Miller & Paterson (1999) and Molyneux & Hutton (2000).

Hot Stokes diapir	**pluton**	**host rocks**
low exposure level	High-T, steep lineation must be present. Strong vertical prolate strain.	High-T shear zone with steep pluton-up kinematic indicators and rim-syncline must be present around the diapir tail.
mid exposure level / pluton equator	Margin: margin-parallel foliation, potentially associated with variable kinematics, no more steep lineations. Centre: no foliation. $0<K<1$ strains with subhorizontal x-axis and pluton-up kinemators	ditto
high exposure level / crest	Radial lineations, increasing in intensity towards the pluton margin. Weak flattening strains.	Narrow, outward dipping shear zone with down-dip lineation, pluton-side up kinematic indicators.
general	Circulation induced characteristic petrological zonation: normal, repeated, or inverse.	

foliations with generally pluton-up kinematic indicators, steep high-temperature marginal shear zones and a well-developed rim-syncline are absent (table 3.3). In contrast, a magmatic-state foliation of varying orientations is developed throughout the quartz monzodiorite and granodiorite of the central complex and igneous minerals locally plunge shallowly to the NE but are never steep. The consistently developed foliation, oblate mafic enclaves and the lack of pluton-up kinematic indicators suggest subhorizontal flattening strain during emplacement. These features are most consistent with *in situ* pluton inflation and ballooning (Fig. 3.23 b). However, evidence for host rock deformation and fabric steepening is localized to the east, north and northwest of the central complex and a consistently developed circular rim-syncline has not been recognized in this study. Although the importance of regional-scale, vertical and horizontal pluton-induced wall rock displacements has been emphasized in pluton emplacement studies from Greenland, Maine and Ireland (e.g. Grocott *et al.* 1999; Tikoff *et al.* 1999; Molyneux & Hutton 2000), the localized host rock deformation around the Rogart central complex suggests that this cannot have been the only emplacement mechanism.

Overall, the pluton fabric pattern suggests that the current exposure level is well below the pluton roof where the structural features exposed are largely inconsistent with diapiric rise. In contrast, pluton and host rock fabrics are most consistent with *in situ* pluton inflation into space created in relation to dextral movements along the Strath Fleet Lineament (Fig. 3.23 b).

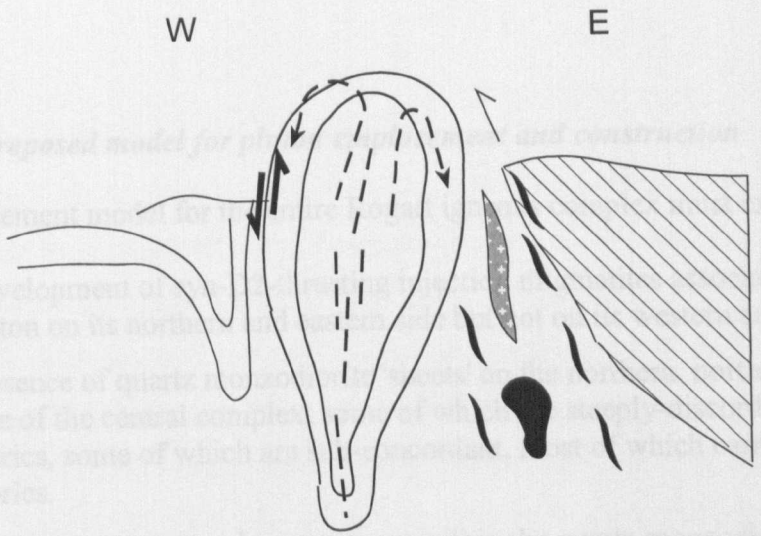

Fig. 3.23a Features to be expected if the Rogart complex was emplaced as a hot Stokes diapir: steep lineations in the pluton centre, radiating lineations in the crestal region, pluton-up shear sense indicators, rim syncline. See text , also compare table 3.3.

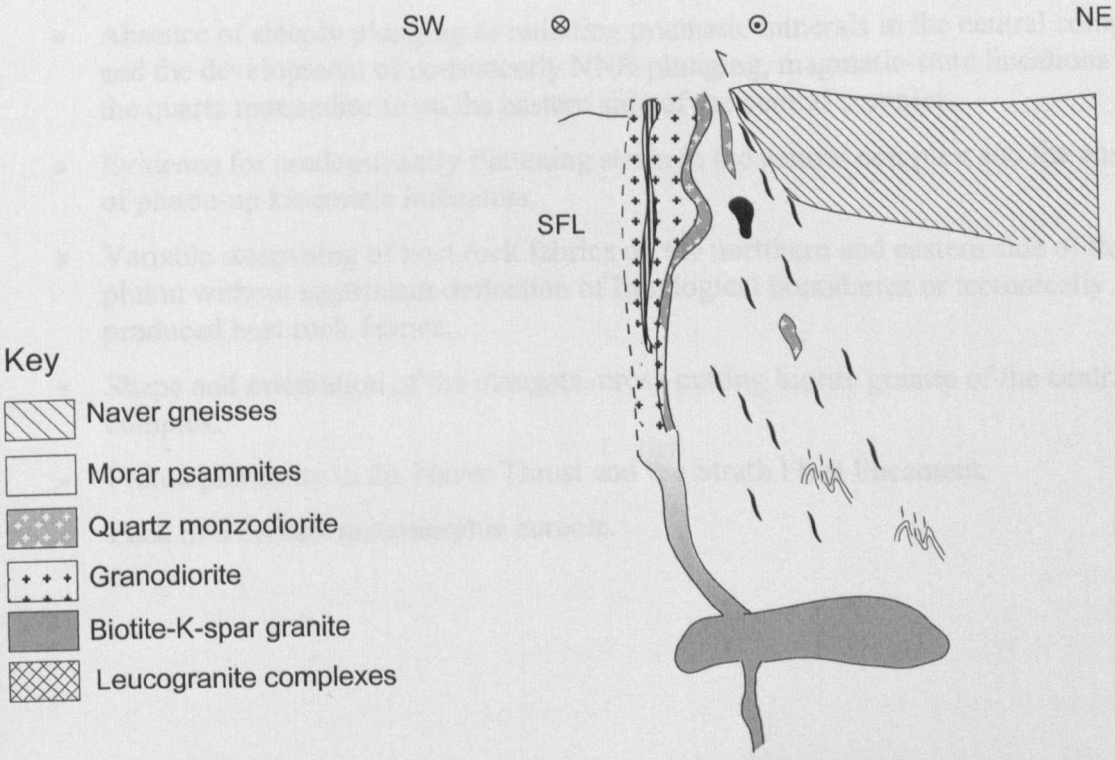

Fig. 3.23b Emplacement of the central complex into void formed by dextral movements along the Strath Fleet Lineament (SFL). Note the the hypothetical fractionating magma chamber at lower crustal levels from which magma is channelled upwards along the lineament and structural anisotropies of the host rocks. See text.

3.6.2.4 Proposed model for pluton emplacement and construction

An emplacement model for the entire Rogart igneous complex must explain the:

- Development of syn-D2-thrusting injection migmatites associated with the Rogart pluton on its northern and eastern side but not on its western and northwestern side.
- Presence of quartz monzodiorite 'sheets' on the northern, northeastern and eastern side of the central complex, some of which are steeply-discordant to the host rock fabrics, some of which are sub-concordant, most of which carry D2 thrust-related fabrics.
- Down-temperature microstructures within the quartz monzodiorite sheets consistent with top-to-the-W movements along the Naver Thrust.
- Absence of quartz monzodiorite sheets piercing the thrust or occurring above it.
- Asymmetrical teardrop-shape of the central complex (2D).
- Petrological zoning of the central complex with transitional / gradational facies boundaries.
- (Micro)fabrics within the central complex that are not D2 thrust-related.
- Pervasive magmatic-state fabrics developed throughout the central complex, which are steeply outward dipping in the north and northeast, subvertical in the east, form a kidney-shaped funnel structure in the west, and locally turn towards the Strath Fleet Lineament.
- Absence of steeply plunging or radiating prismatic minerals in the central complex, and the development of consistently NNE-plunging, magmatic-state lineations in the quartz monzodiorite on the eastern side of the central complex.
- Evidence for predominantly flattening strain in the central complex and the absence of pluton-up kinematic indicators.
- Variable steepening of host rock fabrics on the nortthern and eastern side of the pluton without significant deflection of lithological boundaries or tectonically produced host rock fabrics.
- Shape and orientation of the elongate, cross-cutting biotite granite of the central complex.
- Pluton proximity to the Naver Thrust and the Strath Fleet lineament.
- Lack of a contact metamorphic aureole.

3.6.2.4.1 Early phase of pluton construction

The earliest phase recorded comprised the formation of the injection migmatites, the syn-thrusting emplacement of the leucogranites along the Naver Thrust and the emplacement of the quartz monzodiorite sheets. Leucogranite melt generation and migration towards higher structural levels was syn-tectonic with regional D2 deformation (Fig. 3.24 a). Melt migration occurred in small batches by pervasive flow along foliation planes and active thrust that acted as anisotropic surfaces and were utilized as channels (e.g. Collins & Sawyer 1996; Brown & Solar 1998b; Weinberg & Searle 1998). Leucogranites were focussed into thrust planes where they possibly facilitated thrust movements (e.g. Brown 1994; Brown & Solar 1998b). Syn-thrusting leucogranite emplacement further explains the geographical distribution of the injection migmatites (located in the north and east) and also the absence of a contact metamorphic aureole around the main pluton, as the migmatitic hosts were at high temperatures when the central complex was emplaced. The absence of quartz monzodiorite sheets above the Naver Thrust is interpreted to reflect an impenetrable, thermal barrier formed by the leucogranites.

Post-dating the emplacement of the leucogranites but prior to the end of W-directed, thrust-related deformation several small batches of quartz monzodiorite were emplaced into the Morar Group injection migmatites to the north and east of the pluton below the impenetrable leucogranite cap (Fig. 3.24 a). Emplacement of these small sheets may have taken place by a combination of processes. Individual quartz diorite batches were channelled up along pre-existing anisotropies (foliation planes or thrusts) during W-directed D2 deformation giving the sub-concordant varieties with well developed C-S fabrics. In contrast, buoyancy-driven, discordantly-rising quartz diorite batches that cut across the pre-existing host rock fabrics provided the steeply discordant sheets that nonetheless show thrust-related deformation fabrics.

3.6.2.4.2 Main phase of pluton construction

It is proposed that largely passive emplacement of the Rogart central complex took place into a dilatational void developed along the Strath Fleet lineament during dextral shear associated with sinistral transpression on the Great Glen Fault system (Figs. 3.22; 3.23 b; 3.24 b & c). The main, strike-slip assisted phase of pluton construction may have been preceded by a transitional phase during which thrusting faded and the Strath Fleet

Lineament was activated (Fig. 3.24 b). The fabric pattern of the country rocks indicates that strike-slip movements caused a drag effect at the southeastern, restraining bend thus opening a void (e.g. Hutton 1988). Passive pluton-inflation into this tectonically formed space explains the development of pervasive magmatic-state foliations without diapir-typical lineations or kinematic indicators and microstructures that indicate flattening strain. The gradational boundaries between the quartz monzodiorite and the granodiorite and the widely-developed magmatic-state foliation argue for a quick pluton assembly before the main fabric was formed (e.g. Paterson *et al.* 1998). The steepening of the host rock fabrics and the Naver Thrust to the north and east of the central complex are thus explained by the combined effects of tectonic strike-slip deformation and pluton ballooning. The cross-cutting biotite granite may have been emplaced into an extensional P-shear (e.g. Tikoff & Tessier 1992) developed along the lineament after the emplacement of the quartz monzodiorite and the granodiorite. Finally, the fabric pattern of the central complex suggests that little of the pluton was down faulted during the Mesozoic.

Fig. 3.24 Hypothetical model showing the assembly of the Rogart igneous complex by different mechanisms in simplified maps (left hand diagrams) and cross sections (right hand diagrams).

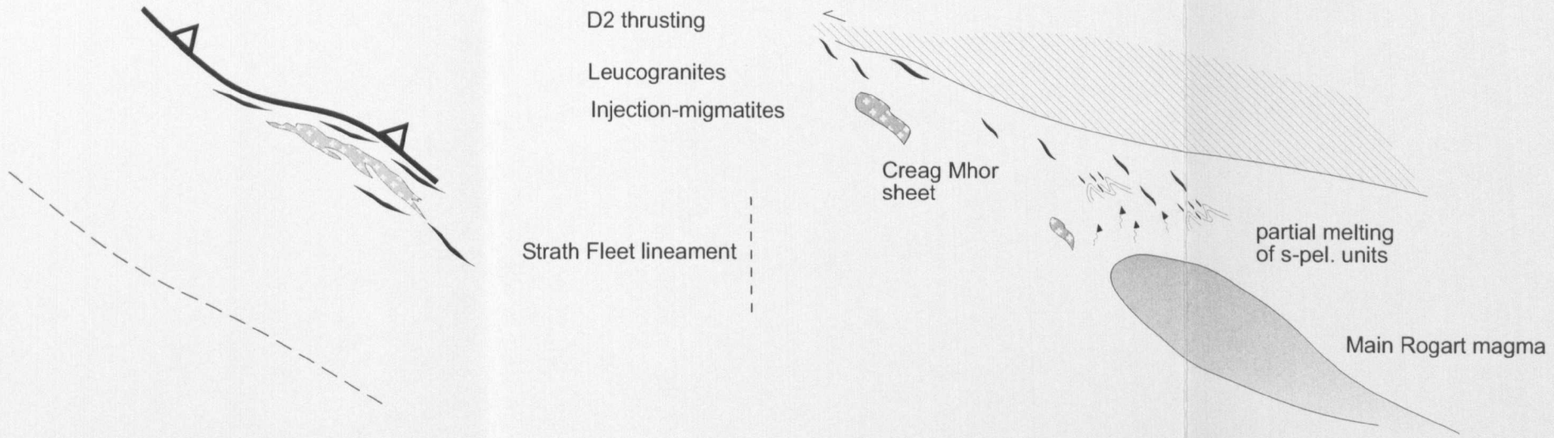

a) Early phase of pluton assembly. Ascending felsic magma chamber sited within the Moine rocks in the footwall of the Naver Thrust. Partial melting of semi-pelitic Morar Group rocks at lower structural levels. Ascent and syn-D2 emplacement of leucogranite sheets at higher structural levels, formation of injection-migmatites. Also separation of early fractionated quartzdiorite batches.

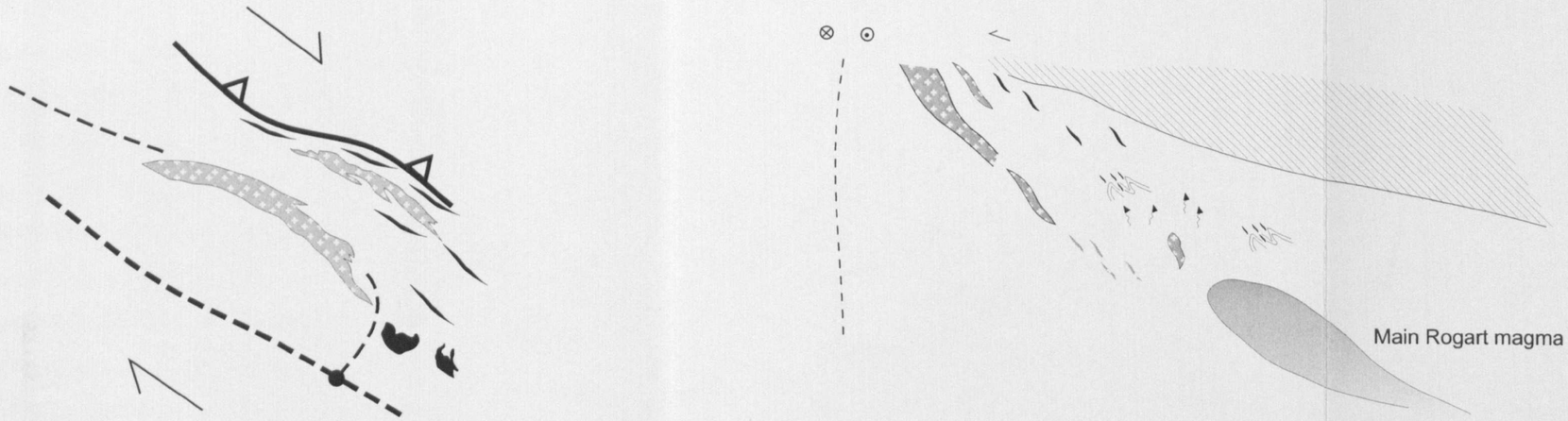

b) Ascent of larger batches of quartz monzodioritic magma by pervasive flow at lower structural levels. Activation of the Strath Fleet lineament .

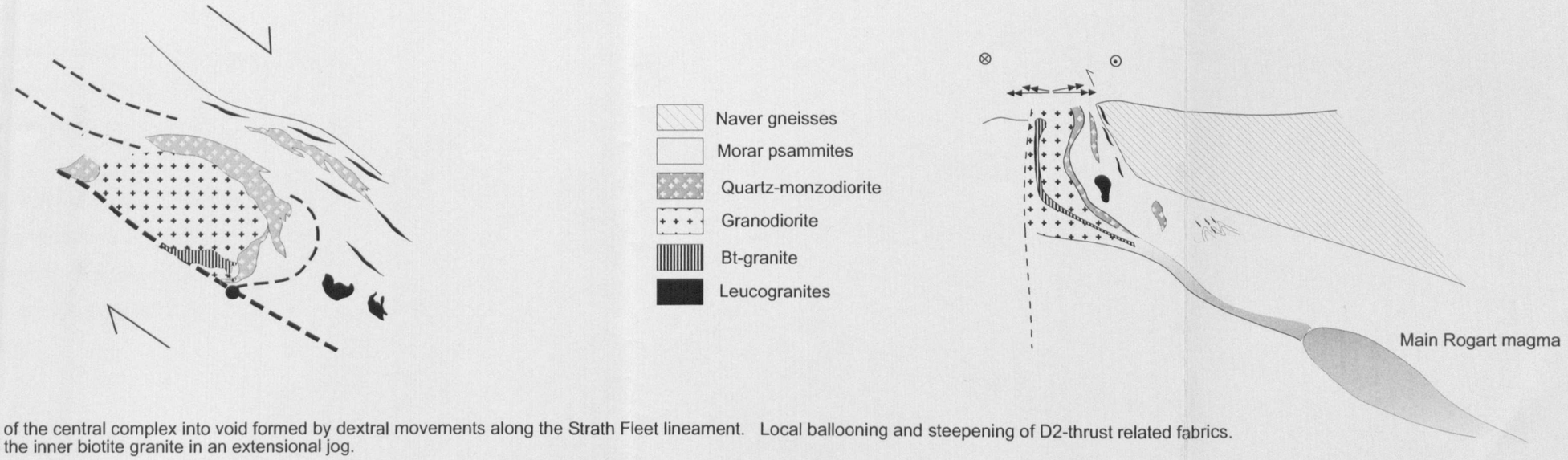

c) Emplacement of the central complex into void formed by dextral movements along the Strath Fleet lineament. Local ballooning and steepening of D2-thrust related fabrics. Emplacement of the inner biotite granite in an extensional jog.

3.6.2.5 Regional significance

The Rogart pluton is so far the only pluton in the Northern Highland Terrane that contains evidence for W-directed thrusting *and* strike-slip related emplacement. Within the terrane, W-NW directed compression is at present (imprecisely) dated by the ages of late syn-D2-thrusting granite sheets at Ben Klibreck (420 ± 6 Ma), Strath Vagastie (424 ± 8 Ma) and Strathnaver (429 ± 11 Ma) (U-Pb SHRIMP zircon, Kinny *et al.* in press). The intrusion of the syn-thrusting Strath Halladale Granite (this study) probably closely pre-dates a U-Pb titanite age of 423 ± 2 Ma (Rogers, G. pers. comm. 1999). Isotopic Rb-Sr and K-Ar ages for syn-kinematically recrystallized micas within the Moine Thrust Zone range from 437 Ma to 408 Ma (Freeman *et al.* 1998). In contrast, precise isotopic constraints exist for sinistral strike-slip movements as early as 427 ± 1.8 Ma along the Great Glen Fault (Clunes Tonalite, Stewart *et al.* 2001) and 425 ± 3 Ma (Strontian pluton, U-Pb bulk zircon, Rogers & Dunning 1991) and at 425 ± 3 Ma along the Strathconon Fault (Ratagain, U-Pb bulk zircon, Rogers & Dunning 1991). The emplacement of the Rogart pluton encompassed the switch from W-NW-directed thrusting to sinistral transpression. A sample from the quartz monzodiorite of the central complex gives a crystallization age of *c.* 431 ± 4 Ma (U-Pb zircon and monazite, preliminary age, Evans, J. pers. comm. 2002) and hence constrains the timing of dextral shearing and emplacement of the central complex to the Silurian. Currently, analytical errors are too large to unravel the emplacement of earlier pluton phases within the Rogart complex and thus the extent of individual periods of regional deformation (e.g. Samson & D'Lemos 1999; Petford *et al.* 2000, see table 2.2). Nonetheless, very high-precision age dating of the syn-thrusting leucogranites, the syn-D2 Creag Mhór sheet might potentially provide better time constraints for W-directed thrusting in the Rogart area. At present, the crystallization age of the central complex indicates that W-directed thrusting in Sutherland was largely accomplished by *c.* 430 - 425 Ma and superseded by strike-slip deformation, consistent with the isotopic ages of strike-slip related granites in Inverness-shire (see Chapter 1, table 1.2). Consequently, the formation of the foreland-propagating thrust system (Barr *et al.* 1986; Butler 1986) and development of the lower to mid-crustal duplexes generating the Assynt Culmination (Butler & Coward 1984) should pre-date the emplacement of the Rogart central complex.

3.6.2.6 Crustal scale model

Any crustal scale model for the generation and emplacement of the Rogart Granite has to consider geochemical arguments as well as the presented structural evidence and regional-scale tectonics. The pluton has been argued to be ultimately mantle-derived (Fowler *et al.* 2001) and its entire volume (excluding *c.* 25% Moine contaminant, Fowler *et al.* 2001) thus had to ascend through the crust. Further, three phases of fractionation at different structural levels plus contamination with Moine are required (e.g. Esperanca & Holloway 1986, 1987; Fowler & Henney 1996; Fowler *et al.* 2001) and the large isotopic heterogeneity of the mafic rocks in contrast to the homogeneity of the felsic rocks needs to be addressed (e.g. Fowler *et al.* 2001). The main structural and tectonic constraints to be considered are the siting of the pluton in the footwall of the Naver Thrust along the Strath Fleet Lineament and above the Assynt culmination, and the pluton emplacement during the switch-over from W-NW-directed compression to sinistral transpression (e.g. Soper *et al.*1992; Hutton & Reavy 1992).

It is proposed that a primary, high-K lamprophyric melt was generated within the metasomatized upper mantle (e.g. Esperanca & Holloway 1986, 1987; Fowler & Henney 1996) in response to the subduction of the Iapetus ocean floor (e.g. Thompson & Fowler 1986). The primary ultramafic magma ascended into the lower crust where minettes & appinites were fractionated (e.g. Esperanca & Holloway 1986), followed by further ascent of small, individual appinitic batches by pervasive flow into the lower & middle crust (e.g. Collins & Sawyer 1996). Contemporaneous fractionation of mafic assemblages and assimilation of Moine at these crustal levels derived felsic magmas (Fowler & Henney 1996, Fowler *et al.* 2001). The proposed individual ascent, fractionation and contamination of small mafic magma batches thus explains the isotopic diversity observed in the mafic rocks (e.g. Fowler *et al.* 2001). The felsic magmas thus generated either continued to ascend and fractionate (such as the early quartz diorite sheets in Rogart), or ponded to form a fractionating mid-crustal magma chamber (resulting in isotopic homogenisation, e.g. Fowler *et al.* 2001) that episodically fed tectonically-created space at a slightly higher structural level (e.g. Rogart central complex). The migration of quartz dioritic and granodioritic magma during the early stages possibly occurred in the footwall of ductile thrusts, followed by pulsed magma migration along crustal-scale lineaments (conduit feeding) during *and* after the switch over to sinistral movements.

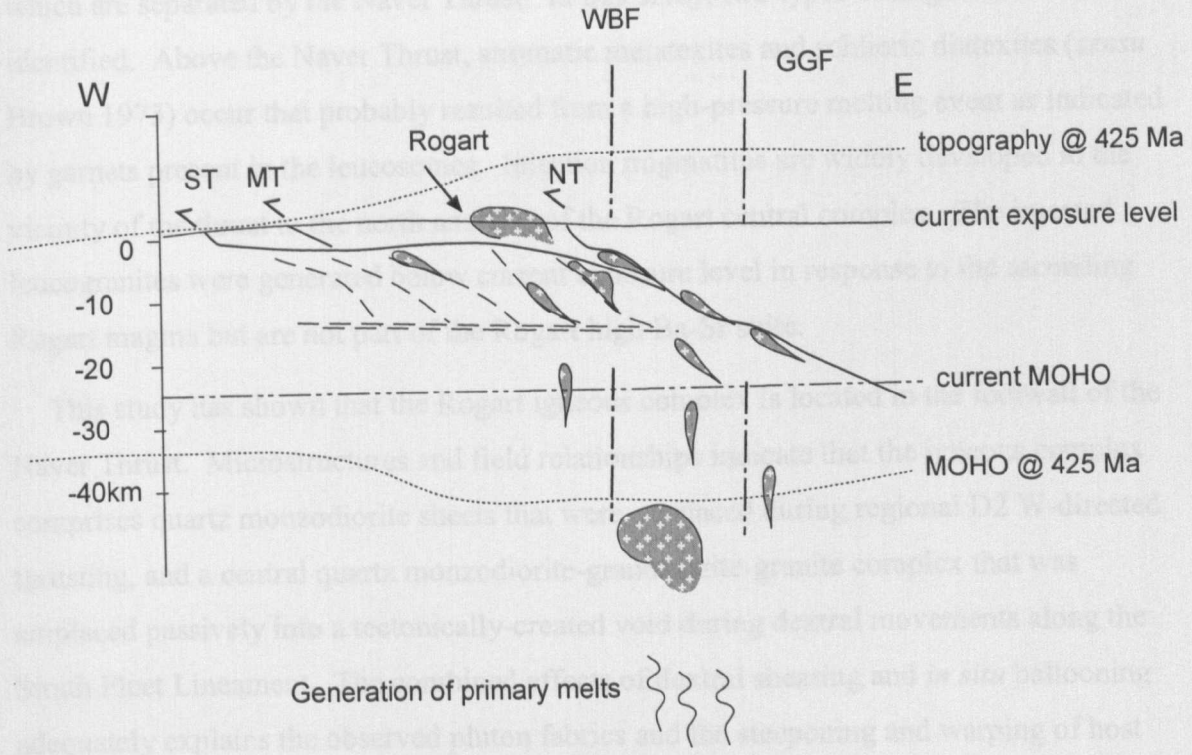

Fig. 3.25 Crustal-scale model of magma ascent and syn-tectonic emplacement of the Rogart (and adjacent) plutons. Magmas are generated in the metasomatized, subcontinental mantle and ascend in small batches whilst fractionating the appinitic parental magmas of the Northen Highland high Ba-Sr granites. Further fractionation of these appinitic parental magmas, and contamination with Moine metasediments occurs at mid to lower crustal levels. Further, possibly deformation-enhanced ascent of felsic magmas along thrusts and shear zones possibly relating to the imbrication in the footwall of the Moine Thrust (e.g. Butler & Coward 1984). Emplacement either as syn-tectonic sheets, or - after the switch over to sinistral strike-slip mode- into extensional jogs along major strike-slip faults. Deep structure based on seismic reflectors after Butler & Coward (1984), see text. Note that the Strath Fleet Fault / Lineament runs parallel to the line of section and is not shown.

3.7 Conclusion

The Rogart igneous complex was emplaced into the Moine metasediments of southeastern Sutherland that comprise Morar Group rocks and Naver Nappe gneisses which are separated by the Naver Thrust. In this study, two types of migmatites have been identified. Above the Naver Thrust, stromatic metatexites and schlieric diatexites (*sensu* Brown 1973) occur that probably resulted from a high-pressure melting event as indicated by garnets present in the leucosomes. Injection migmatites are widely developed in the vicinity of the thrust to the north and east of the Rogart central complex. The injected leucogranites were generated below current exposure level in response to the ascending Rogart magma but are not part of the Rogart high Ba-Sr suite.

This study has shown that the Rogart igneous complex is located in the footwall of the Naver Thrust. Microstructures and field relationships indicate that the igneous complex comprises quartz monzodiorite sheets that were emplaced during regional D2 W-directed thrusting, and a central quartz monzodiorite-granodiorite-granite complex that was emplaced passively into a tectonically-created void during dextral movements along the Strath Fleet Lineament. The combined effects of dextral shearing and *in situ* ballooning adequately explains the observed pluton fabrics and the steepening and warping of host rock fabrics and the Naver Thrust around the Rogart complex. Diapiric rise and emplacement is not considered an important emplacement mechanism in the Rogart scenario (cf. Soper 1963). A preliminary U-Pb age of 431 ± 4 Ma of the central complex (U-Pb, zircon & monazite TIMS, Evans, J. pers. comm. 2002) indicates that in southeastern Sutherland, the switch-over from W-directed compression to sinistral transpression occurred during the middle Silurian. High precision isotopic dating of carefully selected zircons and monazites from leucosomes of the Naver gneisses, leucogranites and thrust-related quartz diorites is needed to unravel the timing of high-pressure metamorphism, leucogranite injection, D2 thrusting and pluton construction.

Chapter 4

Structural geology, fabric development and emplacement of the Strath Halladale and Helmsdale granites.

4 Structural geology, fabric development and emplacement of the Strath Halladale and Helmsdale granites.

4.1 Introduction

The Strath Halladale and Helmsdale granite complexes are located in northeastern Sutherland and Caithness, where they intrude Moine metasediments of the Naver Nappe. The outcrop pattern of the southern part of the study area is dominated by kilometre-scale, NE-SW trending (F3) folds, which form a large synclinorium, here termed the Kildonan synclinorium (Fig. 4.1). The Strath Halladale granite forms an elongate, sheeted complex that is located on the northwestern limb of the Kildonan synclinorium, whereas the Helmsdale granite is an oval shaped intrusion that is located on the southeastern limb of the synclinorium and bounded by the Helmsdale Fault to the southeast. As the two igneous complexes are part of the same regional structure and intrude common host rocks, they will be discussed in the same chapter. Prior to the description and discussion of their respective structural setting, microstructures, and tectonic significance, an overview of the general pluton settings, previous work and host rock lithologies is given.

4.2 Previous work

The Strath Halladale granite complex occurs to the east of the Strath Halladale River, between Achentoul Hill and Reay (Fig. 4.1). The Strath Halladale granite complex comprises a sheeted granodiorite (main Strath Halladale "granite") of *c.*210km^2 that is flanked by the Reay Diorite in the north. The complex is widely covered by boggy grounds and moorlands, and stream sections provide almost the only exposures. The igneous complex and its relationship to the Moine rocks was first described by Horne & Greenly (1896) and a comprehensive summary of the geology of eastern Sutherland and Caithness is provided by Read (1931). The southern part of the Strath Halladale Granite complex (Altnabreac district) was studied by the BGS during the late 1970s as part of the UK research programme into the assessment of the feasibility of the disposal of high-level radioactive wastes in crystalline rocks. Summaries of the geology, geophysics, and geochemistry of the rocks of the Altnabreac area were subsequently published by McCourt (1980), Storey & Lintern (1981), Lintern & Storey (1980), and Lee (1987).

Fig. 4.1 Geological overview of the Strath Halladale and Helmsdale area.
Explanation see text, compiled using data from field seasons 1999 - 2001, BGS 1" Scotland Sheets 103, 109E, 110 & 115E, R. A. Strachan (unpublished).

The Helmsdale granite crops out in the southeast of the study area, around the village of Helmsdale in Sutherland (Fig. 4.1). The Helmsdale granite comprises an outer, coarse grained granodiorite and an inner fine grained granite. To the east, the granite is bounded by the Helmsdale Fault, a Mesozoic normal fault that downthrows to the east. The granite occurs over an area of about 50km^2 and is well exposed along several road sections but inland exposure is largely restricted to stream sections and isolated outcrops on hillsides. The first comprehensive reviews of the geology of the Helmsdale Granite, and lithologies and structures present within the metamorphic rocks of the Scaraben area to its northwest, were given by Read *et al.* (1925), and Read (1931). Subsequently, research on the regional metamorphism of the country rocks was published by Watson (1948) and Soper & Brown (1971), and the currently accepted lithostratigraphy was summarized by Strachan (1988). Palaeomagnetic and geochemical-alteration studies of the Helmsdale granite were published by Torsvik *et al.* (1983) and Tweedie (1979), respectively.

4.3 Aims of this study

Existing published descriptions outline the general geology, metamorphic grade and structural features of the Moine rocks (see above). Published work has recorded that the Strath Halladale Granite is locally foliated (e.g. McCourt 1980) but it has previously been interpreted to post-date the main phase of regional deformation (e.g. McCourt 1980, Lintern & Storey 1980; Strachan 1988). A Rb-Sr whole rock age of 649 ± 30 Ma (M. Brook quoted in Pankhurst 1982) has been used by previous workers to demonstrate Neoproterozoic tectonothermal activity in the Moine rocks of east Sutherland (e.g. Powell *et al.* 1983; Barr *et al.* 1986). However, Kinny *et al.* (1999) questioned this interpretation on the basis that widespread migmatization and regional D2 deformation is dated in the *central belt* of the Naver Nappe at 461 ± 13 Ma (Kirtomy migmatites). A Silurian age for the granite is indicated by a U-Pb titanite age of 423 ± 2 Ma (G. Rogers, pers. comm.) that, in the absence of post-emplacement metamorphism, is interpreted to reflect post-magmatic cooling of the pluton through the closure temperature for radiogenic Pb of titanite.

In this study, the emplacement and fabric development of the Strath Halladale granite complex has been studied by field mapping and microstructural analysis. Additionally, 220 thin sections from surface and drill core samples were kindly loaned by the British Geological Survey to aid fabric analysis.

The focus of previous research within the study area clearly lay in its central and northern parts whereas the area around Helmsdale was less well known. The granite has previously been interpreted to postdate Caledonian deformation (e.g. McCourt 1980; Strachan 1988) and a bulk zircon age of *c.*420 Ma (Pidgeon & Aftalion 1978) is thought to broadly date its emplacement. However, the granite is bounded by the Helmsdale Fault that forms part of the Great Glen- Walls Boundary Fault system. Pluton emplacement along major strike-slip faults that are part of this regional fault system has been envisaged for granites of comparable age to the south (e.g. Hutton 1988b; Hutton & McErlean 1991; Stewart *et al.* 2001). In order to establish the temporal and kinematic relationships between the emplacement of the Helmsdale granite, regional Caledonian deformation and development of the Helmsdale Fault, it was mapped and sampled to investigate the structural setting and fabric development.

4.4 Overview of lithologies

4.4.1 Moine rocks

The Moine rocks of the study area comprise two main metasedimentary sequences: a westerly series of psammitic and semi-pelitic, migmatitic gneisses (provisionally termed the "Loch Coire Formation" according to the geological 1:50000 map sheet of the Kildonan area, BGS in press), and an easterly, predominantly non-migmatitic, continuous sequence of psammites, semi-pelites and quartzite that has been termed the Scaraben succession (Read 1931; Strachan 1988).

Loch Coire Formation

The rocks that crop out to the west and southwest of the Strath Halladale granite comprise two different units that form a structural sequence with no way up criteria. Banded psammitic and semi-pelitic, migmatitic gneisses and associated leucogranitic sheets form the bulk of the bedrock to the west of the Strath Halladale Granite (herein termed "Achentoul Banded Formation") and are overlain by the Badenloch Pelite Formation (Strachan 1988) that forms a thin strip of pelitic gneisses to the south of the Strath Halladale Granite (Figs. 4.1 & 4.5).

The structurally lowest parts of the Achentoul Banded Formation crop out in the far northwest of the study area and comprise medium grained, layered psammites that are

quartz-rich, generally recrystallized and contain subordinate amounts of microcline, plagioclase and micas (McCourt 1980). Towards higher structural levels, rocks that comprise alternating bands of semi-pelite (c. 15cm) and psammite (<30cm) occur. This alternate banding has been interpreted to represent modified bedding (McCourt 1980).

The migmatitic rocks of the Achentoul Banded Formation range from regularly layered stromatic metatexites to disrupted diatexites (Fig. 4.2; sensu Brown 1973). The stromatic varieties comprise alternating thin bands of *c.* 1-3mm thick, biotite-rich, pelitic horizons that alternate with thin, *c.* 1-2mm thick generally concordant leucosomes of granitic composition. Leucosome proportions may locally increase and form individual migmatitic segregation melts of up to 30cm thickness that are progressively discordant to the stromatic layering and may lead to the formation of diatexites and leucosome-engulfed metatexite rafts (Fig. 4.2 b). Over wide areas, the leucosomes coalesce and form leucogranitic sheets that are ubiquitous throughout the Achentoul Banded Formation to the west of the Strath Halladale Granite and locally form large, continuous igneous bodies which have been referred to as G2-phase (see below).

The Badenloch Pelite Formation occurs structurally above the Achentoul Banded Formation. It was previously ascribed to the Scaraben succession (e.g. Strachan 1988) as it was thought to correlate with pelitic rocks exposed on the east side of the Strath Halladale granite. Remapping of the area (Kildonan sheet, BGS in press and this study) now questions this earlier interpretation and the Badenloch Pelite Formation is now assigned to the Loch Coire Formation. The Badenloch Pelite Formation is exposed in the stream sections to the south of the main Strath Halladale Granite. It comprises a coarse grained biotite-muscovite gneiss with subordinate ribs of psammite (c.20-40cm thick). Throughout the Badenloch Pelite Formation, the characteristic gently-discordant leucogranites observed in the Achentoul Banded Formation (G2-phase) are ubiquitous. The contact of the Badenloch Pelite Formation and the lowermost unit of the overlying Scaraben Succession is unexposed in the study area.

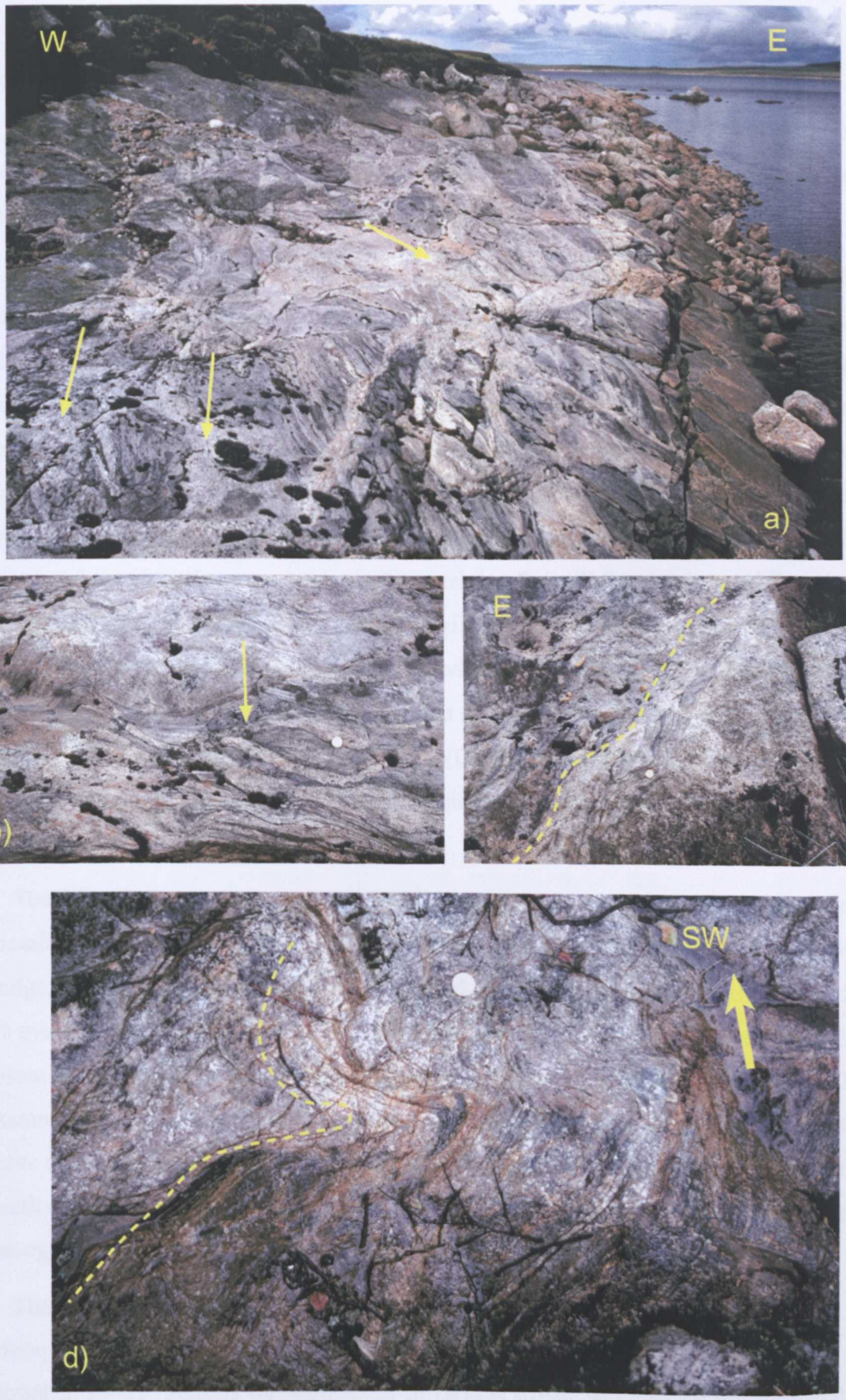

Fig. 4.2 Field photographs of the migmatites of the Achentoul Banded Fm (a-c) and the Kildonan Psammites (d). a) Overview of the southwestern lochside of Loch An Rhutair [NC 8647|3575] showing stromatic metatexites and cross-cutting leucogranites. b) Leucogranite-engulfed metatexite rafts on the southern lochside [NC 8644|3559], looking E. c) Granite sheet correlated with the Strath Halladale Granite cross-cutting the composite S_1/S_2 fabric at [NC8644|3559], looking S. Note that deformation, migmatisation and granite phases in the study area are at present not, or imprecisely, dated. d) Kildonan Psammites exposed in the lower Torrish Burn [NC 9690|1875]. Horizontal surface looking SW (arrow), general dip of $S_0/S_1/S_2$ is 50-60° to the SE. Folds are possibly of F3 age, as they fold the composite planar D2 fabric. See text.

Scaraben Succession

The Scaraben Succession (Read 1931) dominates the basement geology in the southeast part of the study area and in stratigraphic order comprises the Kildonan Psammite, the Suisgill Semi-pelite and the Scaraben Quartzite.

The Kildonan Psammite is well exposed south of the main Strath Halladale Granite, along the Strath of Kildonan and the Kinbrace, Torrish and Kildonan burns. The main lithology is a medium grained, grey to brown, quartzose or micaceous psammite (Fig. 4.2), but subordinate bands of quartzite and semi-pelite are locally common (e.g. Kinbrace Burn). Occasionally, these lithologies are rhythmically interbanded on a scale of 1-3cm and occur as striped, gneissic lithologies. Sedimentary structures such as cross-bedding, cross-lamination and graded bedding are locally common (e.g. Allt Breac and Torrish Burn) and consistently young towards the overlying Suisgill Semi-pelite and Scaraben Quartzite (Strachan 1988). In the upper Suisgill and Torrish burns, semi-pelitic horizons of *c.* 20cm become increasingly interbedded with the psammites and mark a gradational boundary towards the Suisgill Semi-pelite that dominates the geology east of the Strath Halladale Granite. In the Berriedale Water [ND 114 237], the upper Kildonan Psammites comprise increasing amounts of interbedded quartzite and grade into the overlying Scaraben Quartzite (Strachan 1988).

The Suisgill Semi-pelite is a biotite-rich, medium or coarse grained schist that contains occasional psammitic layers. It is well exposed in the stream sections at Dallnawillan Lodge, east of the Strath Halladale Granite, and is repeated by folding in the cores of major D3 synclines at Learable Hill and Beinn Dubhain. It thins towards the southeast and is absent in the Berriedale Water where the Scaraben Quartzite directly overlies the Kildonan Psammite (see above and Fig. 4.1). East of the Strath Halladale Granite, the Suisgill Semi-pelite contains limited evidence for segregation melting and leucogranites are sparse. South of the Strath Halladale Granite, the Suisgill Semi-pelite is decidedly gneissic but leucogranites are rare to absent (Strachan 1988).

The Scaraben Quartzite is a distinct, white, medium grained, well bedded, orthoquartzite that forms the scree-covered mountains of Sron Garb and Scaraben (Strachan 1988). Smaller outcrops occur in various stream sections off the Berriedale Water, and in the upper Suisgill Burn where the quartzite is very pure (>98% quartz), although thin bands of semi-pelite have been reported (e.g. Read 1931; Strachan 1988).

4.4.2 Igneous Rocks

The igneous rocks of the study area have been previously divided into four groups, in order of age (G1-G4) that were thought to form individual, but consecutive intrusive phases (e.g. McCourt 1980; Strachan 1988).

G1 – oldest igneous rocks

Based on cross-cutting relationships and the development of strong solid-state fabrics, the G1 suite is thought be the oldest group of igneous rocks, but individual types are not genetically linked (e.g. McCourt 1980; Strachan 1988). North of the Scaraben area, Strachan (1988) defined G1 to contain augen granites, granodiorite sheets and veins, and pegmatites (Fig. 4.3). Southeast of Braemore Lodge [ND 070|355], the augen granites carry a strong solid-state rodding lineation that plunges both S and SE and K-feldspar augen indicate top-to-the-N to NW sense of shear. Northwest of the Strath Halladale area, McCourt (1980) assigned a fine to medium grained K-feldspar-megacrystic granite to G1 that occurs east of Portskerra [NC882|660].

G2 –phase

In the literature, the G2 igneous phase is either referred to as "white granite" (McCourt 1980), or as "G2-tonalite" (Lintern & Storey 1980; Storey & Lintern 1981; Strachan 1988), or "sodic granite" (Mykura 1985). All workers describe the phase as a sodic, medium grained granitoid of a distinctly white colour that shows intimate association with the migmatitic Moine rocks to the west of the main Strath Halladale Granite (i.e. the Loch Coire Formation) and may be continuous with similar igneous rocks of the Loch Coire Migmatite Complex to the west (Read 1931; Strachan 1988). Petrographically, the G2-phase comprises oligoclase, quartz, biotite, and minor amounts of K-feldspar (<10% modal) with accessory ore minerals. Field investigation of the G2 phase in this study supports the view that it is an intimate part of the migmatites of the Loch Coire Formation and constitutes the leucosomes and leucogranites described above. It is further noted that the leucogranites share common field characteristics, petrography and structural settings with migmatitic segregation granites of Ordovician (Grampian) age described from the Kirtomy and Naver migmatites (Watt *et al.* 1996; Kinny *et al.* 1999; Friend *et al.* 2000) and the Rogart metatexites as described in this study ("Naver gneisses", see Chapter 3). In this Chapter, the G2 phase is simplistically referred to as leucogranites in keeping with the terminology applied in Chapter 3.

G3 – Strath Halladale Granite

In this study, the Strath Halladale granite suite is taken to comprise the main Strath Halladale Granite, the Reay Diorite, and various associated dioritic, and mafic to ultramafic rocks (Fig. 4.3). The main Strath Halladale intrusion (Fig. 4.1) is a sheeted complex of essentially medium to coarse grained, variably-foliated granite of grey to orange colour (Fig. 4.3). It is mainly exposed along the upper parts of stream sections to the east of the Strath Halladale River, in sporadic outcrops on the hillsides east of the Strath Halladale River, and along the Sandside Burn to the south of Reay (Fig. 4.1). Although the Strath Halladale Granite is commonly referred to as 'granite' (e.g. McCourt 1980; Lintern & Storey 1980; Storey & Lintern 1981; Strachan 1988) it is mainly of granodioritic composition and may locally grade into quartz monzonite. Its modal composition is variable but typically, the granodiorites comprise plagioclase (50%), quartz (c. 15%), and K-feldspar (22%) with abundant biotite (c.10%) and minor accessory phases (<3%). Commonly, K-feldspar occurs as subhedral phenocrysts of 5-10mm length that show perthite exolution and contain remnants of twinned plagioclase. The plagioclase is smaller and its cores are often strongly sericitised. Quartz generally forms 2-4mm elongate interstitial multigrain pools, and occasionally titanite and (more often) apatite occurs. Monazite, ilmenite and magnetite form further accessory phases.

The Reay Diorite is a small stock of quartz diorite intruded into the Moine rocks at the northern end of the main Strath Halladale Granite (Fig. 4.1). Outcrops of the Reay Diorite are restricted to a few sparsely exposed hills south of Reay, as much of the intrusion has been quarried. Smaller quartz dioritic intrusions occur on the western and eastern side of the main Strath Halladale granite and, east of Achentoul, as inclusions within it. The quartz diorite contains euhedral hornblende and plagioclase laths with interstitial quartz and varying amounts of fine grained K-feldspar. The feldspars are often strongly sericitised. Clinopyroxene has been reported in the literature (e.g. Lintern & Storey 1980; Dallmeyer *et al.* 2001). Ubiquitous titanite and apatite together with abundant ore and minor zircon form the main accessory minerals. Locally, the diorite contains dark, biotite-rich mafic enclaves and intrusive amphibolite sheets.

Associated with, and included within the main granite are several large mafic enclaves (Fig. 4.3). At Knockfin, these rocks are dark green to black in colour and exclusively made up by small subhedral pyroxenes and euhedral hornblende that are enveloped in large, poikilitic amphiboles. In Trantlebeg Burn, at Gobernuisgeach and at Loch Scye

(Scyelite, Read 1931), further outcrops of comparable lithologies occur and mafic to ultramafic material is sparsely present within the BGS drill-core. Apart from the mafic rocks exposed at Knockfin, other mafic to ultramafic lithologies are strongly netveined by sodic granites and variably deformed. The mafic to ultramafic rocks are thought to correspond to hybrids of the Ach'Uaine type (e.g. Read 1931, McCourt 1980) which are thought to be genetically linked with the Newer Granites (Fowler & Henney 1996). The Strath Halladale Granite complex and the Moine rocks are cut by a set of fine grained, quartzo-feldspathic, unfoliated aplite-granites (Fig. 4.3).

G4 – Helmsdale Granite

The Helmsdale Granite complex is exposed on the hillsides north and south of the Helmsdale River to the east of Torrish Burn. The granite complex comprises an outer very coarse grained, porphyritic granodiorite and an inner, very fine grained adamellite. The outer granodiorite (Fig. 4.4 a) comprises large, euhedral K-feldspar phenocrysts of *c.* 2cm length that show distinct perthite exolution and generally contain small euhedral plagioclase and hornblende inclusions. Locally, the phenocrysts may increase to over 5cm in length. Plagioclase forms smaller, euhedral crystals that are of oligoclase to albite composition (An_{10}) and generally strongly sericitized. Large quartz grains of up to 5mm across are interstitial, of a distinct milky appearance, and often form aggregates of about 1cm across. Brown biotite occurs as small, ragged flakes that are often strongly retrogressed to chlorite. Ore minerals are commonly present and accessory phases comprise apatite, titanite and zircon. Ultramafic rocks of up to 80cm diameter are found within the outer granodiorite. They comprise subhedral amphiboles of up to 0.5mm width that sit within a fine grained matrix of plagioclase and K-feldspar. The enclaves locally show evidence for crystal transfer of K-feldspar megacrysts and large quartz grains derived from the outer granodiorite (Fig. 4.4 b).

The inner Helmsdale granite is very fine grained and comprises almost equal amounts of plagioclase and K-feldspar with subordinate quartz. Plagioclase (oligoclase) generally forms small, eu- to subhedral crystals of *c.*0.5mm length that form aggregates with commonly anhedral, but slightly larger orthoclase. These aggregates are set in a larger groundmass of quartz and rarely small K-feldspar phenocrysts occur (Fig. 4.4). Small biotite is often retrogressed to chlorite. The outer granodiorite grades into the inner granite over a strip of 200-500m. The intermediate lithology is a fine grained, orange granite that comprises abundant, large quartz grains. Occasionally, K-feldspar megacrysts that are

possibly derived from the outer granodiorite occur within the fine grained matrix of small plagioclase, K-feldspar and interstitial quartz (Fig. 4.4 c).

4.4.3 Sedimentary rocks

The basement lithologies of the study area are unconformably overlain by lower- to middle Devonian sedimentary rocks. The Early Devonian sequence comprises a basal breccia that is overlapped by a sequence of dark, red-brown to purple sandstones and siltstones. The unconformably overlying Middle Devonian sediments (Caithness Flagstone Group) locally comprise a basal breccia overlain by a unit of greenish-grey, calcareous siltstones with interbedded carbonates (e.g. Mykura 1985).

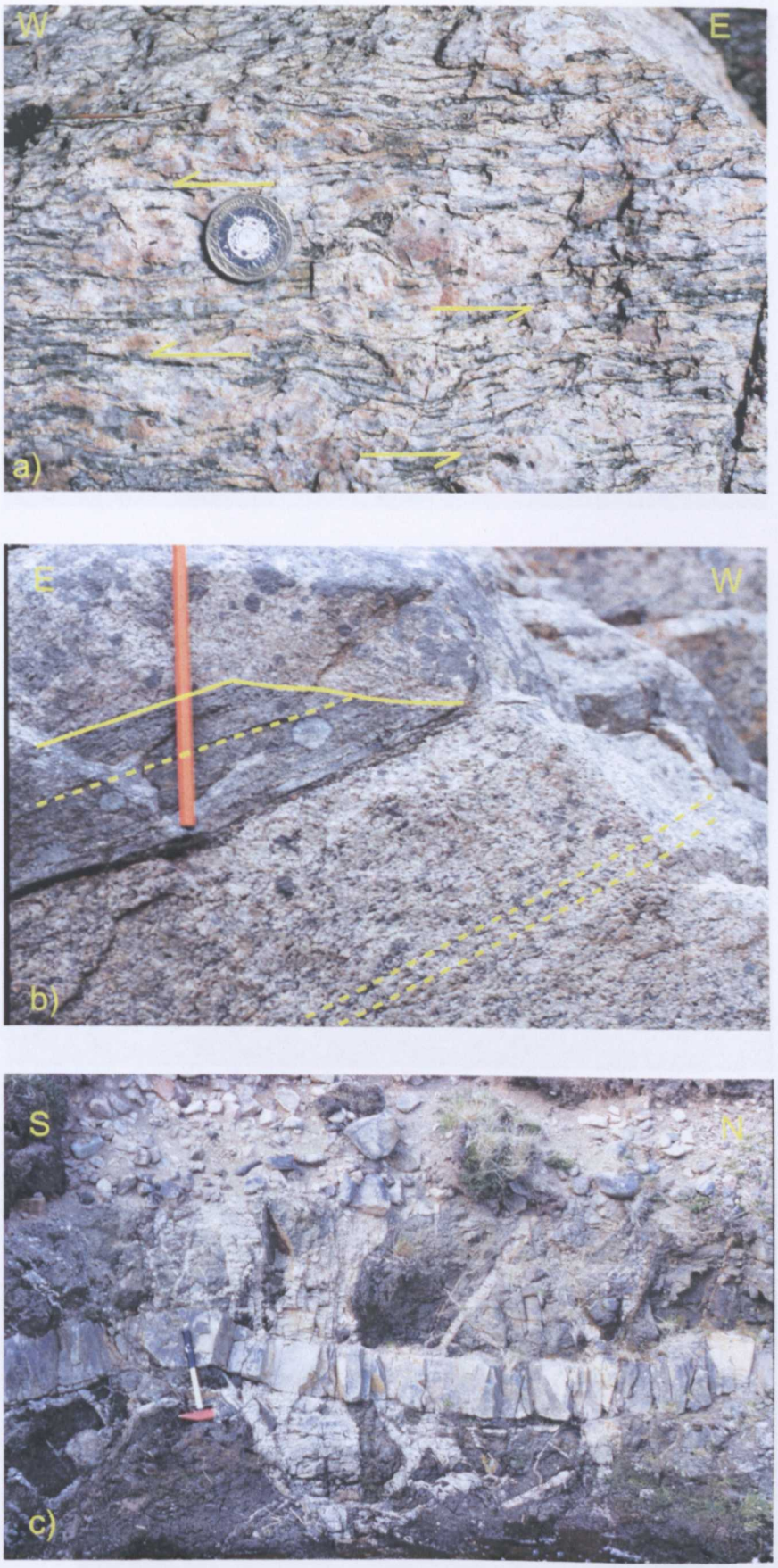

Fig. 4.3 Field photographs of igneous rocks in the Strath Halladale area. a) G-1 augen granites with strong solid-state rodding lineation and asymmetrically sheared K-feldspars exposed southeast of Braemore lodge at [ND0986|2879]. Solid-state lineation plunges 34 => 100°, top-to-the-W sense of shear. b) Foliated Strath Halladale granite exposed at Craigtown Rock [NC8923|5584] cross-cutting S_1/S_2-foliation of Achentoul Banded Fm. c) Ultramafic rocks exposed at Knockfin [NC9000|3600] are cut by foliated Strath Halladale Granite sheet (vertical) and late, cross-cutting, unfoliated aplites (horizontal).

Fig. 4.4 Field photographs of the Helmsdale Granite. a) Outer Helmsdale Granite, cumulate facies with large, randomly orientated K-feldspars and large, milky, interstitial quartz pools exposed at NC9457|1655. b) Ultramafic enclave within the outer Helmsdale Granite, note crystal transfer of K-feldspar [NC9486|1660]. c) Inner Helmsdale Granite, transitional facies exposed at Eldrable [NC9847|1838]. Note large K-feldspars (rectangle) and quartz pools (arrows) which are possibly derived by crystal transfer from the outer Helmsdale Granite.

4.5 Structural and metamorphic history

The previously accepted structural and metamorphic history of the study area is resolved in four separate deformational phases, D1-D4, based on the style and orientation of folding, development of fabrics and cross-cutting relationships with igneous bodies (Read 1931; McCourt 1980; Storey & Lintern 1981; Strachan 1988). Main structural trends are shown on Figure 4.1 and the previously accepted tectono-metamorphic history and timing of igneous events are summarized in Table 4.1.

4.6 Geology of the Strath Halladale Granite

4.6.1 Introduction

The Strath Halladale Granite is located on the western limb of the Kildonan synclinorium, a set of large-scale, open, NE-SW trending F3 folds. It is intruded into Moine rocks of the Loch Coire and Scaraben formations, and cross-cuts the unit boundaries and the regional composite $S_0/S_1/S_2$ foliation at shallow angles (e.g. Figs 4.2 & 4.6). This composite host rock foliation is attributed to ductile D1/D2 deformation (e.g. McCourt 1980; Strachan 1988) and within this part of the study area generally strikes 020-030° and dips consistently to the SE (Fig 4.1). The gentle swing of this foliation from NE-SW in the north, to N-S, back to NE-SW in the south is attributed to late-stage warping of the composite S2 fabric during D3 and D4 (e.g. McCourt 1980). D2 deformation also resulted in the formation of a strong mineral and rodding lineation (L2) that parallels F2 fold axes. In areas of low post-D2 strain, it plunges 10-12° towards 170-180° (McCourt 1980), but southeasterly plunging mineral lineations have also been observed (this study). Whereas large areas of the central granite are unexposed, its northern and southern terminations are moderately to well exposed and are used to describe some of the key structural, igneous and metamorphic features.

Deformation –Igneous phase	Fabrics – Structures – Metamorphism- other features	Exposed at
G4	Helmsdale Granite (2)	
D4	Regional, NW-SE trending open-gentle folds revealed by warping of S0/S1/S2 foliation and refolding of D3 axial traces (2). Rare minor open buckle folds and kink-bands with weak crenulation fabric (S4) (2). Widespread growth of radiating mats of fibrolite and sillimanite, overgrowing S1 and S2 but unconstrained with respect to D3 and D4 (2). Local development of kink bands and monoformal folds, occ. folding the "G3 granite phase" (1).	Helmsdale River to Scaraben area (2). Creag nan Iolair [NC 9030 5900] (1).
G3	Comprises Strath Halladale Granite (SHG), Reay Diorite, associated ultramafic rocks (1). Main SHG poorly exposed, but related granitic sheets x-cut F2 and F3 folds, G3 is therefore post D3 (2). Related SHG granite veins and pegmatites x-cut Reay Diorite (1).	Suissgill Burn, Kinbrace Burn (2). Torran Dubh [NC 9665 6255]
D3	Tight-open, large-scale, ENE-WNW trending F3-folds with subvertical FAP and gently (10°) easterly plunging fold axes. Rare F3 minor folds with weak axial-planar crenulation fabric. Bt-recrystallization at mid-greenschist facies metamorphic conditions (2). Asymmetrical, small-scale open-chevron type F3-folds with FAP (040/40/SE) and F3-hinges plunging gently (c.20°) to 040-050 or 150-170 (saddle structures) (1). Minor F3-folds are generally of S-symmetry, plunging NE in Strath Halladale but of z-symmetry, plunging SSE in Glutt Water (1). Folds G2-leucogranite sheets (1)	Clais nam Bo'Dubha [NC 9092 5364] (1). Strath Halladale area, and Glutt Water (1). Gloval Hill section [NC 9050 6150], Calgarry Beg section [NC9035 5930] (1).
G2	Anatexis and formation of leucogranites [aka "white granite" (1), "tonalite" (2) (3), "sodic granite" (4)] G2 contains xenoliths with F2-folds, therefore post-dates D2 (1), (2); G2 cuts isoclinal F2-folds and L2 (1)	Corrish Hill [NC 820 330] (1), (2) ?
D2	Folding of D1-structures and migmatitic segragations along small scale, tight to isoclinal F2-folds with FAP (020/30/SE), and crenulated S1-fabric in F2-foldhinges (1) (2). Locally transposition of S0/S1 to give strong composite, bedding-parallel S2-foliation (030/30/SE). Strong L2 rodding lineation, parallel to F2-hinges c.12°=>170-180 (1) (2). No retrogression of metamorphic assemblages associated with D1 => amphibolite facies (2).	Beinn Dubhain [NC 920 204] (2); Dun Burn [ND100 250] (2)
G1 ?	Augen granites & pegmatites with solid-state rodding lineations (2).	N of Mt. Morven (2)
D1	Penetrative Bt-fabric (S1) parallel to compositional banding (representing S0) in Moine country rocks. S1 is axial planar to rare isoclinal F1 folds. S1-parallel quartzo-feldspathic leucosomes, upper amphibolite facies (1) (2).	
G1 ?	Augen granites & pegmatites with solid-state rodding lineations (2).	

Table 4.1. Previously accepted tectono-metamorphic/magmatic history of the study area after (1) McCourt 1980; (2) Strachan 1988; (3) Lintern & Storey (1980); (4) Mykura (1985).

4.6.2 Metamorphism of the host rocks

The Moine rocks on the western side of the Strath Halladale Granite are dominated by strongly banded metatexites typical of the Achentoul Banded Formation (Figs. 4.2 & 4.5). The metatexitic banding is essentially parallel to the $S_0/S_1/S_2$-foliation and comprises biotite-rich melanosomes and quartzo-feldspathic leucosomes. Within the leucosomes, garnet is generally present as small, anhedral grains with rare plagioclase rims, but also grows within the biotite-rich melanosomes (Fig. 4.5 a, b, e, f, g & h). Locally, the biotite is embayed and the garnets show plagioclase coronas (Fig. 4.5 g & h). Occasionally, the segregation fabric is reworked by younger D2 fabrics and its formation can hence be attributed to D1 (table 4.1, see below). The preserved mineral assemblage suggests that the anhedral garnet in the leucosomes may represent the peak metamorphic conditions and could have formed by biotite dehydration melting at high pressures (e.g. Miller *et al.* 1997, see also Chapter 3), whereas the plagioclase halos fringing the garnets could have been formed by subsequent biotite and garnet breakdown during decompression (Jones, K. A. pers. comm. 2002). At present, it is, however, unclear whether all the leucogranites within the Achentoul Banded Formation were formed during prograde crustal thickening or post-peak exhumation.

The host rocks on the eastern side of the granite are mainly pelitic to semi-pelitic gneisses assigned to the Suisgill Semi-pelite. They are well exposed along the Glutt Water and in smaller stream sections towards Knockfin Heights (Fig. 4.6). East of the granite, the gneisses also show some evidence for melting which gets less common further towards the south. Where present, the leucosomes contain small, anhedral garnets indicative of high pressure Bt-dehydration melting. Locally, the segregation fabric is crenulated and folded. The newly developed axial planar crenulation fabric is generally defined by kinked biotite of the melanosome and newly grown biotite and muscovite (Fig. 4.5 a - d). Importantly, thin sections from migmatitic semi-pelites exposed in Glutt Water also show that prismatic sillimanite grows within a strongly developed S-C fabric (Fig. 4.5 i - k) suggesting that this second deformation event which crenulates the segregation fabric was accompanied by sillimanite grade metamorphism.

Towards the south, the Suisgill Semi-pelite shows less evidence for in situ melting and a strong D2 S-C fabric is developed in gneissic lithologies. The S-C fabric is defined by sheared biotite grains that wrap around recrystallized quartz aggregates. This fabric is

locally overgrown by radiating mats of fibrolite that have previously been interpreted to post date the shear fabric development and represent mimetic growth induced by the emplacement of the Strath Halladale Granite (e.g. Watson 1948; Strachan 1988). However, thin sections from Suisgill Burn also show that prismatic sillimanite grows within the S-C fabric (Fig. 4.5 l, m, n & o), indicating that fabric development and regional deformation occurred at sillimanite grade conditions, *prior* to mimetic fibrolite growth. Within the core of an F3 syncline developed at Learable Hill (Figs. 4.1 & 4.13) the sillimanite-grade shear fabric and the mimetic fibrolite overgrowths are crenulated, indicating that shear fabric and fibrolite development pre-date D3.

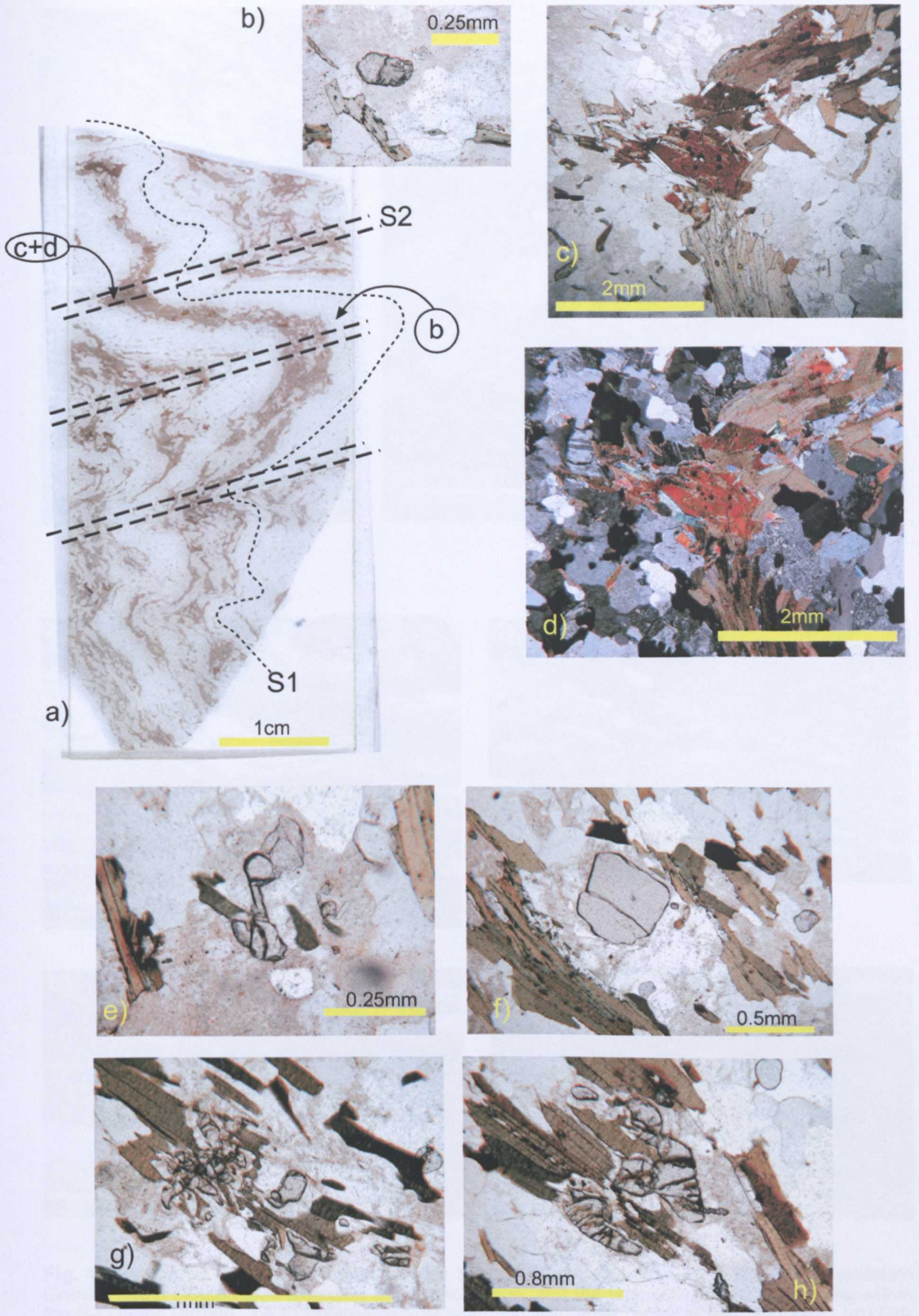

Fig. 4.5 Thin section photographs of the metatexites of the Strath Halladale area. a) Thin section scan showing the folded and crenulated S1-segregation fabric (Glutt Water). b) Small anhedral garnet in the leucosome (PPL, for location see a). c & d) Crenulated biotite (S1) and newly crystallized biotite and muscovite (S2) (for location see a), c) is PPL, d) is XPL). e & f) Small garnets within the metatexitic leucosomes W of the Strath Halladale Granite indicating possible in situ melting by Bt-dehydration at high pressures >10kbar, note biotite fabric wrapping garnet in f). g & h) Scalloped biotite and garnets showing plagioclase coronas, indicating the post-peak decompression reaction Bt+Grt=>Plag. See text.

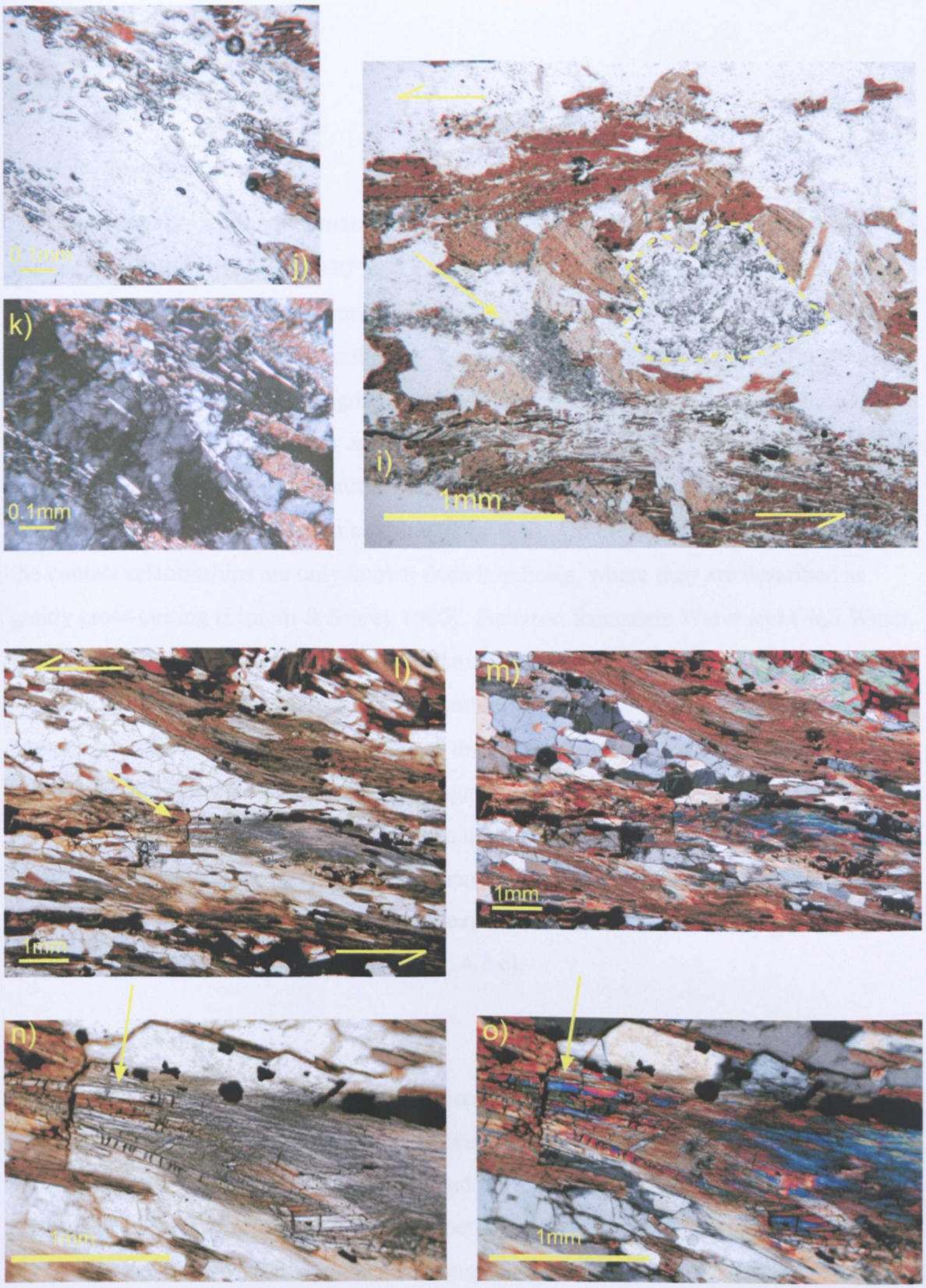

Fig. 4.5 continued. i) Grt-Bt-Sil-gneiss of the Suisgill Semi-pelite to the E of the Strath Halladale Granite. Note biotite fabric wrapping the relictic garnet, and the prismatic sillimanite growing within the S-C fabric (arrow). j & k) Enlargement of prismatic sillimanite grains in PPL and XPL. l-o) Grt-Bt-Sil-gneiss of the Suisgill Semi-pelite to the S of the Strath Halladale Granite. Note the prismatic sillimanite growing within the S-C fabric and the possibly mimetic fibrolite. See text.

4.6.3 The southern domain

4.6.3.1 Structural setting

Throughout the southern domain (Fig. 4.6), the composite S_2 foliation of the Moine rocks consistently strikes 020-030° and generally dips SE to E at 25-80° degrees. The Strath Halladale Granite cuts across the formation boundaries of the Moine rocks at a shallow angle and in the Achentoul Burn. On the southwestern side of Loch An Rhutair [NC864|355], granite sheets assigned to the Strath Halladale Granite cross-cut the composite S_2 foliation at shallow angles. In stream sections on the northwestern side of the granite, a general increase of granitic sheets towards the east is noted and psammitic screens are present within the main granite (Fig. 4.6). On the eastern side of the granite, the contact relationships are only known from boreholes, where they are described as gently cross-cutting (Lintern & Storey 1980). Between Rumsdale Water and Glutt Water, field mapping and core-data indicate large amounts of biotite granite that closely resemble the main Strath Halladale Granite and may either form several granite sheets or a larger igneous body that is also sub-concordant to the country rock foliation (Fig. 4.6). The Strath Halladale Granite carries a strong magmatic-state foliation (see below) that is sub-parallel to the local Moine rock foliation. In the Achentoul area, dioritic and mafic to ultramafic igneous rocks occur within the main granite, but contact relationships are not exposed. The mafic to ultramafic enclaves exposed at Knockfin are cut by granodioritic sheets and fine grained pink aplites (see Fig. 4.3 c).

4.6.3.2 Pluton Fabrics

The Strath Halladale Granite of the southern domain is strongly foliated but lacks macroscopically identifiable lineations. However, the appearance of the fabric intensity and kinematic indicators in handspecimen and thin section depends strongly on the orientation of the cut section (Fig. 4.7). Generally, W-E to NW-SE striking sections that are cut vertical to the foliation show the strongest and best-defined fabrics (Fig. 4.7 b & c). Vertical W-E striking sections also generally show a strong fabric whereas vertical, N-S striking sections only show very weak fabrics (Fig. 4.7 d). Sections cut parallel to the foliation show no preferred linear alignment of any minerals (Fig 4.7 e). To identify the maximum extension direction during fabric formation, a sample was collected for AMS-analysis (anisotropy of magnetic susceptibility) and processed by D. Liss at Birmingham

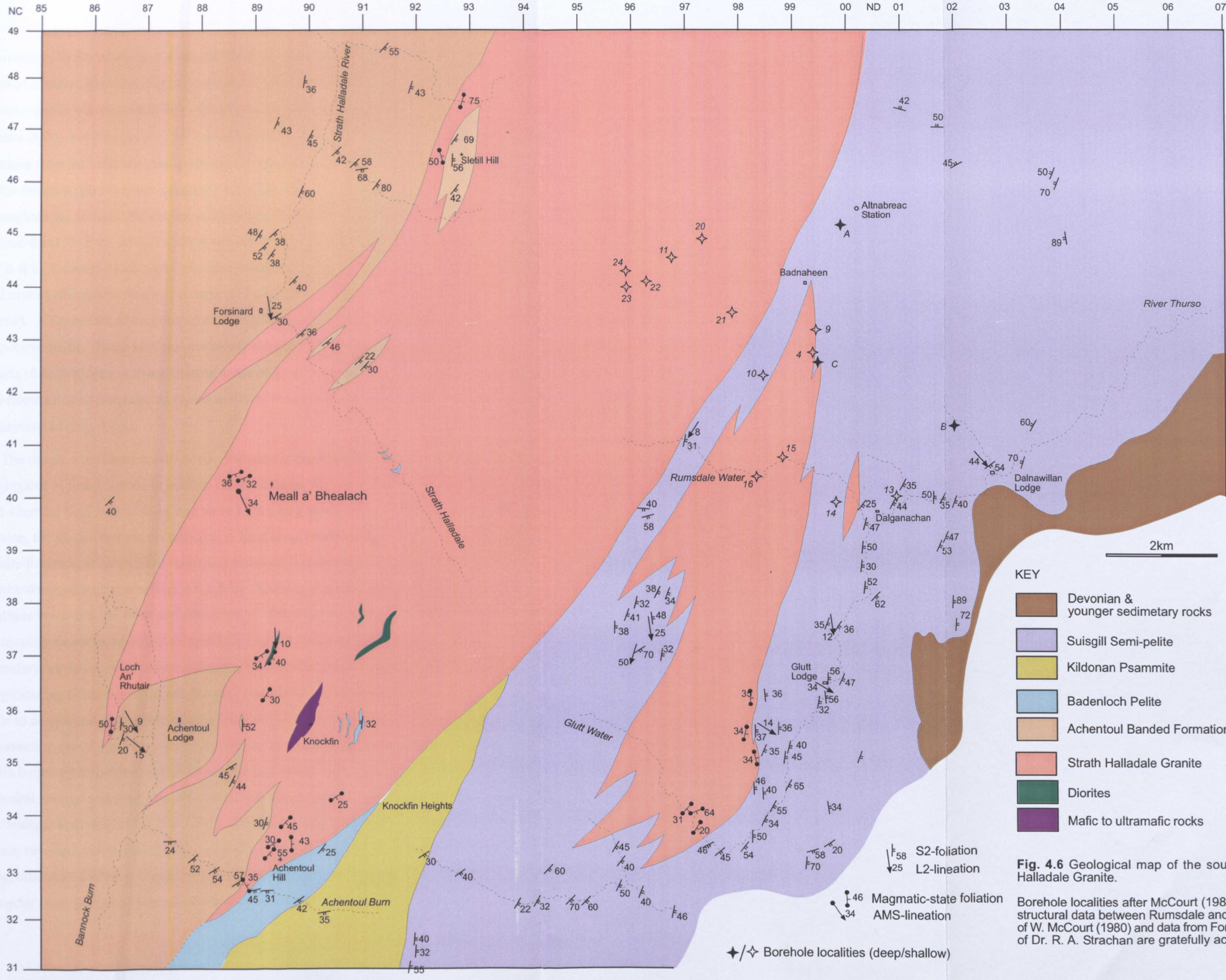

Fig. 4.6 Geological map of the southern Strath Halladale Granite.

Borehole localities after McCourt (1980), additional structural data between Rumsdale and Glutt waters of W. McCourt (1980) and data from Forsinard Lodge of Dr. R. A. Strachan are gratefully acknowledged.

University. In the southern domain, the AMS measurement (Sample SHG 132 collected west of Meall a' Bhealach, Fig. 4.6) defined a foliation that corresponds well with field measurements but also identified a weak lineation that is defined by ilmenite (Liss pers. comm. 2000) and plunges at *c.* 54° towards the SE. Subsequently, polished slabs and thin sections from this domain were generally cut parallel to this AMS-lineation, perpendicular to the foliation (also in other samples). Although this lineation will most likely undulate throughout the domain, the chosen sections generally show a strong, well-defined foliation. Within these W-E to NW-SE striking sections cut perpendicular to the foliation (e.g. Fig. 4.7 b & c), kinematic indicators (elongate feldspar aggregates, elongate K-feldspar augen, and asymmetric quartz ribbons) consistently give top-to-the-west sense of shear (see below). A further set of sections was cut perpendicular to the foliation, parallel to its respective strike. These sections commonly show a strong foliation in which elongate quartz ribbons locally indicate sinistral sense of shear (viewed east), suggesting that fabric development took place during top-to-the-W/NW movements with local, sinistral oblique transpression (Fig. 4.8 g).

The rough, sometimes anastomosing foliation is generally defined by elongate aggregates of fine grained plagioclase and K-feldspar that are wrapped by small biotites and alternate with 1-5mm thick and up to 1.5cm long quartz ribbons (Fig. 4.7). In thin section, the plagioclase occurs either as 2-3mm long, twinned laths that lie within the biotite foliation, or as smaller, subhedral grains of 1-2mm diameter that are part of the biotite-wrapped aggregates (Fig. 4.8 a & b). It shows straight extinction, undeformed multiple twins and has often sericitized cores. There is no evidence for high internal dislocation densities, marginal recrystallization and core mantle structures, or grain boundary migration at intersecting feldspar/plagioclase grains. Grain boundaries with neighbouring biotites are also straight and indicate magmatic-state fabric development with little to no evidence for deformation in the solid state. However, grain boundaries at intersecting quartz grains are generally slightly irregular, indicating some low-temperature grain boundary migration controlled recovery of quartz. K-feldspar occurs either as anhedral, elongate megacrysts within the foliation, or forms a subordinate component of the feldspar aggregates (Fig. 4.8 c & d). The megacrysts are *c.* 6x3mm and often contain small, euhedral, unstrained plagioclase grains that are occasionally aligned parallel to the magmatic-state foliation. The megacrysts, however, show strong undulose extinction and irregular outer grain boundaries, indicating high dislocation densities and limited solid-

state recovery. Biotite commonly occurs as 0.5-1mm long, rectangular crystals wrapping the earlier crystallized phases and defining the foliation. Only rarely, it shows sweeping undulose extinction but is often retrogressed to white mica and chlorite. Quartz occurs in three distinct varieties (Figs. 4.8 e to l). It forms an interstitial phase within the biotite-wrapped feldspar aggregates (Fig. 4.8 b, c & f) and shows little internal subgrain formation but prismatic deformation bands are common (Fig. 4.8 f). Contacts with adjacent feldspars are, however, irregular (Fig. 4.8 b & c) and indicate grain boundary migration. Alternatively, quartz occurs as ribbons that show various microstructures. It may form 2x4mm, biotite-wrapped, elongate grains that show internal subgrains with straight subgrain boundaries and little evidence for high internal strain (Fig. 4.8 e & g). The elongate quartz grains may also be flattened and occur as *c.* 0.5 x 2-4mm wide ribbons that show either grain boundary migration-dominated subgrain formation (Fig. 4.8 g), or little to no internal strain (Fig. 4.8 h). These largely strain-free grains appear to have been formed, aligned and flattened in the magmatic state. Locally, the flattened quartz ribbons comprise strongly developed prismatic deformation bands and sweeping undulose extinction that correspond to type 2 ribbons of Boullier & Bouchez (1978) which indicates weak low-temperature deformation (Fig. 4.8 i to k). Often, quartz occurs a large oval shaped grains that show prismatic deformation bands but are otherwise undeformed (Fig. 4.8 l).

Overall, the microstructures indicate that mineral alignment occurred in the magmatic state with little evidence for down-temperature deformation. Quartz morphologies indicate that most of the flattening of the fabric occurred in the magmatic state followed by limited low-temperature deformation leading to locally higher dislocation densities (undulose extinction) and consequent grain boundary migration controlled recovery. The microstructures suggest that this overprint may have occurred at temperatures corresponding to lower greenschist facies (300-350°C). Brittle cracks are locally abundant and probably result from brittle faulting that is well documented within the overlying sediments of Devonian age to the east of the Strath Halladale Granite (e.g. McCourt 1980). Throughout the southern domain, there is little variation of the microstructures developed within the granite and figure 4.9 shows further polished specimen and thin sections from Achentoul and Sletill Hill (Fig. 4.6) that comprise distinctly magmatic-state fabrics. Fabrics developed within the biotite granite sheet exposed in the Glutt Water (Fig. 4.6) are

similar to the magmatic-state fabrics developed within the main Strath Halladale Granite. However, biotite may locally be sparse.

Dioritic and ultramafic enclaves within the main granite locally show a strong, southerly plunging lineation that is defined by aggregates of small, hornblendic amphiboles sat in a fine grained groundmass of subhedral plagioclase with little K-feldspar and interstitial quartz. Amphibole is locally retrogressed to biotite, and plagioclase is often sericitized. These lineations thus deviate from the locally-dominant SE-plunging lineations in the granite (AMS) and the host rocks. However, magmatic-state, southerly-plunging lineations have been observed in the igneous rocks of northern domain (see below) which may indicate that syn-deformational magmatic flow occurred along sigmoidal trajectories changing from SE-NW to N-S to SE-NW. Alternatively, the N-S trending lineations within the southern domain could be interpreted to have been rotated following the incorporation of the enclaves into the main granite.

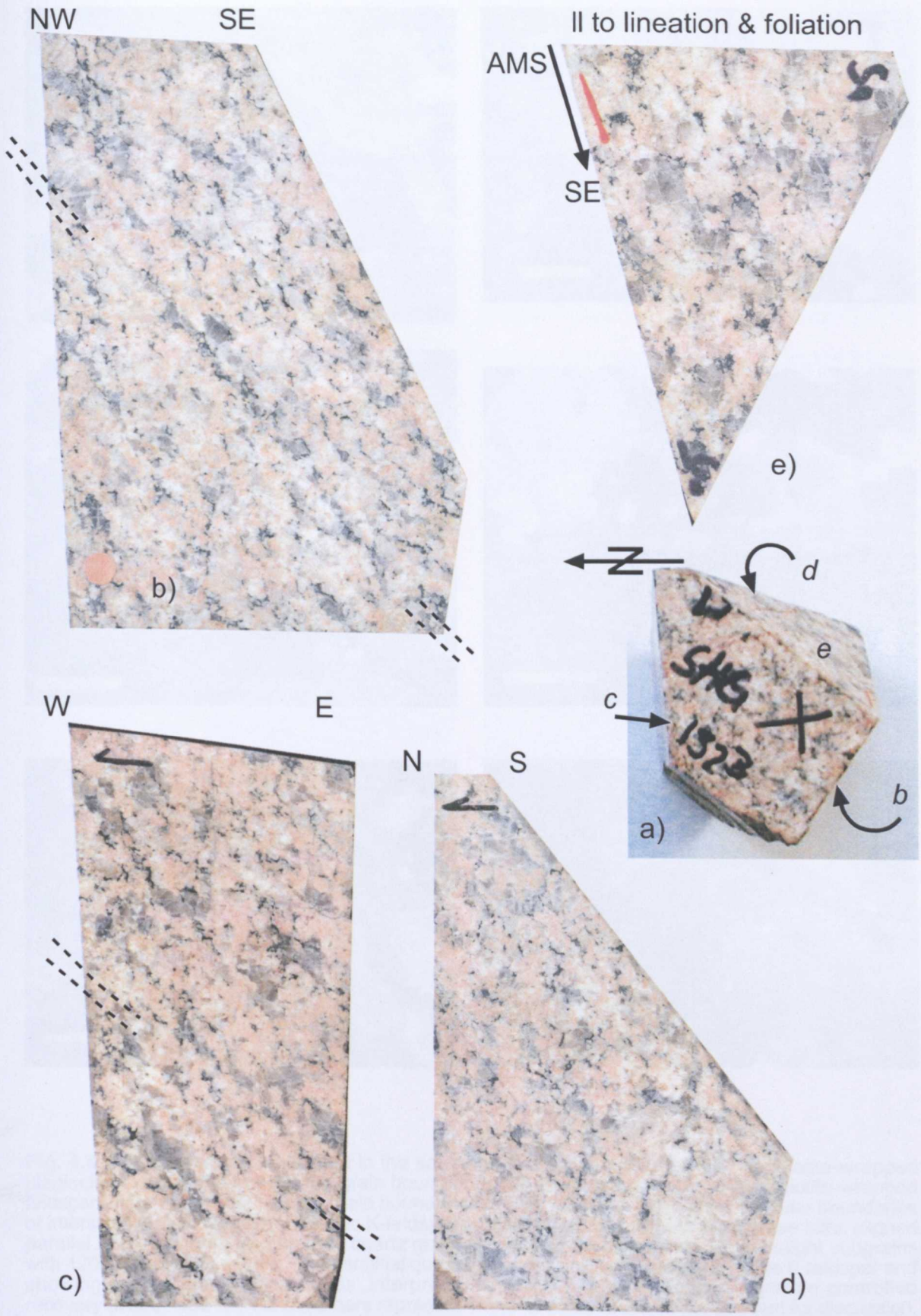

Fig. 4.7 Photographs of polished handspecimen sections of the Strath Halladale Granite cut varying orientations. a) Photo looking down onto the specimen SHG 132B indicating the position of sections b) to e). b) Section cut parallel to the AMS-lineation showing strong foliation. c) Section cut W-E showing strong foliation. d) Section cut N-S showing comparably weak foliation. e) Section cut parallel to the foliation showing no preferred linear mineral allignment. See text for further explanation. Note the coarse, sometimes anastomosing fabric defined by elongate quartz ribbons and biotite-wrapped feldspar aggregates. Black arrows are 1cm long, orange circle is c.0.5cm accross, red line in e) is 1.2cm long.

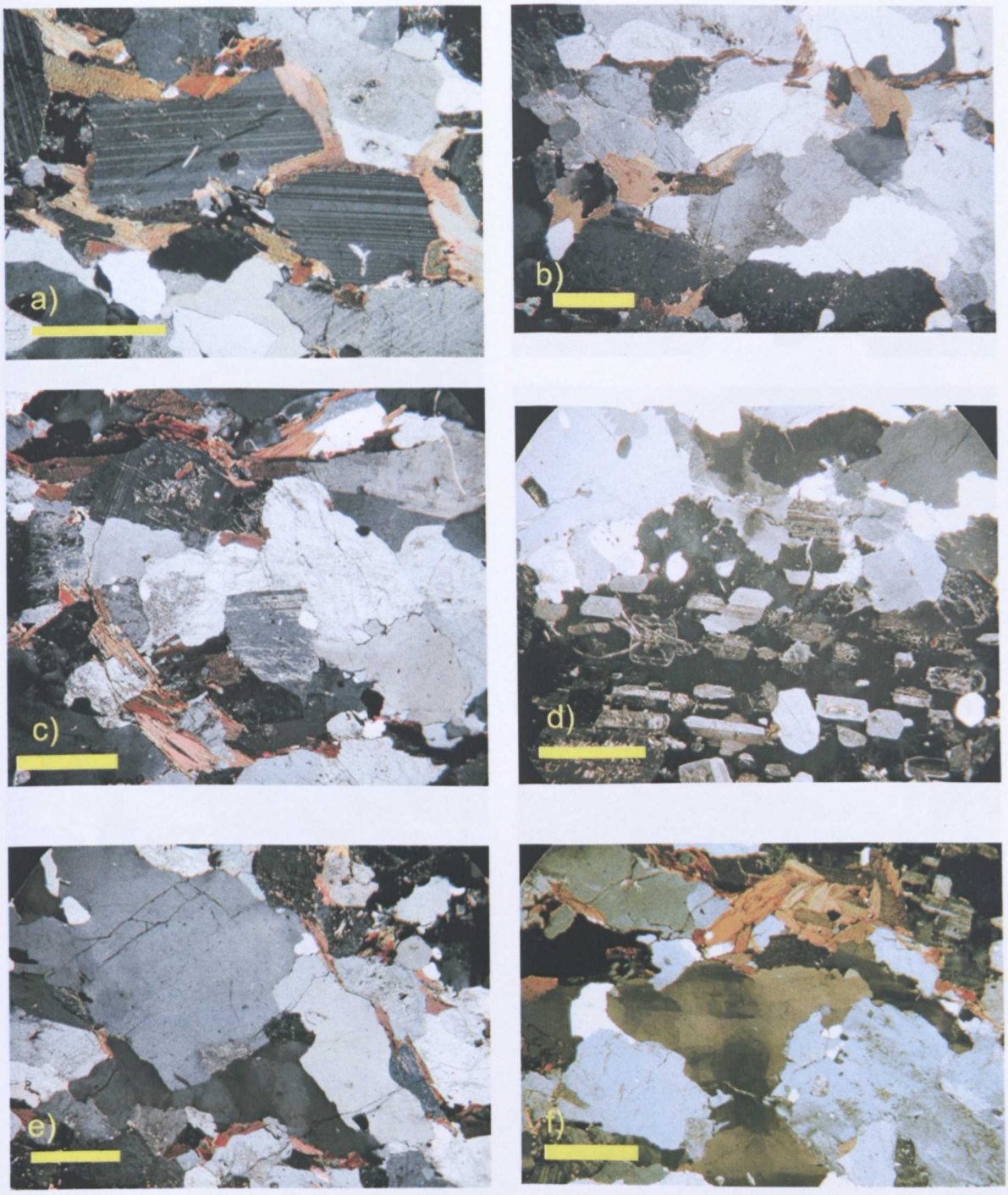

Fig. 4.8 Microstructures developed in the southern Strath Halladale Granite. a) Biotite-wrapped plagioclase laths, note the straight grain boundaries and uniform extinction. b & c) Biotite-wrapped feldspar aggregates, note straight grain boundaries of neighboring feldspars but irregular boundaries of interstitial quartz. d) Large poikilitic K-feldspar containing small euhedral plagioclase laths aligned parallel to the foliation. e) Elongate quartz grain wrapped by biotite and showing straight subgrains with 120° intersection angles. f) Interstitial quartz grain growing in P-shadow of large K-feldspar and showing equant deformation bands: interpreted to indicate grain boundary migration controlled recovery at 350°-400° C. All scale bars represent 1mm, all pictures are XPL. See text for discussion.

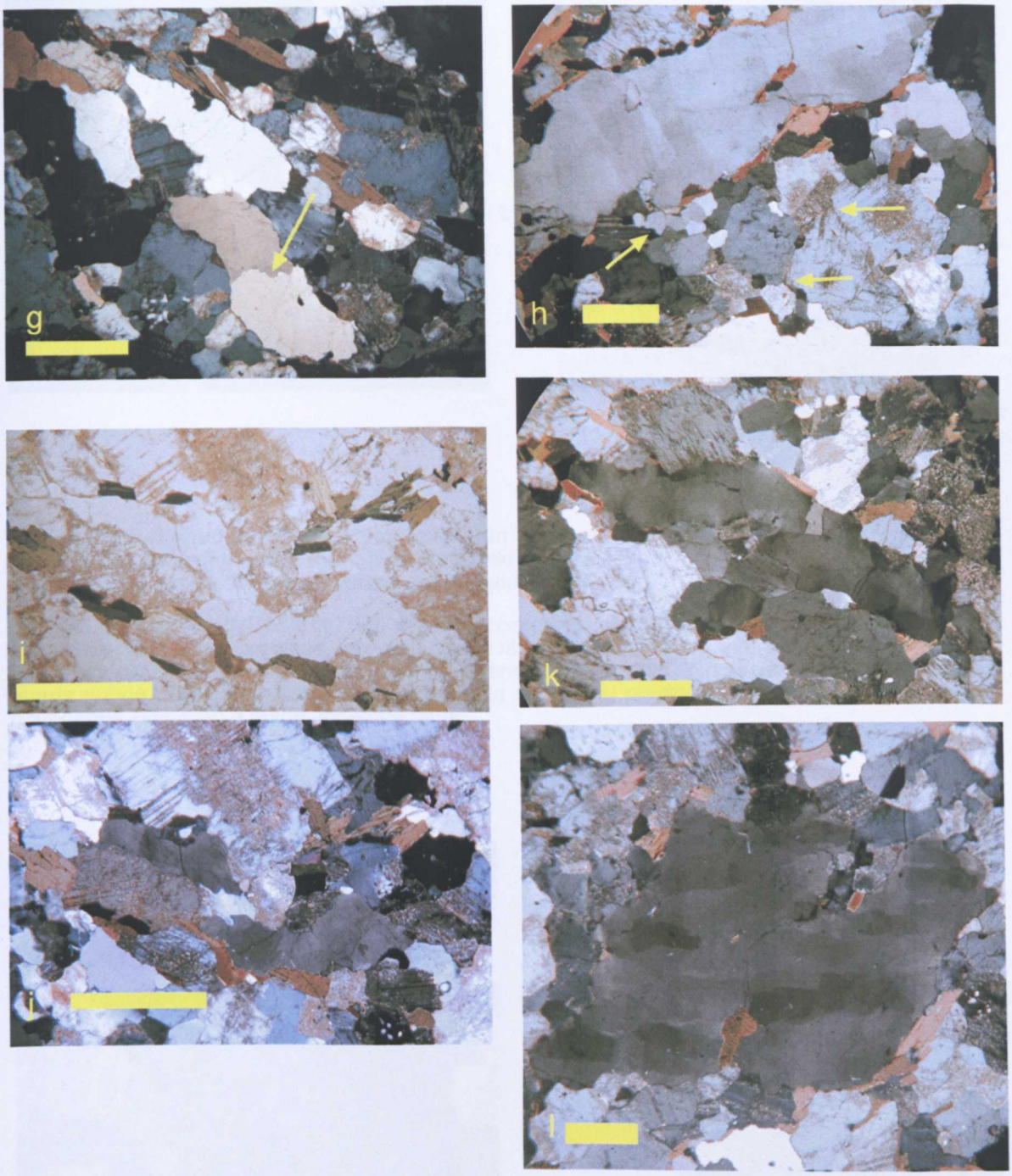

Fig. 4.8 continued. g) Sigmoidal quartz ribbon showing grain boundary migration at sub grain boundary. h) Large, flattened quartz ribbon showing little internal deformation. Also note the 120° intersection angles of the feldspars below. i+j) Flattened quartz ribbon between sericitized plag & K-feldspar in PPl and XPL. k) Flattened quartz ribbon showing undulose extinction (XPL). l) Large, largely undeformed, interstitial quartz grain of c. 6mm radius showing equant internal deformation bands and chess board pattern. All scale bars equal 1mm, see text for further explanation.

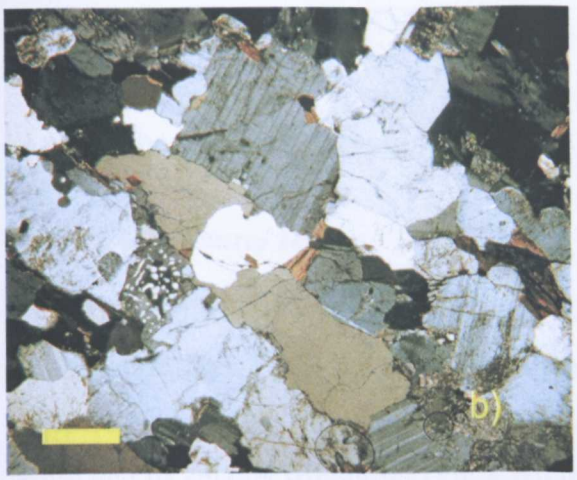

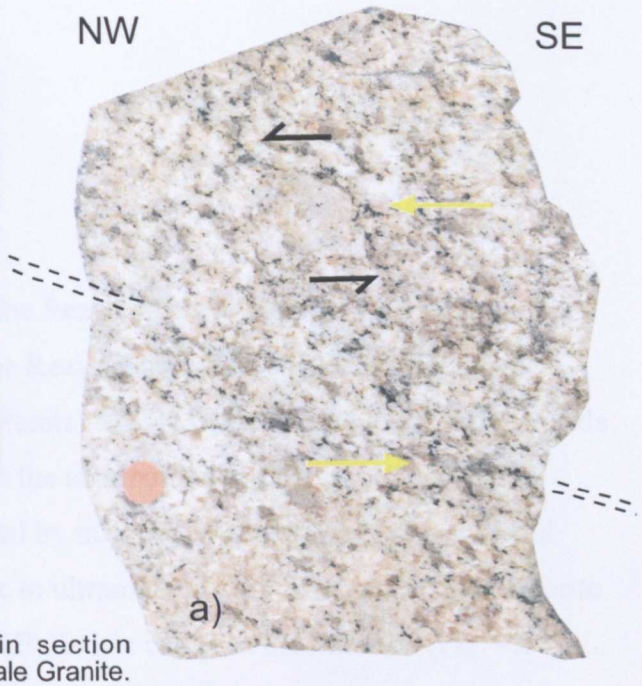

Fig. 4.9 Polished handspecimen and thin section photomicrographs of the southern Strath Halladale Granite. Orange circle is 0.5cm across, yellow scale equals 1mm.

a) Sletil Hill sample [NC9300|4750]: medium-coarse grained granodiorite with strong foliation comprising feldspar aggregates, elongate quartz ribbons, oval-shaped, interstitial quartz pools and asymmetrical K-feldspars giving top-to-the-W sense of shear. b) Thin section showing flattened, quartz ribbon with little internal deformation and subhedral plagioclase laths with straight grain boundaries indicating a magmatic-state fabric.

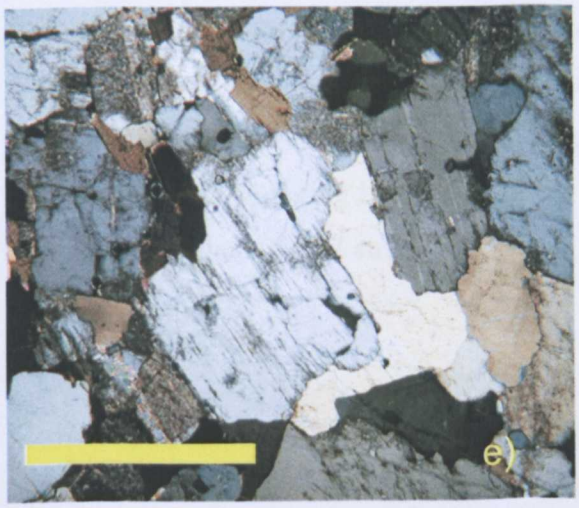

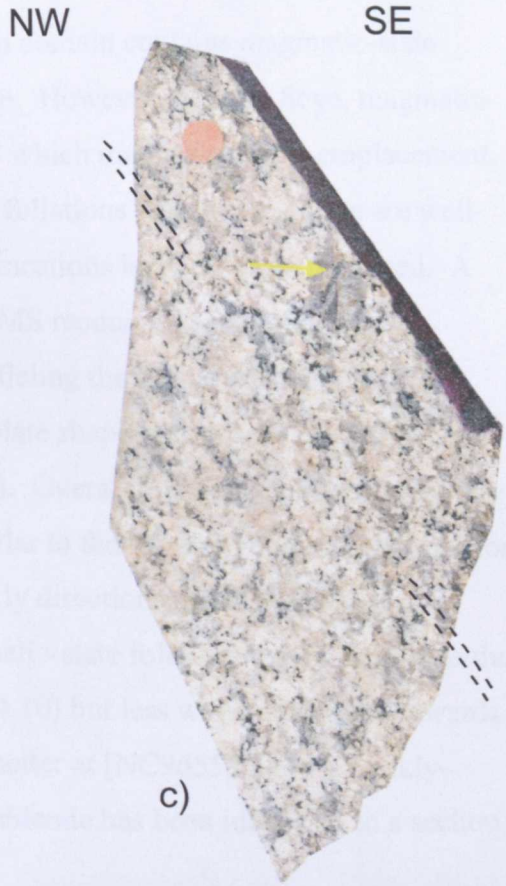

c) Polished handspecimen from Achentoul Hill [NC8963|3391] showing comparable fabrics to Sletil Hill, note the large interstitial quartz pool (arrow). d) Thin section of interstitial quartz grain showing little evidence for solid-state deformation and only equant internal deformation bands. e) Thin section showing subhedral plagioclase laths with interstitial quartz, note the straight grain boundaries and lack of solid-state deformation.

4.6.4 The northern domain

4.6.4.1 Structural setting

In the northernmost part of the domain, the Reay Diorite is intruded into migmatitic, semi-pelitic Moine gneisses that separate the Reay Diorite from the Strath Halladale Granite (Fig. 4.10). The Strath Halladale Granite itself is well exposed along the Sandside Burn and its smaller tributaries (Fig 4.10) to the south of Reay. The geology on the western side of the main granite is dominated by migmatitic gneisses of the Achentoul Banded Formation into which various mafic to ultramafic stocks and isolated granodiorite sheets that closely resemble the main Strath Halladale complex are intruded (Fig. 4.10). On the western side, the composite S_2 foliation developed in the migmatitic Moine gneisses strikes 020° and dips east at mostly 30-50°. North of the lower Trantlebeag burn at [NC9045|5355] a small, mafic to ultramafic stock is exposed. In the north, the composite S_2 foliation developed in the host rocks swings to 040° but still dips at 20-50° to the SE. The Strath Halladale Granite in the northern domain contains magmatic-state foliations that parallel the local S_2 host rock foliation. However, at Loch Scye, magmatic-state foliations developed within the granite dip SW which may reflect post-emplacement, large-scale, open folding. Throughout this domain, foliations within the granite are well-developed in W-E to NW-SE striking sections but lineations have not been observed. A second sample from the granite was collected for AMS reconnaissance work from Sandside Burn, and again identified a foliation paralleling the field measurements. The AMS-ellipsoid is defined by magnetite and of an oblate shape with a very weak magnetic lineation that plunges SSW (Liss pers. comm. 2000). Overall this indicates predominantly flattening strain during fabric development and similar to the southern domain, sections for structural work were cut in westerly or north-westerly directions, perpendicular to the foliations. The Reay Diorite locally carries a magmatic-state foliation that is parallel to the host rock foliation towards the pluton margin (Fig. 4.10) but less well constrained towards its centre. Within a sample collected south of Helshetter at [NC9655|6240], a weakly-developed, SSW-plunging lineation defined by hornblende has been identified in a section cut parallel to the NE-SW striking foliation.

KEY

- Devonian & younger sedimetary rocks
- Suisgill Semi-pelite
- Achentoul Banded Formation
- Strath Halladale Granite
- Reay Diorite
- Mafic to ultramafic rocks

- S2-foliation
- L2-lineation
- Magmatic-state foliation
- AMS-lineation
- Sense of shear (top)
- Sample locallity (AMS/chron)

Fig. 4.10 Geological map of the northern Strath Halladale Granite.

Note the magmatic-state fabric of the granite and the shear sense indicators. Devonian boundary and Devonian structural data after BGS sheet 115, additional structural data W of the Strath Halladale Granite after McCourt 1980.

4.6.4.2 Pluton Fabrics

In the lower Trantlebeg Burn [NC9045|5355] (Fig. 4.10), mafic to ultramafic igneous rocks are intruded into the Achentoul migmatites and locally carry strong foliations paralleling the local Moine fabric (Fig. 4.10). The foliation in the meta-igneous rocks strikes 004° and dips at 44° to the east. In thin section, the hornblende is strongly recrystallized indicating solid-state fabric development that suggests the intrusion had cooled prior to the main phase of deformation (D2).

At Craigtown Rock (Fig. 4.10) a large granite sheet that petrographically and geochemically resembles the main Strath Halladale granite is intruded into metatexitic Moine gneisses. The metatexitic banding and the composite S_2 foliation strikes 054° and dips SE at 57° and locally, small-scale easterly-plunging sheath folds are developed. The granite cross-cuts the composite S_2 foliation of its host rocks (see Fig. 4.3 b) but also carries a strong magmatic-state foliation that is subparallel to the host rock foliation (041/47/SE). Dm-scale shear zones are well-developed in outcrop faces trending E-W and indicate an overall top-to-the-W sense of shear (Fig. 4.11 a). The foliation anastomoses around feldspar aggregates and elongate quartz grains that are occasionally wrapped by small biotite grains. In thin section, plagioclase and K-feldspar occur as aligned, undeformed, small, eu- to subhedral grains that are embayed by neighbouring quartz grains (Fig. 4.11 c, d & e). However, at intersecting feldspar boundaries, no recrystallization is observed and 120° intersection angles indicate undeformed equilibrium assemblages. Quartz also occurs as large, oval-shaped grains that are wrapped by biotite (Fig. 4.11f). These quartz grains show subgrains that also intersect at 120° angles and show no evidence for internal high strain. The granite fabric is therefore clearly magmatic and carries no solid-state overprint, similar to the fabrics observed within the main Strath Halladale Granite to the south. The shear zones further indicate that this sheet was emplaced syn-tectonically during broadly west-directed thrusting during D2-deformation.

Within the northern Strath Halladale Granite, comparable magmatic-state shear zones are widely developed and have been observed at Sandside Burn and west of Creag Mor (Fig. 4.10). A polished section (Fig. 4.12 a) cut NW-SE with abundant, anastomosing shear bands indicates top-to-the-NW sense of shear. In handspecimen, the S-fabric is defined by aligned eu- to subhedral crystals that are comparatively large with respect to the finer grained aggregates of feldspars and quartz which define the C-fabric. In thin section,

however, both assemblages appear undeformed and show no evidence for solid-state deformation (Fig. 4.12 b). The S-fabric is largely defined by euhedral, longitudinally-twinned plagioclase with subhedral K-feldspars and large, interstitial, elongate quartz grains. Fine grained aggregates of feldspars and quartz that are mantled by small biotite flakes form the C-fabric but consistently show magmatic-state microstructures such as straight grain boundaries, straight extinction, abundant 120° intersection angles and only little, low-temperature grain boundary migration recrystallization.

The foliation developed in the Reay Diorite is defined by aggregates of small, hornblendic amphibole (0.25-0.5mm) and biotite that alternate with aggregates of subhedral plagioclase, K-feldspar, and interstitial quartz. Plagioclase shows straight grain boundaries, multiple twins with straight extinction but is often strongly sericitized. Amphibole shows predominantly irregular grain boundaries and is often replaced by biotite. Small, interstitial quartz grains show abundant undulose extinction and equant deformation bands. Overall, the fabric is interpreted to have formed in the magmatic state but has subsequently been strongly retrogressed.

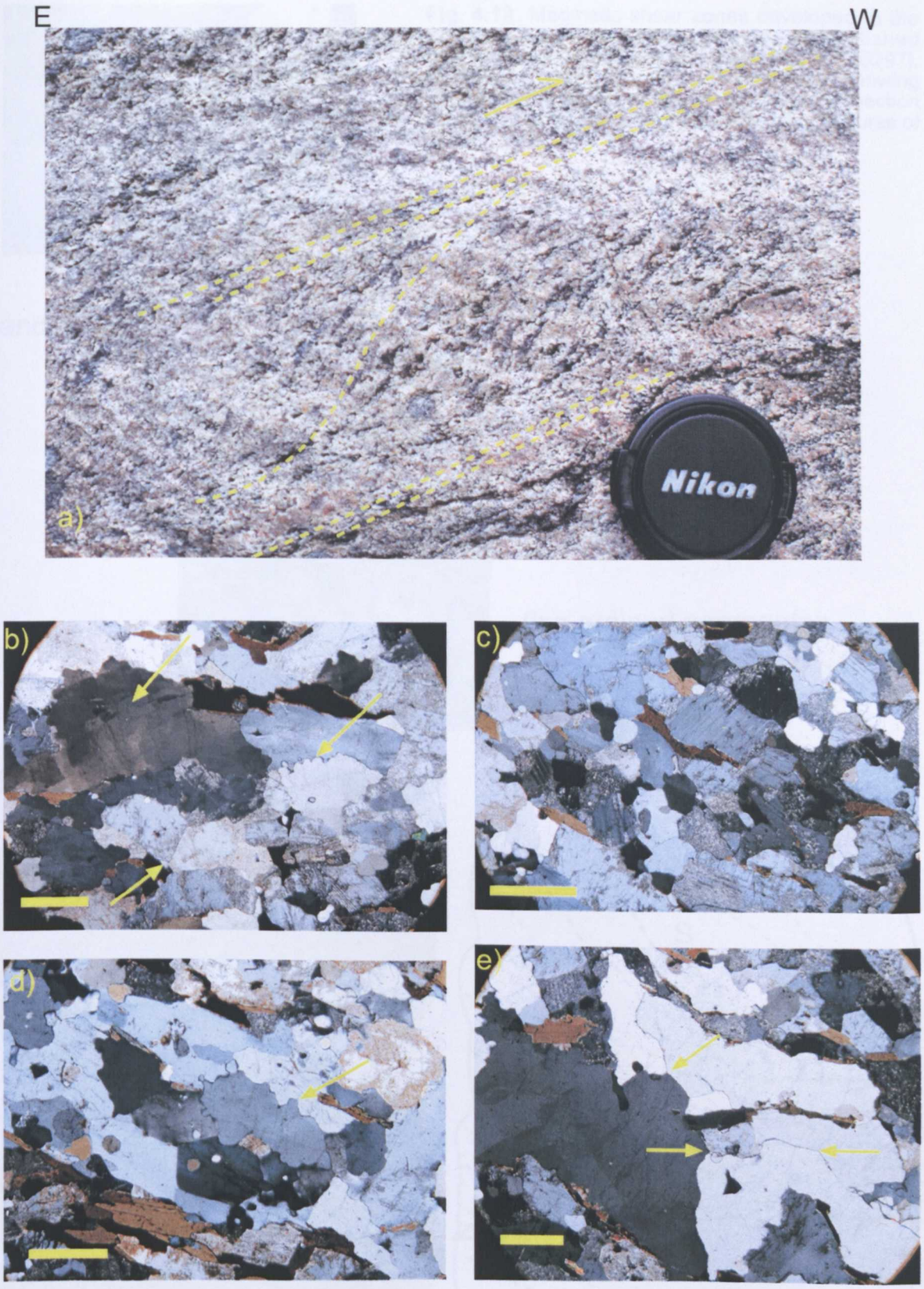

Fig. 4.11 Magmatic, top-to-the-W shear zone developed within a satellite sheet W of the main Strath Halladale Granite at Craigtown Rock [NC8923|5584]. a) Field photograph showing C-S fabric. b-e) XPL thin section photomicrographs showing the magmatic nature of the shear fabric. b) Typical alternating feldspar aggregates and elongate quartz define the planar fabric. Note the grain boundary migration between the quartz subgrains, the undulose extinction, and the tripple points between the feldspars . c) Smaller, equigranular quartz and feldspar aggregates. d) Larger domain of quartz grains showing grain boundary migration and undulose extinction. e) Large quartz grain with well defined sub grains showing 120° intersection angles. Scale bars equal 1mm.

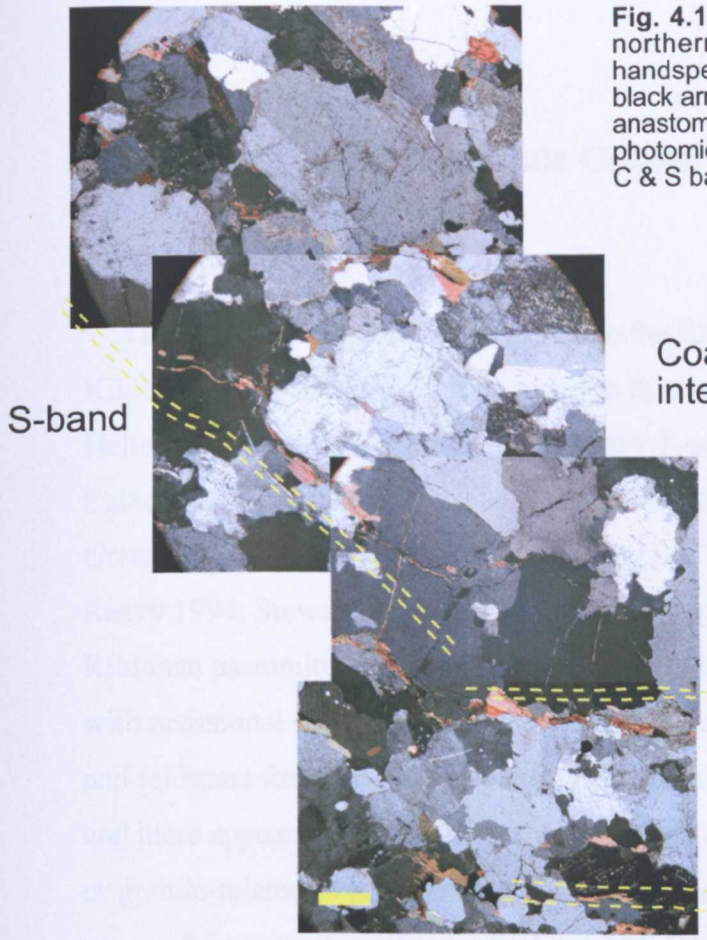

Fig. 4.12 Magmatic shear zones developed in the northern Strath Halladale Granite. a) Polished handspecimen from Creag Leathan [NC9875|6297], black arrow equals 1cm. b) Structural sketch showing anastomozing shear bands. c) Collage of thin section photomicrographs showing magmatic-state features of C & S bands. See text.

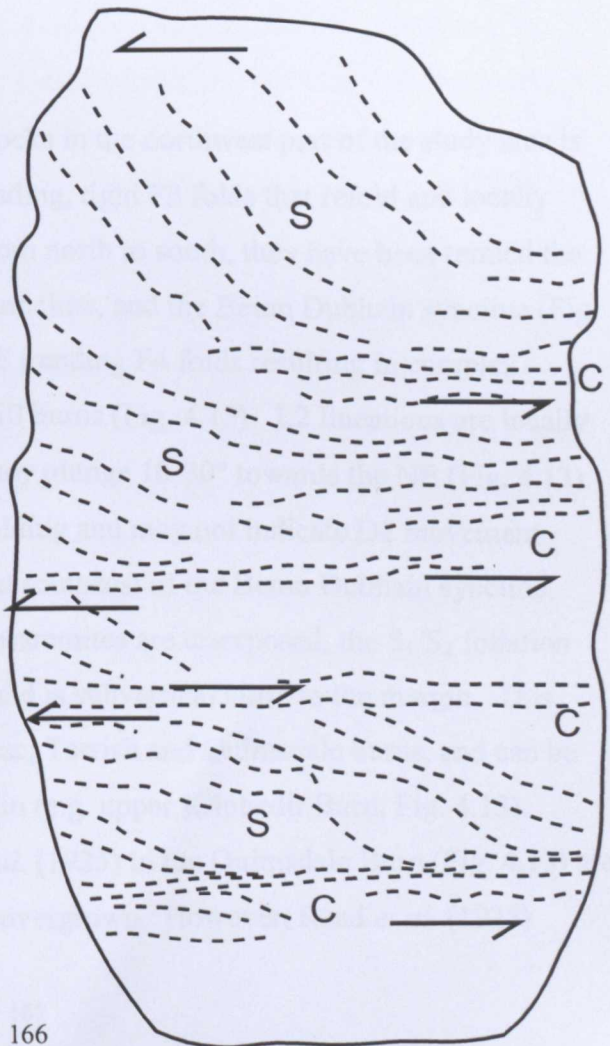

4.7 Geology of the Helmsdale Granite

4.7.1 Introduction

The Helmsdale Granite is intruded into the Kildonan psammites on the SE limb of the Kildonan Synclinorium and is bounded to the southeast by the Helmsdale Fault. The Helmsdale Fault is a Mesozoic normal fault downthrowing to the southeast, an older Caledonian history has been inferred in the context of the sinistral movements along the Great Glen – Walls Boundary fault system (e.g. Watson 1984; Leake 1990a; Jacques & Reavy 1994; Stewart *et al.* 1997, 1999). Throughout this part of the study area, the Kildonan psammites are mostly dark-grey to light-brown coloured, flaggy metasediments with occasional semi-pelitic bands. In thin section, quartz appears strongly recrystallized and feldspars form small aggregates. No metamorphic index minerals have been observed and there appears to be no contact metamorphic aureole developed within the host rocks, or granite-related fibrolite growth as reported further north. The granite and its host rocks are overlain unconformably by Early and Middle Devonian sediments (Fig. 4.13).

4.7.2 Structural setting

The structural geology of the basement rocks in the northwest part of the study area is dominated by three large-scale, NE-SW trending, tight F3 folds that refold and locally crenulate the penetrative S_1/S_2 foliation. From north to south, they have been termed the Learable Hill syncline, the Kildonan Burn anticline, and the Beinn Dubhain syncline (Fig. 4.13). These F3 folds are kinked by NW-SE trending F4 folds resulting in complex foliation patterns in the Kildonan and Suisgill burns (Fig. 4.13). L2 lineations are locally observed in this northwestern area, where they plunge 10-30° towards the NE (Fig. 4.13). However, they are clearly effected by D3 folding and may not indicate D2 movement directions. The Helmsdale Granite crops out southeast of the Beinn Dubhain syncline. Although its contact relationships with the psammites are unexposed, the S_1/S_2 foliation steepens progressively towards the pluton, and is subvertical close to the margin. This steepening is well developed in the Allt Breac, Torrish and Oulmsdale burns, and can be seen all along the northwestern pluton margin (e.g. upper Kilphedir Burn, Fig. 4.13). Contact relationships described by Read *et al.* (1925) in the Oulmsdale Burn (Fig. 4.13) are no longer exposed and appear to have been overgrown. However, Read *et al.* (1925)

reported that the contact is subvertical, that the Moine rocks in the contact zone are extremely 'shattered' and that the granite contains angular Moine xenoliths (Read *et al.* 1925, p. 41).

North of the pluton, the Kildonan psammites are well exposed along the Langwell Water, on Mid Hill, in various stream sections towards Scaraben and in the Berriedale Water (Fig. 4.13). The contact relationships of pluton and host rocks along the northern pluton margin are not exposed, however, the S_2 foliation steepens towards the pluton and is vertical in its vicinity (e.g. Mid Hill, Fig. 4.13), comparable to the relationships described previously (see above). The S_1/S_2-foliations further indicate a set of large-scale, tight, E-W striking folds, that occur south of the Beinn Dubhain syncline which occurs west of Scaraben (Fig. 4.13). The W-E trending, southward-verging anticline is tight in the west and its trace can be inferred from the upper Langwell Water towards the lower Berriedale Water in the east where the structure is open and rather upright (Fig. 4.13, 4.13). In the Langwell Water, the S_2 foliations south of the anticline steepen towards the pluton and are generally subvertical. However, way-up criteria show younging towards the north which requires the existence of an otherwise unobservable, tight syncline, the trace of which lies on the northwestern flank of Mid Hill (Fig. 4.13). This structure is not traceable to the west and thus probably dies out laterally. In the area between Scaraben and Berriedale Water, the Moine rocks are only mildly affected by post D2 deformation and an L_2 lineation is well developed that plunges gently (10-20°) towards the NNE (Strachan 1988).

The western and northeastern margin of the Helmsdale Granite are unconformably overlain by sediments of Early to Middle Devonian age and contact relationships of granite and host rocks are unexposed. The contact between pluton and host rocks in the far southwest (Fig. 4.13) is unexposed and has been inferred from the geological map (sheet Nr. 103). On the coast north of Berriedale, granitic rocks that are comparable to the outer Helmsdale Granite have been reported but are inaccessible from the landward side. The Devonian rocks that unconformably overly the Moine rocks and the Helmsdale Granite display two sets of open to gentle folds (Fig. 4.13). These are interpreted to form by progressive tightening of the underlying basement structures during the Devonian and are not considered to be Caledonian F3 folds.

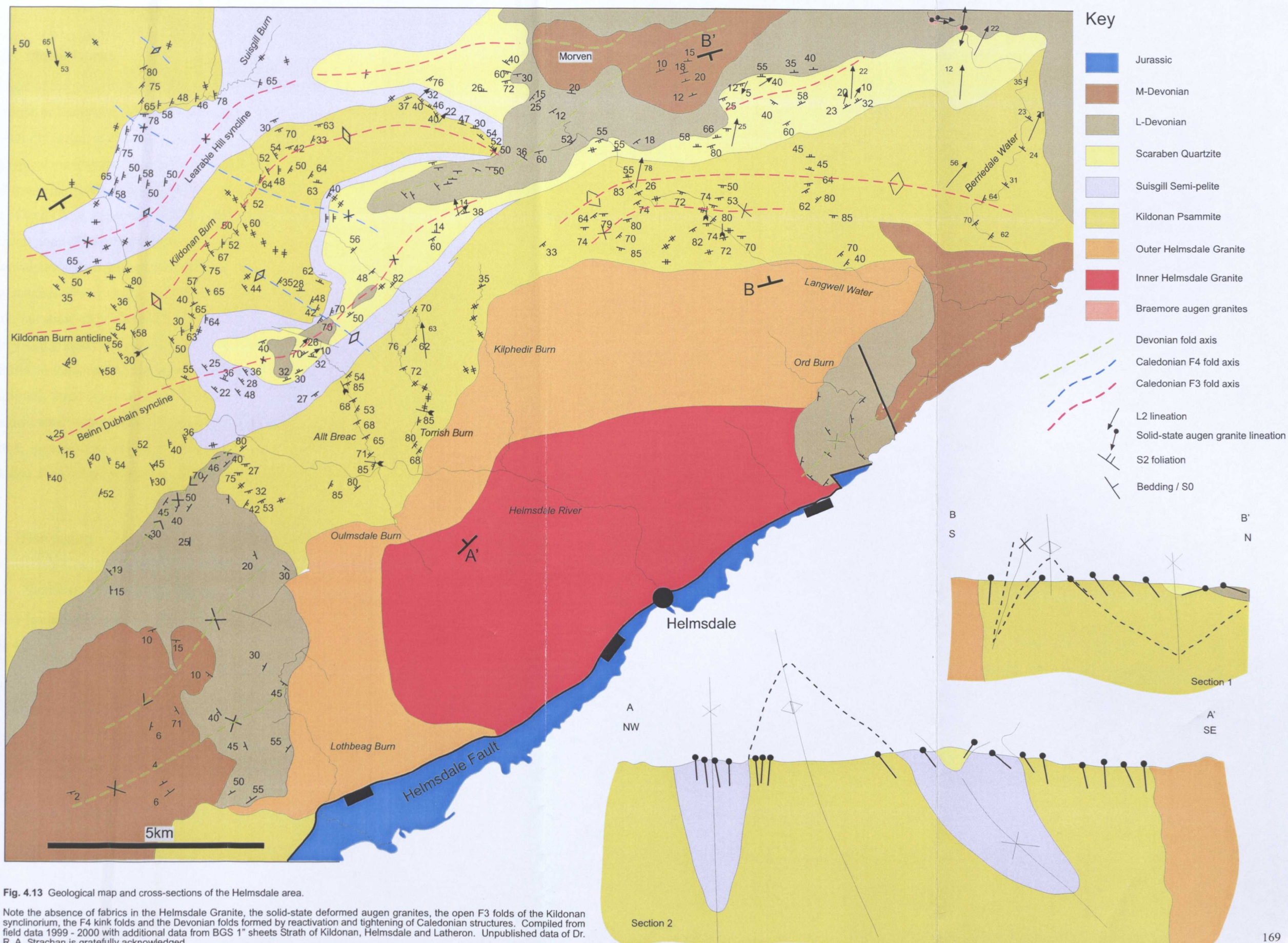

Fig. 4.13 Geological map and cross-sections of the Helmsdale area.

Note the absence of fabrics in the Helmsdale Granite, the solid-state deformed augen granites, the open F3 folds of the Kildonan synclinorium, the F4 kink folds and the Devonian folds formed by reactivation and tightening of Caledonian structures. Compiled from field data 1999 - 2000 with additional data from BGS 1" sheets Strath of Kildonan, Helmsdale and Latheron. Unpublished data of Dr. R. A. Strachan is gratefully acknowledged.

4.7.3 Pluton fabrics

None of the granitic facies carries macroscopically identifiable magmatic or solid-state foliations or lineations. The outer granodiorite is variably coarse grained, but always structurally isotropic and shows no fabric or preferred alignment of K-feldspar megacrysts. The typical outer granodiorite facies crops out to the east of Torrish Burn along the main road from Helmsdale to the north, and in the lower Langwell Water (Fig. 4.13). To the east of Ben Uarie, the coarse grained granodiorite comprises both, ultramafic and silicic enclaves none of which are flattened or deformed. In the lower Glen Loth, the granodiorite is considerably finer grained but again carries no fabrics. In the upper Kilphedir Burn, local patches of very coarse grained outer granodiorite with K-feldspars of up to 5 x 8cm occur, but show no preferred flow alignment or other fabrics. The inner Helmsdale granite is very fine grained and generally lacks minerals that could form a macroscopically identifiable foliation (biotite, mica) or lineation (hornblende or suitably-sized feldspars). It is distinctly structurally isotropic throughout the study area although transected by abundant small-scale brittle faults towards its eastern margin. Overall, the Helmsdale Granite appears to be an undeformed, slowly cooled (coarse outer granodiorite) igneous rock that does not show any record of syn- or post-emplacement deformation.

4.8 Discussion

4.8.1 Summary of key features

Key features of the Moine rocks and igneous rocks of the study area are summarized in table 4.2.

Summary of key features

Metasedimentary Moine rocks	
Formation	**Features**
Scaraben Succession	Comprises Kildonan Psammite, Suisgill Semi-pelite and Scaraben Quartzite. Structurally dominated by several large, NE-SW trending F3 folds that refold and locally crenulate the regionally developed S2 foliation. F3-folds are kinked by NW-SE trending F4-folds leading locally to complex interference patterns. S2 foliation steepens towards the margin of the Helmsdale Granite and is generally vertical in its vicinity. L2 mineral lineations are widely developed to the north of the granite. In the NW, they generally plunge NE but are affected by D3-folding and consequently may not indicate D2 transport direction. In the NE, post-D2 deformation appears limited and L2-lineations plunge NNE.
Scaraben Quartzite	Pure quartzite with locally strongly developed L2 lineation, plunging NNE in low post-D2-strain areas.
Suisgilll Semi-pelites	Biotite rich, medium- or coarse grained schist, that contains occasional psammitic layers. Locally evidence for segregation melting decreasing to the S. Carries strong D2 S-C fabric with prismatic sillimanite growth.
Kildonan Psammites	Grey to brown psammites host to the Helmsdale Granite but without contact metamorphic aureole.
Loch Coire formation	Comprises Achentoul banded formation and Badenloch Pelite.
Badenloch Pelite	Coarse-grained biotite-muscovite gneiss with abundant leucogranites (G2-phase).
Achentoul Banded Formation	Characterized by migmatites that show a strong segregation banding and comprise abundant leucogranite sheets (G2-phase). The metatexitic banding and the formation of the leucogranites may relate to a high pressure melting event at P>10 kbars that has also been recognized in the Kirtomy and Naver migmatites on the north coast (Kinny et al. 1999; Friend et al. 2000). Evidence for post peak decompression is also locally preserved. The metatexitic segregation fabric is locally crenulated by an S-C fabric that was formed at sillimanite grade conditions during regional D2 deformation.
	Structurally dominated by composite S2 foliation that generally strikes 020-030° and dips consistently to the E. S2 fabric locally crenulates the S1 segregation fabric. S2 fabric is folded /warped by D3. Pervasive mineral and rodding lineation (L2) that parallel F2-foldaxes are present and two lineation trends have been observed: A N-S trending lineation plunges 10-12° towards 170-180° (McCourt 1980). However, pre-dominantly SE plunging mineral lineations that are most likely of a D2 age have been observed in this study. Shear sense indicators parallel to this L2 verge generally NW

Igneous rocks	
Phase	Features
G4 - Helmsdale Granite	Oval shaped with apparently steep sides, comprising a coarse grained outer granodiorite and a fine-grained, inner adamellite. Does not carry any evidence for syn- or post-emplacement deformation but host rock foliations steepen towards the pluton and are subvertical in its vicinity.
G3	Comprises Strath Halladale Granite, Reay Diorite & associated mafic- to ultramafic rocks.
G3 - Strath Halladale Granite	Forms a set of NE-SW trending granodioritic sheets that cross-cut the regional composite S0/S1/S2 foliation at shallow angles but carry a strong S2-parallel, magmatic-state foliation. AMS-reconnaissance work identified a prolate magnetic elipsoid defining a easterly dipping foliation and a SE plunging lineation within the southern domain. In the northern domain, the magnetic elipsoid is rather oblate and indicates a very weak southerly plunging lineation. Shear sense indicators within the granite and associated sheets to the west show consistent magmatic-state top-to-the-W-to-NW movements throughout the pluton.
G3 - Reay Diorite	Cut by granitic sheets assigned to the Strath Halladale Granite and therefore pre-dates it. Locally carries a magmatic-state foliation that parallels the host rock fabrics towards the pluton margin but is of varying orientations towards the centre. No kinematic indicators have been observed. Dioritic enclaves within the main Strath Halladale Granite carry a foliation that parallels the granite foliation but locally show a southerly plunging lineation.
G2	Leucosomes of the Achentoul banded formation that coalesce to form leucogranitic sheets and larger igneous bodies. Variably foliated and locally containing Moine rafts that comprise F2-folds (McCourt 1980; Strachan 1988)
G1	Coarse grained augen granites with strong solid-state L-fabric that, from S to N, swings from plunging SE to E to N-S and back to SE.

4.8.2 Emplacement and significance of the Strath Halladale Granite

4.8.2.1 Timing of emplacement

The four phase deformational history of the study area as outlined by McCourt (1980), Lintern & Storey (1980) and Strachan (1988) (see also table 4.1) is accepted in this study. However, the currently accepted timing of fabric development, metamorphism and granite emplacement (table 4.1) is questioned. The precise timing of emplacement of the Strath Halladale Granite (G3) with respect to the regional deformational sequence (D1-D4) is disputed amongst previous workers. McCourt (1980) stated that the Strath Halladale Granite post-dates regional D3 deformation and is folded by a "late monoformal fold episode (F4)" exposed at [NC9030 | 5900] (McCourt 1980, p. 9), but does not present evidence for the post-D3 status. Support for the pre-D4 status of the Strath Halladale Granite comes from Strachan (1988) who quoted Read (1931) who suggested that apophyses relating to the Strath Halladale Granite are folded on a large scale by F4 folds in the Suisgill area, but stated that the evidence is now obscured by vegetation. Lintern & Storey (1980) argued that the granite must post-date D2, as granite sheets correlated with the main granite cut across the S_2-foliation and the associated L_2 lineation in the Glutt Water (Lintern & Storey 1980, p.27). They further inferred the granite to be emplaced during or after the D3 open folding event (Lintern & Storey 1980, p28) but presented no data to evaluate this. Strachan (1988) argued that the granite post-dates D3, as granitic sheets that correlate with the main Strath Halladale Granite cut across F2 and F3 fold hinges in the Suisgill and Kinbrace burns.

Problems in precisely determining the relative age of the Strath Halladale Granite with respect to regional deformation are two-fold. Firstly, exposure is locally extremely poor and all pluton boundaries are covered either by glacial deposits or peat. The currently accepted timing therefore relies exclusively on cross-cutting relationships of sheets that are *thought* to correspond to the main granite. Secondly, only recently have the rates of pluton emplacement processes, orogenic activity and fabric development been delineated (e.g. Paterson & Tobisch 1992; Karlstrom & Williams 1995; Samson & D'Lemos 1999; Petford *et al.* 2000) and suggest that the time interval over which a pluton is partially molten and may record magmatic-state fabrics is comparatively short (10.000-100.000 years, e.g. Karlstrom & Williams 1995; Tribe & D'Lemos 1996) with respect to regional deformation events that may last 10's of Ma (e.g. Samson & D'Lemos 1999, see also table 2.1). As

such, it is possible that a granite may be emplaced within a deformational event but post-date fabrics which were developed early during the same event.

The Strath Halladale Granite and its associated sheets clearly cross-cut the migmatitic layering of the host rock metatexites and also the superimposed composite $S_0S_1S_2$ foliation (e.g. Loch An'Rhutair, Craigtown Rock). It must therefore post-date the formation of these fabrics but not necessarily the entire deformational phase (D2) (see above). The problem with a post-D3 emplacement age of the Strath Halladale Granite (e.g. McCourt 1980; Strachan 1988) lies in the widely developed magmatic-state foliation that throughout the pluton records ductile, west-directed deformation which, in western Sutherland, is related to late Caledonian "Scandian" D2 deformation (e.g. Barr *et al.* 1986; Strachan & Holdsworth 1988; Kinny *et al.* 1999, in press.). In addition to the composite $S_0S_1S_2$ foliation, the host rocks of the Strath Halladale Granite in the southern domain also carry a SE-plunging mineral lineation (Fig. 4.6) that is paralleled by a magmatic-state SE-plunging lineation (determined by AMS) within the southern Strath Halladale Granite. This paralellism of host rock and magmatic-state pluton fabrics indicates contemporaneous fabric development. The (micro) structural age of the Strath Halladale Granite with respect to country rock deformation in the *eastern belt* is therefore thought to be late D2 after the initial $S_0S_1S_2$ fabric had formed within the host rocks but prior to the cessation of NW-directed ductile deformation. The Reay Diorite is cut by granitic sheets that are thought to correspond to the Strath Halladale Granite (table 4.1; McCourt 1980; this study) and thus pre-dates its emplacement. Geochemical evidence further suggests that the Reay Diorite and the Strath Halladale Granite form a single intrusive suite (Storey & Lintern 1981, see also Chapter 5). Together, this suggests that the emplacement of the entire suite took place over a short time interval late during D2 west-directed thrusting and pre-dates the D3-phase of regional deformation. This further implies that the granitic sheets which reportedly cross-cut F3 folds in the Suisgill Burn (Strachan 1988) are either a very late magmatic pulse of, or unrelated to the main Strath Halladale Granite.

4.8.2.2 Fabric development

The fabrics developed within the pluton are strictly formed within the magmatic state and do not show evidence for pervasive, continuous down-temperature deformation, or a strong solid-state overprint. Only locally, weak low-temperature ductile deformation is indicated by undulose extinction in K-feldspar and equant to prismatic deformation bands

developed in quartz which indicate high dislocation densities and grain boundary migration controlled recovery at temperatures of *c.* 350-400° C. This regionally homogeneous, magmatic-state fabric is peculiar, as within a set of separately emplaced sheets, one might expect to see a variety of fabrics throughout the pluton. Sheets emplaced early during the deformation should be comparatively cool to later emplaced sheets and hence carry solid-state fabrics, which are not observed. Also, pluton size should exert a major influence on fabric formation and small sheets, like the sheets on the west side of the main granite, should have cooled faster and thus also show solid-state fabrics. This is again not observed and the homogeneity of magmatic-state fabrics in the Strath Halladale Granite is, for example, very different to the fabrics developed within the granites emplaced along the Naver Thrust. These granite sheets were also emplaced late during the D2 thrusting but do carry pervasive solid-state deformation fabrics (Kinny *et al.* in press.). A possible explanation is that deformation was partitioned into other, structurally lower parts of the westward propagating thrust belt (e.g. Barr *et al.* 1986; Tribe & D'Lemos 1996; Kinny *et al.* 1999).

4.8.2.3 Mode of emplacement

The elongate shape, the petrographical changes, the easterly dipping magmatic-state foliations and the granodiorite sheets on the western flank of the main Strath Halladale Granite suggest that the entire complex consists of broadly contemporaneously emplaced granitic sheets. Structural and microstructural evidence presented in this chapter strongly suggests that the Strath Halladale Granite records evidence of broadly W-directed thrusting contemporaneous with its emplacement. Within the Caledonian belt exposed in Sutherland, numerous sheeted granite complexes have been reported within the vicinity of the Naver Thrust (e.g. Strachan & Holdsworth 1988; Kinny *et al.* in press.) and it has been shown in Chapter 3 that ductile thrusting and the emplacement of granite sheets along thrust planes is a process that operated within the Rogart area. Although the structural data presented here strongly favours thrust-related granite emplacement, to date, no major ductile thrust has been identified within the Strath Halladale area.

Importantly, the Strath Halladale Granite is emplaced broadly along the boundary between the migmatitic rocks of the Loch Coire Formation and the gneisses of the Scaraben Succession. However, identifying this boundary as a major tectonic break in this area has prooved impossible due to the limited exposure. Nonetheless, reconnaissance

mapping in the Black Water *c.* 25km to the southwest of the Strath Halladale Granite has identified the Loch Coire Formation-Scaraben Succession boundary to be of very high strain with shear sense indicators giving top-to-the-NW movements (Strachan pers. comm. 2002). Based on their borehole data, Lintern & Storey (1980) inferred the existence of a ductile D2 thrust to the east of the main granite (Lintern & Storey, 1980, Fig.3, p13) but could not prove a surface expression.

Overall, the available data indicates that a ductile thrust may exist to the east of the Strath Halladale Granite, or coincide with its eastern margin and the Loch Coire Formation – Scaraben Succession boundary, but this is not proven. Alternatively, this boundary could be regarded as a strained, tectonised lithological boundary that acted as a plane of weakness along which the granite was emplaced during west-directed deformation. If so, the eastward decrease of migmatization could simply reflect cooler, structurally higher parts of the sequence that were less prone to partial melting during crustal thickening, rather than constituting fundamentally different and tectonically juxtaposed rocks. Whatever the case, magmatic-state shear zones consistently show top-to-the-NW movements throughout the Strath Halladale Granite and indicate that ductile D2 deformation was contemporaneous with its emplacement.

4.8.3 Emplacement of the Helmsdale Granite

The emplacement of the Helmsdale Granite remains somewhat enigmatic. The pluton-host rock contacts and the pluton-fault contacts are unexposed and the intrusion does not contain any macroscopically identifiable fabrics that can be related to magmatic activity during its emplacement, or any movements along regional tectonic structures. The pre-Mesozoic role of the Helmsdale Fault and possible interactions between lateral fault movements and pluton emplacement therefore remain speculative, although strike-slip related pluton emplacement has been demonstrated in other comparable settings within the Northern Highland Terrane (e.g. Strontian, Hutton 1988b; Ratagain, Hutton & McErlean 1991; Clunes, Stewart *et al.* 2001). However, the host rock fabrics steepen considerably towards the intrusion and the syncline- anticline pair north of the pluton could conceivably have been produced by pluton induced deformation, i.e. ballooning. The emplacement of the Helmsdale Granite clearly post-dates D2 deformation and the lack of any deformation-induced fabrics within the pluton suggests that the pluton is entirely post-tectonic to Caledonian deformation.

4.8.4 Regional significance and geochronology

4.8.4.1 Migmatization and metamorphism of the Moine country rocks

The oldest metamorphic phase in the study area, M1, has been inferred to be of mid to upper amphibolite conditions. During M1 segregation melting of the more pelitic units resulted in the formation of regional metatexites (table 4.1, e.g. Strachan 1988, McCourt 1980). This study has shown, that anatexis and segregation melting probably occurred under high-pressure conditions (8-10 kbars) as suggested by the presence of garnet in the leucosomes (e.g. Patino Douce & Beard 1995; Miller *et al.* 1997; Whittington & Treloar 2002 and references therein). Scalloped biotite and abundant plagioclase coronas around garnets may further indicate a post-peak decompression reaction (Bt+K-spar=>Plag, K. A. Jones pers. comm. 2002). The M1 segregation fabric was reworked but not retrogressed during a second phase of deformation (D2) indicating that D2 was associated with metamorphic conditions similar to M1 (McCourt 1980; Strachan 1988). This study has further shown that the pervasive D2-related S-C fabric developed within the Suisgill Semi-pelite to the east and southeast of the granite occurred at sillimanite grade conditions (M2). To the east of the Strath Halladale Granite, post-M2, mimetic fibrolite mats radiate across this S_2 S-C fabric developed within the Suisgill gneisses and have been interpreted to represent a thermal overprint, possibly related to the emplacement of the Strath Halladale Granite (M3; Watson 1948; Strachan 1988).

The metatexites exposed on the western side of the Strath Halladale Granite (i.e. the Achentoul Banded Formation) have common lithological, structural and metamorphic characteristics with the metatexites observed above the Naver and Swordly thrusts to the northwest of the study area (e.g. Watt *et al.* 1996; Kinny *et al.* 1999; Friend *et al.* 2000). The formation of these migmatites has been related to a high-pressure melting event thought to represent crustal thickening between *c.* 460 – 470 Ma (Kinny *et al.* 1999; Friend *et al.* 2000). Therefore, at present, the migmatization of the country rocks in the northwestern parts of the study area (M1) is inferred to relate to the same Grampian aged high-pressure event, although this needs to be confirmed by isotopically dating D1/M1 leucosomes of the Achentoul Banded Formation. Post-peak exhumation is indicated by decompression textures which are most likely of a pre-D2 age. The Strath Halladale Granite was probably emplaced late during D2 deformation (see above) and therefore closely post-dates the formation of the sillimanite grade S_2 shear fabric (M2) which

overprints and crenulates the migmatitic segregation fabric (M1). The fibrolite growth within the Suisgill Semi-pelites (M3) may relate to and closely post-date the emplacement of the Strath Halladale Granite (Watson 1948; Strachan 1988).

4.8.4.2 Regional deformation and fabric development

The Caledonian thrust pile in Sutherland is commonly divided into the Moine and Naver nappes, the latter of which comprises three separate belts that show internally consistent fabric patterns (Fig. 4.14).

Moine Nappe & Western belt of the Naver Nappe

In western Sutherland, top-to-the-W-to-NW D2 ductile thrusting that resulted in isoclinal folding and the formation of a pervasive, SE-dipping, composite $S_0S_1S_2$ foliation (e.g. Barr *et al.* 1986; Moorhouse & Moorhouse 1988; Strachan & Holdsworth 1988). An associated L_2 mineral lineation plunges SSE in the vicinity of the Naver Thrust and ESE in the vicinity of the Moine Thrust, suggesting that Caledonian transport direction changed from early NNW- to later WNW directed thrusting (Strachan & Holdsworth 1988, Alsop *et al.* 1996). Recently, fabric development and D2 deformation in this domain have been identified to be of Silurian, i.e. Scandian age by dating the syn-tectonic Ben Klibreck (420 ± 6 Ma), Strathnaver (429 ± 11 Ma) and Strath Vagastie (424 ± 8 Ma) granites (U-Pb zircon SHRIMP; Kinny *et al.* in press) which cut early D2-folds but carry pervasive D2, L-S fabrics (Strachan & Holdsworth 1988; Kinny *et al.* in press).

Central belt of the Naver Nappe

In the central belt of the Naver Nappe above the Swordly Thrust, the Kirtomy migmatites comprise a strong foliation that is generally parallel to the stromatic layering of the metatexites and dips to the SE. A mineral lineation consistently plunges to the S (Strachan, pers. comm., see Fig. 4.14). Small scale, ductile, tight-to-close folds commonly deform this migmatitic fabric and are themselves cut by migmatitic segregations indicating that migmatization was contemporaneous with deformation (Kinny *et al.* 1999). Therefore, the 461 ± 13 Ma U-Pb SHRIMP age of zircons derived from the migmatitic leucosomes at Kirtomy are thought to date both, migmatization and D2 deformation in this domain which thus corresponds to the Grampian event (Kinny *et al.* 1999, Fig. 4.14). As the fabrics are not reworked during later deformation events, the *central belt* constitutes an area of low Scandian strain. A 431 ±10 Ma U-Pb SHRIMP age derived from monazites in

the Kirtomy migmatites is interpreted by Kinny *et al.* (1999) to either represent an amphibolite facies overprint, very slow cooling of the rocks through the closure temperature of monazite for radiogenic Pb, or the cessation of fluid flow along the Kirtomy Thrust.

Eastern belt of the Naver Nappe

The study area constitutes the *eastern belt* of the Naver Nappe above the Swordly Thrust. The fabric pattern in the Moine rocks of the study area is characterized by a northern domain of strong local D2 deformation that shows little reworking during D3 and D4 (Strath Halladale area), and a southern domain dominated by large, open F3 folds that significantly re-orientate earlier formed fabrics (Helmsdale area).

In the Strath Halladale area, it has been shown that D2 fabrics rework an earlier segregation fabric that is correlated with the migmatitic layering to the northwest (see above). The composite $S_0S_1S_2$ Moine rock foliation in this domain generally strikes NE-SW and dips to the SE, and locally small scale tight to isoclinal F2-folds plunge SE. However, the lineations developed in the Moine rocks in this northern domain show two orientations (Fig. 4.14): one trending broadly N-S and another one trending NW-SE. The G1 augen granites also show two sets of solid-state lineations, predominantly trending NNE-SSW but also trending WNW-ESE. Further, the preliminary AMS analysis (this study) has identified two sets of magnetic lineations within the Strath Halladale Granite: in the north an oblate magnetic strain ellipsoid indicates a SSW-plunging preferred linear alignment, whereas in the south a prolate ellipsoid indicates a SE-plunging preferred linear alignment. The importance and formation of this linear fabric pattern is somewhat inconclusive, as it has not been possible to demonstrate a relative age relationship between the two sets of lineations. It is therefore unclear whether they represent a phase of continuous deformation with changing movement directions comparable to western Sutherland and are of Scandian age (see above, grey arrow in Fig. 4.14), or whether they relate to separate phases of deformation with earlier, Grampian aged, N-S trending lineations (identical to the dated N-S lineations in the central belt) being preserved in localized low Scandian D2-strain domains of the *eastern belt.*

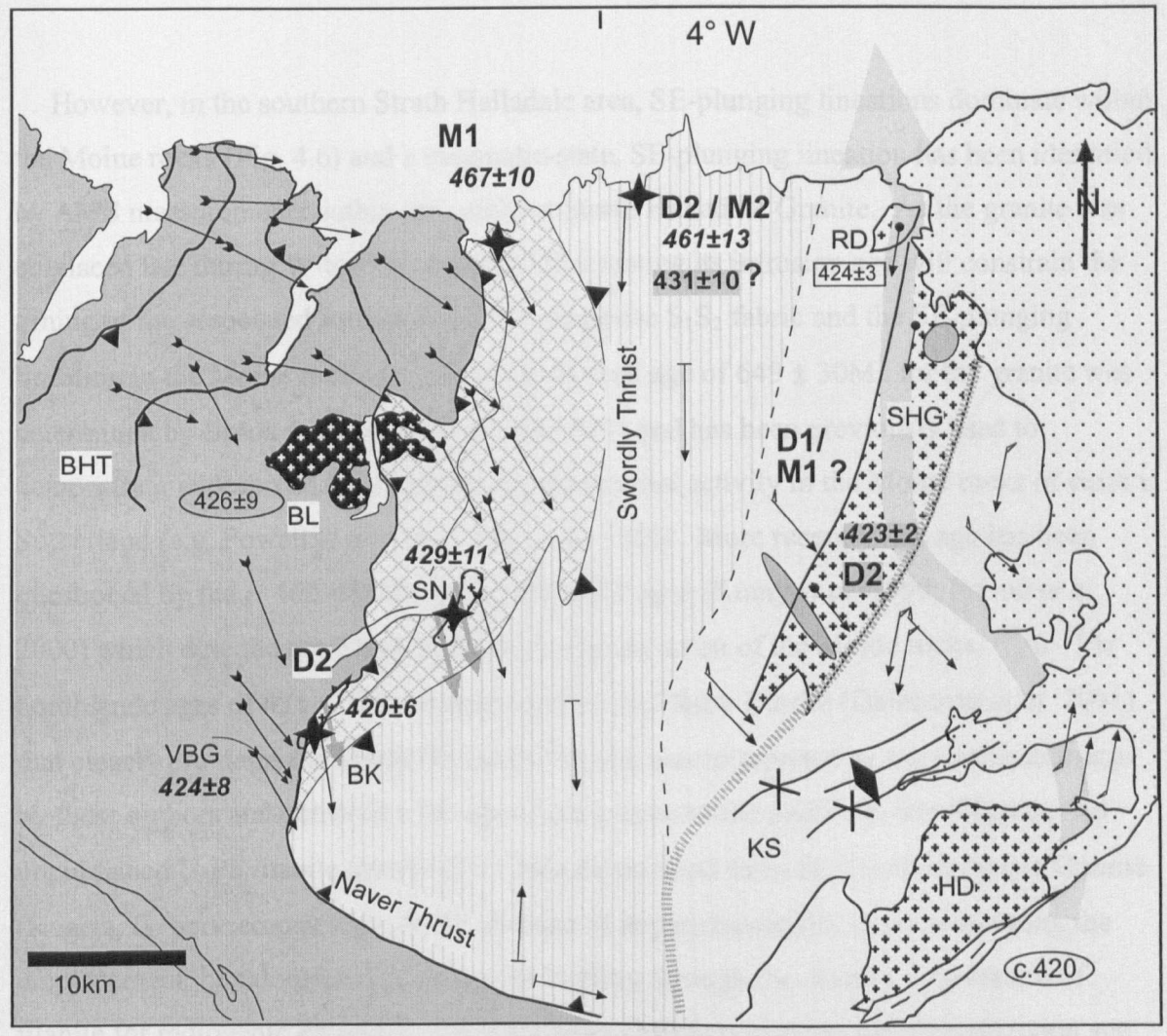

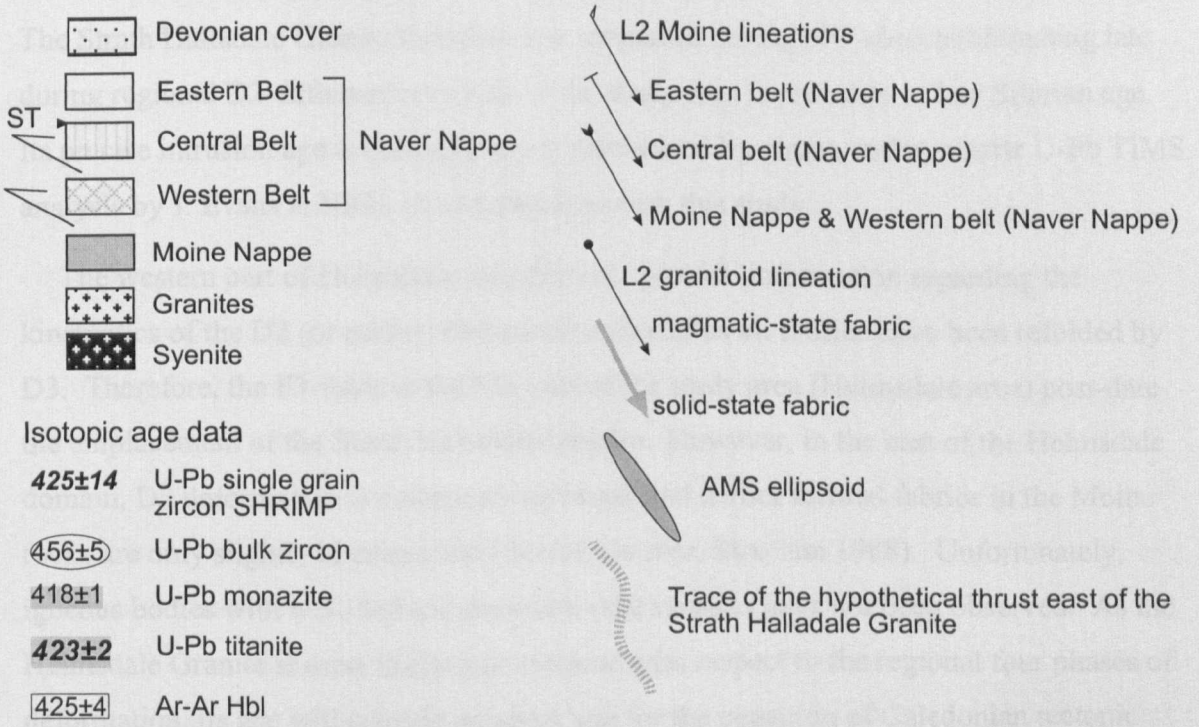

Isotopic age data

425±14	U-Pb single grain zircon SHRIMP
(456±5)	U-Pb bulk zircon
418±1	U-Pb monazite
423±2	U-Pb titanite
[425±4]	Ar-Ar Hbl

Fig. 4.14 Lineation patterns in the structural domains of Sutherland. Structural data compiled from Strachan & Holdsworth 1988, Holdsworth & Strachan 1988, Holdsworth 1990, Alsop *et al.* 1996, and Strachan & Kocks (unpublished data). Isotopic age data is referrenced in table 1.2 , also see text.. Note the prolate AMS ellipsoid in SE-plunging southern Strath Halladale and the oblate ellipsoid in northern Strah Halladale (flattening). Also shown is a hypothetical Scandian deformation trajectory (large grey arrow). BL= Ben Loyal syenite, RG= Rogart granite, VBG= Vagastie Bridge granite, SN= Strath Naver granite, SHG= Strath Halladale granite, HD= Helmsdale granite, BK= Ben Klibreck, BHT= Ben Hope Thrust, D2 = locally dominant deformation event, M = dated migmatization.

However, in the southern Strath Halladale area, SE-plunging lineations dominate within the Moine rocks (Fig. 4.6) and a magmatic-state, SE-plunging lineation has been identified by AMS measurements within the southern Strath Halladale Granite. As the granite was emplaced late during W-to-NW-directed D2 thrusting its intrusion age will constrain the timing of the associated formation of the composite S_1S_2 fabric and the SE-plunging lineation in the Moine rocks. A Rb-Sr whole rock age of 649 ± 30Ma for the granite was determined by Brook (quoted in Pankhurst 1982) and has been previously used to demonstrate widespread Precambrian tectonothermal activity in the Moine rocks of eastern Sutherland (e.g. Powell *et al.* 1983; Barr *et al.* 1986). More recently this age has been questioned by the *c.* 460-470Ma zircon SHRIMP ages (Kinny *et al.* 1999; Friend *et al.* 2000) which date the pre-Strath Halladale migmatization of the Moine rocks. ^{40}Ar-^{39}Ar hornblende ages of 424 ± 3Ma determined from the Reay Diorite (Dallmeyer *et al.* 2001) that closely pre-dates the Strath Halladale Granite was interpreted as a crystallisation age by these authors and constrains the age of the granite to the middle to late Silurian. An unpublished U-Pb titanite age of 423 ± 2Ma determined from the Strath Halladale Granite (Rogers, G. pers. comm.) can, in the absence of any metamorphic event post-dating the emplacement, be interpreted as an age for cooling through the closure temperature of titanite for radiogenic Pb which hence probably closely post-dates the crystallization age. The Strath Halladale Granite therefore was emplaced during NW-directed thrusting late during regional D2-deformation which in the study area is probably of late Silurian age. Its precise intrusion age is currently being determined by zircon and monazite U-Pb TIMS analysis by J. Evans at NIGL in collaboration with this study.

The western part of Helmsdale area does not provide information regarding the kinematics of the D2 (or earlier) deformation phases as all fabrics have been refolded by D3. Therefore, the F3-folds in the SW part of the study area (Helmsdale area) post-date the emplacement of the Strath Halladale Granite. However, in the east of the Helmsdale domain, D3 deformation is comparatively weak and earlier formed fabrics in the Moine rocks are only slightly re-orientated (Berriedale area, Strachan 1988). Unfortunately, igneous bodies with well-defined structural relationships have not been observed. As the Helmsdale Granite is most likely post-tectonic with respect to the regional four phases of deformation, its age will provide an upper age for the cessation of Caledonian tectonic activity in the study area.

4.9 Conclusions

The regional Caledonian geology of the study area can be summarized in terms of a complex sequence composed of four deformational phases, three distinct metamorphic events, and two phases of Caledonian granite emplacement. The migmatization of the Moine rocks and partial melting leading to abundant leucogranites during M1 is tentatively correlated with comparable lithologies and events at Kirtomy and Strathnaver. M1 is thought to have occurred under high-pressure conditions during crustal thickening between 470-460 Ma (e.g. Friend *et al.* 2000). There is (undated) evidence for post-peak-metamorphic decompression. The main ductile deformation affecting the rocks in the study area is of D2 age as it reworks the earlier migmatite fabric. D2 is associated with W-to-NW directed thrusting and ductile deformation that occurred under sillimanite grade, amphibolite facies conditions. The Strath Halladale Granite was emplaced as a series of sheets late during D2 deformation after the initial formation of the $S_0S_1S_2$ fabric and contains magmatic-state shear zones that consistently record top-to-the-NW-to-W directed movements. Available evidence is consistent with the existence of a ductile thrust to the east of Strath Halladale Granite that possibly coincides with the boundary between the Loch Coire Formation and the Scaraben Succession. The fibrolite growth in the Suisgill Semi-pelite (M3) is thought to relate to the emplacement of the Strath Halladale Granite (Watson 1948; Strachan 1988). Currently, the intrusion age of the Strath Halladale Granite is imprecisely constrained by an ^{40}Ar-^{39}Ar hornblende age form the Reay Diorite of 424 ± 3 Ma (Dallmeyer *et al.* 2001), that is interpreted to represent post-crystallization cooling, and by a titanite age of 423 ± 2 Ma (Rogers, G. pers. comm. 2000) of the Strath Halladale Granite interpreted to date post-emplacement cooling. These ages therefore indicate that ductile D2 deformation, NW-directed thrusting and S2 fabric development under sillimanite grade conditions in the study area are of middle Silurian, Scandian age. It should be noted that D2 deformation in the *eastern belt* of the Naver Nappe is therefore *c.*40 Ma younger than D2 deformation in the *central belt.* A precise U-Pb TIMS age of the Strath Halladale Granite is needed to test this. D3 deformation post-dates the emplacement of the Strath Halladale Granite and M3, but pre-dates the emplacement of the Helmsdale Granite. The age and emplacement mechanism of the Helmsdale Granite is enigmatic. As is contains no macroscopic fabrics it most likely post-dates all Caledonian deformational phases in the study area. Pluton emplacement may have been assisted by Caledonian lateral movements along the Helmsdale Fault but remain speculative.

4.10 Future work

Structurally well-defined leucosomes and leucogranite sheets of the Achentoul Banded Formation should be dated to test whether the M1 metamorphic event correlates with the 460 – 470 Ma event recorded in adjacent areas.

The formation and significance of the linear fabric pattern in the Moine rocks of the Strath Halladale area needs to be further resolved. The SE-plunging lineations are most likely Silurian in age (see above) but the age of the N-S trending lineations is unknown. Isotopic dating of metamorphic titanite from the solid-state deformed G1 augen granites which carry the N-S lineation may solve this problem and is currently being undertaken (Kinny, P. pers. comm. 2002).

The magmatic-state fabrics developed within the Strath Halladale Granite should be further investigated by AMS studies to clarify the orientation and distribution of magnetic lineations throughout the pluton.

The inner Helmsdale Granite should be investigated by AMS to test whether there are mapable, magnetic fabric patterns that clarify its emplacement and the role of the Helmsdale Fault.

Chapter 5

Geochemistry of Caledonian high Ba-Sr granitoids in the Northern Highland Terrane

5 Geochemistry of Caledonian high Ba-Sr granitoids in the Northern Highland Terrane

5.1 Introduction

Today, petrologists recognise many different groups of granite: I- and S-type granites are thought to derive from igneous and sedimentary protoliths respectively (Chappell & White 1974), A-type granites are anorogenic (or alkaline) and have several possible sources (Eby 1990) and M-type granites are mantle-derived via extended crystal fractionation in regions otherwise dominated by basalt (Pitcher 1993). Recently, high Ba-Sr granitoids have been defined in the Scottish Caledonides (Tarney & Jones 1994), on the basis of trace element characteristics complementary to those of I- and S-types. These include high Ba, Sr and light REEs; low Nb, Ta and heavy REEs; consequent high LILE/HFSE ratios and high K/Rb. The petrogenesis of Scottish Caledonian "Newer Granites" (Read 1948) has been much debated within a framework of mantle and crustal contributions and theories for late Caledonian magma generation and evolution are numerous (e.g. Hamilton *et al.* 1980; Thirlwall 1982, 1986, 1988; Halliday 1984; Halliday *et al.* 1985; Harmon *et al.* 1984; Frost & O'Nions 1985; Thompson & Fowler 1986; Holden *et al.* 1987; Fowler 1988 a,b, 1992; Thirlwall & Burnard 1990; Fowler *et al.* 2001).

The Newer Granites of the Northern Highland Terrane represent the type high Ba-Sr class of Tarney & Jones (1994) and whole rock major element, trace element and isotope data from the Northern Highland Newer Granite suite have grown significantly since the reconnaissance work of the 1980s (e.g. Harmon *et al.* 1984; Stephens & Halliday 1984). Several studies have detailed the magmatic histories, petrogenetic processes and contributing sources of individual syenite-dominated and granite-dominated complexes in the Northern Highland Terrane e.g. at Strontian (Pankhurst 1979), at Loch Borralan (Thirlwall & Burnard 1990), at Glen Dessarry (Fowler 1992), at Ach' Uaine (Fowler & Henney 1996) and at Rogart (Fowler *et al.* 2001). These have shown that the high Ba-Sr characteristics can be traced back to associated appinitic rocks, and that high Ba-Sr granitoids may be generated from such mantle-derived magmas by protracted crystal fractionation coupled with crustal contamination ("AFC" - *assimilation fractional crystallization*, De Paolo 1981) (e.g. Thirwall & Burnard 1990; Fowler 1992; Fowler & Henney 1996). Since both granites and syenites possess the high Ba-Sr elemental

signature, a genetic relationship has been proposed (Thompson & Fowler 1986; Fowler & Henney 1996), but the cause of the divergent silica saturation trends has remained obscure. Also, three isotopically-distinct mantle sources have been postulated beneath the Northern Highland Terrane, delineating the nebulous "enriched subcontinental lithospheric mantle" of the literature (Halliday *et al.* 1985; Menzies *et al.* 1987; Menzies & Halliday 1988): the depleted source of the Glen Dessarry syenite (Fowler 1992), the Loch Borralan source which approximates to Bulk Earth (Thirlwall & Burnard 1990) and the significantly enriched Rogart source (Fowler *et al.* 2001).

5.2 Aims of this study, approach and acknowledgement

The studies of Thirlwall & Burnard (1990), Fowler (1992), Fowler & Henney (1996), and Fowler *et al.* (2001) of Northern Highland granitoids have clearly shown the value of detailed elemental and isotopic approaches involving all lithologies of composite plutons, as within-pluton variations, especially of the isotope systems, may be significant. The aims of this study have been to: (1) further investigate the extent of the high Ba-Sr class in the granites of the Northern Highland Terrane, (2) investigate the genetic relationships between granites and syenites, and (3) to delineate the nature and extent of the previously described source regions. Given the size of this project, the approach has been two fold: within the remapping and structural analysis of the Strath Halladale, and Helmsdale granites numerous samples were collected by the author to detail their magmatic evolution. Further samples were collected (or provided by various colleagues) within the framework of Dr. M. B. Fowler's continuing research of Caledonian magmatism of the Cluanie granite, the Strontian granite complex, the Loch Loyal syenites and the Ratagain complex, spanning the lithological range where possible. Thus a regional data set showing elemental and isotopic variations in the high Ba-Sr granitoids of the Northern Highland Terrane has been assembled. Published data have been incorporated where necessary and unpublished data of Mike Fowler and Peter Greenwood are gratefully acknowledged, as are invaluable discussions with Mike Fowler, Fiona Darbyshire and Peter Greenwood. Previous case studies (Pankhurst 1979; Fowler 1988a,b, 1992; Thirlwall & Burnard 1990; Fowler & Henney 1996; Fowler *et al.* 2001) and the regional study carried out in this project provide a useful background against which the geochemical characteristics, systematics and significance of the lithologically less diverse Strath Halladale and Helmsdale granites can be discussed. The chapter therefore starts with a summary of the elemental geochemistry

of all the plutons comprising the regional study leading into the detailed analysis of the Strath Halladale and Helmsdale intrusions, prior to a discussion of the regional isotopic variations.

5.3 Regional study – rock types, major and trace element data, and genetic relationships

5.3.1 Petrography: syenites, granites and appinites

The igneous complexes exposed in the Northern Highland Terrane which share the characteristic high Ba-Sr trace element signature can be divided petrographically into two groups: a western belt of syenites (Glen Dessarry, Loch Borralan, Loch Ailsh, Loch Loyal) and a central to eastern belt of granitic complexes (Strontian, Cluanie, Rogart, Helmsdale, Strath Halladale; Fig. 5.1). The Ratagain pluton has features transitional between the syenites and the granites, including local syenites within the main diorite and granodiorite units (Stephens 1999).

The syenites mainly comprise medium grained mela to leucosyenites (Thompson & Fowler 1986, Thirlwall & Burnard 1990) with minor monzodiorite and associated coarse mafic to ultramafic appinitic rocks, such as biotite or hornblende pyroxenites (Thirlwall & Burnard 1990, Fowler 1992). At Loch Borralan, a range of strongly silica-undersaturated rocks is developed, including nepheline and pseudoleucite-bearing syenites.

The granite complexes are dominated by medium to coarse grained granodiorites that are typically K-feldspar porphyritic. Medium grained biotite granites account for large volumes although finer grained adamellites can also be extensive (e.g. Helmsdale). Medium grained quartz diorites and diorites extend the spectrum to lower silica content and mafic to ultramafic appinitic rocks are often present as enclaves or discrete facies (Holden *et al.* 1987; Highton 1999; Fowler *et al.* 2001).

The appinite suite (see Appendix 1) itself is found both within and outwith the granitoids, and comprises a wide variety of rock types from the typical medium grained hornblende-meladiorites to hornblende peridotites (cortlandite), phlogopite-bearing picrites (kentallinite), hornblendites, hornblende gabbros and a variety of hornblende or biotite-bearing granodiorites and granites (Smith 1979). Rock (1984) suggested that the suite represents the plutonic equivalents of calc-alkaline lamprophyres.

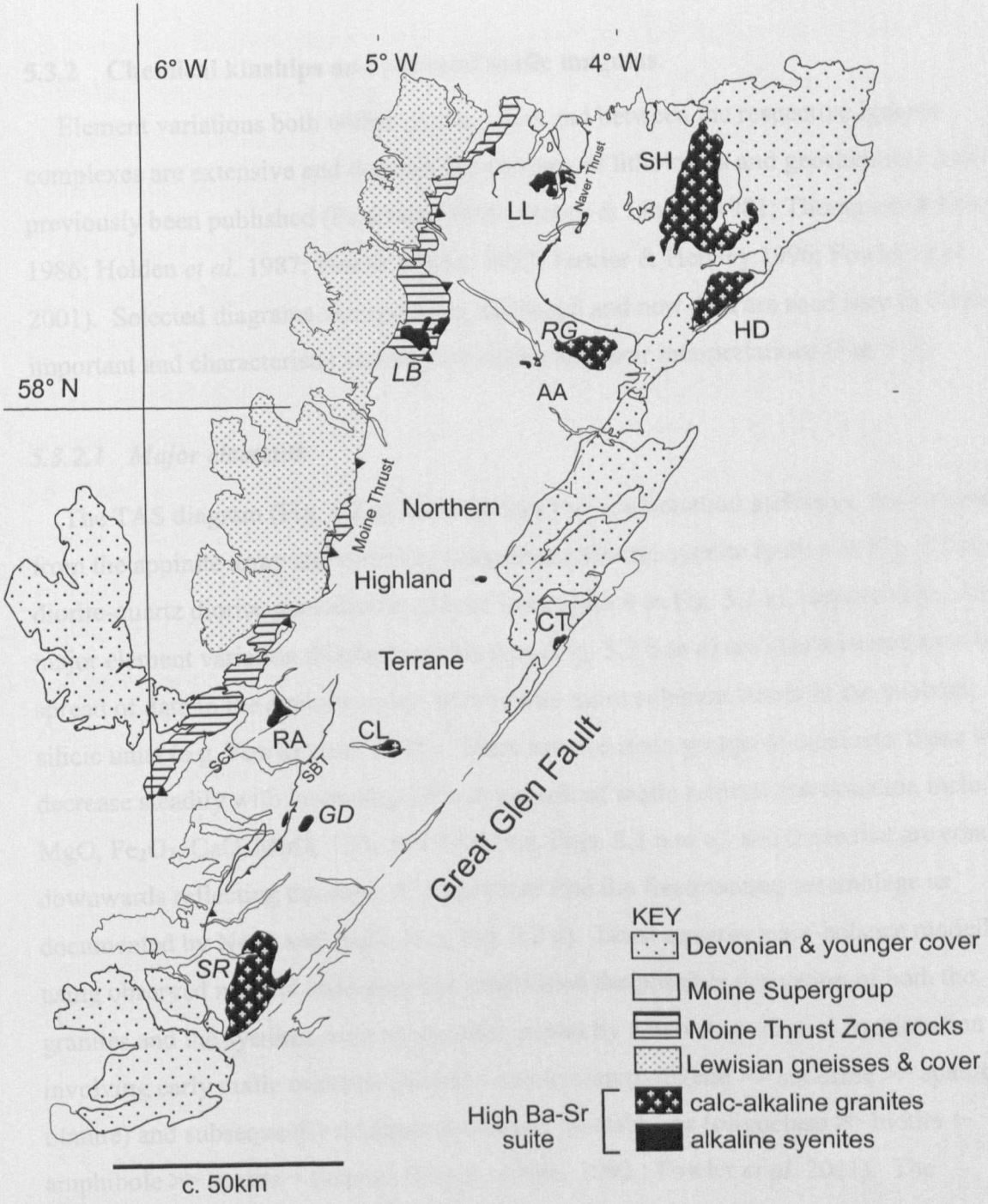

Fig. 5.1 Location map showing the western belt of syenite-dominated complexes and the central to eastern granitoid belt in the Northern Highland Terrane. SR = Strontian, GD = Glen Dessarry, CL = Cluanie, RA = Ratagain, LB = Loch Borralan, RG = Rogart, HD = Helmsdale, LL = Loch Loyal, SH = Strath Halladale, AA = Ach'Uaine. *Italic* typeset indicates previously studied complexes where published data is available, see text.

5.3.2 Chemical kinships and parental mafic magmas.

Element variations both within pluton suites and between the respective igneous complexes are extensive and detailed descriptions of lithologies and geochemical data have previously been published (Pankhurst 1979; Storey & Lintern 1981; Thompson & Fowler 1986; Holden *et al.* 1987; Fowler 1988a, 1992; Fowler & Henney 1996; Fowler *et al.* 2001). Selected diagrams incorporating published and new data are used here to illustrate important and characteristic element variations and their interpretations (Fig. 5.2).

5.3.2.1 Major elements

The TAS diagram (Fig. 5.2 a) demonstrates two fractionation pathways, both stemming from the appinite array and evolving along monzodiorite-syenite (path ***a*** in Fig. 5.2 a) and diorite-quartz diorite-granodiorite-granite lines (path ***b*** in Fig. 5.2 a), respectively. All major element variation diagrams of this type (Fig. 5.2 b to d) are characterized by a broad spread of data in the appinite array, settling into more coherent trends in the evolved, silicic units (e.g. Fowler *et al.* 2001). There are two main groups of elements: those which decrease steadily with increasing SiO_2 as a result of mafic mineral fractionation including MgO, Fe_2O_3, CaO, MnO, TiO_2 and P_2O_5 (e.g. Figs. 5.2 b to c), and those that are concave downwards reflecting the entry of plagioclase into the fractionating assemblage as documented by Na_2O and Al_2O_3 (e.g. Fig. 5.2 d). Least-squares mass-balance modelling using observed mineral chemistry has established the possible derivation of both the granites and the syenites from an appinitic parent by a two stage crystal fractionation involving early mafic minerals (biotite + calcic clinopyroxene >> andesine >> apatite + titanite) and subsequently feldspar-dominated assemblages (oligoclase >> biotite + amphibole >> apatite + titanite) (Fowler 1988a, 1992 ; Fowler *et al.* 2001). The differences in major element chemistry between the silica-undersaturated syenites and the silica-oversaturated granites have been attributed to the earlier involvement of feldspar fractionation in the latter case (Fowler *et al.* 2001, p527).

5.3.2.2 Trace elements

Minor element variations are extensive, but all igneous complexes share the characteristic high Ba-Sr contents (thousands of ppm) throughout the lithological range, low Rb leading to high K/Rb, high LILEs and generally low HFSEs producing high LILE/HFSE ratios proposed in the literature (e.g. Tarney & Jones 1994). The greatest

LILE and light REE enrichment is seen in some of the syenites (especially Loch Loyal), which thus represent the extreme of the high Ba-Sr class. Within the high Ba-Sr granites, elemental abundances of LILE are high compared to other granites (I- or S-type) but do not reach enrichment levels of the high Ba-Sr syenites.

REE diagrams (Fig. 5.2 e to g) of all plutons consistently show highly fractionated patterns, which have light REE up to several hundred times chondrite, heavy REE only about ten times chondrite and small or negligible Eu anomalies, all of which suggest a genetic kinship of the suite. Further, REE diagrams clearly distinguish the high Ba-Sr granitoids from other granitoid types (e.g. I and S-types, Fig. 5.2 g) which have comparatively shallow REE patterns (low La/Yb) that generally contain well developed, negative Eu anomalies (e.g. Taylor & McLenan 1985). In previously studied plutonic suites (e.g. Glen Dessarry –Fowler 1992; Ach'Uaine – Fowler & Henney 1996; Rogart-Fowler *et al.*2001), appinitic rocks (where available) have the highest REE concentration and lie at the top of the array. Towards higher silica contents, the REE abundances systematically decrease towards granite or syenite (e.g. Strontian – Pankhurst 1979; Glen Dessarry –Fowler 1992). This progressive downward shift has been interpreted to result from fractional crystallisation of observed REE-rich accessory phases such as titanite, apatite, zircon and allanite during the felsic fractionation step (Fowler *et al.* 2001). The similarity of REE patterns of different facies within each pluton has been interpreted to demonstrate the genetic link of rocks throughout the respective suite (e.g. Pankhurst 1979, Fowler 1988a, 1992; Thirlwall & Burnard 1990; Fowler *et al.* 2001) whereas the downward shift of the REE pattern from mafic to felsic compositions has been interpreted to signal a direct parental status of the mantle-derived mafic magmas (e.g. Fowler 1988a, 1992; Fowler & Henney 1996; Fowler *et al.* 2001). This previously established REE-behaviour is observed in all newly studied granite plutons throughout the intermediate-to-felsic lithologies. However, not everywhere do mafic rocks of the individual complexes lie at the top of the range (e.g. Strath Halladale) and within the intermediate-to-felsic lithologies considerable overlap of REE patterns locally exists (e.g. Helmsdale, Cluanie, Strontian). Further, the degree of REE-enrichment and REE-fractionation varies regionally as the slope of the pattern steepens significantly from the southwest (Glen Dessarry, Strontian, Cluanie, Fig. 5.2) towards the northeast (Loch Loyal, Rogart, Strath Halladale and Helmsdale; Fig. 5.2).

Spider diagrams emphasize the similarities of the high Ba-Sr syenites and granites (both newly and previously studied complexes) and can be used to adequately summarize their key features (Fig. 5.3). The spider diagrams consistently slope from left to right in keeping with element incompatibility with respect to mantle parageneses. Well developed peaks at Ba, K and Sr occur throughout the lithological range and indicate enriched precursors and highlight the importance of feldspar during the fractionation process. Troughs at Nb, P and Ti occur throughout the lithological range and have previously been interpreted as a source signature indicating subduction-related origin (e.g. Saunders *et al.* 1980).

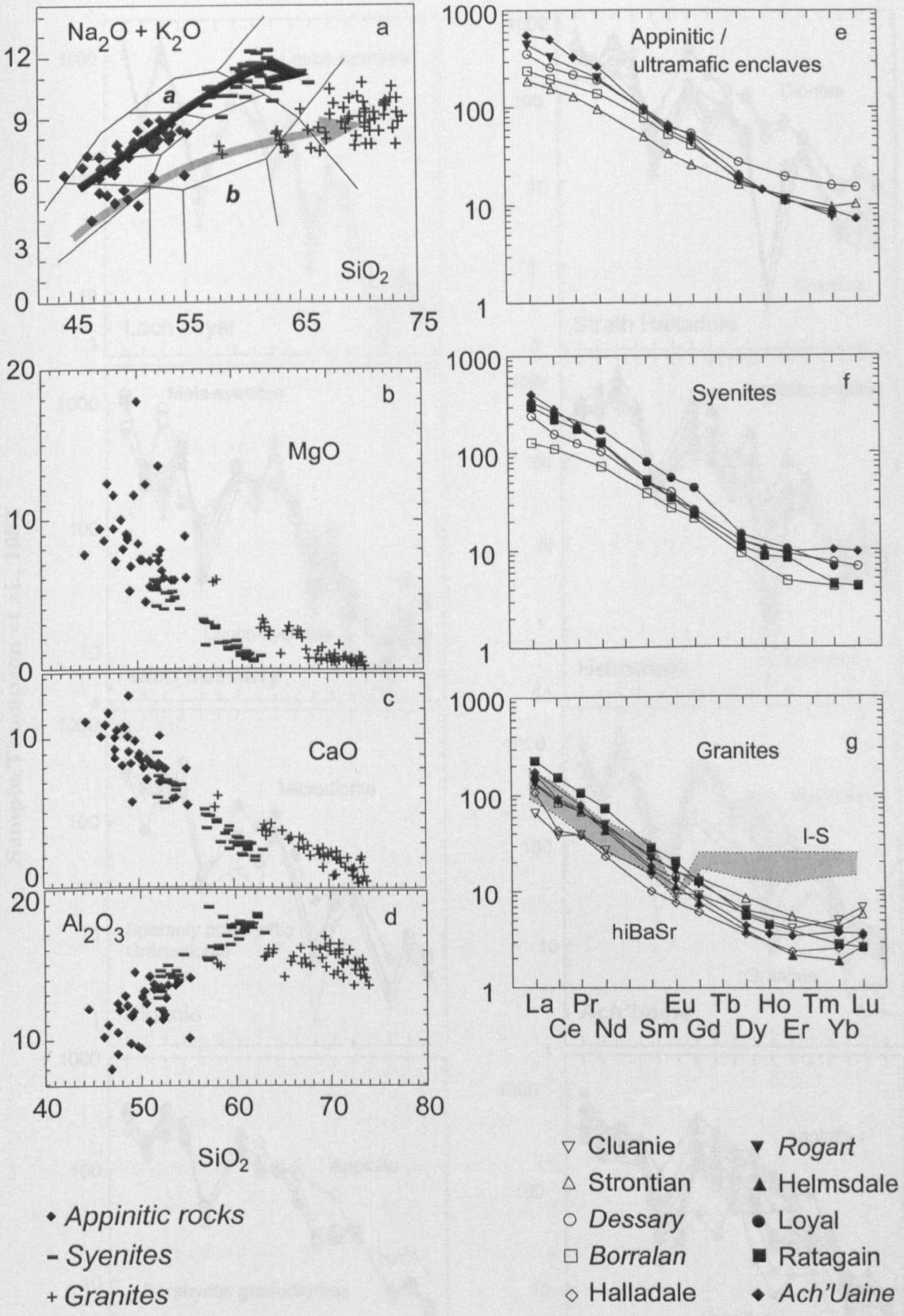

Fig. 5.2 Major element and REE plots of the Northern Highland high Ba-Sr granitoids. a) TAS-diagram showing syenitic and granitic fractionation trends. b-d) Harker diagrams showing steadily decreasing and concave downwards trends with increasing SiO2. e-g) Chondrite normalized REE plots. Note fractionated patterns, general absence of Eu-anomalies and dish-shaped hREE. Published data (*italicized* typeset) from Fowler (1988 a, b,1992), Thirlwall & Burnard (1990), Fowler & Henney (1996) and Fowler et al. (2001). Data for I and S-type granites from Taylor & McLennan 1985.

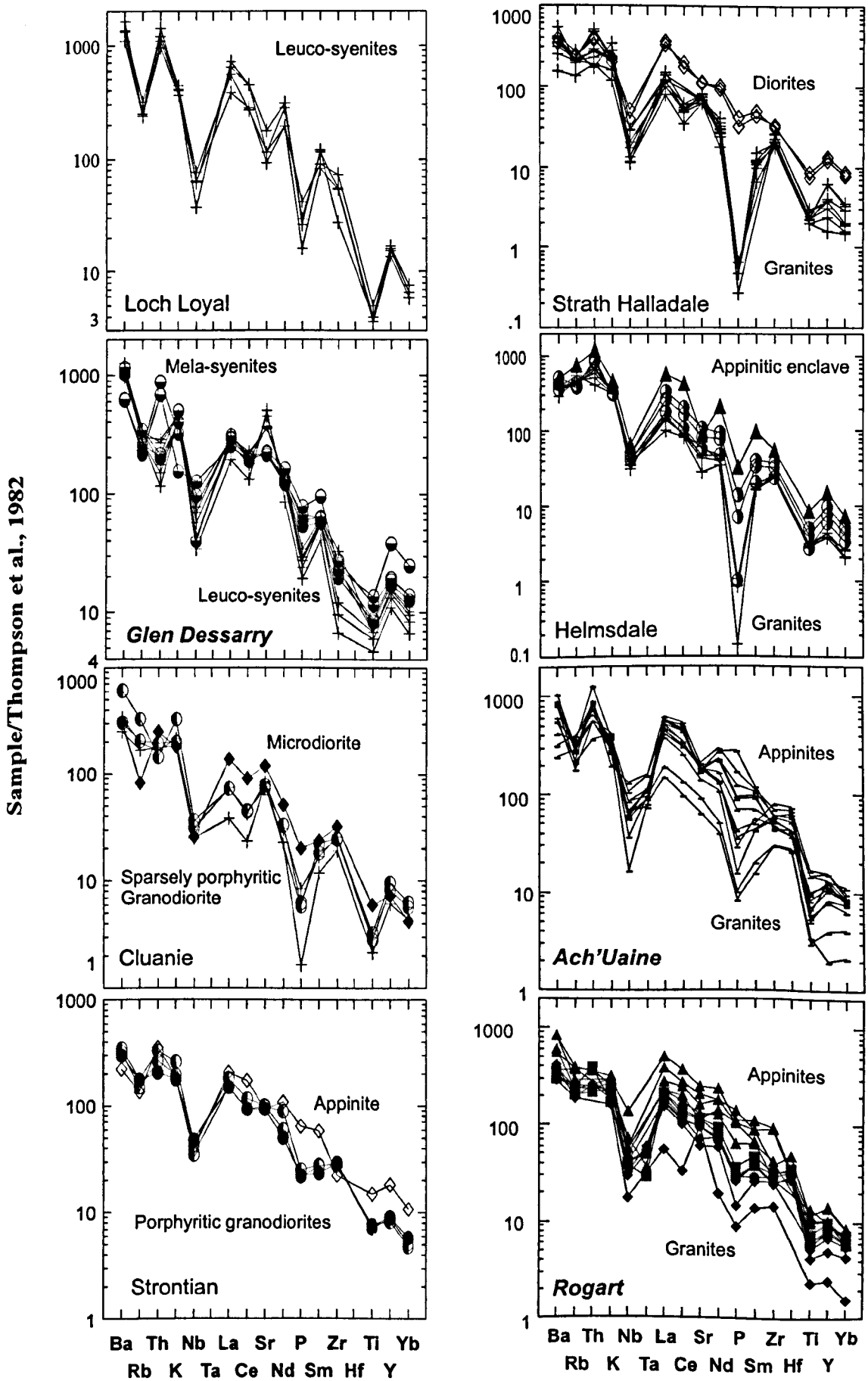

Fig. 5.3 Spiderdiagrams showing available data for high Ba-Sr plutons of the Northern Highland Terrane. ***Bold italicized*** typing indicates published data, see text. All plots are normalized to Thompson et al. 1982.

5.4 Case studies

5.4.1 Strath Halladale Granite

The rock types studied include the Strath Halladale granodiorites/granites, the Reay diorites and a variety of mafic to ultramafic rocks, either forming enclaves within the main felsic plutons or stocks on the western side of the Strath Halladale Granite (see chapter 4).

5.4.1.1 Major elements

The range of compositions is extensive with SiO_2 varying between 44.5% and 73% forming clusters at 45-50%, 60% and 69-73%. On the TAS diagram (Fig. 5.4 a) the suite forms an array from monzogabbro through monzodiorite to quartz monzonite and granite, corresponding to fractionation pathway ***b*** described in the regional study. The variation of the remaining major elements is depicted in a series of Harker diagrams (Fig. 5.4) which are characterized by coherent trends in the felsic lithologies but display great variety within the mafic suite (open and filled squares and circles). Mafic rocks analysed occupy distinct fields situated off the backwards extension of the major element trends defined by the diorites and granites and plot away from the areas where suitable precursors to the diorites would be expected. Petrographically, two main types of mafic rocks have been observed. Coarse grained pyroxene-bearing hornblendite is found in the southern Strath Halladale area (filled squares) whereas medium to fine grained enclaves rich in amphibole, biotite and plagioclase are found within the Reay Diorite (semi-filled circles). Compared to the mantle-derived Northern Highland minettes (Canning *et al.* 1996), some of the mafic rocks of the Strath Halladale suite are very high in, for example, MgO, Fe2O3 and CaO ruling them out as direct precursors to the diorites and granites (Fig. 5.4). Instead, the major element chemistry and mineralogy suggest that the majority of mafic rocks in Strath Halladale may represent cumulus phases to an unexposed precursor of the diorites and granites. Thus, it is impossible to define well-constrained fractionation trends spanning the entire lithological range on Harker diagrams. However, assuming a precursor to the diorites at the felsic end of the observed mafic array with SiO_2=52%, Na_2O=3%, K_2O=5.5%, Al_2O_3=12.5%, CaO=8%, MgO=7.5%, MnO=0.13%, Fe_2O_3=8%, TiO_2=1.2% and P_2O_5=0.55% that corresponds to the mantle-derived, parental minettes and appinites of Canning *et al.* (1996) and Fowler & Henney (1996), two elemental trends may be

envisaged (Fig. 5.4): those elements which decrease constantly with increasing SiO_2 (Fe_2O_3, MnO, MgO, CaO, TiO_2 & P_2O_5; e.g. Fig. 5.4 b to g) and those which are concave downwards such as Al_2O_3 and Na_2O+K2O (e.g. Fig. 5.4 a & h). In Strath Halladale, the data are consistent with feldspar-dominated fractional crystallization in the diorite to granite step as previously proposed for adjacent high Ba-Sr plutons (e.g. Fowler & Henney 1996; Fowler *et al.* 2001), but do not allow the precise identification of earlier fractionating assemblages or a precursor to the diorites.

5.4.1.2 Trace elements

5.4.1.2.1 Bivariate plots

Trace element behaviour throughout the suite is also not straightforward. Some of the "classic" bivariate trace elements plots are shown in figure 5.5. Fig. 5.5a illustrates the high concentrations of Ni (250-300ppm) and Cr (430 - 1400ppm) in the mafic facies indicating derivation from a mantle source (table 2.3). This plot also documents the expected progressive compatibility of Ni and Cr throughout fractionation and a proportional decrease of Ni and Cr towards felsic lithologies. The contemporaneous, parallel decrease of V and Ti (Fig. 5.5 b) suggests the involvement of ilmenite or titanomagnetite during fractionation (e.g. Fowler & Henney 1996) which is supported by the presence of abundant ore minerals throughout the suite. Other bivariate trace element plots are characterized by a wide spread in the data, which is again very pronounced in the mafic lithologies. Zr vs. Y (Fig. 5.5c) is generally taken to monitor zircon fractionation (e.g. Fowler *et al.* 2001) but does not seem a useful petrogenetic indicator for the entire Strath Halladale suite. However, excluding the mafic phases, a very steep trend results in the diorite to granite step. This may reflect the importance of apatite and titanite over zircon fractionation and agrees well with abundant titanite and apatite in the Reay diorites. Ba vs. Sr and Rb vs. Sr are usually taken to monitor the substitution of Ba, Rb and Sr into feldspars (and subordinate hornblende & biotite for Ba & Rb, table 2.3). Only rarely are trends smooth, more often showing considerable spread and overlap between rock types, especially within the mafic facies, (e.g. Glen Dessarry, Fowler 1992; Rogart, Fowler *et al.* 2001) which these authors interpret to reflect incomplete *in situ* crystal-liquid separation. In the Strath Halladale suite, the fields of the Reay Diorite and the Strath Halladale Granite form rather tight, neighbouring clusters with the diorites showing higher Sr but equal Ba and Rb (Fig. 5.5 d & e). The mafic rocks, however, plot in a wide field to the bottom-left

of the felsic varieties, partially overlapping with the granitoids and as such need to be excluded from the "trend construction". Thus trends fitted through the remaining two point clusters cannot unequivocally establish crystallizing minerals that control element substitution. However, plotted against SiO_2 as a fractionation monitor, a systematic behaviour of Sr can be shown (Fig. 5.5 f). The elemental Sr-content increases steadily during early stages (c. 50% SiO_2), and is interpreted to reflect the incompatibility of Sr for early fractionating amphibole and biotite-dominated assemblages. Once plagioclase fractionation becomes dominant (c. 55% SiO_2), Sr behaves compatibly and correspondingly decreases in the diorite to granite step. A comparable trend can be inferred for Rb vs. SiO_2 in the diorite to granite step (Fig. 5.5 g). However, the spread of Rb in the mafic rocks (Fig. 5.5 g) is considerable and may reflect varying abundance of Rb-rich minerals such as biotite or even K-feldspar in the matrix of (appinitic) cumulates. Overall, the disposition and scatter of the mafic rocks of the Strath Halladale suite on most trace element plots (e.g. Ba-Rb vs. Sr, Y vs. Zr) strongly argues that these do not form direct parental liquids to the diorites and granites.

5.4.1.2.2 Chondrite-normalized plots

The Strath Halladale granites have already been shown to possess a distinct REE pattern identifying it as part of the high Ba-Sr granitoids (Fig. 5.2, see above). Fig. 5.6 shows a series of REE diagrams and spider diagrams separately showing mafic rocks, Reay diorites and Strath Halladale granites.

The REE patterns of the diorites and granodiorites are highly fractionated with La/Yb ratios of 60-70 and show negligible negative Eu-anomalies and characteristically dish-shaped heavy REE (Fig. 5.6 a). The light REE enrichment argues for the importance of accessory phases such as titanite, apatite, allanite and monazite during fractionation and the dish-shaped heavy REE pattern is consistent with amphibole fractionation (e.g. Rollinson 1993). REE patterns of the felsic rocks exposed in Strath Halladale support a genetic link between them. The downward shift of REE patterns in the diorite to granite step is consistent with the removal of accessory-rich feldspar-dominated assemblages as previously proposed for adjacent high Ba-Sr plutons (Fowler & Henney 1996; Fowler *et al.* 2001). The lack of significantly developed Eu-anomalies in feldspar-dominated fractionation processes has commonly been interpreted to demonstrate high fO_2 during feldspar crystallization (Drake & Weill 1975).

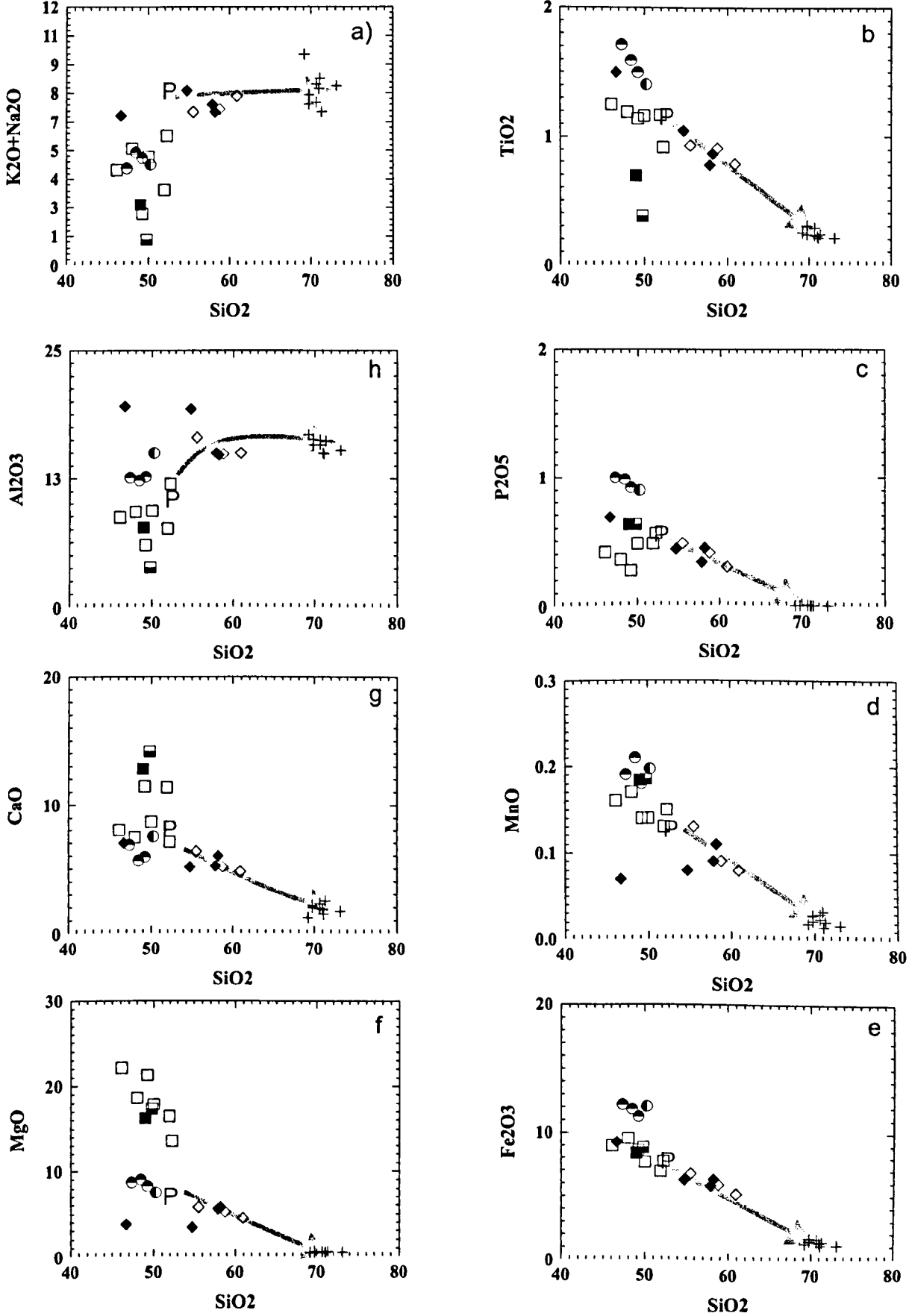

Fig. 5.4 Harker diagrams for the Strath Halladale suite depicting possible fractionation trends (grey arrows), open symbols = published data (Storey & Lintern 1981). Explanation see text.

P: hypothetical parent, that corresponds to the mantle-derived minettes of Canning *et al.* (1996).

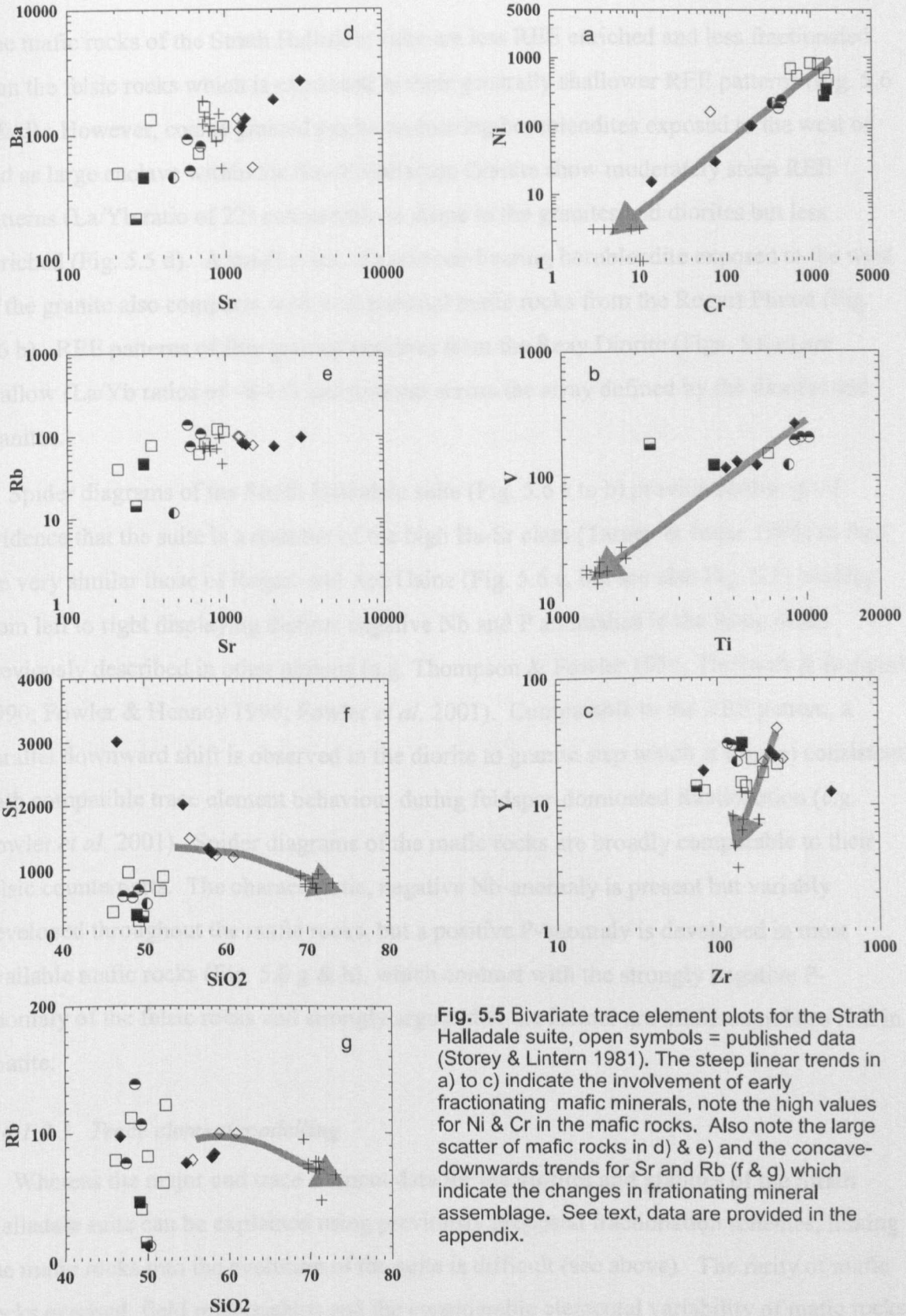

Fig. 5.5 Bivariate trace element plots for the Strath Halladale suite, open symbols = published data (Storey & Lintern 1981). The steep linear trends in a) to c) indicate the involvement of early fractionating mafic minerals, note the high values for Ni & Cr in the mafic rocks. Also note the large scatter of mafic rocks in d) & e) and the concave-downwards trends for Sr and Rb (f & g) which indicate the changes in frationating mineral assemblage. See text, data are provided in the appendix.

The mafic rocks of the Strath Halladale suite are less REE enriched and less fractionated than the felsic rocks which is expressed in their generally shallower REE patterns (Fig. 5.6 c & d). However, coarse grained pyroxene-bearing hornblendites exposed to the west of and as large enclave within the Strath Halladale Granite show moderately steep REE patterns (La/Yb ratio of 22) comparable in shape to the granites and diorites but less enriched (Fig. 5.5 d). A small stock of pyroxene-bearing hornblendite exposed to the west of the granite also compares well with parental mafic rocks from the Rogart Pluton (Fig. 5.6 b). REE patterns of fine grained enclaves from the Reay Diorite (Figs. 5.6 c) are shallow (La/Yb ratios of ~8-11) and thus cut across the array defined by the diorites and granites.

Spider diagrams of the Strath Halladale suite (Fig. 5.6 e to h) provide further good evidence that the suite is a member of the high Ba-Sr class (Tarney & Jones 1994) as they are very similar those of Rogart and Ach'Uaine (Fig. 5.6 e, but see also Fig. 5.3), sloping from left to right displaying distinct negative Nb and P anomalies in the felsic rocks previously described in other plutons (e.g. Thompson & Fowler 1986; Thirlwall & Burnard 1990; Fowler & Henney 1996; Fowler *et al.* 2001). Comparable to the REE pattern, a parallel downward shift is observed in the diorite to granite step which is (again) consistent with compatible trace element behaviour during feldspar-dominated fractionation (e.g. Fowler *et al.* 2001). Spider diagrams of the mafic rocks are broadly comparable to their felsic counterparts. The characteristic, negative Nb-anomaly is present but variably developed throughout the mafic rocks, but a positive P-anomaly is developed in most available mafic rocks (Fig. 5.6 g & h), which contrast with the strongly negative P-anomaly of the felsic rocks and strongly argues that the former are mafic cumulates rich in apatite.

5.4.1.2.3 Trace element modelling

Whereas the major and trace element data for the diorites and granites of the Strath Halladale suite can be explained using previously proposed fractionation schemes, linking the mafic rocks into the evolution of the suite is difficult (see above). The rarity of mafic rocks exposed, field relationships and the considerable elemental variability of mafic rocks available further severely restrict the choice in identifying a suitable parent to the suite.

The coarse grained pyroxene-bearing hornblendite (SHG 450) which forms a large enclave within the southern Strath Halladale Granite shows a comparable but less enriched REE

pattern to the diorites (and the granites). Its spider diagram further shows a positive P anomaly which strongly suggests that it is a cumulate. Using observed mineralogy and the REE concentration of this cumulate, a parental melt from which it separated was modelled using the fractional crystallisation equations of Allegre & Minster (1978) and mineral/melt distribution coefficients for basaltic compositions of Arth (1976) (Fig. 5.7, table 5.1). Compared to the observed cumulate, the modelled parent (at 10% cumulus) shows an enriched REE pattern that reflects the incompatibility of REE for the fractionating mafic assemblages. The modelled parental pattern is also very similar to the diorite pattern (Fig. 5.7). It is therefore proposed that the diorites were derived from a parental magma comparable to the modelled liquid by continued segregation of mafic cumulates consistently shifting the REE pattern of the evolving liquid upwards. Once the fractionating assemblage became feldspar-dominated and accessory phases started to crystallize, the REE behaved compatible resulting in a downward shift of the pattern as proposed by Fowler *et al.* (2001). The modelled parental melts are similar to rocks that form small stocks within the Moine to the west of the granite (as exemplified by sample SHG 65) which may therefore approximate potential parental magmas, similar to relationships described from Ach'Uaine and Rogart (e.g. Fowler & Henney 1996; Fowler *et al.* 2001).

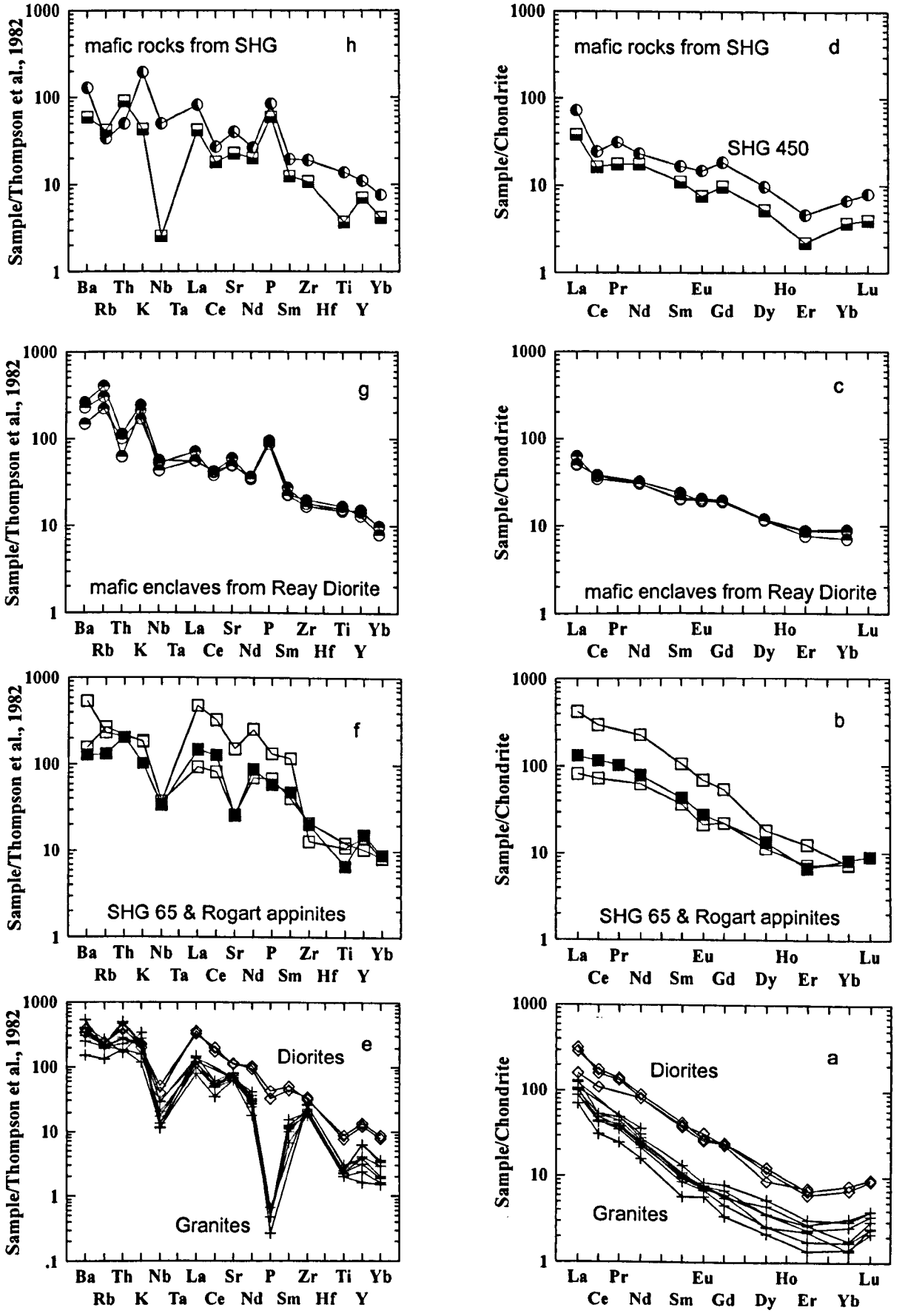

Fig. 5.6 REE & Spiderdiagrams for the Strath Halladale suite (SHG), showing individual mafic and felsic lithologies from top to bottom. Note diversity in mafic rocks contrasting the homogeneity in the intermediate-felsic lithologies. a & e) Diorites and granites. b & f) Px-bearing hornblendite exposed to the west of the Strath Halladale Granite compared to appinitic rocks from Rogart (pjh215 & RA1, data from Fowler et al. 2001). c & g) Shallow cross-cutting enclaves from the Reay Diorite. d& h) Mafic rocks from the SHG including SHG 450. Note the positive P anomaly in g) & h) indicating cumulates rich in apatite. Symbols as in Fig. 5.4, see text.

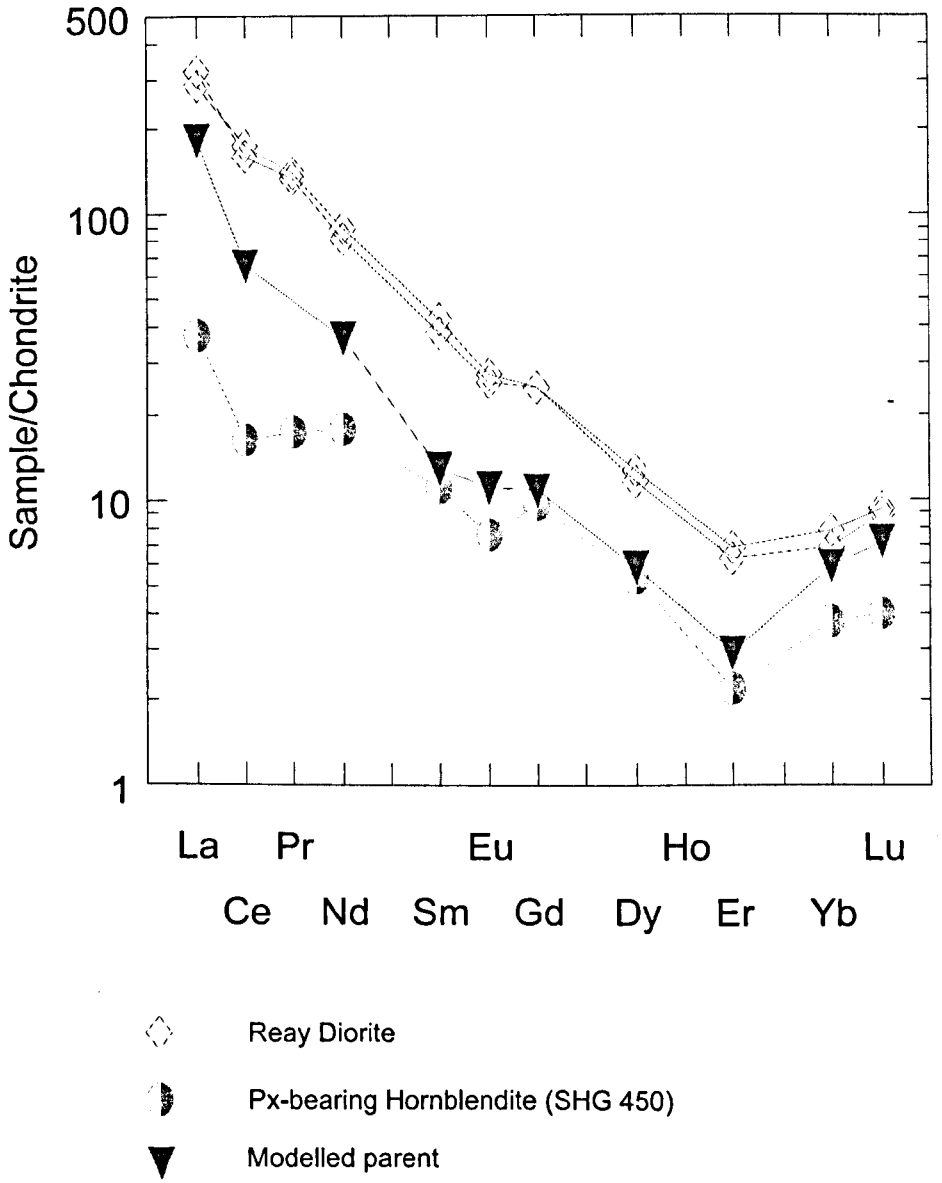

Fig. 5.7 REE diagram showing SHG450 (cumulate), two Reay Diorite samples (RD90, RD84) and a parental melt. The parent was modelled based on the cumulate chemistry and mineralogy using fractional crzstallization equations after Allegre & Minster (1978) and D-values for basalts-basaltic andesites of Arth (1976). Note that at 10% cumulate fractionation, the shape of the parent is very similar to the shape of the Reay diorites. Thus it is suggested, that during the early evolution of the Strath Halladale suite, cumulate fractionation lead to an upward shift of the REE pattern (incompatible trace element behaviour) that has not previously been recognized in other high Ba-Sr plutons. For modelling parameters see table 5.1

Table 5.1 Modelling parameters used in figure 5.7

	mineralogy	La	Ce	Nd	Sm	Eu	Gd	Dy	Er	Yb	Lu
hbl	0.95	0.11	0.2	0.33	0.55	0.4	0.63	0.64	0.55	0.49	0.43
bt	0		0.7		1.3		1.1			0.8	
pl	0		0.2		0.2		0.14			0.12	
ap	0.0148	6	3	10	20	19	18	18	13	9	8
ti	0		80		270		260			72	
zr	0		2.2		33		180			120	
other	0										
Cpx	0.0362	0.1	0.15	0.31	0.5	0.51	0.61	0.68	0.65	0.62	0.56
sum	1.001										
Bulk-Kd		0.19692	0.23983	0.472722	0.8366	0.679662	0.886982	0.899016	0.73843	0.621144	0.547172

			F
	SHG 450	**PARENT**	0.9
La	13.9	67.69313	
Ce	15.6	62.51996	
Pr	2.4	0	
Nd	12.7	26.13909	
Sm	2.54	3.010494	
Eu	0.667	0.965188	
Gd	3	3.36251	
Dy	2.01	2.224113	
Er	0.55	0.734785	
Yb	0.922	1.45544	
Lu	0.153	0.273117	

Allegre & Minster (1978)
PARENT: Co = (Cs*(1-F))/(1-(F^D))

The enrichment of a trace element in the residue,i.e. the mean concentration of the cumulate (Cs), relative to the parental liquid (Co). F = fraction of remaining liquid. D = bulk partition coefficient. Kd-values after Arth (1976).

5.4.1.3 Isotopes

Six samples were selected for Sr and Nd radiogenic and oxygen isotope analysis. Based on their elemental geochemistry and field evidence, five samples including the mafic cumulate (SHG 450), two diorites (RD1 & SHG 403) and two granodiorites (SHG-c & SHG 132) have been interpreted to be cogenetic. A sixth sample (SHG 65) from outside the pluton has been analysed as its elemental geochemistry suggested that it could represent an analogue of a potential mafic parent to the suite. Initial isotope ratios were calculated to 423Ma based on the titanite age produced by G. Rogers (pers. comm.) and are presented in table 5.2. The radiogenic data form an array of $\varepsilon Nd_{(i)}$ from –0.9 to –2.3 and of $^{87}Sr/^{86}Sr_{(i)}$ from 0.70579 to 0.70694. $\delta^{18}O$ values range from 7.1‰ in the mafic rocks to 10.1‰ in the intermediate to felsic rocks. Fig. 5.8a shows the data in relation to the positions of various possible contributory reservoirs including depleted mantle, Lewisian basement in amphibolite and granulite facies and Moine metasediments (data from Harmon *et al.* 1984). On a large scale, the samples of the Strath Halladale suite define a coherent and characteristic array that plots between a depleted component and the Moine metasediments (Fig. 5.8a) and distinguishes the suite from adjacent high Ba-Sr plutons (see below and Fig. 5.11). In detail, the variations of the initial isotopes within the cogenetic suite (excluding SHG 65) are complex (Fig. 5.8 b) as the more felsic samples do not necessarily possess more "evolved" radiogenic isotopic signatures. Instead, the diorites posses a more evolved radiogenic isotope signature than the granodiorites which plot very close to the mafic cumulate (SHG 450; Fig. 5.8b). The oxygen data show comparable behaviour as some diorites have a higher $\delta^{18}O$ than related granites (Fig. 5.8b). The radiogenic and stable isotope data thus argue against close-system evolution but suggest the involvement of a contaminant and further render a straightforward evolution of the cogenetic suite by AFC from mafic to felsic as proposed for adjacent plutons (e.g. Fowler *et al.* 2001) impossible. As the samples plot on a trajectory from Bulk Earth towards Moine metasediment and show varying high $\delta^{18}O$, Moine-derived material is considered a likely contaminant (Figs. 5.8a & b). Although the external sample (SHG 65) plots within the array, isotopically it does not approximate a suitable parent for the Strath Halladale suite which should have the least evolved radiogenic signature present (Fig. 5.8b).

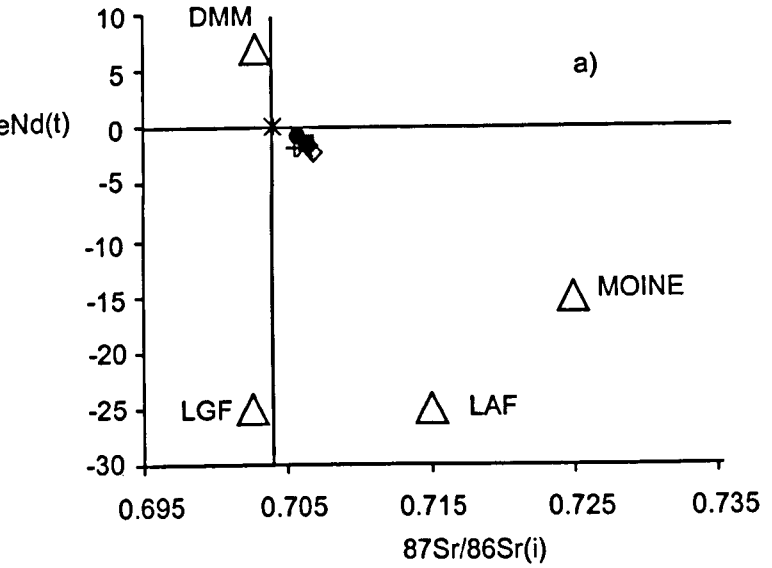

Fig. 5.8 Isotope systematics of the Strath Halladale suite. a) Overview plot showing the suite with respect to possible contributing reservoirs. Initial ratios calculated based on published age data (table 5.1), DMM= depleted mantle, LAF/LGL= Lewisian in amphibolite / granulite facies (data from Harmon et al. 1984). b) detailed plot showing radiogenic and stable isotope covariations. Note the "out of sequence" AFC behaviour of the suite, the hypothetical AFC-trajectories, and the hypothetical parent melt "P", see text. Data are summarized in table 5.2. c) Flow diagram illustrating the hypothetical fractionation scheme of a parent magma (imprecisely constrained), from which mafic & felsic melts separate prior to individual contamination.

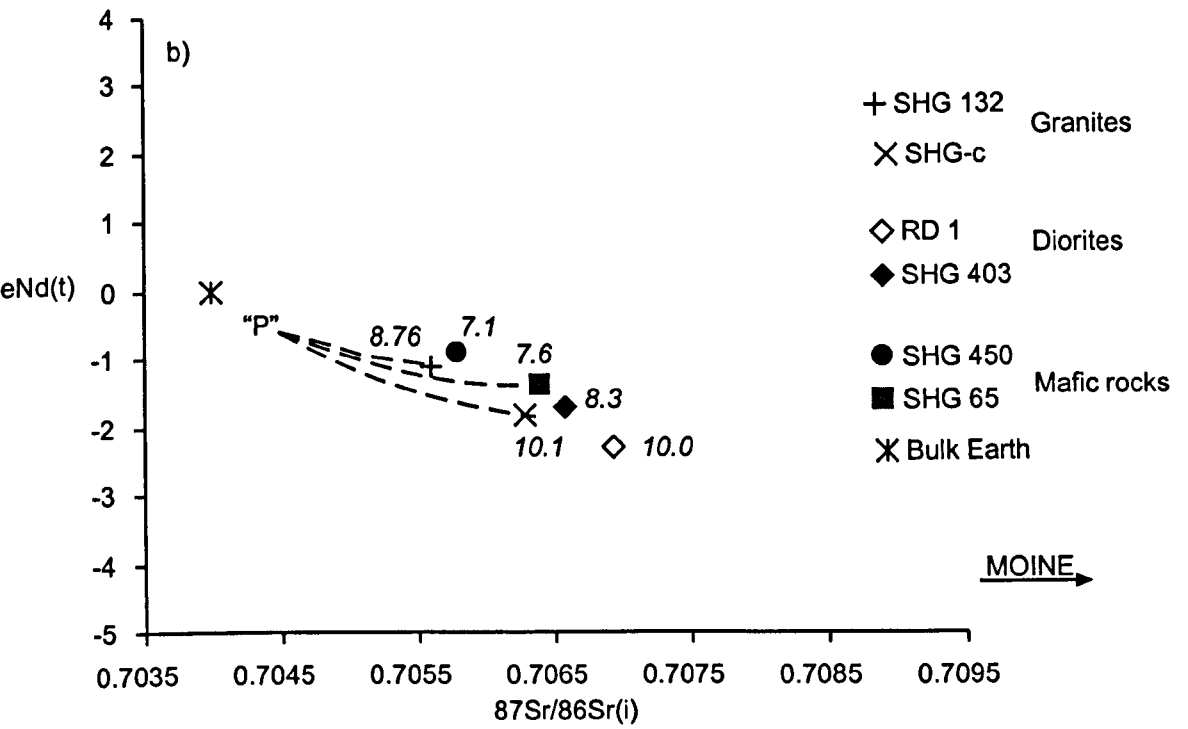

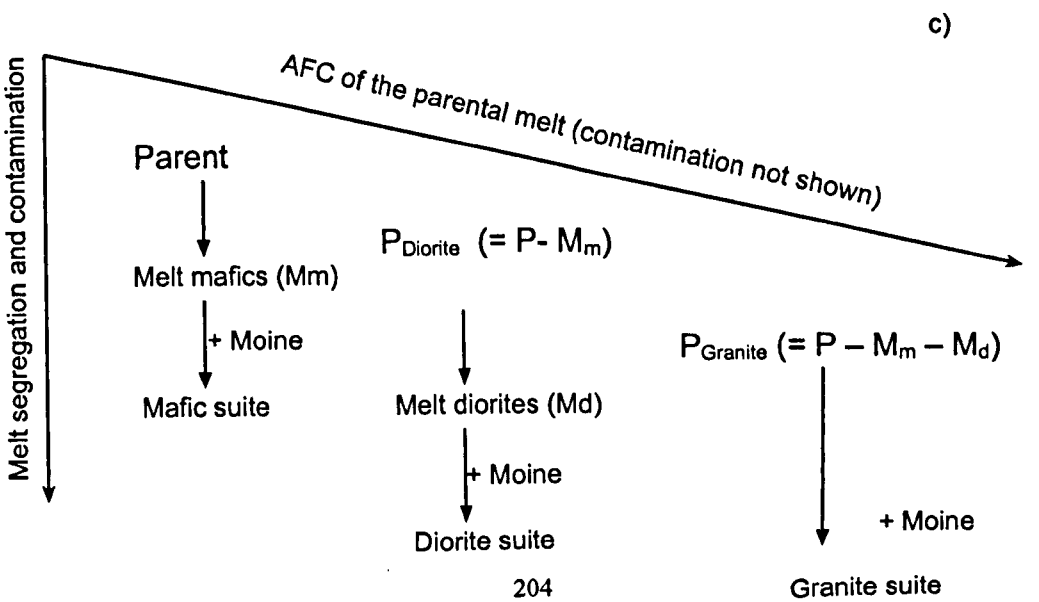

5.4.1.4 Petrogenetic model

In keeping with the elemental and isotopic data of the suite, the following hypothetical model is proposed. A parental melt approximating the composition modelled from the cumulate SHG 450 (section 5.4.1.2.4) was derived in response to the subduction of Iapetus. From this parental melt ("P" in Fig. 5.8b) mafic, dioritic and granitic melts separated and individually became contaminated to varying degrees with Moine metasediment (Fig 5.8c). The samples are therefore genetically linked and possess the elemental characteristics of the evolving parent but in detail contain an *individual* isotopic signature reflecting individual contamination. Discrete magma pulses were clearly able to assimilate more or less metasediment during ascent to the site of pluton construction, presumably related to the details of the plumbing system that each traversed. Similar models have been invoked to explain such 'out of sequence' isotopic variations in the Tertiary lavas of Skye (Thirlwall & Jones 1983).

5.4.1.5 Summary of the Strath Halladale suite

In summary, the geochemistry of the Strath Halladale suite clearly indicates that the pluton is a member of the high Ba-Sr class (Tarney & Jones 1994). The major and trace element geochemistry of the diorites and granites is consistent with fractional crystallization of felsic, accessory-rich, feldspar-dominated assemblages as proposed for adjacent plutons (e.g. Fowler *et al.* 2001). Mineralogy and trace element geochemistry of the mafic rocks suggests that they were most likely not direct parents to the diorites (and granites) but instead represent a variety of cumulates. However, the elemental composition of a precursor to the diorites may be modelled using observed chemistry and defines a previously-unseen shift of the REE pattern in the early stages of the magmatic evolution of the suite. This and the subsequent, familiar decrease can be explained in a two stage fractional crystallization model involving early mafic crystal fractionation during which the REE behaved incompatibly and the established subsequent feldspar-dominated fractionation (e.g. Fowler *et al.* 2001) during which they behaved compatibly. The radiogenic and stable isotopes are consistent with the sequential segregation of mafic, dioritic and granitic melts from a fractionating parental melt followed by individual contamination with Moine metasediment. The isotopic composition of such a potential parental melt for the suite is not well constrained, but may be similar to the source of the Loch Borralan complex (see below). Although complex in detail, the isotopic range of all

analysed samples displays a characteristic and coherent trend distinguishing the Strath Halladale suite from adjacent high Ba-Sr plutons (see below).

5.4.2 Helmsdale granite

The Helmsdale suite comprises the variably K-feldspar-porphyritic granodiorite and the central, fine grained adamellite which grade into each other over short distances and show evidence for mixing in a narrow, intermediate zone (chapter 4). Mafic enclaves have been observed in the porphyritic granodiorite and the largest (c.80cm diameter) has been included in the geochemical study. However, since equilibration of small mafic enclaves with their felsic hosts has been well documented (e.g. Holden *et al.* 1987; Stephens *et al.* 1991) the interpretation of the mafic enclave needs to remain tentative. In particular large-ion-lithophile-elements and isotopes are prone to lose useful petrogenetic information by diffusion across the enclave/host contact whereas high-field-strength-elements may retain original magmatic concentrations (Fowler & Henney 1996, p202). The range of composition is therefore clearly limited and it is impossible to establish unequivocal fractionation trends.

5.4.2.1 Major elements

Harker diagrams are shown in figure 5.9 for the sake of consistency, as all samples (excluding the enclave) plot within 65-74% SiO_2 and show typical but unspecific major element abundances. The spread of SiO_2 in the granodiorites may reflect the varying abundance of megacrystic K-feldspar, with the megacryst-poor rocks overlapping with the adamellites. The 'mafic' enclave actually shows intermediate SiO_2, which may be explained by quartz-crystal-transfer from the porphyritic granodiorite that could not be totally removed during sample preparation. However, apart from the misplacement on diagrams involving silica, this should not significantly affect the abundance of other major elements or trace element or isotopic behaviour, as distribution coefficients of elements other than Si are low for quartz.

5.4.2.2 Trace elements

5.4.2.2.1 bivariate plots

Again, the limited compositional variety restricts the usefulness of bivariate trace element plots to demonstrating trace element abundances. Fig 5.9a emphasizes high values

for Ba (1000-2000ppm) and Sr (400-1500ppm), high K/Rb (Fig. 5.10b) and low HFSE element abundances in the granites and granodiorites, characteristic of high Ba-Sr granites (Tarney & Jones 1994; Fowler & Henney 1996). Scatter inherent in the granodiorites may reflect varying abundances of ore minerals and apatite (e.g. V & Ti, Fig. 5.10c), or zircon (e.g. Y & Zr, Fig. 5.10d). Trace element abundances in the enclave are generally higher than in the granitoids. However, Ni and Cr (Fig. 5.10e) are lower (150ppm and 200ppm respectively) than in similar mafic rocks from other intrusions (e.g. Ach'Uaine: Cr up to 585ppm and Ni up to 163ppm, Fowler & Henney 1996) and thus do not indicate direct mantle derivation (e.g. table 2.3).

5.4.2.2.2 Chondrite-normalized plots

The REE patterns and spider diagrams (Fig. 5.10 f& g) summarize the geochemical features of the Helmsdale suite and again emphasize their membership within the high Ba-Sr class. The REE-pattern is characteristically fractionated with high La/Yb (>50), no Eu-anomalies and typical dish-shaped heavy REE, as already described in the Strath Halladale suite. The spider diagrams show the characteristic high Ba-Sr, left-to-right sloping pattern with negative troughs developed at Nb and P throughout the suite. The REE and spiderpatterns shift progressively downwards with increasing SiO_2 consistent with a model of progressive fractionation of accessory phases towards higher silica abundance. Interestingly, the mafic enclave always lies at the top of the range in both diagrams, suggesting that interaction with its felsic host did not affect the REE.

5.4.2.3 Isotopes

Five samples were selected for isotopic analysis, comprising two porphyritic granodiorites, two adamellites and the mafic enclave. Initial isotopic ratios were calculated to 420Ma based on a U-Pb zircon age published by Pidgeon & Aftalion (1978). The isotopic range within the Helmsdale granite suite is very narrow (Fig. 5.10h), ranging from $\varepsilon Nd_{(i)}$ –5.4 to –6.0, $^{87}/^{86}Sr_{(i)}$ 0.70636 to 0.70657 and $\delta^{18}O$ 10.4 to 12.6 thus forming a well defined cluster. On a regional scale, the Helmsdale granite represents the most radiogenically enriched (Sr_i) granite in the terrane (complementary most depleted $\varepsilon Nd_{(i)}$) and also shows the highest $\delta^{18}O$ values.

5.4.2.4 Summary of the Helmsdale suite

Major and trace element geochemistry of the Helmsdale Granite indicate that the granite is a member of the high Ba-Sr class (Tarney & Jones 1994). Although unconstrained towards lower silica-contents, the elemental and isotopic chemistry is consistent with the derivation of the granites by assimilation fractional crystallization processes involving Moine rocks from an ultimately mantle derived precursor, as proposed for other high Ba-Sr plutons (Fowler 1988 a, b, 1992; Thirlwall & Burnard 1990; Fowler *et al.* 2001; Tarney & Jones 1994; Fowler & Henney 1996). The analysed mafic enclave may be tentatively interpreted as a trapped liquid within the outer granodiorite. The isotopic variation throughout the granite is small and the well-defined cluster represents the most radiogenically-enriched granite facies (coupled with highest $\delta^{18}O$) encountered in this study.

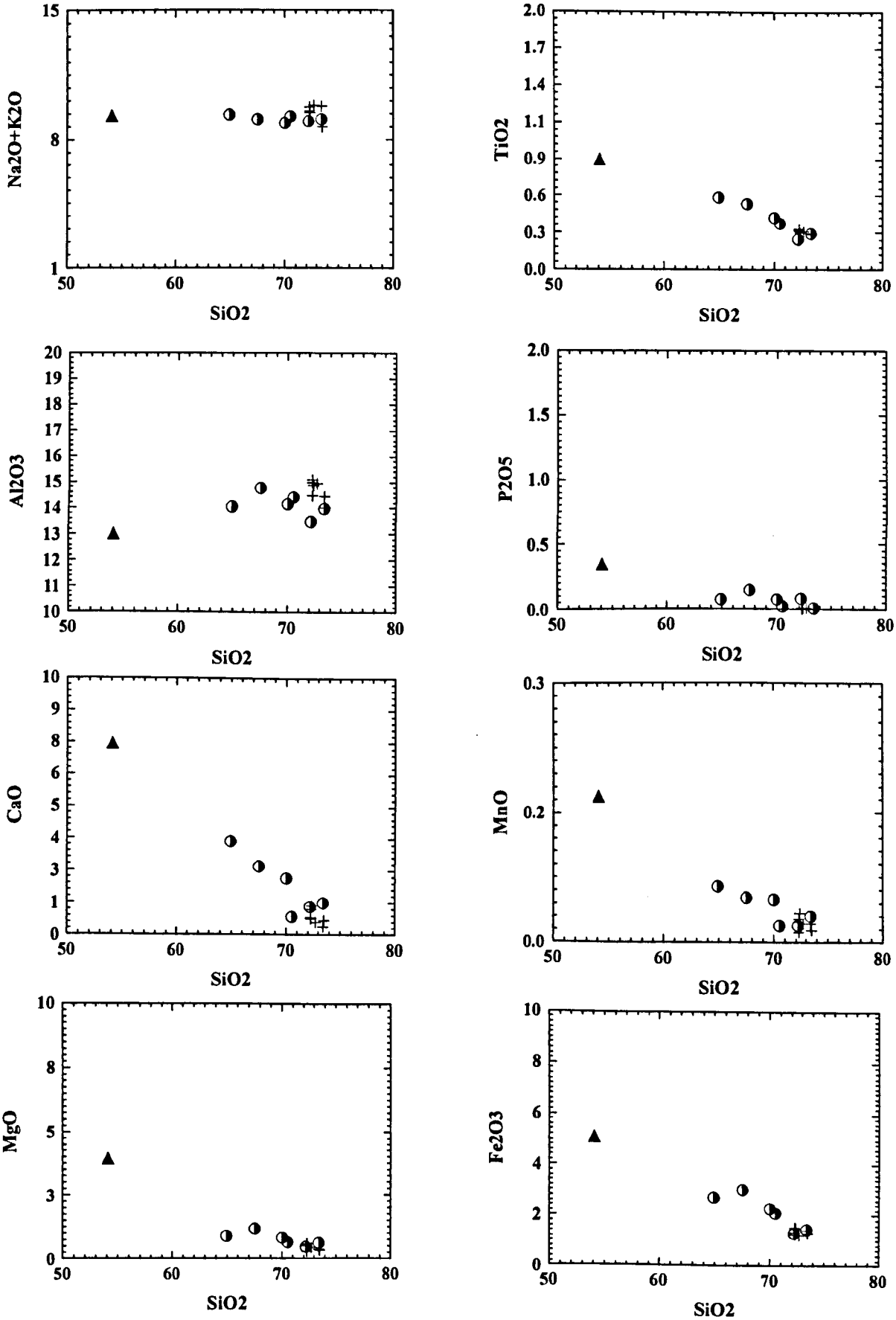

Fig. 5.9 Harker diagrams for the Helmsdale suite. Note that lithological diversity is sparse and that the mafic enclave is tentatively interpreted to show the potential composition of a possible parent to the Helmsdale granites. Thus, fractionation trends have not been plotted (two points only, i.e. any line will fit). The scatter within the porphyritic outer granite facies is interpreted to depend on the abundance of K-feldspar megacrysts.

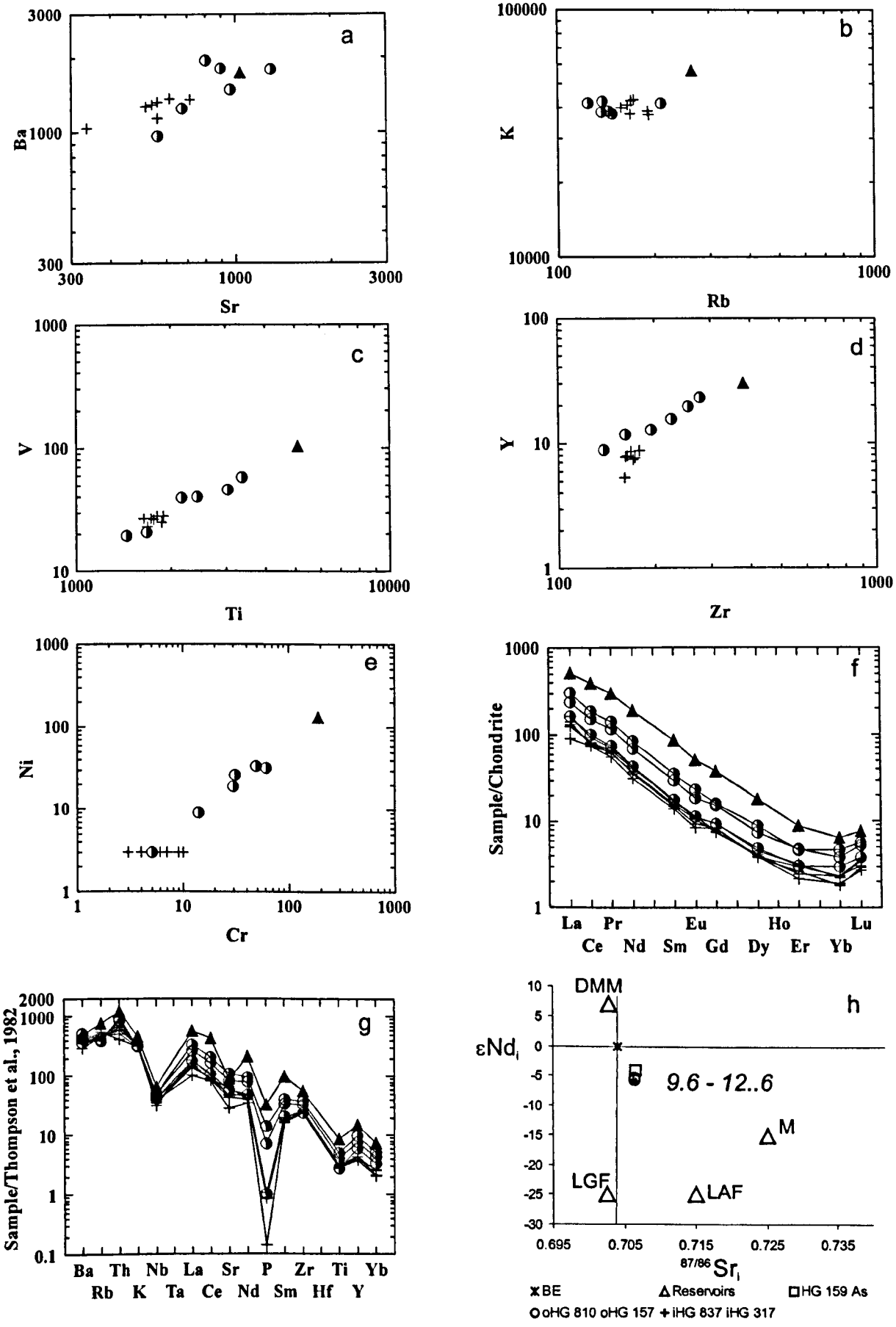

Fig. 5.10 Trace element and isotope variations of the Helmsdale Granite suite. a) to e) bivariate plots showing trace element abundances. f) Characteristic, steep, fractionated high Ba-Sr REE pattern. Note the appinitic enclave at the top and the overlap in the granitic facies. Key as in Fig. 5.9. h) Radiogenic isotopes at c. 420 Ma (see table 5.2) in relation to possible reservoirs. DMM= depleted morb mantle; LGF= Lewisian granulite facies; LAF=Lewisian amphibolite facies; M=Moine (data after Harmon et al. 1985). Note the tight cluster of radiogenic values and the high, but homogenous oxygen (italics). oHG= porphyritic outer granodiorite, iHG = inner Helmsdale granite; HG 159AS = appinitic enclave.

5.5 Regional isotopic study

5.5.1 Isotopic range

In addition to the Strath Halladale and Helmsdale granites, samples of the Cluanie and Strontian granites, the Loch Loyal syenites and the diverse Ratagain complex were analysed for Nd-Sr radiogenic and stable isotope ratios (table 5.2, Fig. 5.11). Initial isotopic ratios were calculated to the time of crystallization according to published age data (table 5.2). Cluanie shows the lowest $^{87}Sr/^{86}Sr_{(i)}$ (0.70472-0.70521), highest εNd_i (+2.6-3.2) and homogenous $\delta^{18}O$ (8.0-8.7) of the analysed suite. Strontian shows initial $^{87}Sr/^{86}Sr_{(i)}$ and εNd_i intermediate between Cluanie and Strath Halladale with $\delta^{18}O$ ranging from 6.7-8.0. Comparable to the Strath Halladale suite both plutons indicate internal complexities and "out-of-sequence" AFC behaviour, as the most mafic phases analysed do not always possess the most primitive isotopic signature. The radiogenic data for the Loch Loyal syenites are more akin to the Helmsdale granite suite and plot close to it in a narrow but well defined cluster with $^{87}Sr/^{86}Sr_{(i)}$ (0.70603-0.70612), εNd_i (-5.6 to –5.9) and $\delta^{18}O$ of 8.1-10‰. The diverse Ratagain complex shows the widest spread of data with $^{87}Sr/^{86}Sr_{(i)}$ ranging from 0.70512 to 0.70943, εNd_i from –3.7 to – 11.6, and $\delta^{18}O$ of 7.9-8.9‰.

5.5.2 Isotopic covariations

Fig. 5.11b shows the isotopic Nd-Sr-$\delta^{18}O$ covariations of all Caledonian plutons assigned to the high-Ba-Sr suite in the Northern Highland Terrane, including published data for Glen Dessarry (Fowler 1992), Loch Borralan (Thirlwall & Burnard 1990), Ach'Uaine (Thompson & Fowler 1996) and Rogart (Fowler *et al.* 2001). Comparable to Strath Halladale and Helmsdale, all samples belonging to the remaining high Ba-Sr complexes define well constrained, separate and characteristic trends, although within-pluton covariations may be complex (e.g. Strontian, Cluanie, Glen Dessarry). Importantly, on a regional scale, radiogenic and stable oxygen isotopes show a positive correlation, as plutons with the least radiogenic signatures also show the lowest $\delta^{18}O$ ratios. Further, the isotopic covariations for the main Caledonian Newer Granite complexes (Cluanie, Strontian, Strath Halladale, Ratagain diorite facies, Rogart, Helmsdale) define subhorizontal fractionation pathways which project towards the field defined by the Moine

Supergroup, whereas the Caledonian syenite complexes (e.g. Glen Dessarry & Loch Borralan) project towards the characteristic Rb-depleted field of Lewisian granulites.

5.5.3 Discussion

5.5.3.1 Disposition of the data arrays

The clear separation of the individual plutons on the Nd-Sr covaration-plot and the positive correlation with the $\delta^{18}O$ data suggests that despite internal complexity, systematic and significant regional and temporal differences must occur in the source region of the parental magmas as represented by their felsic derivatives. Further, the distinct subhorizontal AFC arrays of the granites point towards the Moine, suggesting Moine-involvement during granite evolution. In contrast, the subvertical syenite AFC arrays point towards the Rb-depleted field of granulite facies Lewisian basement and suggest its significance in syenite generation.

5.5.3.2 Fractionation mechanisms

Thirlwall & Burnard (1990) successfully modelled Nd – Pb isotope relationships of the Loch Borralan quartz syenites in terms of AFC of a mantle-derived mafic parent with a Lewisian granulite contaminant. As the published data for Glen Dessarry (Fowler 1992) and –to a lesser extent - the Ratagain syenites (this study) define subparallel Nd-Sr arrays to the Loch Borralan array (Fig. 5.11c) it is suggested that AFC-controlled syenite petrogenesis involving minor crustal assimilation of Lewisian granulites is a regionally important process. The Loch Loyal syenites are rather homogenous and lack an extended fractionation array which therefore do not allow this model to be tested. The Ratagain complex is lithologically and isotopically diverse. Although it is beyond the scope of this study to detail its precise magmatic evolution, it is noteworthy that the observed isotopic separation of syenitic and granitic facies of the Ratagain complex (Fig. 5.11 b& c) is consistent with the proposed importance of contaminant control.

The granite complexes have also been viewed in the context of AFC processes (Fowler *et al.* 2001; this study) and in the cases of the Rogart pluton and the closely-associated Ach'Uaine appinites a maximum of *c.* 25% crustal input using Moine metasediments has been proposed (Fowler & Henney 1996; Fowler *et al.* 2001). The parallel disposition of the data arrays for the other granite plutons (all trending towards Moine) suggests a similar

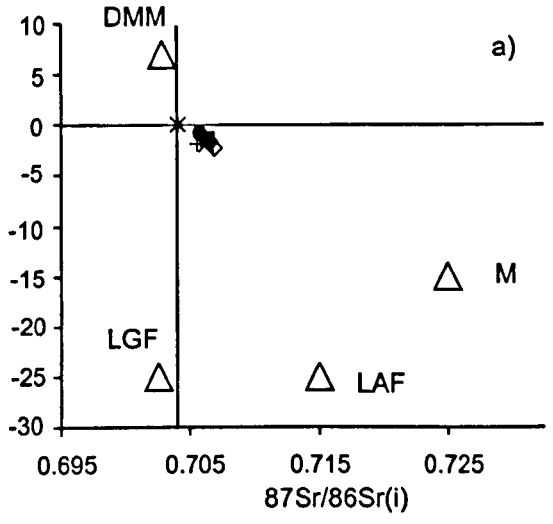

Fig. 5.11 Isotope correlation plots of the Northern Highland Granitoids. a) Overview plot showing the Strath Halladale suite with respect to possible contributing reservoirs as a reference (DMM = depleted mantle, M = Moine, LAF/LGF = Lewisian in amphibolite / granulite facies, data from Harmon et al. 1984). b) Radiogenic and stable isotope data for all plutons. Initial ratios calculated to time of intrusion (tables 1.2 & 5.2). Filled symbols = this study (CL = Cluanie, SR = Strontian, SHG = Strath Halladale, Rad = Ratagain diorite facies, Ras = Ratagain syenite facies, HD = Helmsdale, BL = Ben Loyal. Published data: LB = Loch Borallan (Thirlwall & Burnard 1990), GD = Glen Dessary (Fowler 1992), RG = Rogart (Fowler et al. 2001). BE = Bulk Earth. *Italicized* numbers show the range of oxygen isotope ratios, ***bold italic*** = mean value (table 5.2). c) Interpreted covariation of isotopic systems identifying an array of parental magmas (CPMA). Stars = descriptive extremes of the array, see text.

$\varepsilon Nd_{(t)}$

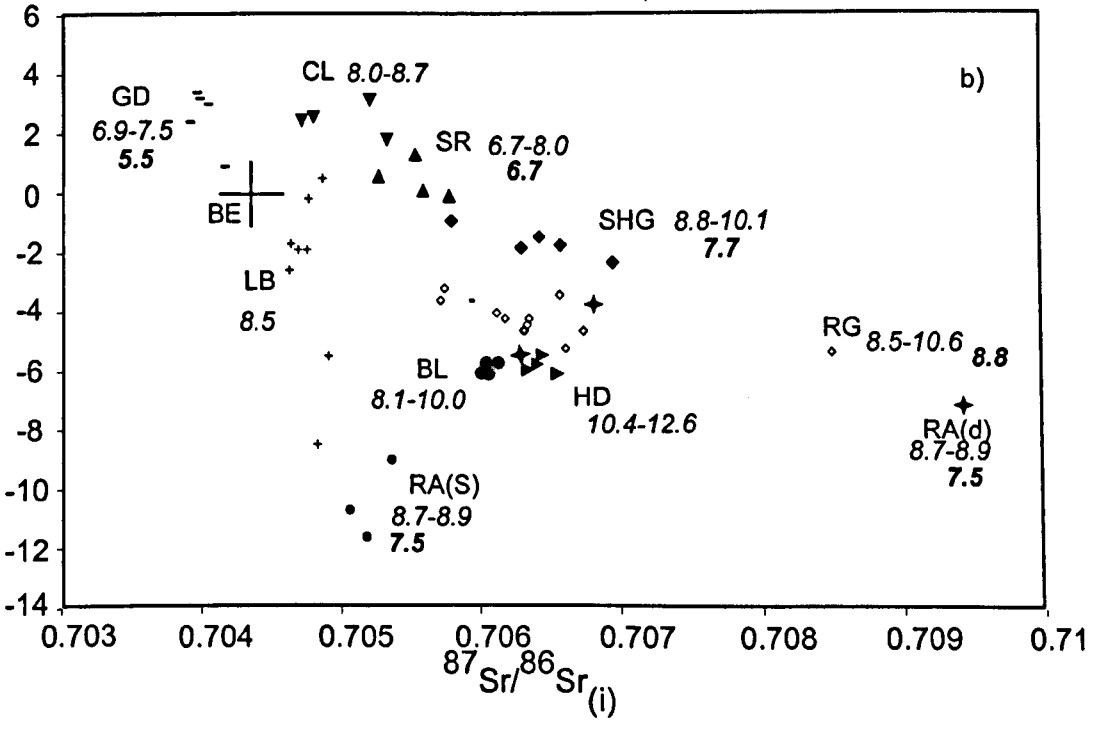

$\varepsilon Nd_{(t)}$

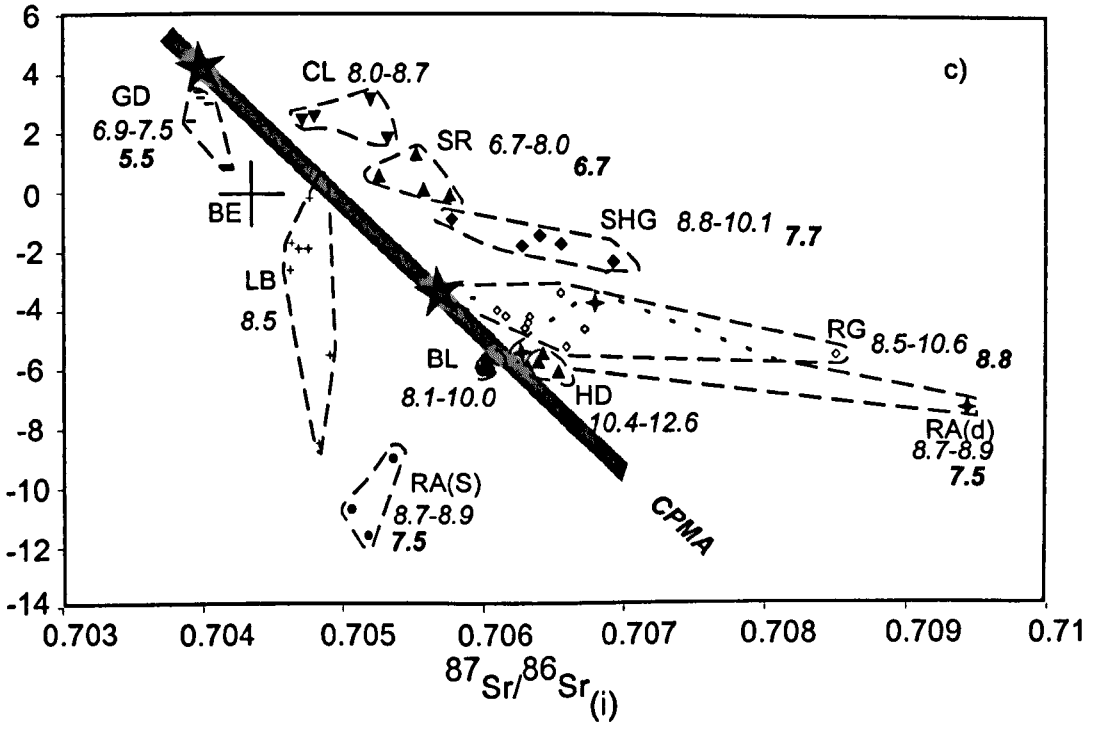

Table 5.2 New Sr, Nd and O isotope data from high Ba-Sr granitoids, Northern Highland Terrane.

Sample	Rocktype *	Rb	Sr	$^{87}Sr/^{86}Sr$	$^{87}Sr/^{86}Sr_i$	Sm	Nd	$^{143}Nd/^{144}Nd$	εNd_i	$\delta^{18}O$	Pluton / age
CL 9	g	62.9	901	0.705946	0.70472	2.29	10.6	0.512587	2.6	8.2	
CL 6	g	108	815	0.707118	0.70481	4.00	19.9	0.512567	2.7	8.7	Cluanie
CL 4	g	54.2	946	0.706212	0.70521	3.49	17.7	0.512587	3.2	8.0	425
SR 1	g	57.8	1102	0.706187	0.70527	6.27	40.4	0.512383	0.6	8.0	
SR 2	a	45.0	1042	0.706530	0.70577	14.0	77.2	0.512393	-0.1	6.7	Strontian
SR 3	g	45.6	1096	0.706317	0.70559	5.25	32.4	0.512371	0.1	7.8	425
SR 4	g	55.8	1023	0.706490	0.70554	5.41	32.7	0.512435	1.3	6.7	
SHG 450	u	13.0	258	0.706663	0.70579	2.64	11.1	0.512445	-0.9	7.1	
SHG 65	u	43.7	289	0.709052	0.70641	12.2	66.2	0.512329	-1.4	7.6	
SHG 403	d	70.2	187	0.707220	0.70657	6.19	55.7	0.512193	-1.7	8.3	Strath Halladale
SHG-c	g	68.1	710	0.707957	0.70628	2.46	17.7	0.512236	-1.8	10.1	423
SHG-132	g	71.6	691	0.2997	0.70506	2.30	14.3	0.512308	-1.1	8.76	
RD 1	d	86.4	2729	0.707487	0.70694	9.68	60.4	0.512244	-2.3	10.0	
RD 3	u	134	516	0.713686	0.70916	5.44	23.5	0.512293	-3.7	8.3	
DRR 207	d	66.4	2894	0.706710	0.70631	23.0	155	0.512061	-5.4	7.9	
DRR 206	d	32.1	3313	0.706973	0.70680	11.7	72.9	0.512173	-3.7	7.4	
DRR 213	d	54.0	9045	0.709536	0.70943	18.5	115	0.511991	-7.2	7.2	Ratagain
MS 405	s	62.0	2073	0.705930	0.70541	12.1	91.0	0.511854	-9.0	8.7	425
MS 434	g	76.0	1667	0.705920	0.70512	6.60	52.0	0.511756	-10.9	8.9	
SRR 653	g	64.3	1748	0.705825	0.70518	7.55	54.9	0.511730	-11.6	8.7	
OHG 810	g	140	641	0.710258	0.70646	4.85	34.0	0.512058	-5.4	10.7	
OHG 157	g	202	535	0.712958	0.70643	3.53	24.7	0.512041	-5.7	10.4	Helmsdale
IHG 837	g	152	514	0.711478	0.70636	4.89	34.8	0.512036	-5.8	12.6	420
IHG 317	g	185	680	0.711275	0.70657	4.40	30.0	0.512031	-6.0	11.4	
BL 1	s	77.9	1020	0.707408	0.70608	20.3	132	0.512048	-5.9	8.1	
BL 4	s	76.0	1946	0.706808	0.70612	26.9	190	0.512043	-5.6	8.2	
BLSE	s	105	1243	0.707546	0.70606	18.6	133	0.512037	-5.6	10.0	Ben Loyal
BL 9	s	81.3	1267	0.707153	0.70603	24.2	168	0.512028	-5.9	8.9	426
MS 390	s	87.0	1661	0.706980	0.70606	21.7	167	0.512009	-5.8	8.2	

* g = granite/granodiorite, d = diorite, s = syenite, a = appinite, u = ultramafic

process, but originating from systematically less enriched parental magmas (i.e. with lower initial $^{87}Sr/^{86}Sr$ and higher initial $^{143}Nd/^{144}Nd$) for Strath Halladale, Cluanie and Strontian granites and more enriched parental magmas for the Helmsdale Granite and the Ratagain diorite facies.

The elemental and isotopic data of the studied Caledonian high Ba-Sr granitoids have been discussed in sections 5.1 to 5.5 in terms of subduction-related generation, fractional crystallization, pre-emplacement differentiation and contamination, and it is clear that individual magmas have protracted histories. However, based on the characteristic multielement "high Ba-Sr" signature that unites all plutons and the systematic covariations of the isotope systems it is suggested that the broadly contemporaneous Caledonian syenites and granites may have been derived from similar mantle materials, underwent similarly extensive crystal fractionation, but were contaminated by different crust-derived materials *en route* to emplacement.

5.5.3.3 Parental magmas & source material(s)

The true nature of the ultimate source of the subduction-generated high Ba-Sr granitoids in the Northern Highland Terrane has been widely debated in previous case studies: Thompson & Fowler (1986) suggested an asthenospheric source containing back-mixed oceanic lithosphere, whereas Halliday *et al.* (1987) preferred a source in the subcontinental lithospheric mantle. Thirlwall & Burnard (1990) argued for a slightly enriched source for the Loch Borralan syenites (compared to Bulk Earth) which they compared to the source of the Lorne lavas, interpreted to be a sediment contaminated mantle source (Thirlwall 1986). Fowler (1992) added various possibilities of contaminated mantle (amphibolite facies Lewisian, Moine metasediments, Southern Uplands Lower Palaeozoic Sediments) for the depleted Glen Dessarry source and Fowler *et al.* (2001) pointed out the enriched, but unspecified character of the Rogart source.

However, it has been demonstrated above, that at least within the studied granite complexes detailed constraints on the ultimate source are sparse and in a recent study of the Lachlan fold belt granitoids, Keay *et al.* (1997) rightly comment that granitoids "reflect the chemistry of the parent magma ..... and generally do not image their source rocks". As these parental magmas may themselves be multicomponent mixtures (e.g. Collins 1996; Keay *et al.*1997) care should be taken in postulating ultimate sources. The systematic isotopic covariations inbetween the high Ba-Sr plutons of the Northern Highland Terrane

are therefore considered to (only) allow the definition of an array of parental magmas, here termed the Caledonian Parental Magma Array (CPMA, see Fig. 5.11c). It is defined by the converging isotopic trends and coincides with and contains the postulated "model sources" of Glen Dessarry and Loch Borralan (Fowler 1992; Thirlwall & Burnard 1990) at the depleted end, and with the "model sources" of Rogart and the Ach'Uaine appinites (Fowler *et al.* 2001; Fowler & Henney 1996) at the enriched end. Its extremes can be described by a depleted model parental melt with $^{87}Sr/^{86}Sr_i = 0.7040$, $\varepsilon Nd_i = +4.5$ and $\delta^{18}O = +6.0‰$ which is located on the back-extrapolations of the Cluanie and Glen Dessarry data, and a modelled, enriched parental melt with $^{87}Sr/^{86}Sr_i = 0.7062$, $\varepsilon Nd_i = -5.9$, and $\delta^{18}O = +8.5‰$ defined at the intersection of Helmsdale and Loch Loyal (Fig. 5.11c). Importantly, the Northern Highland lamprophyres, thought to represent rapidly-emplaced mantle-derived liquids, extend the CPMA further into the enriched quadrant ($^{87}Sr/^{86}Sr = 0.7075$, $\varepsilon Nd = -7$, and $\delta^{18}O = +9.5‰$ - Canning *et al.* 1996 and MBF unpub. $\delta^{18}O$ data). It needs to be stressed that this array merely represents the compositional field of parental magmas from which the high Ba-Sr granitoids appear to have evolved by AFC processes and is not considered equivalent to ultimate mantle sources.

5.5.3.4 Possible causes for the enrichment of the parental melts

The CPMA thus reconstructs variations in the mafic parental magmas of the Caledonian granitoids, which span from depleted (e.g. Glen Dessarry) to enriched (e.g. Rogart) (Fig. 5.11). Since there is a clear temporal association of the high Ba-Sr magmas with active subduction (Thirlwall 1988; Fowler 1988 a, b; 1992; Fowler *et al.* 2001), subduction-modified arc-source mantle is a suitable depleted end member. As time-integrated isotopic evolution of the depleted component over a period of *c.* 35 Ma (i.e. between the emplacement ages of Glen Dessarry and Helmsdale) cannot account for the observed enrichment in the CPMA, contamination is required to explain the enrichment of the parental melts. Fowler *et al.* (2001) argued that source-contamination was to be favoured over gross contamination with crustal sources such as Moine metasediment or Lewisian gneiss during ascent and emplacement as, in the Rogart case, there is a severe mismatch between the volume of contaminant required by the radiogenic isotopes (< 30%) and that which would satisfy the oxygen isotope data (>> 50%).

Heterogeneous enrichment of the subcontinental lithospheric mantle (SCLM), has been traditionally ascribed to fluid or melt percolation into normal mantle peridotite (e.g. Wilson

1989). With reference to Achaean TTG's, Tarney & Jones (1994) suggested that subduction and subsequent melting of enriched portions of the ocean crust (islands or plateaux), or mafic underplating with similar magmas that subsequently undergo hydrous melting could also account for the enrichment observed in the high Ba-Sr plutons. However, although both these latter hypotheses could produce the enriched high Ba-Sr signature, stable garnet or amphibole in the melting residue would produce depleted heavy REEs and Y (Defant & Drummond 1990; Drummond *et al.* 1996; Martin 1999) which has not been observed in the Caledonian high Ba-Sr granitoids or mafic rocks representing their parental melts.

The data presented in sections 5.1 to 5.4 show that the enriched component, i.e. the contaminant should posses high $\delta^{18}O$, high $^{87}Sr/^{86}Sr$, but low $^{143}Nd/^{144}Nd$, high Ba, Sr and light REE, which is most consistent with the incorporation of a sedimentary component. Pelagic sediments, for example, would be suitable as they commonly have enhanced Ba (in biogenic barite), Sr (in carbonate) and light REEs (Hole *et al.* 1984; Weaver 1991; Plank & Langmuir 1998) which thus could imprint the high Ba-Sr signature to the mantle source of the Caledonian Newer Granites and syenites (c.f. Harmon *et al.* 1984). Studies of modern subduction zones have used short-lived isotopic tracers like ^{10}Be (Tera *et al.* 1986; Morris & Tera 1989), ^{207}Pb (e.g. Kay *et al.* 1978; Miller *et al.* 1994), and major and trace element studies (e.g. Hole *et al.* 1984; Plank & Langmuir 1998) to show the significance of recycled sedimentary components in the petrogenesis of subduction-generated magmas. However, these studies have also demonstrated the great variety of contamination processes (e.g. summary in Clift *et al.* 2001).

The geochemical data and the elemental and isotopic variability observed in the high Ba-Sr plutons of the Northern Highland Terrane are consistent with heterogeneous recycling of a sedimentary-derived component ultimately contributing to the variably enriched parental high Ba-Sr melts. However, the present data cannot unequivocally identify the precise contaminant or the recycling process (fluid or melt percolation) in this *c.* 425Ma old calc-alkaline arc.

5.5.3.5 Regional and temporal isotopic variations

The products derived from isotopically-enriched (with respect to Sr_i) parental sources are presently located in a broad, orogen-parallel belt running from Ratagain to Loch Loyal and Helmsdale in the northeast that is wrapped by comparatively depleted (with respect to Sr_i) mantle-derived plutons in the far northeast (Strath Halladale), the west (Loch Borralan) and the southwest (Strontian, Cluanie and Glen Dessarry) (Fig. 5.12). This relative geographical disposition of isotopic signatures within the terrane remains intact despite any effects of post-emplacement fault movements and thrust stacking which may have modified this arrangement but cannot have reversed it. The observed distribution of depleted and enriched isotopic signatures within the terrane thus has no simple geographical control from the southwest to the northeast. Further, its complexity and the presence of plutons derived from depleted parental melts in the Northern Highland Terrane strongly argue against the simple regional model of an enriched Caledonian mantle domain that is separated from a depleted mantle domain underlying the Grampian Terrane by the Great Glen Fault (cf.Canning *et al.* 1998). There is also no straightforward temporal dependence, since although the oldest syenite (Glen Dessarry, 456 ± 5 Ma, van Breemen *et al.* 1979b) is derived from the most depleted parent (with respect to Sr_i)and the youngest (Loch Loyal, 426 ± 9 Ma, Halliday *et al.* 1987) from the most enriched (with respect to Sr_i), the two youngest granite plutons (Helmsdale and Cluanie, 425 to 420 Ma, Pidgeon & Aftalion 1978) stem from opposite ends of the CPMA. One possible solution to this temporal and spatial disposition is that the subcontinental (lithospheric) mantle actually comprises several adjacent cells/ domains that are variably enriched or depleted (e.g. Thompson & Fowler 1986) and from which the differing parental melts are randomly produced, sometimes contemporaneously. However, syenite emplacement spans a comparatively long time of *c.* 30 Ma whereas reliable emplacement ages of the granites range from *c.* 429 Ma (Clunes tonalite, Stewart *et al.* 2001) to *c.* 420 Ma (Helmsdale, Pidgeon & Aftalion 1978) and show a distinct plutonic peak at *c.* 425 Ma (Strontian, Cluanie, Ratagain, Rogart). The isotopically-diverse granitic plutonism thus marks a comparatively short period within the tectonomagmatic evolution of the Northern Highland Terrane (Fig. 5.13). It is therefore proposed that the variations observed in the isotopic record of the Caledonian granitoids of the Northern Highland Terrane are process-related and not geographically or temporally controlled. The syenites record progressive enrichment with respect to Sr_i (and a complementary depletion in Nd_i) in their source

regions underlying the Northern Highland Terrane during the subduction of the Iapetus ocean between *c.*456 Ma and *c.* 425 Ma that was followed by a comparatively short event during which isotopically diverse melts, generated from different source regions within the mantle wedge overlying the Iapetus subduction zone, were emplaced (Fig. 5.13).

Several mechanisms are capable of producing such a short lived, isotopically diverse and voluminous magmatic pulse have been discussed in the literature, including the delamination of orogenic roots (e.g. Bird 1978, 1979; Houseman *et al.* 1981; Nelson 1992), slab break-off (e.g. Davies & von Blanckenburg 1995; von Blankenburg & Davies 1995), or episodic emplacement of ponded magmas in response to changing tectonic regimes (e.g. Karlstrom 1989; Glazner 1991). Most of these have also been discussed within the late Caledonian context (e.g. Soper 1986; Whalen *et al.* 1994, 1996a; D'Lemos *et al.* 1997; Atherton 1999; Schofield & D'Lemos 2000; Atherton & Ghani 2002) and will be discussed in chapter 6.

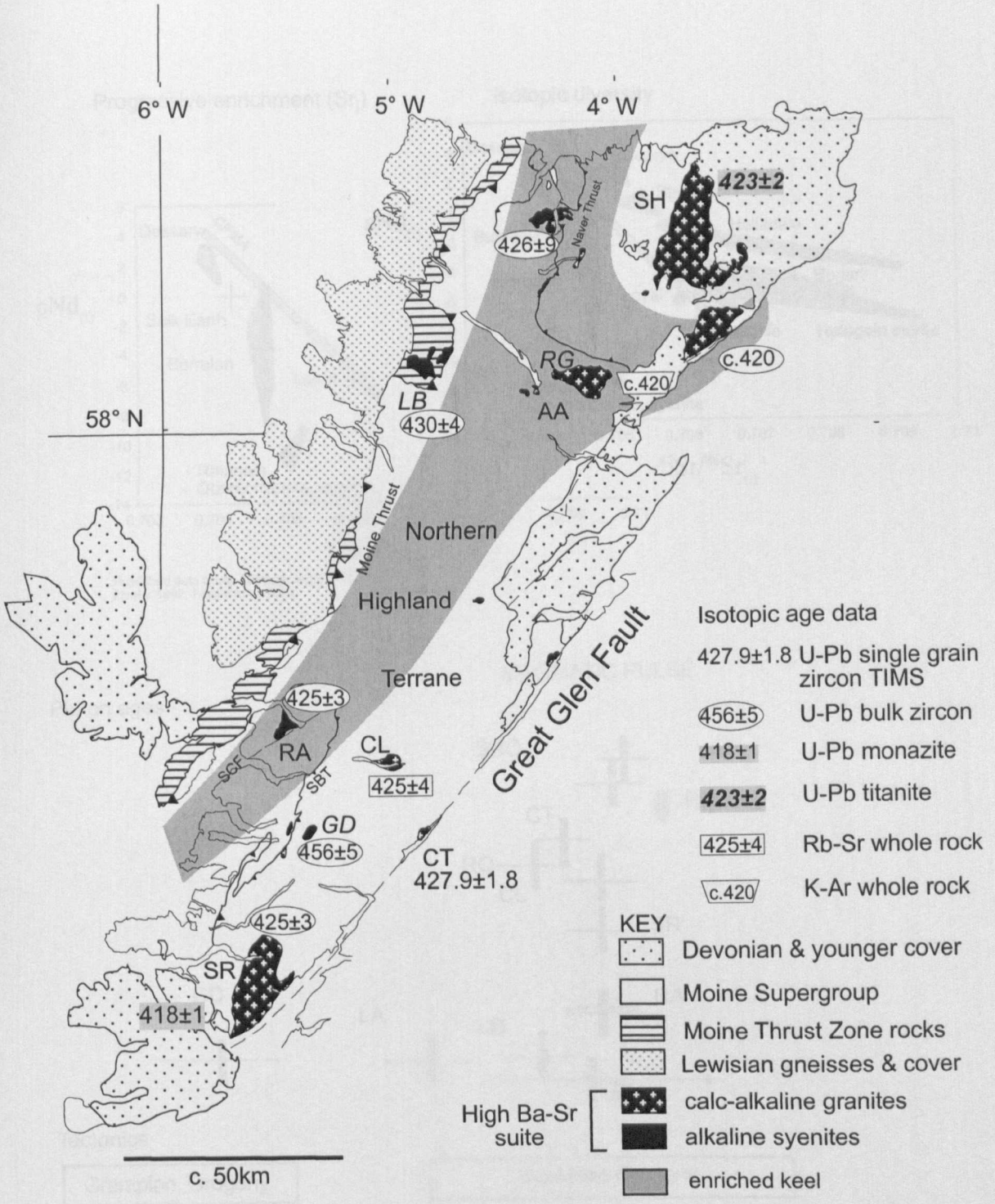

Fig. 5.12 Map showing the distribution of granitoids derived from enriched parental magmas (enriched keel) that are bounded by plutons derived from less enriched to depleted sources. Also shown are available isotopic ages for all complexes (table 1.2). SR = Strontian, GD = Glen Dessarry, CL = Cluanie, RA = Ratagain, LB = Loch Borralan, RG = Rogart, HD = Helmsdale, LL = Loch Loyal , SH = Strath Halladale, AA = Ach'Uaine.

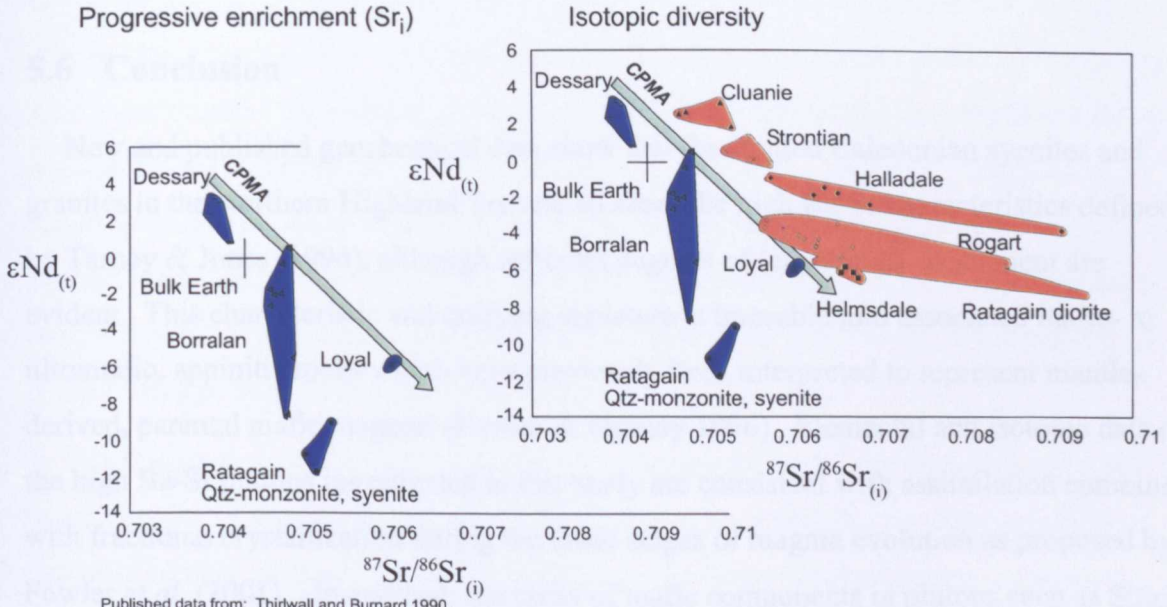

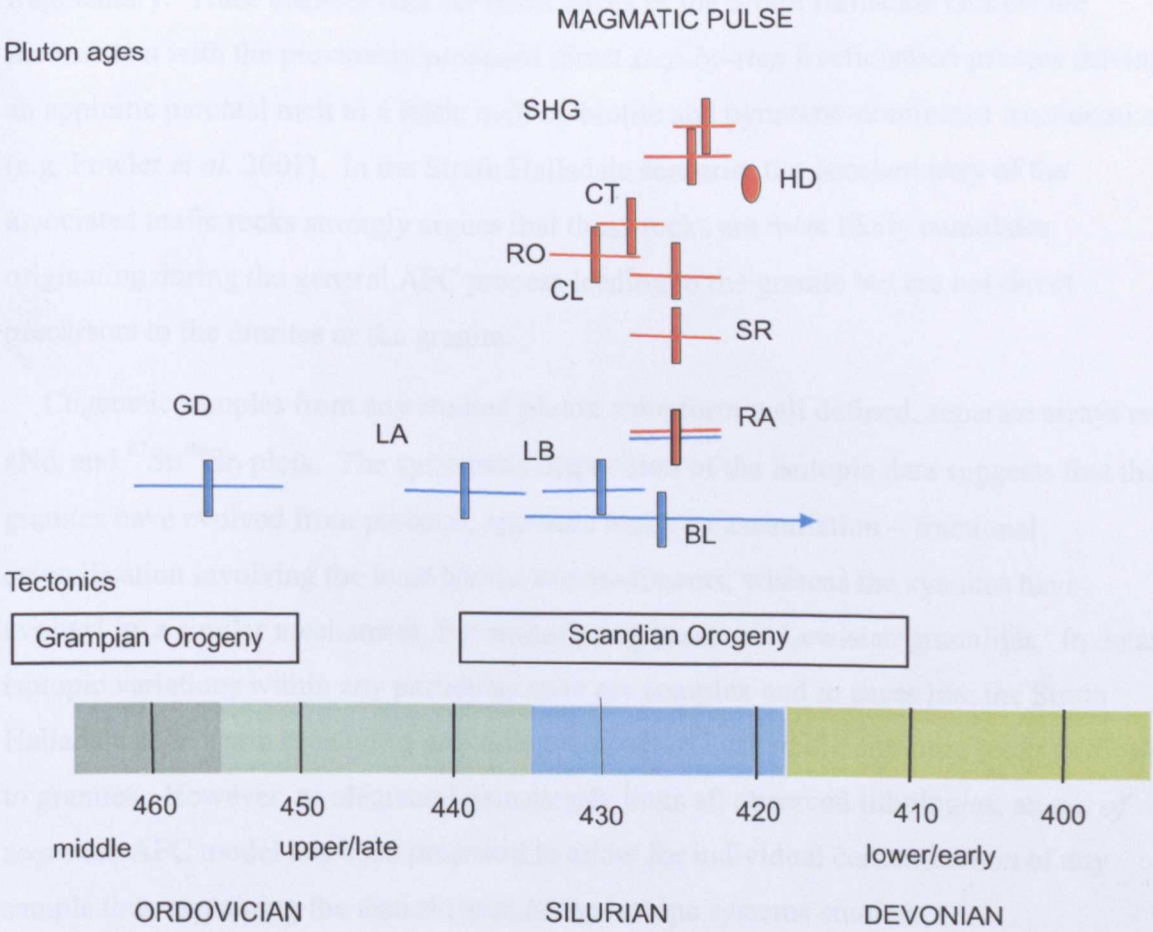

Fig. 5.13 Correlation diagram showing the mid Silurian magmatic pulse leading to great isotopic diversity in the Northern Highland high Ba-Sr granitoids. Age data see table 1.2.

5.6 Conclusion

New and published geochemical data show that the studied Caledonian syenites and granites in the Northern Highland Terrane all share the high Ba-Sr characteristics defined by Tarney & Jones (1994), although different degrees of (elemental) enrichment are evident. This characteristic and unifying signature is traceable into associated mafic- to ultramafic, appinitic rocks which have previously been interpreted to represent mantle-derived, parental mafic magmas (Fowler & Henney 1996). Elemental and isotopic data of the high Ba-Sr plutons investigated in this study are consistent with assimilation combined with fractional crystallization during the felsic stages of magma evolution as proposed by Fowler *et al.* (2001). In contrast, the rarity of mafic components in plutons such as Strath Halladale and Helmsdale granites renders the picture of early magma evolution fragmentary. Trace element data for mafic rocks of the Strath Halladale Granite are inconsistent with the previously proposed direct *step-by-step* fractionation process driving an appinitic parental melt to a felsic melt by biotite and pyroxene-dominated fractionation (e.g. Fowler *et al.* 2001). In the Strath Halladale scenario, the geochemistry of the associated mafic rocks strongly argues that these rocks are most likely cumulates originating during the general AFC process leading to the granite but are not direct precursors to the diorites or the granite.

Cogenetic samples from any studied pluton suite form well defined, separate arrays on εNd_i and $^{87}Sr/^{86}Sr_i$ plots. The systematic disposition of the isotopic data suggests that the granites have evolved from parental, appinitic melts by assimilation – fractional crystallisation involving the local Moine metasediments, whereas the syenites have evolved by a similar mechanism, but assimilating basement Lewisian granulites. In detail, isotopic variations within any particular suite are complex and in cases like the Strath Halladale suite again preclude a sequential derivation from mafic appinitic rocks to diorites to granites. However, as elemental data clearly links all observed lithologies, an *out of sequence* AFC model has been proposed to allow for individual contamination of any sample thus explaining the disturbances of the isotope systems studied.

The Caledonian granitoids have been interpreted to reflect their parental magmas which form a Caledonian Parental Magma Array (CPMA) extending from depleted to significantly enriched compositions (with respect to Sr_i), with high $\delta^{18}O$ in the latter.

Given the long-lived, subduction-related setting of the Palaeozoic Laurentian margin, it is proposed that the depleted source component is likely to have been subduction-modified arc-source mantle. Time-integrated closed-system evolution of this end member cannot account for the observed enrichment. Thus, in keeping with previously published mass balance considerations (Fowler *et al.* 2001), the significance of possible source contaminants has been investigated. Data produced during this study are most consistent with a recycled sedimentary component contaminating the high Ba-Sr source but the precise identification of the enrichment process is not possible.

The distribution of isotopic signatures of granitoids derived from enriched and depleted parental melts in the Northern Highland Terrane has no straightforward geographical or temporal control. Instead, it is proposed that the syenites record progressive mantle enrichment over *c.* 30 Ma, whereas the granites were derived from isotopically diverse mantle domains and emplaced in a short time interval at *c.* 425 Ma. Several tectono-magmatic processes such as slab break-off, delamination of orogenic roots and plume activity are capable of producing such a short-lived, isotopically diverse pulse.

Part C

Summary of conclusions and regional significance of the study

Chapter 6

Summary of conclusions and regional significance of the study

6 Summary of conclusions and regional significance of the study

6.1 Introduction

This study has investigated the structural geology, fabric development and emplacement of the Rogart, Strath Halladale and Helmsdale granites in Sutherland, Scotland (Fig. 6.1). A regional elemental and isotopic study has been carried out across the Northern Highlands Terrane and confirmed that the Strontian, Cluanie, Strath Halladale and Helmsdale granites as well as the Ratagain complex and the Loch Loyal syenites are part of the Caledonian high Ba-Sr suite (*sensu* Tarney & Jones 1994). Against this regional background, the petrogenesis of the lithologically restricted Strath Halladale and Helmsdale granites was investigated in detail.

6.2 Granite emplacement – implications for Caledonian tectonics in Sutherland

The studied plutons contain structural features that allow them to be assigned a relative age with respect to the main phase of Caledonian deformation, that in the study area is of a D2 age (e.g. McCourt 1980; Strachan & Holdsworth 1988, Strachan 1988). The sequence of intrusion has been established as: Strath Halladale (syn-D2-thrusting), Rogart (late syn-D2-thrusting to transcurrent faulting), Helmsdale (post-D2, possibly post-D4).

6.2.1 Strath Halladale

The Strath Halladale Granite was emplaced as a series of sheets into the Moine metasediments of northeastern Sutherland, and structurally lies in the *eastern belt* of the Naver Nappe (Fig. 6.1). The pluton is intruded between two major tectono-stratigraphic units, the migmatitic Loch Coire Formation and the generally non-migmatitic Scaraben Succession. The migmatization of the Moine rocks assigned to the Loch Coire Formation occurred during a pre-D2 event (D1/M1) that is tentatively correlated with a high pressure melting event between 470-460 Ma identified at Kirtomy Point (Kinny *et al.* 1999) and Strathnaver (Friend *et al.* 2000).

The granite was emplaced late during D2 deformation after the initial formation of the $S_0S_1S_2$ host rock fabric and contains magmatic-state shear zones that consistently record top-to-the-NW-to-W directed movements. W-to-NW directed thrusting and ductile

deformation of the host rocks occurred under sillimanite grade, amphibolite facies conditions. Available evidence is consistent with the existence of a ductile thrust to the east of the Strath Halladale Granite that possibly coincides with the Loch Coire Formation-Scaraben Succession boundary. Thrust-related emplacement of the Strath Halladale Granite is thus a likely mechanism and the structurally highest part of the Naver Nappe may therefore form a previously unrecognised thrust sheet.

Deformation in adjacent areas to the west has lately been attributed to the Grampian (the *central belt*, Kinny *et al.* 1999) and Scandian (the *western belt* and Moine Nappe – Alsop *et al.* 1996; Kinny *et al.* in press) orogenic episodes (Fig. 6.1). This study has shown that deformation trajectories during ductile D2 deformation and the syn-tectonic emplacement of the Strath Halladale Granite into Moine rocks of the *eastern belt* may have been complex, comparable to deformation trajectories in the *western belt* and the Moine Nappe (Alsop *et al.* 1996). The precise intrusion age of the Strath Halladale Granite is unknown. However, a titanite age of 423±2Ma (Rogers, G. pers. comm. 2000) is interpreted to reflect post emplacement cooling and assigns D2 deformation and fabric development in the *eastern belt* of the Naver Nappe to the Scandian event. D2 in the *eastern belt* is therefore c.40Ma younger than D2 deformation in the *central belt* (e.g. Kinny *et al.* 1999) but contemporaneous with D2 deformation in the *western belt* and the Moine Nappe (Kinny *et al.* in press; Fig. 6.1).

6.2.2 Rogart

The Rogart igneous complex was emplaced into the Moine metasediments of SE Sutherland that comprise Morar Group rocks and Naver Nappe gneisses, which are separated by the Naver Thrust. It is located in the footwall of the Naver Thrust (Fig. 6.1) which is locally steepened by pluton-related deformation. Microstructures and field relationships indicate that a series of quartz monzodiorite sheets of the igneous complex were emplaced during regional D2 W-directed thrusting, whereas the central quartz monzodiorite-granodiorite-granite complex was most likely emplaced by a combination of dextral shear along the Strath Fleet lineament and ballooning. The pluton is thus not post-tectonic with respect to late Caledonian deformation nor is diapirism considered a major pluton emplacement mechanism as has been previously proposed (cf. Soper 1963, 1999). A *preliminary* U-Pb age of *431 ±4 Ma* for the central complex (U-Pb zircon & monazite TIMS, small fractions of 5 grains, J. Evans pers. comm. 07/2002) indicates that in SE Sutherland, the switchover from W-directed compression to sinistral transpression

(e.g. Soper *et al.* 1992) occurred during the middle Silurian. The doming of the Assynt culmination and W-directed movements in the Moine Thrust Zone c. 50km to the west of the Rogart complex were completed by this time.

6.2.3 Helmsdale

The Helmsdale Granite was intruded into the Moine metasediments of eastern Sutherland in the structurally highest part of the *eastern belt* of the Naver Nappe (Fig. 6.1). The timing of emplacement of the Helmsdale Granite with respect to regional deformation is not well constrained. It post-dates D2-deformation and is possibly post-tectonic with respect to all Caledonian deformation. As the pluton is bounded by the Helmsdale Fault for which a Caledonian strike-slip history has been envisaged (Watson 1984; Stewart *et al.* 1997), pluton emplacement may have been assisted by Caledonian transcurrent movements. However, as the high-level pluton shows no deformation fabrics this role of the Helmsdale Fault remains speculative. The intrusion age of the granite is to date imprecisely defined as c. 420 Ma (U-Pb zircon Pidgeon & Aftalion 1978) and is taken to identify an upper age limit for Caledonian deformation.

6.2.4 Regional correlations

The isotopic ages produced in conjunction with this study combined with the newly established syn-tectonic status of the Strath Halladale and Rogart granites provide new evidence for Silurian D2 deformation during the Scandian orogeny in eastern Sutherland (Fig. 6.1). The new data further support evidence for Scandian thrusting documented in central Sutherland (Kinny *et al.* in press) and are consistent with earlier views of a westward propagating, kinematically linked Caledonian thrust system (Barr *et al.* 1986; Butler 1986). However, the correlation of deformation events between Sutherland, Ross-shire and Inverness-shire remains difficult, as Caledonian D2 deformation and associated metamorphism in the Morar, Glenfinnan and Loch Eil groups of Inverness-shire is currently believed to be of Ordovician age (e.g. van Breemen *et al.* 1974, Brewer *et al.* 1979; Rogers *et al.* 2001). This could be viewed as a large-scale analogue of the *central belt* of the Naver Nappe that forms a Scandian low-strain domain within Sutherland, or alternatively the structural interpretation of dated pegmatites of Inverness-shire (van Breemen *et al.* 1974) may require re-investigation.

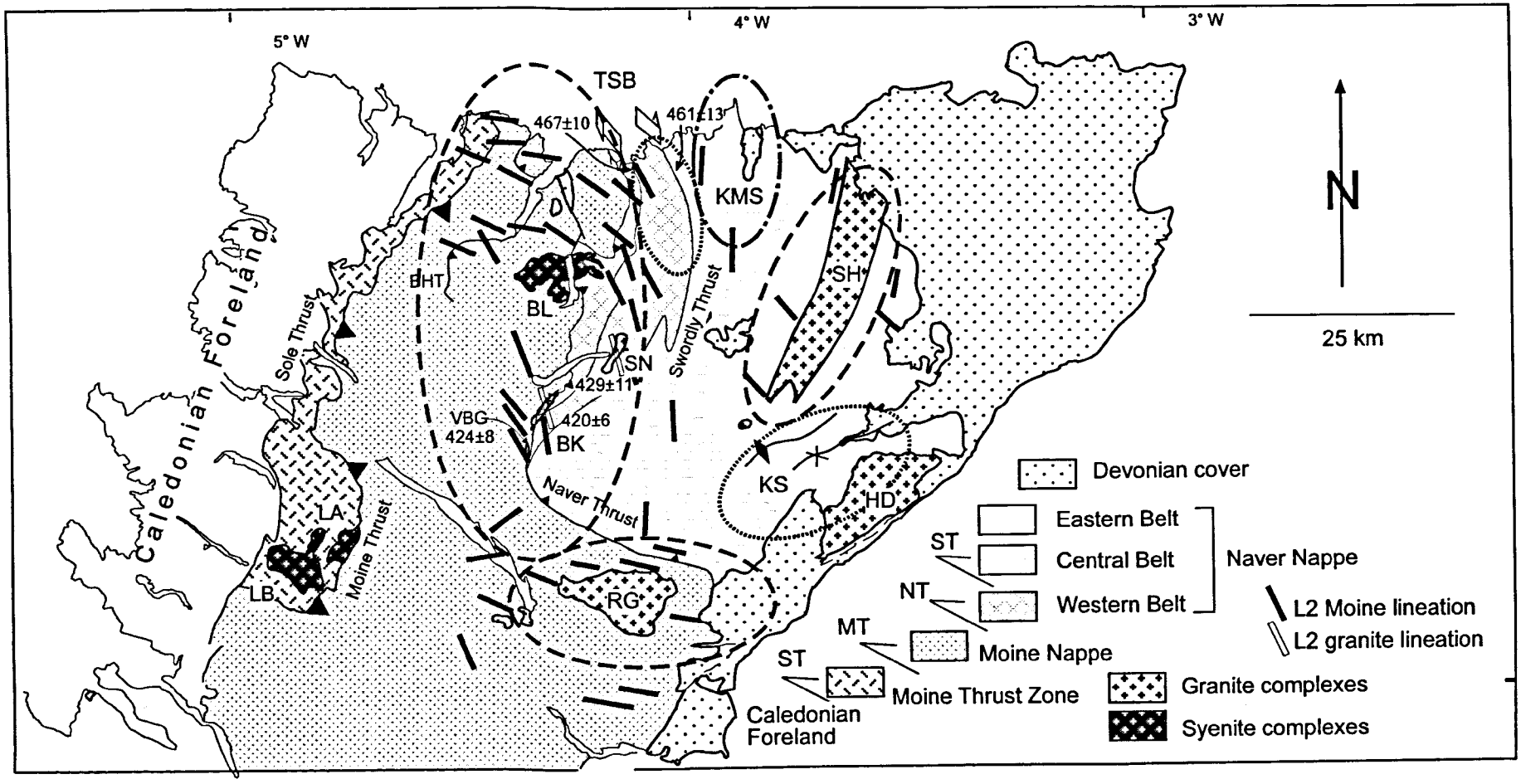

Fig. 6.1 Structural domains of Sutherland showing areas dominated by Scandian D2 deformation (dashed ellipses) , Scandian D3 deformation (dotted ellipses) and Grampian D2 deformation (dashed-dotted ellipses). Compiled from Strachan & Holdsworth 1988, Holdsworth & Strachan 1988, Holdsworth 1990, Burns 1994; Alsop *et al.* 1996, Kinny *et al.* 1999; Friend *et al.* 2000; Kinny *et al.* in press and this study. RG= Rogart granite, SH= Strath Halladale granite, HD= Helmsdale granite, TSB= Torrisdale Steep Belt, KMS = Kirtomy migmatite suite, KS = Kildonan Synclinorium.

6.3 Geochemistry – implications for Caledonian high Ba-Sr magmatism

6.3.1 Extent of high Ba-Sr magmatism in the Northern Highlands Terrane

New elemental whole rock data produced in this study confirm that the Cluanie, Ratagain, Helmsdale, Strath Halladale, and Loch Loyal plutons and the previously described Strontian (Pankhurst 1979), Loch Borralan (Thirlwall & Burnard 1990), Glen Dessarry (Fowler 1992) and Rogart plutons (Fowler *et al.* 2001) belong to the Caledonian high Ba-Sr suite (sensu Tarney & Jones 1994) in the Northern Highlands Terrane. Major element chemistry identifies well-defined, separate fractionation trends for syenite-dominated and granite-dominated complexes, respectively. REE patterns and spiderdiagrams not only demonstrate a genetic relationship of all studied plutons but also show that the syenites generally seem to be elementally more enriched than comparable granites. Radiogenic and stable isotopes show systematic variations throughout the suite. Plutons with the highest initial $^{87}Sr/^{86}Sr$ have the lowest initial εNd and the highest $\delta^{18}O$, whereas plutons with lower initial $^{87}Sr/^{86}Sr$ have complementary higher $\varepsilon Nd_{(i)}$ and lower $\delta^{18}O$. Overall this suggests that all studied high Ba-Sr plutons were derived from comparable parental magmas by comparable but varied melt evolution processes (see below).

6.3.2 Fractionation mechanisms

Previous case studies have shown that the characteristic and unifying high Ba-Sr signature of the granitoids is traceable into associated mafic to ultramafic appinitic rocks that have been interpreted to represent their mantle-derived, parental mafic magmas (Fowler 1992; Fowler & Henney 1996; Fowler *et al.* 2001). A two-stage AFC model involving early mafic and subsequent felsic crystallizing assemblages has been previously described as the main evolutionary process of the high Ba-Sr magmas (Fowler 1992; Fowler *et al.* 2001). For all plutons studied, the newly produced geochemical data are consistent with the evolution of the intermediate to felsic magmas by accessory-rich, feldspar-dominated crystal fractionation as previously proposed (e.g. Fowler 1992; Fowler & Henney 1996; Fowler *et al.* 2001). However, in some instances (e.g. Strath Halladale), it has not been possible to link associated mafic rocks to the high Ba-Sr granites using the previously described fractionation scheme. The new elemental and isotopic data thus preclude the definition of a universal, simple "step-by-step" AFC mode for the entire suite. Locally (e.g. Strath Halladale, Cluanie) the new isotopic data favour an "out of sequence"

AFC mode by which individual batches of magma may separate from a fractionating parent and become contaminated individually en route to emplacement. Notwithstanding this internal complexity, isotopic data for individual plutons define well-constrained and characteristic arrays on $\varepsilon Nd_{(i)}$-$^{87/86}Sr_{(i)}$-$\delta^{18}O$ correlation diagrams. The disposition of these arrays suggests that the granites have evolved from the parental, appinitic melts by AFC involving the local Moine metasediments, whereas the syenites have evolved by a similar mechanism, but assimilating basement Lewisian granulites.

6.3.3 Isotopic implications for parental melts

The Caledonian granitoids reflect their parent magmas and the characteristic $\varepsilon Nd_{(i)}$-$^{87/86}Sr_{(i)}$-$\delta^{18}O$ arrays described above allow the definition of a Caledonian Parental Magma Array (CPMA) extending from depleted to significantly enriched compositions, with high $\delta^{18}O$ in the latter. Given the long-lived, subduction-related setting of the Palaeozoic Laurentian margin and its temporal coincidence with high Ba-Sr magmatism (e.g. Thirlwall 1988, Fowler 1988a, 1992), the depleted component is likely to have been derived from subduction-modified arc-source mantle. However, time-integrated closed system evolution of a depleted parental reservoir cannot account for the observed enrichment and thus a contamination process is required. Following Fowler *et al.* (2001), the nature of a possible source contaminant has been investigated using new and published data. Although this study cannot unambiguously prove the nature of the contaminant or delineate the precise enrichment process, new and published data require the contaminant to have high $^{87}Sr/^{86}Sr_i$, low $^{143}Nd/^{144}/Nd_i$, high $\delta^{18}O$, high Ba, Sr and light REE. A contaminant derived from pelagic sediment is most consistent with this.

6.3.4 Spatial and temporal variations of Caledonian high Ba-Sr isotopic signatures

The distribution of granitoids derived from enriched parental melts form a central, orogen-parallel belt that is bordered to the west and north by plutons derived from comparatively depleted parents. There is therefore no straightforward south-to-north geographical control over the enrichment signature within the Northern Highland Terrane. Neither is there a straightforward time dependence as contemporaneous plutons such as Helmsdale and Cluanie occupy opposite positions in the $\varepsilon Nd_{(i)}$-$^{87/86}Sr_{(i)}$-$\delta^{18}O$ isotope covariation diagrams. However, combining available age data with the observed isotope systematics suggests, that the syenites record progressive (source) enrichment over c. 30 Ma followed by a short isotopically diverse, magmatic pulse at c. 425 Ma.

6.3.5 Caledonian high Ba-Sr magma generation

The petrogenesis of the Scottish calc-alkaline and alkaline suites as a whole has been addressed in models of continuous subduction (e.g. Thompson & Fowler 1986; Thirlwall 1988; Thirlwall & Burnard 1990; Fowler 1992; Fowler *et al.* 2001) and Andean style batholith formation (Oliver 2001). However, these continuum models for syn-orogenic, subduction-related Caledonian magmatism are difficult to reconcile with the newly-discovered, systematic isotopic variability and the established episodic timing of granitic plutonism in the Northern Highlands Terrane. Nonetheless, pluton emplacement is often controlled by active deformation and changes of tectonic regime (e.g. Karlstrom 1989; Glazner 1991), and in the northern Highlands, the change from west-directed compression to sinistral transpression coincides with the observed plutonic pulse at c. 425 Ma. Thus continuously-generated magmas may have ponded at the base of the crust only to be emplaced when deformation allowed, therefore resembling episodic magma generation.

Alternative approaches to explain short lived, syn-orogenic magmatism may lie in tectonically induced processes such as crustal delamination of thickened orogenic roots (e.g. Bird 1978, Houseman *et al.* 1981, Nelson 1992), or slab break-off (e.g. Davies & von Blanckenburg 1995; von Blanckenburg & Davies 1995) and have been discussed within the late Caledonian context (e.g. Soper 1986; Whalen *et al.* 1994, 1996a; D'Lemos *et al.* 1997; Atherton 1999; Schofield & D'Lemos 2000; Atherton & Ghani 2002). The absence of exhumed lower crustal rocks or wholesale lower crustal melting in the Northern Highland Terrane suggest that delamination of a thickened orogenic root following continent-continent collision is an unlikely explanation for the late Caledonian magmatism. The slab-breakoff alternative has recently been promoted by Atherton & Ghani (2002) as *the* unifying model to explain *all* late Caledonian magmatism in the British Caledonides. It is appropriate to test the validity of this wholesale approach in the light of the new data presented here.

In studies from the Alps, Davies & von Blanckenburg (1995) and von Blanckenburg & Davies (1995) have shown that slab breakoff may have provided a short-lived thermal instability in the lithospheric mantle, capable of generating a wide spectrum of melts about 5-10 Ma after continent collision. The time gap of c. 10 Ma between collision and magma generation reflects an estimate for the time necessary for the subduction system to lock up and to initiate slab detachment. The magmatic pulse in the Northern Highlands Terrane occurred at c.425 Ma, therefore any causal collision to this pulse must have occurred at least 10 Ma earlier. In published models, the Scottish terranes have been located in the

collision zone between Avalonia and Laurentia (e.g. Soper *et al.* 1992). Although initial soft docking between Avalonia and the Scottish segment of Laurentia may have occurred during the Silurian, convergent movements occurred until the early Devonian (e.g. Thirlwall 1988; Oliver 2001). If slab-pull drives subduction systems and deformation in the overriding plate (e.g. Bott 1993), the northward subducting slab attached to Avalonia cannot have been detached prior to the latest phase of compressional deformation. A slab breakoff in this palaeogeographic context therefore most likely post-dates the observed magmatic pulse in the Northern Highland Terrane and thus cannot explain it.

Recently, it has become increasingly clear that the dominant ductile deformation in the Northern Highlands Terrane is of Scandian age, i.e. Silurian (e.g. Kinny *et al.* in press) whereas the majority of deformation fabrics in the Grampian Terrane are of Grampian age, i.e. Ordovician (e.g. Oliver 2001). Conversely, Caledonian deformation in Scandinavia and Eastern Greenland is thought to be of Late Ordovician to Early Silurian age (e.g. Hartz *et al.* 2001; Anderson *et al.* 1992– see Fig. 6.2). Further, there still is considerable uncertainty surrounding late Caledonian, sinistral movements along the Great Glen Fault (e.g. Coward 1990; Stewart *et al.* 1997, 2000). Overall, it is therefore entirely possible that during the Silurian the Northern Highlands Terrane was situated in between Laurentia and Baltica (Fig. 6.2). Published data for ductile deformation in these terranes (e.g. Anderson *et al.* 1992; Hartz *et al.* 2001; Kinny *et al.* in press) indicates that a slab breakoff on the Scandinavia-Greenland segment of the Caledonian belt could have occurred as early as c. 435-440 Ma and therefore could have induced a diverse magmatic pulse in the Northern Highlands Terrane at c.425Ma. However, the precise timing of compressional Caledonian deformation even within the Northern Highlands Terrane is not agreed (see table 1.1) and the matter is far from resolved.

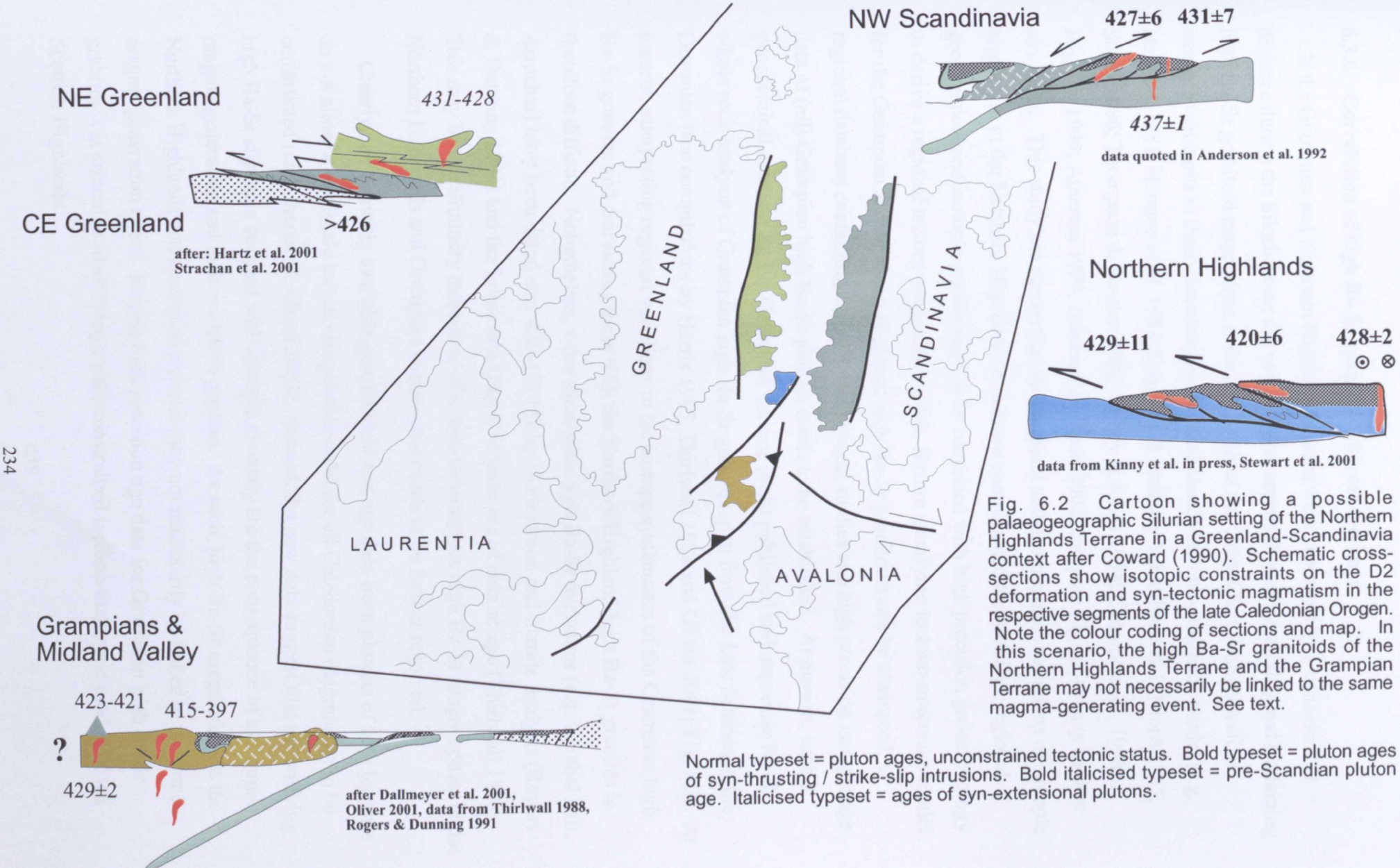

Fig. 6.2 Cartoon showing a possible palaeogeographic Silurian setting of the Northern Highlands Terrane in a Greenland-Scandinavia context after Coward (1990). Schematic cross-sections show isotopic constraints on the D2 deformation and syn-tectonic magmatism in the respective segments of the late Caledonian Orogen. Note the colour coding of sections and map. In this scenario, the high Ba-Sr granitoids of the Northern Highlands Terrane and the Grampian Terrane may not necessarily be linked to the same magma-generating event. See text.

Normal typeset = pluton ages, unconstrained tectonic status. Bold typeset = pluton ages of syn-thrusting / strike-slip intrusions. Bold italicised typeset = pre-Scandian pluton age. Italicised typeset = ages of syn-extensional plutons.

6.3.6 Correlation of high Ba-Sr granitoids across terranes

If the Grampian and Northern Highland terranes were separated by a considerable distance during the Silurian (see above), previous approaches of classifying and explaining high Ba-Sr granitoid magmatism north and south of the Great Glen Fault as well as isotopic variations in their source regions in a wholesale tectono-magmatic model (e.g. Halliday 1984; Harmon *et al.* 1984; Stephens & Halliday 1984; Frost & O'Nions 1985; Soper 1986; Thompson & Fowler 1986; Tarney & Jones 1994; Canning *et al.* 1998; Highton 1999; Atherton 1999; Atherton & Ghani 2002, compare Fig. 1.10) may be over simplistic. This study has shown that the temporal and geographical variations of isotopic signatures in the Northern Highland Terrane are complex and that detailed, regional geochemical and isotopic studies need to be combined with high precision geochronology to derive a regional tectono-magmatic model. Before a unifying tectono-magmatic model for the Grampian and Northern Highland high Ba-Sr granitoids can be attempted, a regional database containing detailed geochemical studies and high precision isotopic age data of (all) Grampian high Ba-Sr plutons needs to be established. At present, such a geochemical database for the Grampian Terrane is not published and imprecise Rb-Sr whole rock analysis of Grampian high Ba-Sr granites span from the Late Silurian to the Devonian (see compilations by Harris 1985, Thirlwall 1988 and Oliver 2001; Fig. 6.2). At present, interpreting regional variations in the isotope systematics of the Grampian high Ba-Sr granites and correlating these with the Northern Highland high Ba-Sr granites is therefore difficult. Nonetheless, a few Grampian high Ba-Sr intrusions (e.g. Garabal Hill, Arrochar) have been dated at c. 426-429 Ma by U-Pb zircon and titanite analysis (Rogers & Dunning 1991) and the Lorne and Glen Coe lavas are of similar age (Thirlwall 1988). This may be a preliminary indication of a contemporaneous high Ba-Sr magma pulse in the Northern Highlands and Grampian terranes but needs to be further resolved.

Clearly, the currently available geochemical and age data from plutons of both terranes do not allow a wholesale tectono-magmatic model for all Caledonian magmatism to be constructed (cf. Atherton & Ghani 2002). Instead, the new data suggest that the unifying high Ba-Sr signature coupled with isotopic diversity are the consequence of a common magma generation and melt evolution process. As such, high Ba-Sr magmatism in the Northern Highlands and Grampian terranes may not necessarily be linked to the same magma generation event. Further high precision age data for Grampian high Ba-Sr granitoids is critical in identifying a well-constrained tectono-magmatic model for the Scottish Highlands.

Aftalion, M. & Van Breemen, O. 1980. U—Pb zircon, monazite and Rb—Sr whole-rock systematics of granitic gneiss and psammitic to semipelitic host gneiss from Glenfinnan, northwestern Scotland. *Contributions to Mineralogy and Petrology,* **72,** 87-98.

Aftalion, M., Van Breemen, O. & Bowes, D. R. 1984. Age constraints on the basement of the Midland Valley of Scotland. *Transactions of the Royal Society of Edinburgh* **77,** 53-64.

Aitchison, J. 1986. The statistical analysis of compositional data. Methuen, New York.

Allègre, C. J. & Minster, J. F. 1978. Quantitative models of trace element behaviour in magmatic processes. *Earth and Planetary Science Letters* **38,** 1-25.

Alsop, G. I. & Holdsworth, R. E. 1993. The distribution, geometry and significance of Caledonian buckle folds in the western Moine Nappe, northwestern Scotland. *Geological Magazine* **130,** 353-362.

Alsop, G. I., Holdsworth, R. E. & Strachan, R. A. 1996. Transport-parallel cross folds within a mid-crustal Caledonian thrust stack, northern Scotland. *Journal of Structural Geology* **18**(6), 783-790.

Anderson, M. W., Barker, A.J., Bennett, D.G. & Dallmeyer, R. D. 1992. A tectonic model for Scandian terrane accretion in the northern Scandinavian Caledonides. *Journal of the Geological Society of London* **149,** 727-741.

Anderton, R. 1982. Dalradian deposition and the late Precambrian-Cambrian history of the N Atlantic region; a review of the early evolution of the Iapetus Ocean. *Journal of the Geological Society of London* **139**(4), 421-431.

Anderton, R. 1985. Sedimentation and tectonics in the Scottish Dalradian. *Scottish Journal of Geology* **21**(4), 407-436.

Armstrong, H. A., Owen, A. W., Scrutton, C. T., Clarkson, E. N. K. & Taylor, C. M. 1996. Evolution of the Northern Belt, Southern Uplands: implications for the Southern Uplands controversy. *Journal of the Geological Society of London* **153,** 197-205.

Armstrong, H. A. & Owen, A. W. 2001. Terrane evolution of the paratetconic Caledonides of northern Britain. *Journal of the Geological Society of London* **158** (3), 475-486.

Arth, J. G. 1976. Behaviour of trace elelments during magmatic processes – a summary of theoretical models and their applications. *Journal of Research, U.S. Geological Survey* **4,** 41-47.

Arzi, A. A. 1978. Critical phenomena in the rheology of partially melted rocks. *Tectonophysics* **44,** 173-184.

Atherton M. P. 1999. Slab breakoff: A consistent model for Caledonian late granite magmatism in the British Isles. In: *The origin of granites and related rocks.* 4th Hutton Symposium, Clermont-Ferrand, France.

Atherton, M. P. & Ghani, A.A. 2002. Slab breakoff: a model for Caledonian, late-granite syn-collisional magmatism in the orthotectonic (metamorphic) zone of Scotland and Donegal, Ireland. *Lithos* **62** (2-3), 65-85.

Bailey, E.B. 1960. *Geology of Ben Nevis and Glencoe.* Memoir of the Geological Survey of Great Britain (2nd edition).

Barber, A. J. & May, F. 1976. The history of the western Lewisian in the Glenelg Inlier, Lochalsh, northern Highlands. *Scottish Journal of Geology* **12**(1), 35-50.

Barr, D., Holdsworth, R. E. & Roberts, A. M. 1986. Caledonian ductile thrusting in a Precambrian metamorphic complex; the Moine of northwestern Scotland. *Geological Society of America Bulletin* **97**(6), 754-764.

Bateman, R. 1984. On the role of diapirism in the segregation, ascent and final emplacement of granitoids. *Tectonophysics* **10,** 211-231.

Bird, P. 1978. Initiation of intracontinental subduction in the Himalaya. *Journal of Geophysical Research* **84**, 4975-4987.

Bird, P. 1979. Continental delamination and the Colorado Plateau. *Journal of Geophysical Research* **84**, 7561-7571.

Bluck, B. J. 1983. Role of the Midland Valley of Scotland in the Caledonian Orogeny. *Transactions of the Royal Society of Edinburgh: Earth Sciences* **74**(3), 119-136.

Bluck, B. J.. 1984. Pre-Carboniferous history of the Midland Valley of Scotland. *Transactions of the Royal Society of Edinburgh* **75** (2), 275-295.

Bluck, B. J. 1985. The Scottish paratectonic Caledonides. *Scottish Journal of Geology* **21**(4), 437-464.

Bluck, B J. 2001. Caledonian and related events in Scotland. *Transactions of the Royal Society of Edinburgh: Earth Sciences* **91**, 375-404.

Bluck, B. J. & Leake, B. E. 1986. Late Ordovician to Early Silurian amalgamation of the Dalradian and adjacent Ordovician rocks in the British Isles. *Geology* **14**(11), 917-919.

Bluck, B. J. & Dempster, T. J. 1991. Exotic metamorphic terranes in the Caledonides; tectonic history of the Dalradian Block, Scotland. *Geology* **19**(11), 1133-1136.

Bluck, B. J., Dempster, T. J. & Rogers, G. 1997. Allochtonous metamorphic blocks on the Hebridean passive margin, Scotland. *Journal of the Geological Society of London* **154**, 921-924.

Bluck, B. J., Halliday, A. N., Aftalion, M. & Macintyre, R. M. 1980. Age and origin of Ballantrae ophiolite and its significance to the Caledonian Orogeny and Ordovician time scale. *Geology* **8**(10), 492-495.

Bluck, B. J., Ingham, J. K., Curry, G. B. & Williams, A. 1984. Stratigraphy and tectonic setting of the Highland Border Complex. *Transactions of the Royal Society of Edinburgh* **75**, 124-133.

Bott, M. H. P. 1993. Modelling the plate-driving mechanisms. *Journal of the Geological Society of London* **150** (5), 941-951.

Bouchez, J-L., Delas, C., Gleizes, G., Nébélec, A. & Cuney, M. 1992. Submagmatic microfractures in granites. *Geology* **20**, 35-38.

Boullier, A. M. & Bouchez, J-L. 1978. Le quartz en rubans dans les mylonites. *Bulletin de la Societe Geologique de France* **7**, 235-253.

Bowes, D.R. 1968. The absolute time scale and the subdivision of Precambrian rocks in Scotland. *Geologiska Föreningens i Stockholm Förhandlingar* **90**, 175-188.

Brewer, M. S., Brook, M. & Powell, D. 1979. Dating of the tectono-metamorphic history of the southwestern Moine, Scotland. *In:* Harris, A. L., Holland, C. H. & Leake, B. E.(eds): *The Caledonides of the British Isles -Reviewed.* Special Publication - Geological Society of London **8**, 129-137.

British Geological Survey. 1985. Geological map of Reay 1:50.000. Scotland Sheet 115E. Keyworth, UK.

British Geological Survey. 1985. Geological map of Latheron 1:50.000. Scotland Sheet 110. Keyworth, UK.

British Geological Survey. 1998 Geological map of Helmsdale 1:50.000. Scotland Sheet 103E, provisional series. Keyworth, UK.

British Geological Survey, in press. Geological map of Kildonan 1:50.000. Scotland Sheet 109E. Keyworth, UK.

Brook, M., Brewer, M. S. & Powell, D. 1976. Grenville age for rocks in the Moine of north-western Scotland. *Nature (London)* **260**, 515-517.

Brown, G.C. 1979. Geochemical and geophysical constraints on the origin and the evolution of Caledonian granites. *In*: Harris, A.L., Holland, C.H. & Leake, B.E. (eds) *The Caledonides of the British Isles — Reviewed.* Geological Society, London, Special Publications, **8**, 645-652.

Brown, G.C., Francis, E.H., Kennan, P. & Stillman, C.J. 1985. Caledonian igneous rocks of Britain and Ireland. *In*: Harris, A.L. (ed.) *The Nature and Timing of Orogenic Activity in the Caledonian Rocks of the British Isles.* Geological Society, London, Memoirs **9**, 1-15.

Brown, M. 1973. The definition of metatexis, diatexis and migmatite. *Proc. Geol. Ass.* **84** (4), 371-382.

Brown, M. 1994. The generation, segregation, ascnet and emplacement of granite magma: the migmatite-to-crustally-derived granite connection in thickened orogens. *Earth-Science Reviews* **36**, 83-130.

Brown, M. & Rushmer, T. 1997. The role of deformation in the movement of granitic melt: views from the laboratory and the field. *In*: Holness, M. B.(ed): *Deformation-enhanced fluid transport in the Earths crust and mantle*, Chapman & Hall, London.

Brown, M. & Solar, G. S. 1998a. Shear zones and melts: Positive feedback in orogenic belts. *Journal of Structural Geology* **20** (2-3), 211-227.

Brown, M. & Solar, G. S. 1998b. Granite ascent and emplacement in contractional orogenic belts. *Journal of Structural Geology* **20** (9-10), 1365-1393.

Brown, R. L., Dalziel, I. W. D. & Johnson, M. R. 1970. A review of the structure and stratigraphy of the Moinian of Ardgour, Moidart and Sunart-Argyll and Inverness-shire. *Scottish Journal of Geology* **6**, 309-335.

Brown, P. E. 1991. Caledonian and earlier magmatism. *In*: Craig, G. Y. (ed): *Geology of Scotland.* Geological Society, London, 229-295.

Bryon, D. N., Atheron, M. P. & Hunter, R. H. 1994. The description of the primaty textures of 'Cordilleran' granitic rocks. *Contributions to Mineralogy and petrology* **117**, 66-75.

Burns, I. M. 1994. Tectonothermal evolution and petrogenesis of the Naver and Kirtomy nappes, North Sutherland, Scotland. Unpublished Ph.D. thesis, Oxford Brookes University.

Butler, R. W. H. 1986. Structural evolution in the Moine of northwestern Scotland: a Caledonian linked thrust system?. *Geological Magazine*, **123**, 1-11.

Butler, R. W. H. & Coward, M. P. 1984. Geological constraints, structural evolution, and deep geology of the Northwest Scottish Caledonides. *Tectonics* **3**(3), 347-365.

Canning, J.C., Henney, P.J., Morrison, M.A. & Gaskarth, J.W. 1996. Geochemistry of late Caledonian minettes from Northern Britain: Implications for the Caledonian sub-continental lithospheric mantle. *Mineralogical Magazine,* **128**, 385-388.

Canning, J.C., Henney, P.J., Morrison, M.A., Van Calsteren, P.W., Gaskarth, J.W. & Swarbrick, A. 1998. The Great Glen Fault: A major lithospheric boundary. *Journal of the Geological Society, London* **155**, 424-427.

Castro, A. & Fernandez, C. 1998. Granite intrusion by externally induced growth and deformation of the magma reservoir, the example of the Plasenzuela pluton, Spain. *Journal of Structural Geology* **20** (9-10), 1219-1228.

Chappell, B. W. & White, A. J. R. 1974. Two contrasting granite types. *Pacific Geology* **8**, 173-174.

Chappell, B. W., White, A. J. R. 1992. I- and S-type granites in the Lachlan fold belt. *Transactions of the Royal Society of Edinburgh* **272**, 1-26.

Chivas, A. R., Andrew, A.S., Sinah, A. K. & O'Neil, J. R. 1982. Geochemistry of a Plio-Pleistocene oceanic-arc plutonic complex, Guadalcanal. *Nature* **300**, 139-143.

Clemens, J. D. & Mawer C. K. 1992. Granite magma transport by fracture propagation. *Tectonophysics* **204**, 339-360.

Clemens, J. D., Petford, N. & Mawer, C. K. 1997. Ascend mechanisms of granitic magmas: causes and consequences. *In*: Holness, M. B. (ed): *Deformation-enhanced fluid transport in the Earths crust and mantle*. Chapman & Hall, London, 144-171.

Cliff, R. A. 1985. Isotopic dating in metamorphic belts. *Journal of the Geological Society of London* **142**, 97-110.

Clifford, T.N. 1957. The stratigraphy and structure of part of the Kintail district of southern Ross-shire – its relationship to the Northern Highlands. *Quarterly Journal of the Geological Society of London* **113**, 57-92.

Clift, P. D., Rose E.F., Shimizu, N., Layne, G.D., Draut, A.E. & Regelous, M. 2001. Tracing the evolving flux from the subducting plate in the Tonga-Kremadec arc system using boron in volcanic glass. *Geochimica Cosmochimica Acta* **65**(15), 3347-3364.

Collins, W. J. 1996. Lachlan Foldbelt granitoids: products of three-component mixing. *Transactions of the Royal Society of Edinburgh* **87**, 171-181.

Collins, W. J & Sawyer, E. W. 1996. Pervasive granitoid magma transfer through the lower-middle crust during non-coaxial compressional deformation. *Journal of Metamorphic Geology* **14**, 565-579.

Condon, D. J. & Prave, A. R. 2000. Two from Donegal; Neoproterozoic glacial episodes on the northeast margin of Laurentia. *Geology* **28**(10), 951-954.

Coward, M. P. 1983. The thrust and shear zones of the Moine Thrust zone and the NW Scottish Caledonides. *Journal of the Geological Society of London* **140**, 795-812.

Coward, M. P. 1985. The thrust structures of southern Assynt, Moine thrust zone. *Geological Magazine* **122**(6), 595-607.

Coward, M. P. 1990. The Precambrian, Caledonian and Variscan framework of NW Europe. *In*: Hardman, R. F. P. & Brooks, J. (eds): *Tectonic events responsible for Britain's oil and gas reserves*, Geological Society of London – Special publication **55**, 1-34.

Cowie, J.W., Rushton, A.W.A. & Stubblefield, C.J. 1972. *A correlation of Cambrian rocks in the British Isles*. Geological Society, London, Special Reports, **2**.

Cox, K. G., Bell, J. D. & Pankhurst, R. J. 1979. The interpretation of igneous rocks. George, Allen & Unwin, London.

Cruden, A. R. 1988. On the emlpacement of tabular granites. *Journal of the Geological Society of London* **156**, 853-862.

Curry, G. B., Ingham, J. K., Bluck, B. J. & Williams, A. 1982. The significance of a reliable Ordovician age for some Highland Border rocks in central Scotland. *Journal of the Geological Society of London* **139**(4), 451-454.

Curry, G. B., Bluck, B. J., Burton, C. J., Ingham, J. K., Siveter, D. J., Williams, A. & Bowes, D. R. 1984. Age, evolution and tectonic history of the Highland Border Complex, Scotland. *Transactions of the Royal Society of Edinburgh* **75** (2), 113-133.

Dallmeyer, R. D., Strachan, R. A., Rogers, G., Watt, G. R. & Friend, C. R. L. 2001. Dating deformation and cooling in the Caledonian thrust nappes of North Sutherland, Scotland; insights from (super 40) Ar/ (super 39) Ar and Rb-Sr chronology. *Journal of the Geological Society of London* **158** (3), 501-512.

Dalziel, I. W. D. & Soper, N. J. 2001. Neoproterozoic extension on the Scottish Promontory of Laurentia; paleogeographic and tectonic implications. *Journal of Geology* **109**(3), 299-317.

Davies, J. H. & von Blanckenburg, F. 1995. Slab breakoff; a model of lithosphere detachment and its test in the magmatism and deformation of collisional orogens. *Earth and Planetary Science Letters* **129**(1-4), 85-102.

De Saint Blanquat, M. & Tikoff, B. 1997. Development of magmatic to solid-state fabrics during syntectonic emplacement of the Mono Creek Granite, Sierra Nevada Batholith. *In*: Bouchez, J. L., Hutton, D. H. W. & Stephens, W. E. (eds): *Granite: from segregation of melt to emplacemnet fabrics*. Kluwer Academic Publishers.

Defant M.J. & Drummond M.S. 1990. Derivation of some modern arc magmas by melting of young subducted lithosphere. *Nature* **347**, 662-665.

Dempster, T.J., Rogers, G., Tanner, P.W.G., Bluck, B.J., Muir, R.J., Redwood, S.D., Ireland, T.R. & Paterson, B.A. 2002. Timing of deposition, orogenesis and glaciation within the Dalradian rocks of Scotland: constraints from U—Pb zircon ages. *Journal of the Geological Society, London* **159**, 83-94.

De Paolo, D. J. 1981. Trace element and isotopic effects of combined wall rock assimilation and fractional crystallisation. *Earth and Planetary Science Letters* **53**, 189-202.

Dewey, J. F. 1969. Evolution of the Appalachian/Caledonian orogen. *Nature (London)* **222**(5189), 124-129.

Dewey, J. F. 1971. A model for the Lower Palaeozoic evolution of the southern margin of the early Caledonides of Scotland and Ireland. *Scottish Journal of Geology* **7** (3), 219-240.

Dewey, J. F. & Pankhurst, R. J. 1970. The evolution of the Scottish Caledonides in relation to their isotopic age pattern. *Transactions of the Royal Society of Edinburgh* **68**(11), 361-387.

Dewey, J.F. & Ryan, P.D. 1990. The Ordovician evolution of the South Mayo Trough, western Ireland. *Tectonics,* **9**, 887-903.

Dickin, A. 1995. Radiogenic isotope geology. Cambridge University Press, UK.

D'Lemos, R., Brown, M. & Strachan, R. A. 1992. Granite magma gemeration, ascent and emplacement within a transpressional orogen. *Journal of the Geological Society of London* **149**, 487-490.

D'Lemos, R. S., Schofield, D. I., Holdsworth, R. E. & King, T. R. 1997. Deep crustal and rheological controls on the siting and reactivation of fault and shear zones, northeastern Newfoundland. *Journal of the Geological Society of London* **154** (1), 117-121.

Drake, M. J. & Weill, D. F. 1975. Partition of Sr, Ba, Ca, Y, Eu2+, Eu3+ and other REE between plagioclase feldspar and magmatic liquid: an experimental study. *Geochimica and Cosmaochimica acta* **39**, 689-712.

Drummond M.S., Defant M.J. & Kepezhinskas P.K. 1996. Petrogenesis of slab-derived trondhjemite-tonalite-dacite/adakite magmas. *Transactions of the Royal Society of Edinburgh – Earth Sciences* **87**, 205-215.

Eby, G. N. 1990. The A-type granitoids; a review of their occurrence and chemical characteristics and speculations on their petrogenesis. *Lithos* **26**(1-2), 115-134.

Elliott, D. & Johnson, M. R. W. 1980. Structural evolution in the northern part of the Mopine thrust belt, NW Scotland. *Transactions of the Royal Society of Edinburgh* **71**, 69-96.

England, P. C. & Thompson, A. 1986. Some thermal and tectonic models for crustal melting in continental collision zones. *In*: Coward, M. P. & Ries, A. C. (eds): *Collision tectonics*. Geological Society of London, Special Publication **19**, 83-94.

Esperanca, S. & Holloway, J. R. 1986. The origin of high-K latites from Camp Creek, Arizona: Constraints from experiments with variable fO_2 and aH_2O. *Contributions to Mineralogy and PetrologyI* **93**, 504-512.

Esperanca, S. & Holloway, J. R. 1987. On the origin of some mica lamprophyres: experimental evidence from a mafic minette. *Contributions to Mineralogy and PetrologyI* **95**, 207-216.

Faure, G. 1986. Principles of isotope geology. Wiley, New York.

Fettes, D. J., Graham, C. M., Harte, B. & Plant, J. A. 1986. Lineaments and basement domains; an alternative view of Dalradian evolution. *Journal of the Geological Society of London* **143** (3), 453-464.

Ferré, E., Gleizes, G., Djouadi, M. T., Bouchez, J-L. & Ugodulunwa, X. O. 1997. Drainage and emplacement of magmas along an inclined transcurrent shear zone: Petrophysical evidence from a granite-charnockite pluton (Rahama, Nigeria). *In*: Bouchez, J. L., Hutton, D. H. W. & Stephens, W. E. (eds): *Granite: from segregation of melt to emplacemnet fabrics*. Kluwer Academic Publishers.

Fowler, M. B. 1988a. Ach'uaine hybrid appinite pipes; evidence for mantle-derived shoshonitic parent magmas in Caledonian granite genesis. *Geology* **16**(11), 1026-1030.

Fowler, M. B. 1988b. Elemental evidence for crustal contamination of mantle-derived Caledonian syenite by metasediment anatexis and magma mixing. *Chemical Geology* **69**(1-2), 1-16.

Fowler, M. B. 1992. Elemental and O-Sr-Nd isotope geochemistry of the Glen Dessary Syenite, NW Scotland. *Journal of the Geological Society of London* **149** (2), 209-220.

Fowler, M. B. & Henney, P. J. 1996. Mixed Caledonian appinite magmas; implications for lamprophyre fractionation and high Ba-Sr granite genesis. *Contributions to Mineralogy and Petrology* **126**(1-2), 199-215.

Fowler, M. B., Henney, P. J., Darbyshire, D. P. F. & Greenwood, P. B. 2001. Petrogenesis of high Ba-Sr granites: the Rogart Pluton, Sutherland. *Journal of the Geological Society of London* **158**, 521-534.

Freeman, S. R., Butler, R. W. H., Cliff, R. A. & Rex, D. C. 1998. Direct dating of mylonite evolution; a multi-disciplinary geochronological study from the Moine thrust zone, NW Scotland. *Journal of the Geological Society of London* **155** (5), 745-758.

Friedrich, A. M., Bowring, S. A., Martin, M. W. & Hodges, K. V. 1999a. Short-lived continental magmatic arc at Connemara, western Irish Caledonides; implications for the age of the Grampian Orogeny. *Geology* **27**(1), 27-30.

Friedrich, A. M., Hodges, K. V., Bowring, S. A. & Martin, M. W. 1999b. Geochronological constraints on the magmatic, metamorphic and thermal evolution of the Connemara Caledonides, western Ireland. *Journal of the Geological Society of London* **156** (6), 1217-1230.

Friend, C. R. L. & Kinny, P. 2001. A reapraisal of the Lewisian complex. *Contributions to Mineralogy and Petrology* **142**, 198-218.

Friend, C. R. L., Jones, K. A. & Burns, I. M. 2000. New high-pressure granulite event in the Moine Supergroup, northern Scotland; implications for Taconic (early Caledonian) crustal evolution. *Geology* **28**(6), 543-546.

Friend, C. R. L., Strachan, R. A. Kinny, P. K. & Watt, G. R. in press. Provenance of the Moine Supergroup of NW Scotland: evidence from geochronology of detrital and inherited zircons from (meta) sedimentary rocks, granites and migmatites. *Journal of the Geological Society of London.*

Friend, C. R. L., Kinny, P. D., Rogers, G., Strachan, R. A. & Paterson, B. A. 1997. U-Pb zircon geochronological evidence for Neoproterozoic events in the Glenfinnan Group (Moine Supergroup); the formation of the Ardgour granite gneiss, North-west Scotland. *Contributions to Mineralogy and Petrology* **128**(2-3), 101-113.

Frost, C. D. & O'Nions, R. K. 1985. Caledonian magma genesis and crustal recycling. *Journal of Petrology* **26 (2)**, 515-544.

Gapais, D. 1989. Shear structures within deformed granites: Mechanical and thermal indicators. *Geology* **17**, 1144-1147.

Gibbons, W. & Gayer, R.A. 1985. British Caledonian Terranes. *In*: Gayer, R.A. (ed.) *The tectonic evolution of the Caledonian-Appalachian Orogen*. Viewseg, Brunswick, 3-16.

Giletti, B. J., Moorbath, S. & St. J. Lambert, R. 1961. A geochronological study of the metamorphic complexes of the Scottish Highlands. *Quarterly Journal of the Geological Society of London* **117** (3), 233-272.

Glazner, A. F. 1991. Plutonism, oblique subduction, and continental growth; an example from the Mesozoic of California. *Geology* **19**(8), 784-786.

Gleizes, G., Leblanc, D., Santana, V., Olivier, P. & Bouchez, J. L. 1998. Sigmoidal structures featuring dextral shear during emplacement of the Hercynian granite complex of Cauterets-Panticosa (Pyrenees). *Journal of Structural Geology* **20** (9-10), 1229-1245.

Glendinning, N. R. W. 1988. Sedimentary structures and sequences within a late Proterozoic tidal shelf deposit; the upper Morar Psammite Formation of northwestern Scotland. *In*: Winchester, J. A.(ed): *Later Proterozoic stratigraphy of the northern Atlantic regions*, Blackie, Glasgow 14-31.

Gray, C. M. 1984. An isotopic mixing model for the origin of granitic rocks in southeastern Australia. *Earth and Planetary Science Letters* **70**, 47-60.

Grocott, J., Brown, M., Dallmeyer, R.D. Taylor, G. K. & Treloar, P. J. 1994. Mechanisms of continental growth in extensional arcs: An example from the Andean plate boundary zone. *Geology* **22** , 391-394.

Grocott, J., Garde, A. A., Chadwick, B., Cruden, A. R. & Swager, C. 1999. Emplacement of rapakivi granite and syenite by floor depression and roof uplift in the Palaeoproterozoic Ketilidian Orogen, South Greenland. *Journal of the Geological Society of London* **156** (1), 15-24.

Hall, A. 1987. Igneous petrology. Longman, London.

Halliday, A. N. 1984. Coupled Sm-Nd and U-Pb systematics in late Caledonian granites and the basement under northern Britain. *Nature (London)* **307**, 229-233.

Halliday, A. N., Graham, C. M., Aftalion, M. & Dymoke, P. 1989. The depositional age of the Dalradian Supergroup; U-Pb and Sm-Nd isotopic studies of the Tayvallich Volcanics, Scotland. *Journal of the Geological Society of London* **146**(1), 3-6.

Halliday, A. N., Aftalion, M., Parsons, I., Dickin, A. P. & Johnson, M. R. W. 1987. Syn-orogenic alkaline magmatism and its relationship to the Moine Thrust zone and the thermal state of the lithosphere in NW Scotland. *Journal of the Geological Society of London* **144**(4), 611-617.

Halliday, A. N., Stephens, W. E., Hunter, R. H., Menzies, M. A., Dickin, A. P. & Hamilton, P. J. 1985. Isotopic and chemical constraints on the building of the deep Scottish lithosphere. *Scottish Journal of Geology* **21**(4), 465-491.

Halliday, A. N., Dickin, A. P., Hunter, R. H., Davies, G. R., Dempster, T. J., Hamilton, P. J. & Upton, B. G. J. 1993. Formation and composition of the lower continental crust: evidence from scottish xenolith suites. *Journal of Geophysical Research* **98**, 581-607.

Hamilton, P. J., O'Nions, R. K. & Pankhurst, R. J. 1980. Isotopic evidence for the provenance of some Caledonian granites. *Nature (London)* **287**(5780), 279-284.

Harmon, R. S., Halliday, A. N., Clayburn, J. A. P. & Stephens, W. E. 1984. Chemical and isotopic systematics of the Caledonian intrusions of Scotland and northern England; a guide to magma source region and magma-crust interaction. *Transactions of the Royal Society of Edinburgh* **A 310**, 709-742.

Harris, A. L. 1985. Enclosure 1 - map and isotopic ages of igneous rocks in Great Britain. *In*: Harris, A.L. (ed.) *The Nature and Timing of Orogenic Activity in the Caledonian Rocks of the British Isles.* Geological Society, London, Memoirs **9**.

Harris, A.L., Haselock, P.J., Kennedy, M.J. & Mendum, J.R. 1994. The Dalradian Supergroup in Scotland, Shetland and Ireland. *In*: Gibbons, W. & Harris, A.L. (eds) *A revised correlation of Precambrian rocks in the British Isles*. Geological Society, London, Special Report, **22**, 33-53.

Harris, A.L., Baldwin, C.T., Bradbury, H.J., Johnson, H.D. & Smith, R.A. 1978. Ensialic basin sedimentation: the Dalradian Supergroup: *In*: Bowes, D.R. & Leake, B.E. (eds) *Crustal evolution in Northwestern Britain and adjacent regions*. Geological Journal Special Issue, **10**, 115-138.

Harrison, T.N. 1987. The granitoids of eastern Aberdeenshire. *In*: Trewin, N.H., Kneller, B.C. & Gillen, C. (eds): *Excursion Guide to the Geology of the Aberdeen area*. Scottish Academic Press, Edinburgh, 243-250.

Haughton, P. D. W., Rogers, G. & Halliday, A. N. 1990. Provenance of Lower Old Red Sandstone conglomerates, SE Kincardineshire; evidence for the timing of Caledonian terrane accretion in central Scotland. *Journal of the Geological Society of London* **147**(1), 105-120.

Hartz, E. H., Andresen, A. , Hodges, K.V. & Martin, M. W. 2001. Syncontractional extension and exhumation of deep crustal rocks in the east Greenland Caledonides. *Tectonics* **20**(1), 58-77.

Highton, A. J. 1999. Late Silurian and Devonian granitic intrusions of Scotland-Introduction. *In*: Stephenson, D., Bevins, R.E., Millward, D., Highton, A.J., Parsons, I., Stone, P. & Wadsworth, W.J. (eds): *Caledonian Igneous Rocks of Great Britain*. Geological Conservation Review Series, **17**, 1-48.

Highton, A. J., Hyslop, E. K., Noble, S. R.. 1999. U-Pb zircon geochronology of migmatization in the northern central Highlands; evidence for pre-Caledonian (Neoproterozoic) tectonometamorphism in the Grampian Block, Scotland. *Journal of the Geological Society of London* **156** (6), 1195-1204.

Hirth, G. & Tullis, J. 1992. Dislocation creep regimes in quartz aggregates. *Journal of Structural Geology* **14** (2), 145-159.

Hodges, K. V., Parrish, R. R., Housh, T. B., Lux, D. R., Burchfiel, B. C., Royden, L. H. & Chen, Z. 1992. Simultaneous Miocene extension and shortening in the Himalayan orogen. *Science* **258**, 1466-1470.

Hofmann, A. W. 1997. Mantle geochemistry: the message from oceanic volcanism. *Nature* **385**, 219-229.

Holden P., Halliday A.N. & stephens W.E. 1987. Neodymium and strontium isotope content of microdiorite enclaves points to mantle input to granitoid production. *Nature* **330**, 53-56.

Holdsworth, R. E. 1989a. The geology and structural evolution of a Caledonian fold and ductile thrust zone, Kyle of Tongue region, Sutherland, northern Scotland. *Journal of the Geological Society of London* **146**(5), 809-823.

Holdsworth, R. E. 1989b. Late brittle deformation in a Caledonian ductile thrust wedge; new evidence for gravitational collapse in the Moine thrust sheet, Sutherland, Scotland. *Tectonophysics* **170**(1-2), 17-28.

Holdsworth, R. E. 1990. Progressive deformation structures associated with ductile thrusts in the Moine Nappe, Sutherland, N. Scotland. *Journal of Structural Geology* **12**(4), 443-452.

Holdsworth, R. E. & Roberts, A. M. 1984. Early curvilinear fold structures and strain in the Moine of the Glen Garry region, Inverness-shire. *Journal of the Geological Society of London* **141**, 327-338.

Holdsworth, R. E. & Strachan, R. A. 1988. The structural age and possible origin of the Vagastie Bridge Granite and associated intrusions, central Sutherland. *Geological Magazine* **125**(6), 613-620.

Holdsworth, R. E., Strachan, R. A. & Harris, A. L. 1994. Precambrian rocks in northern Scotland east of the Moine Thrust; the Moine Supergroup. *In*: Gibbons, W. & Harris, A. L.(eds): A revised correlation of Precambrian rocks in the British Isles. *Special Report - Geological Society* **22**, 23-32.

Holdsworth, R. E., McErlean, M. A. & Strachan, R. A. 1999. The influence of country rock structural architecture during pluton emplacement; the Loch Loyal Syenites, Scotland. *Journal of the Geological Society of London* **156**(1), 163-175.

Holdsworth, R. E., Strachan, R. A. & Alsop, G. I. 2001. *Geology of the Tongue District (Sheet 114E, Scotland)*. HMSO.

Hole M.J., Saunders A.D., Marriner G.F. & Tarney J. 1984. Subduction of pelagic sediments: implications for the origin of Ce-anomalous basalts from the Mariana Islands. *Journal of the Geological Society, London* **141**, 453-472.

Hollister, L. S. & Crawford, M. A. 1986. Melt-enhanced deformation: A major tectonic process. *Geology* **14**, 558-561.

Houseman, G.A., McKenzie D.P. & Molnar, P. 1981. Convective instability of a thickened boundary layer and its relevance for thermal evolution of convergent continental belts. *Journal of Geophysical Research* **86**, 6135-6155.

Horne, J. & Greenly, E. 1986. On foliated granites and their relations to crystalline schists in Eastern Sutherland. *Quarterly Journal of the Geological Society of London* **52**, pp 633.

Hutton, D. H. W. 1982. A tectonic model for the emplacement of the Main Donegal granite, N.W. Ireland. *Journal of the Geological Society of London* **139**, 615-631.

Hutton, D. H. W. 1987. Strike-slip terranes and a model for the evolution of the British and Irish Caledonides. *Geological Magazine* **124**(5), 405-425.

Hutton, D. H. W. 1988. Granite emplacement mechanisms and tectonic controls; inferences from deformation studies. *Transactions of the Royal Society of Edinburgh: Earth Sciences* **79**(2-3), 245-255.

Hutton, D. H. W. 1988b. Igneous emplacement in a shear-zone termination; the biotite granite at Strontian, Scotland. *Geological Society of America Bulletin* **100**(9), 1392-1399.

Hutton, D. H. W. & Murphy, F. C. 1987. The Silurian of the Southern Uplands and Ireland as a successor basin to the end-Ordovician closure of Iapetus. *Journal of the Geological Society of London* **144**(5), 765-772.

Hutton, D. H. W. & McErlean, M. 1991. Silurian and Early Devonian sinistral deformation of the Ratagain Granite, Scotland; constraints on the age of Caledonian movements on the Great Glen fault system. *Journal of the Geological Society of London* **148** (1), 1-4.

Hutton, D. H. W. & Reavy, R. J. 1992. Strike-slip tectonics and granite petrogenesis. *Tectonics* **11**(5), 960-967.

Hutton, D. H. W., Dempster, T. J., Brown, P. E. & Becker, S. D. 1990. A new mechanism of granite emplacement: intrusion in active extensional shear zones. *Nature* **343**, 452-455.

Ingram, G. M. & Hutton, D. H. W. 1994. The Great Tonalite Sill; emplacement into a contractional shear zone and implications for Late Cretaceous to early Eocene tectonics in Southeastern Alaska and British Columbia. *Geological Society of America Bulletin* **106**(5), 715-728.

Jacques, J. M. & Reavy, R. J. 1994. Caledonian plutonism and major lineaments in the SW Scottish Highlands. *Journal of the Geological Society of London* **151** (6), 955-969.

Jessell, M. 1987. Grain-boundary migration microstructures in naturally deformed quarzite. *Journal of Structural Geology* **9**, 1007-1014.

Johnson, M. R. W. 1991. Dalradian. *In*: Craig, G. Y. (ed): *Geology of Scotland.* Geological Society, London, 125-160.

Johnstone, G.S., Smith, D.I. & Harris, A.L. 1969. The Moinian Assemblage of Scotland. *In*: Kay, M. (ed.) *North Atlantic geology and continental drift.* American Association of Petroleum Geologists, Memoirs, **12**, 159-180.

Karlstrom, K. E. 1989. Towards a syntectonic paradigm for granitoids. *EOS* **70**, 762-763.

Karlstrom, K. E. & Williams, M. L. 1995. The case for simultaneous deformation, metamorphism and plutonism; an example from Proterozoic rocks in central Arizona. *Journal of Structural Geology* **17**(1), 59-81.

Kay, R. W., Sun, S. S. & Lee-Hu, C. N. 1978. Pb and Sr isotopes in volcanic rocks from the Aleutian Islands and Pribilof Islands, Alaska. *Geochimica et Cosmochimica Acta* **42**(3), 263-274.

Keay, S., Collins, W. J. & McCulloch, M. T. 1997. A three-component Sr-Nd isotopic mixing model for granitoid genesis, Lachlan fold belt, eastern Australia. *Geology* **25 (4)**, 307-310.

Kelley, S. P. & Powell, D. 1985. Relationships between marginal thrusting and movement on major, internal shear zones in the northern Highland Caledonides, Scotland. *Journal of Structural Geology* **7**(2), 161-174.

Kinny, P. D., Friend, C. R. L., Strachan, R. A., Watt, G. R. & Burns, I. M. 1999. U-Pb geochronology of regional migmatites in East Sutherland, Scotland; evidence for crustal melting during the Caledonian Orogeny. *Journal of the Geological Society of London* **156**(6), 1143-1152.

Kinny, P., Strachan, R. A., Friend, C. R. L., Kocks, H., Rogers, G. & Paterson, B. in press. U-Pb geochronology of deformed meta-garnites in central Sutherland, Scotland: evidence for widespread late Silurian metamorphism and ductile deformation of the Moine Supergroup during the Caledonian Orogeny. *Journal of the Geological Society of London.*

Kneller, B. C. & Aftalion, M. 1987. The isotopic and structural age of the Aberdeen Granite. *Journal of the Geological Society of London* **144**(5), 717-721.

Kneller, B. C. & Leslie, A. G. 1984. Amphibolite facies metamorphism in shear zones in the Buchan area of NE Scotland. *Journal of Metamorphic Geology* **2**(2), 83-94.

Lambert, R. S. J. & McKerrow, W. S. 1976. The Grampian Orogeny. *Scottish Journal of Geology* **12** (4), 271-292.

Leake, B. E. 1990a. Finding space for granite intrusions. *Nature (London)* **343**(6257), 413.

Leake, B. E. 1990b. Granite magmas; their sources, initiation and consequences of emplacement. *Journal of the Geological Society of London* **147**(4), 579-589.

Leedal, G.P. 1952. The Cluanie igneous intrusion, Inverness-shire and Ross-shire. *Quarterly Journal of the Geological Society of London*, **108**, 35-63.

Leggett, J. K. 1987. The Southern Uplands as an accretionary prism; the importance of analogues in reconstructing palaeogeography. *Journal of the Geological Society of London* **144**(5), 737-752.

Leggett, J. K., McKerrow, W. S. & Eales, M. H. 1979. The Southern Uplands of Scotland; a lower Palaeozoic accretionary prism. *Journal of the Geological Society of London* **136** (6), 755-770.

Lee, M. K. 1987. Geophysical investigations in the Strath Halladale-Altnabreac distric (NE Scotland) in relation to radioactive waste disposal. *Journal of Geophysical Research* **92**(8), 7807-7819.

Le Maitre, R. W. (ed). 1989. A classification of igneous rocks and glossary of terms. Blackwell Scientific Publications, Oxford, UK.

Lintern, B. C. & Storey, B. C. 1980. Geology of the Altnabreac research site, Caithness. ENPU 80-14, Rep. Inst. Geol. Sci.

Longman, C. D., Bluck, B. J. & Van Breemen, O. 1979. Ordovician conglomerates and the evolution of the midland valley. *Nature (London)* **280**, 578-581.

Marsh, B. D. 1982. On the mechanichs of igneous diapirism, stoping and zone melting. *American Journal of Science* **282**, 808-855.

Martin H. 1999. Adakitic magmas, modern analogues of Archaean granitoids. *Lithos* **46**, 411-429.

May, F., Peacock, J.D., Smith, D.I. & Barber, A.J. 1993. *Geology of the Kintail District.* Memoir of the British Geological Survey, HMSO.

McCaffrey, K.J.W. 1992. Igneous emplacement in a transpressive shear zone: Ox Mountains Igneous complex. *Journal of the Geological Society of London* **149**, 221-235.

McCaffrey, K. J. W., Miller, C. F., Karlstrom, K. E. & Simpson, C. 1999. Synmagmatic deformation patterns in the Old Woman Mountains, SE California. *Journal of Structural Geology* **21**(3), 335-349.

McCourt, W.J. 1980. The Geology of the Strath Halladale-Altnabreac district. ENPU 80-1. Rep. Inst. Geol. Sci.

McCulloch, M. T. & Chappell, B. W. 1982. Nd isotopic characteristics of S- and I-type granites. *Earth and Planetary Science Letters* **58**, 51-64.

McKerrow, W. S. & Soper, N. J. 1989. The Iapetus suture in the British Isles. *Geological Magazine* **126**(1), 1-8.

McKerrow, W. S., Mac Niocaill, C. & Dewey, J. F. 2000. The Caledonian Orogeny redefined. *Journal of the Geological Society of London* **157** (6), 1149-1154.

Menuge, J. F. & Daly, J. S. 1994. The Annagh Gneiss Complex in County Mayo, Ireland. *In*: Gibbons, W. & Harris, A. L. (eds): *A revised correlation of Pre-cambrian rocks in the British Isles.* Geological Society of London, Special reports **22**, 59-62.

Menzies M.A. & Halliday A.N.1988. Lithospheric mantle domains beneath the Scottish Highlands. *In*: Menzies M.A. and Cox K.G. (eds): *Oceanic and continental lithosphere: similarities and differences.* Journal of Petrology Special Lithosphere Issue, 275-302.

Menzies M.A., Halliday A.N. Palacz Z., Hunter R.H., Upton BGJ, Aspen, P. & Hawkesworth C.J. 1987. Evidence from mantle xenoliths for an enriched lithospheric keel under the Outer Hebrides. *Nature*, **325**, 44-47.

Michard, A. 1989. Rare earth element systematics in hydrothermal fluids. *Geochimica Cosmochimica Acta* **53**, 745-750.

Millar, I. L. 1999. Neoproterozoic extensional basic magmatism associated with the West Highland granite gneiss in the Moine Supergroup of NW Scotland. Journal of the Geological Society of London **156** (6), 1153-1162.

Miller, B. V., Samson, S. D. & D'Lemos, R. S. 2001. U-Pb geochronological constraints on the timing of plutonism, volcanism, and sedimentation, Jersey, Channel Islands, UK. *Journal of the Geological Society of London* **158**, 243-252.

Miller, D. M., Goldstein, S.L. & Langmuir, C.H. 1994. Cerium/lead and lead isotope ratios in arc magmas and the enrichment of lead in the continents. *Nature* **368**, 514-520.

Miller, H. 1893. quoted in Read et al. 1925.

Miller, J. A., Cartwright, I. & Buick, I. S. 1997. Granulite facies metamorphism in the Mallee Bore area, northern Harts Eange: implications for the thermal evolution of the eastern Arunta Inlier, Australia. *Journal of metamorphic Geology* **15**, 613-629.

Miller, R. B. & Paterson, S. R. 1994. The transition from magmatic to high-temperature solid-state deformation: implications from the Mount Stuart batholith, Washington. *Journal of Structural Geology* **16** (6), 853-865.

Miller, R. B. & Paterson, S. R. 1999. In defense of magmatic diapirs. *Journal of Structural Geology* **21**, 1161-1173.

Miller, R. B. & Paterson, S. R. 2001. Construction of mid-crustal sheeted plutons: Examples from the North Cascades, Washington. *GSA Bulletin* **113**(11), 1423-1442.

Molyneux, S. G. 1998. An upper Dalradian microfossil reassessed. *Journal of the Geological Society of London* **155** (5), 741-743.

Molyneux, S. J. & Hutton, D. H. W. 2000. Evidence for significant granite space creation by the ballooning mechanism: The example of the Ardara pluton, Ireland. *GSA Bulletin* **112** (10), 1543-1558.

Moorhouse, S. J. & Moorhouse, V. E. 1977. A Lewisian basement sheet within the Moine at Ribigill, north Sutherland. *Scottish Journal of Geology* **13**, 289-300.

Moorhouse, S. J. & Moorhouse, V. E. 1979. The Moine amphibolite suites of central and northern Sutherland, Scotland. *Mineralogical Magazine* **43**(326), 211-225.

Moorhouse, S.J. & Moorhouse, V.E. 1988. The Moine Assemblage in Sutherland. *In*: Winchester, J.A. (ed.) *Later Proterozoic Stratigraphy in the Northern Atlantic Regions*. Blackie, Glasgow, 54-73.

Moorhouse, S. J., Moorhouse, V. E. & Holdsworth, R. E. 1988. Excursion 12. North Sutherland. *In*: Allison, I., May, F. & Strachan, R. A. (eds): *An Excursion Guide to the Moine Geology of the Scottish Highlands*. Scottish Academic Press, Edinburgh, 216-248.

Moorhouse, V. E. & Moorhouse, S. J. 1983. The geology and geochemistry of the Strathy Complex of North-East Sutherland, Scotland. *Mineralogical Magazine* **47**(2), 123-137.

Morris, J. H. 1987. The northern belt of the Longford-Down Inlier, Ireland and Southern Uplands, Scotland; an Ordovician back-arc basin. *Journal of the Geological Society of London* **144**(5), 773-786.

Morris, J. & Tera, F. 1989. ^{10}Be and ^{9}Be in mineral separates and whole rocks from volcanic arcs; implications for sediment subduction. *Geochimica et Cosmochimica Acta* **53**(12), 3197-3206.

Muir, R. J., Fitches, W. R., Maltman, A. J. & Bently, M. R. 1994. Pre-cambrian rocks in the southern Inner Hebrides - Malin Sea region: Colonsay, West Islay, Inishtrahul and Iona. *In*: Gibbons, W. & Harris, A. L. (eds): *A revised correlation of Pre-cambrian rocks in the British Isles*. Geological Society of London, Special reports **22**, 59-62.

Musumeci, G. 1999. Magmatic belts in accretionary margins, a key for tectonic evolution; the tonalite belt of North Victoria Land (East Antarctica). *Journal of the Geological Society of London* **156** (1), 177-189.

Mykura, W. 1991. Old Red Sandstone. *In*: Craig, G. Y.(ed): *Geology of Scotland* , Geological Society, London 297-344.

Mykura, W. 1985. Explanations to the Geological map 1:50000, Reay, sheet 115E. *British Geological Survey,* Keyworth.

Needham, D. T. 1993. The structure of the western part of the Southern Uplands of Scotland. *Journal of the Geological Society of London* **150**(2), 341-354.

Nelson, K.D. 1992. Are crustal thickness variations in old mountain belts like the Appalachians a consequence of lithospheric delamination? *Geology* **20**, 498-502.

Noble, S. R., Hyslop, E. K. & Highton, A. J. 1996. High-precision U-Pb monazite geochronology of the c. 806 Ma Grampian shear zone and the implications for the evolution of the Central Highlands of Scotland. *Journal of the Geological Society of London* **153** (4), 511-514.

Oliver, G. J. H. 2001. Reconstruction of the Grampian episode in Scotland; its place in the Caledonian Orogeny. Tectonophysics **332**(1-2), 23-49.

Oliver, G. J. H., Chen, F., Buchwaldt, R. & Hegner, E. 2000. Fast tectonometamorphism and exhumation in the type area of the Barrovian and Buchan zones. *Geology* **28**(5), 459-462.

Owen, A. W., Armstrong, H. A. & Floyd, J. D. 1999. Rare earth element geochemistry of Upper Ordovician cherts from the Southern Uplands of Scotland. *Journal of the Geological Society of London* **156**(1), 191-204.

Pankhurst, R.J. 1970. The geochronology of the basic igneous complexes. *Scottish Journal of Geology,* **6**, 83-107.

Pankhurst, R. J. 1974. Rb-Sr Whole-Rock Chronology of Caledonian Events in Northeast Scotland. *Geological Society of America Bulletin* **85**(3), 345-350.

Pankhurst, R.J. 1979. Isotope and trace element evidence for the origin and evolution of Caledonide granites in the Scottish Highlands. *In*: Atherton, M.J. & Tarney, J. (eds) *The Origin of Granite Batholiths: Geochemical Evidence*, Shiva, Nantwich, 18-33.

Pankhurst, R. J. 1982. Geochronological tables for British igneous rocks (Appendix C). *In*: Sutherland, D. S.(ed): *Igneous rocks of the British Isles*. Wiley & Sons Ltd., 575-581.

Pankhurst, R. J. & Sutherland, D. S. 1982. Caledonian granites and diorites of Scotland and Ireland. *In*: Sutherland, D. S.(ed): *Igneous rocks of the British Isles*. Wiley & Sons Ltd., 149-190.

Park, R. G., Cliff, R. A., Fettes, D. J., Stewart, A. D. 1994. Precambrian rocks in Northwest Scotland west of the Moine Thrust; the Lewisian Complex and the Torridonian. *In*: Gibbons, W. & Harris, A. L.(eds): *A revised correlation of Precambrian rocks in the British Isles*. Geological Society of London, Special Report **22**, 6-22.

Paterson, S. R. & Tobisch, O. T. 1988. Using pluton ages to date regional deformations; problems with commonly used criteria. *Geology* **16**(12), 1108-1111.

Paterson, S. R. & Tobisch, O. T. 1992. Rates of processes in magmatic arcs; implications for the timing and nature of pluton emplacement and wall rock deformation. *Journal of Structural Geology* **14**(3), 291-300.

Paterson, S. R. & Vernon, R. H. 1995. Bursting he bubble of ballooning plutons: A return to nested diapirs emplaced by mutiple processes. *GSA Bulletin* **107** (11), 1356-1380.

Paterson, S. R. & Schmidt, K. L. 1999. Is there a close spatial relationship between faults and plutons? *Journal of Structural Geology* **21**(8-9), 1131-1142.

Paterson, S. R., Vernon, R. H. & Tobisch, O. T. 1989a. A review of criteria for the identification of magmatic and tectonic foliations in granitoids. *Journal of Structural Geology* **11**(3), 349-363.

Paterson, S. R., Tobisch, O. T. & Vernon, R. H. 1989b. Criteria for establishing the relative timing of pluton emplacement and regional deformation. *Geology* **17**(5), 475-476.

Paterson, S. R., Vernon, R. H. & Fowler, T. K., Jr. 1991. Aureole tectonics. *In*: Kerrick, D. M. (ed): *Contact metamorphism*. Mineralogical Society of America Special Publication **26**, 673-722.

Paterson, S. R., Fowler, T. K. Jr, Schmidt, K. L., Yoshinobu, A. S., Yuan, E.S. & Miller, R. B. 1998. Interpreting magmatic fabric patterns in plutons. *Lithos* **44**, 53-82.

Passchier, C. W. & Trouw, R. A. J. 1996. Microtectonics. Springer Verlag.

Patino Douce, A. E. & Beard, J. S. 1995. Dehydration-melting of Biotite Gneiss and Quartz Amphibolite from 3 to 15 kbar. *Journal of Petrology* **36** (3), 707-738.

Peacock, J. D., Mendum, J. R. & Fettes, D. J. 1992. *Geology of the Glen Affric District.* Memoir of the Geological Survey, 81p.

Pearce, T. H. , Gorman B. E. & Birkett, T.C. 1977. The relationship between major element chemistry and tectonic environment of basic and intermediate volcanic rocks. *Earth and Planetary Science Letters* **36**, 121-132.

Pearce, T. H., Harris, N. B. W. & Tindle, A.G. 1984. Trace element discrimination diagrams for the tectonic interpretation of granitic rocks. *Journal of Petrology* **25**, 956-983.

Petford, N., Cruden, A. R., McCaffrey, K. J. W. & Vigneresse, J-L. 2000. Granite magma formation, transport and emplacement in the Earth's crust. *Nature* **408**, 669-673.

Petford, N., Kerr, R. C. & Lister J. R. 1993. Dike transport of granitoid magmas. *Geology* **21**, 845-848.

Piasecki, M. A. J. 1980. New light on the Moine rocks of the Central Highlands. *Journal of the Geological Society of London* **137**, 41-59.

Pickering, K. T., Bassett, M. G. & Siveter, D. J. 1988. Late Ordovician-Early Silurian destruction of the Iapetus Ocean; Newfoundland, British Isles and Scandinavia; a discussion. *Transactions of the Royal Society of Edinburgh: Earth Sciences* **79**(4), 361-382.

Pidgeon, R. T. & Aftalion, M. 1978. Cogenetic and inherited zircon U-Pb systems in granites; Palaeozoic granites of Scotland and England. *In*: Bowes, D. R. & Leake, B. E.(eds): *Crustal evolution in northwestern Britain and adjacent regions.* Geological Journal Special Issue, 183-220.

Pitcher, W. S. 1987. Granites and yet more granites forty years on. *Geologische Rundschau* **76**(1), 51-79.

Pitcher, W. S. 1993. The Nature and origin of granite. Blackie, London, 322p.

Plank T. & Langmuir C.H. 1998. The geochemical composition of subducting sediment and its consequences for the crust and mantle. *Chemical Geology*, **145**, 325-344.

Powell, D. 1966. The Structure of the South-Eastern Part of the Morar Antiform, Inverness-shire. *Proceedings of the Geologists' Association*, **77**, 79-100.

Powell, D. 1974. Stratigraphy and structure of the Western Moine and the problem of Moine orogenesis. *Journal of the Geological Society of London* **130**(6), 575-593.

Powell, D. & Phillips, W. E. A. 1985. Time of deformation in the Caledonide Orogen of Britain and Ireland *In*: Harris, A. L.(ed): *The nature and timing of orogenic activity in the Caledonian rocks of the British Isles*. Memoir of the Geological Society of London **9**, 17-39.

Powell, D. & Glendinning, R. 1988. Excursion 4: Glenfinnan to Morar. *In*: Allison, I., May, F. & Strachan, R.A. (eds) *An Excursion Guide to the Moine Geology of the Scottish Highlands*. Scottish Academic Press, Edinburgh, 80-102.

Powell, D., Brook, M. & Baird, A.W. 1983. Structural dating of a Precambrian pegmatite in Moine rocks of northern Scotland and its bearing on the status of the 'Morarian Orogeny'. *Journal of the Geological Society, London,* **140**, 813-823.

Prave, A. R. 1999. The Neoproterozoic Dalradian Supergroup of Scotland: an alternative hypothesis. *Geological Magazine* **136**(6), 609-617.

Pressley, R. A. & Brown, M. 1999. The Phillips Pluton, Maine, USA: Evidence for heterogeneous crustal sources, and implications for granite ascent and emplacement mechanisms in convergent orogens. *Lithos* **46** (13), 335-366.

Ramsay, J. G. 1956. The structural geology of a double fold system at Loch Monar, Inverness-shire and Ross-shire [Scotland]. *Proceedings of the Geological Society of London* **154**(1), 121-124.

Ramsay, J. G. 1958. Moine-Lewisian relations at Glenelg, Inverness-shire. *Quarterly Journal of the Geological Society of London* **113**(4), 487-523.

Ramsay, J. G. 1963. Structure and metamorphism of the Moine and Lewisian rocks of the northwest Caledonides. *In*: Johnson, M. R. & Stewart, F. H. (eds): *The British Caledonides*. Oliver & Boyd, Edingburgh, 143-176.

Ramsay, J.G. 1989. Emplacement kinematics of a granite diapir: The Chindamora batholith, Zimbabwe. *Journal of Structural Geology* **11**, 191-210.

Ramsay, J. G. & Spring, J. 1962. Moine stratigraphy in the western Highlands of Scotland [with discussion]. *Proceedings of the Geologists' Association* **Part 3**.

Rathbone, P.A. & Harris, A.L. 1979. Basement-cover relationships at Lewisian inliers in the Moine rocks. *In*: Harris, A.L., Holland, C.H. & Leake, B.E. (eds) *The Caledonides of the British Isles – Reviewed.* Geological Society, London, Special Publications **8**, 101-107.

Read, H.H. 1931. *The Geology of Central Sutherland.* Memoir of the Geological Survey of Great Britain. HMSO.

Read, H., H. 1948. A commentary on place in plutonism [presidential address]. *Quarterly Journal of the Geological Society of London* **413**(1), 155-205.

Read, H. H. 1961. Aspects of Caledonian magmatism in Britain. *Liverpool Manchester geol. J.* **2**, 653-683.

Read, H.H., Phemister, J. & Ross, G. 1926. *The geology of Strath Oykell and lower Loch Shin.* Memoir of the Geological Survey **102**, Scotland. HMSO.

Read, H.H., Ross, G., Phemister, J. & Lee, G.W. 1925. *The geology of the country around Golspie, Sutherlandshire*. Memoir of the Geological Survey **103**, Scotland. HMSO.

Reymer, A. & Schubert, G. 1984. Phanerozoic addition rates to the continental crust and crustal growth. *Tectonics* **3**(1), 63-77.

Reymer, A. & Schubert, G. 1986. Rapid growth of some major segments of continental crust. *Geology* **14**(4), 299-302.

Roberts, A. M. & Harris, A. L. 1983. The Loch Quoich Line - alimit of early Paleozoic crustal reworking in the Moine of the Northern Highlands of Scotland. *Journal of the Geological Society of London* **140**,883-892.

Roberts, A.M. & Holdsworth, R.E. 1999. Linking onshore and offshore structures: Mesozoic extension in the Scottish Highlands. *Journal of the Geological Society, London,* **156,** 1061-1064.

Roberts, A. M., Smith, D. I. & Harris, A. L. 1984. The structural setting and tectonic significance of the Glen Dessary Syenite, Inverness-shire. *Journal of the Geological Society of London* **141**(6), 1033-1042.

Roberts, A. M., Strachan, R. A., Harris, A. L., Barr, D. & Holdsworth, R. E. 1987. The Sgurr Beag Nappe; a reassessment of the stratigraphy and structure of the Northern Highland Moine. *Geological Society of America Bulletin* **98**(5), 497-506.

Robertson, S. & Smith, M. 1999. The significance of the Geal Charn-Ossian steep belt in basin development in the central Scottish Highlands. *Journal of the Geological Society of London* **156** (6), 1175-1182.

Rock, N. M. S. 1984. Nature and origin of calc-alkaline lamprophyres: minettes, vosgesites, kersantites and spassartites. *Transactions of the Royal Society of Edinburgh, Earth Sciences* **74**, 193-227.

Rock, N. M. S. 1990. Lamprophyres. Kluwer Academic Publishers (Netherlands), 296 p.

Rock, N.M.S., MacDonald, R., Walker, B.H., May, F., Peacock, J.D. & Scott, P. 1985. Intrusive metabasite belts within the Moine assemblage, west of Loch Ness, Scotland: evidence for metabasite modification by country rock interactions. *Journal of the Geological Society, London* **142,** 643-661.

Rogers, G. & Dunning, G. R. 1991. Geochronology of appinitic andrelated granitic magmatism in the W Highlands of Scotland: constraints on the timing of transcurrent fault movement. *Journal of the Geological Society of London* **148**, 17-27.

Rogers, G. & Pankhurst, R. J. 1993. Unravelling dates through the ages; geochronology of the Scottish metamorphic complexes. *Journal of the Geological Society of London* **150** (3), 447-464.

Rogers, G., Paterson, B. A., Dempster, T. J. & Redwood, S. D. 1994. U-Pb geochronology of the 'Newer gabbros', NE Grampians. *In: Caledonian terrane relationships in Britain.* Program with abstracts, British Geologigal Survey, Keyworth, p8.

Rogers, G., Hyslop, E. K., Strachan, R. A., Peterson, B. A. & Holdsworth, R. E. 1998. The structural setting and U-Pb geochronology of Knoydartian pegmatites in W Inverness-shire; evidence for Neoproterozoic tectonothermal events in the Moine of NW Scotland. *Journal of the Geological Society of London* **155** (4), 685-696.

Rogers, G., Kinny, P. D., Strachan, R. A., Friend, C. R. L. & Paterson, B. A. 2001. U-Pb geochronology of the Fort Augustus granite gneiss; constraints on the timing of Neoproterozoic and Palaeozoic tectonothermal events in the NW Highlands of Scotland. *Journal of the Geological Society of London* **158** (1), 7-14.

Rollinson, H. 1993. Using geochemical data. Longman, London.

Roman-Berdiel, T., Gapais, D. & Brun, J.P. 1997. Granite intrusion along strike-slip zones in experiment and nature. *American Journal of Science* **297**, 651-678.

Rubin, A. M. 1995. Getting granite dikes out of the source region. *Journal of Geophysical Research* **100** (4), 5911-5929.

Ryan, P.D. & Soper, N.J. 2001. Modelling anatexis in intra-cratonic rift basins: an example from the Neoproterozoic rocks of the Scottish Highlands. *Geological Magazine* **138**, 577-588.

Samson, S. D. & D'Lemos, R. S. 1999. A precise late Neoproterozoic U-Pb zircon age for the syntectonic Perelle quartz diorite, Guernsey, Channel Islands, UK. *Journal of the Geological Society of London* **156** (1), 47-54.

Saunders, A. D., Tarney, J. & Weaver S. D. 1980. Transverse variations across the Antarctic Peninsula: implications for the genesis of calc-alkaline magmas. *Earth and Planetary Science Letters* **46**, 344-360.

Schmid, S. M. & Handy, M. 1991. Towards a genetic classification of fault rocks: Geological usage and tectonic implications. *In*: Moeller, D. W., McKenzie, J. A. & Weissert. H.(eds): *Controversies in modern geology*. Kluwer Academic press, 339-361.

Schofield, D. I. & D'Lemos, R. S. 1998. Relationships between syn-tectonic granite fabrics and regional PTtd paths; an example from the Gander-Avalon boundary of NE Newfoundland. *Journal of Structural Geology* **20**(4), 459-471.

Schofield, D. I. & D'Lemos, R. S. 2000. Granite petrogenesis in the Gander Zone, NE Newfoundland: mixing of melts from multiple sources and the role of lithospheric delamination. *Canadian Journal of Earth Sciences* **37**, 535-547.

Schofield, D., D'Lemos, R. & King, T. 1996. Evidence and implications for the syntectonic emplacement of the Cape Freels Granite; a Silurian pluton emplaced into the Gander Lake subzone, Northeast Newfoundland. *Newfoundland Department of Natural Resources, Geological Survey Report* **96-1**, 329-342.

Searle, M. P. 1999. Extensional and compressional faults in the Everest-Lhotse massive, Khumbu-Himalaya, Nepal. *Journal of the Geological Society of London* **156**, 227-240.

Searle, M.P., Parrish, R. R., Hodges, K. V. Hurford, A., Ayres, M. W. & Whitehouse, M. J. 1997. The Shishi Pangma leucogranite, south Tibetan Himalaya: Filed relations, geochemistry, age, origin and emplacement. *Journal of Geology* **105**, 295-317.

Smith, D.I. 1979. Caledonian minor intrusions of the N Highlands of Scotland. *In*: Harris A.L., Holland C.H. & Leake B.E. (eds). *The Caledonides of the British Isles – reviewed*. Geological Society of London, Special Publication **8**, 683-697.

Smith, M., Robertson, S. & Rollin, K. E. 1999. Rift basin architecture and stratigraphical implications for basement-cover relationships in the Neoproterozoic Grampian Group of the Scottish Caledonides. *Journal of the Geological Society of London* **156** (6), 1163-1173.

Solar, G. S., Pressley, R. A., Brown, M. & Tucker, R. D. 1998. Granite ascent in convergent orogenic belts: Testing a model. *Geology* **26** (8), 711-714.

Soper, N. J. 1963. The structure of the Rogart igneous complex, Sutherland, Scotland. *Quarterly Journal of the Geological Society of London* **119** (4), 445-478.

Soper, N. J. 1986. The Newer Granite problem; a geotectonic view. *Geological Magazine* **123**(3), 227-236.

Soper, N. J. 1994a. Was Scotland a Vendian RRR junction? *Journal of the Geological Society of London* **151** (4), 579-582.

Soper, N. J. 1994b. Neoproterozoic sedimentation on the northeast margin of Laurentia and the opening of Iapetus. *Geological Magazine* **131**(3), 291-299.

Soper, N. J. 1999. Loch Airighe Bheg. *In*: Stephenson, D., Bevins, R.E., Millward, D., Highton, A.J., Parsons, I., Stone, P. & Wadsworth, W.J. (eds): *Caledonian Igneous Rocks of Great Britain.* Geological Conservation Review Series **17**, .

Soper, N. J. & Brown, P. E. 1971. Relationship between metamorphism and migmatization in the northern part of the Moine Nappe. *Scottish Journal of Geology* 7(4), 305-325.

Soper, N. J. & Wilkinson, P. 1975. The Moine Thrust and Moine Nappe at Loch Eriboll, Sutherland. *Scottish Journal of Geology* **11** (4), 339-359.

Soper, N. J. & Hutton, D. H. W. 1984. Late Caledonian sinistral displacements in Britian; implications for a three-plate collision model. *Tectonics* **3**(7), 781-794.

Soper, N. J. & England, R. W. 1995. Vendian and Riphean rifting in NW Scotland. *Journal of the Geological Society of London* **152**(1), 11-14.

Soper, N. J. & Harris, A. L. 1997. Proterozoic orogeney questioned: a view from the Scottish Highland Field Workshops, 1995-1996. *Scottish Journal of Geology* **33**, 188-190.

Soper, N. J., Harris, A. L. & Strachan, R. A. 1998. Tectonostratigraphy of the Moine Supergroup; a synthesis. *Journal of the Geological Society of London* **155**, (1), 13-24.

Soper, N. J., Ryan, P. D. & Dewey, J. F. 1999. Age of the Grampian Orogeny in Scotland and Ireland *Journal of the Geological Society of London* **156** (6), 1231-1236.

Soper, N. J., England, R. W., Snyder, D. B. & Ryan, P. D. 1992b. The Iapetus suture zone in England, Scotland, and eastern Ireland; a reconciliation of geological and deep seismic data. *Journal of the Geological Society of London* **149** (5), 697-700.

Soper, N. J., Strachan, R. A., Holdsworth, R. E., Gayer, R. A. & Greiling, R. O. 1992. Sinistral transpression and the Silurian closure of Iapetus. *Journal of the Geological Society of London* **149** (6), 871-880.

Steenken, A., Siegesmund, S. & Heinrichs, T. 2000. The emplacement of the Rieserferner Pluton (Eastern Alps, Tyrol); constraints from field observations, magnetic fabrics and microstructures. *Journal of Structural Geology* **22**(11-12), 1855-1873.

Stephens, W. E. & Halliday, A. N. 1984. Geochemical contrasts between late Caledonian granitoid plutons of northern, central and southern Scotland. *Transactions of the Royal Society of Edinburgh* **75** (2), 259-273.

Stephens, W.E. 1988. Granitoid plutonism in the Caledonian orogen of Europe. *In*: Harris, A.L. & Fettes, D.J. (eds) *The Caledonian-Appalachian Orogen.* Geological Society, London, Special Publications, **38**, 389-403.

Stephens, W. E., Holden, P. & Henney, P. J. 1991. Microdioritic enclaves withn the Scottish Caledonian granitoids and their significance for crustal magmatism. *In*: Didier, J. & Barbarin, B. (eds): *Enclaves and granite petrology.* Elsevier, Amsterdam, 125-133.

Stephens, W. E. 1999. The Ratagain Complex. *In*: Stephenson, D., Bevins, R.E., Millward, D., Highton, A.J., Parsons, I., Stone, P. & Wadsworth, W.J. (eds). *Caledonian Igneous Rocks of Great Britain.* Geological Conservation Review Series, **17**,.

Stephenson, D. & Gould, D. 1995. British regional geology: the Grampian Highlands (4th edition). HMSO, London, for the British Geological Survey.

Stephenson, D., Bevins, R.E., Millward, D., Highton, A.J., Parsons, I., Stone, P. & Wadsworth, W.J. 1999. *Caledonian Igneous Rocks of Great Britain.* Geological Conservation Review Series, **17**, 1-648. Joint Nature Conservation Committee.

Stewart, M., Strachan, R.A. & Holdsworth, R.E. 1997. Direct field evidence for sinistral displacements along the Great Glen Fault Zone: late Caledonian reactivation of a regional basement structure? *Journal of the Geological Society, London* **154**, 135-139.

Stewart, M., Strachan, R. A. & Holdsworth, R. E. 1999. Structure and early kinematic history of the Great Glen Fault Zone, Scotland. *Tectonics* **18**, 326-342.

Stewart, M., Strachan, R. A., Martin, M. W. & Holdsworth, R. E. 2001. Constraints on early sinistral movements along the Great Glen Fault Zone, Scotland: structural setting, U-Pb geochronology and emplacement of the syn-tectonic Clunes tonalite. *Journal of the Geological Society of London* **158**(5), 821-830.

Stone, P., Floyd, J. D., Barnes, R. P. & Lintern, B. C. 1987. A sequential back-arc and foreland basin thrust duplex model for the Southern Uplands of Scotland. *Journal of the Geological Society of London* **144**(5), 753-764.

Storey, B. C. & Lintern, B. C. 1981. Geochemistry of the rocks of the Strath Halladale-Altnabreac district. Rep. Inst. Geol. Sci., ENPU 81-12.

Strachan, R. A. 1985. The stratigraphy and structure of the Moine rocks of the Loch Eil area, West Inverness-shire. *Scottish Journal of Geology* **21**(1), 9-22.

Strachan, R. A. 1988. The metamorphic rocks of the Scaraben area, East Sutherland and Caithness. *Scottish Journal of Geology* **24**(1), 1-13.

Strachan, R. A. & Holdsworth, R. E. 1988. Basement-cover relationships and structure within the Moine rocks of central and Southeast Sutherland. *Journal of the Geological Society of London* **145**(1), 23-36.

Strachan, R. A., Martin, M. W. & Friderichsen, J. D. 2001. Evidence for contemporaneous yet contrasting styles of granite magmatism during extensional collapse of the northeast Greenland Caledonides. *Tectonics* **20**(4), 458-473.

Tanner, P. W. G. & Bluck, B. J. 1999. Current controversies in the Caledonides; introduction. *Journal of the Geological Society of London* **156** (6), 1137-1141.

Tanner, P. W. G., Johnstone, G. S., Smith, D. I. & Harris, A. L. 1970. Moinian stratigraphy and the problem of the central Ross-shire inliers. *Geological Society of America Bulletin* **81**(1), 299-305.

Tarney, J. & Jones, C. E. 1994. Trace element geochemistry of orogenic igneous rocks and crustal growth models. *Journal of the Geological Society of London* **151**(5) 855-868.

Taylor, S. T. & McLennan, S. M. 1985. *The continental crust: its composition and evolution.* Blackwell Scientific Publications, Oxford.

Tera, F., Brown, L., Morris, J., Sacks, I. S., Klein, J. & Middleton, R. 1986. Sediment incorporation in island-arc magmas; inferences from ^{10}Be. *Geochimica et Cosmochimica Acta* **50**(4), 535-550.

Thirlwall, M. F. 1981. Implications for Caledonian plate tectonic models of chemical data from volcanic rocks of the British Old Red Sandstone. *Journal of the Geological Society of London* **138** (2), 123-138.

Thirlwall, M. F. 1982. Systematic variation in chemistry and Nd-Sr isotopes across a Caledonian calc-alkaline volcanic arc; implications for source materials. *Earth and Planetary Science Letters* **58**(1), 27-50.

Thirlwall, M. F. 1983. Systematic variation in chemistry and Nd-Sr isotopes across a Caledonian calc-alkaline volcanic arc; implications for source materials; reply. *Earth and Planetary Science Letters* **65**(1), 208.

Thirlwall, M. F. 1986. Lead isotope evidence for the nature of the mantle beneath Caledonian Scotland. *Earth and Planetary Science Letters* **80**, 55-70.

Thirlwall, M. F. 1988. Geochronology of late Caledonian magmatism in northern Britain. *Journal of the Geological Society of London* **145** (6), 951-967.

Thirlwall, M. F. & Jones, H. W. 1983. Isotope geochemistry and contamination mechanisms of Tertiary Lavas from Skye, NW Scotland. *In*: Hawksworth, C.J. & Norry, M. J.(eds): *Continental basalts and mantle xenoliths*. Shiva geology series, 186-208.

Thirlwall, M. F. & Burnard, P. 1990. Pb-Sr-Nd isotope and chemical studies of the origin of undersaturated and oversaturated shoshonitic magmas from the Borralan Pluton, Assynt, NW Scotland. *Journal of the Geological Society of London* **147**(2), 259-269.

Thompson, R. N. 1985. Model for Grampian tract evolution. *Nature (London)* **314**, 562.

Thompson, R. N. & Fowler, M. B. 1986. Subduction-related shoshonitic and ultrapotassic magmatism; a study of Siluro-Ordovician syenites from the Scottish Caledonides. *Contributions to Mineralogy and Petrology* **94**(4), 507-522.

Tikoff, B. & Tessier, C. 1992. Crustal –scale, en-echelon "P-shear" tensional bridges: a possible solution to the batholithic room problem. *Geology* **20**, 927-930.

Tikoff, B. , De Saint Blanquat, M. & Tessier, C. 1999. Translation and the resolution of the space problem. *Journal of Structural Geology* **21**, 1109-1117.

Tobisch, P. T., Fleuty, M. J., Merh, S. S., Mukhopadyay, D. & Ramsay, J. G. 1970. Deformational and metamorphic history Moinian and Lewisian rocks between Strathconon and Glen Affric. *Scottish Journal of Geology* **6**, 243-265.

Tommasi, A., Vauchez, A., Fernandes, L.A.D. & Porcher, C.C. 1994. Magma-assisted strain localization in an orogen parallel transcurrent shear zone of southern Brazil. *Tectonics* **13**, 421-437.

Torsvik, T. H., Storevedt, K. M. & Loevlie, R. 1983. Multicomponent magnetization in the Helmsdale granite, NE Scotland. *Tectonophysics* **98**(1-2), 111-129.

Tribe, I. R. & D'Lemos, R. S. 1996. Significance of a hiatus in down-temperature fabric development within syntectonic quartz diorite complexes, Channel Islands, UK. *Journal of the Geological Society of London* **153** (1), 127-138.

Tweedie, J. R. 1979. Origin of uranium and other metal enrichments in the Helmsdale Granite, eastern Sutherland, Scotland. *Institution of Mining and Metalurgy*, B145-153.

Upton, B. G. J., Aspen, P., Hunter, R. H. & Bowes, D. R. c. 1984. Xenoliths and their implications for the deep geology of the Midland Valley of Scotland and adjacent regions. *Transactions of the Royal Society of Edinburgh* **75** (2), 65-70.

Van Breemen, O. & Bluck, B. J. 1981. Episodic granite plutonism in the Scottish Caledonides. *Nature (London)* **291**(5811), 113-117.

Van Breemen, O., Pidgeon, R. T. & Johnson, M. R. W. 1974. Precambrian and Palaeozoic pegmatites in the Moines of northern Scotland. *Journal of the Geological Society of London* **130**(6), 493-507.

Van Breemen, O., Aftalion, M. & Johnson, M. R. W. 1979b. Age of the Loch Borrolan Complex, Assynt, and late movements along the Moine thrust zone. *Journal of the Geological Society of London* **136** (4), 489-495.

Van Breemen, O., Aftalion, M., Pankhurst, R. J. & Richardson, S. W. 1979a. Age of the Glen Dessary Syenite, Inverness-shire; diachronous Palaeozoic metamorphism across the Great Glen. *Scottish Journal of Geology* **15, Part 1**, 49-62.

Van Der Molen, I. & Paterson, M. S. 1979. Experimental deformation of partially-melted granite. *Contributions to mineralogy and petrology* **70**, 299-318.

Vance, D., Strachan, R. A. & Jones, K. A. 1998. Extensional versus compressional settings for metamorphism; garnet chronometry and pressure-temperature-time histories in the Moine Supergroup, Northwest Scotland. *Geology* **26**(10), 927-930.

Varne, R. 1985. Ancient subcontinental mantle; a source for K-rich orogenic volcanics. *Geology* **13**(6), 405-408.

Vernon, R. H., Paterson, S. R., Geary, E.E. 1989. Evidence for syntectonic intrusion of plutons in the Bear Mountains fault zone, California. *Geology* **17**, 723-726.

Vigneresse, J. L. 1995. Control of granite emplacement by regional deformation. *Tectonophysics* **249**(3-4), 173-186.

Vigneresse, J. L. & Tikoff, B. 1999. Strain partitioning during partial melting and crystallizing felsic magmas. *Tectonophysics* **312**, 117-132.

Von Blanckenburg, F. & Davies, J. H. 1995. Slab breakoff; a model for syncollisional magmatism and tectonics in the Alps. *Tectonics* **14**(1), 120-131.

Watson, J. 1948. Late sillimanite in the migmatites of Kildonan, Sutherland. *Geological Magazine* **85**, 145-158.

Watson, J. 1984. The ending of the Caledonian Orogeny in Scotland. *Journal of the Geological Society of London* **141**, 193-214.

Watt, G.R., Burns, I.M. & Graham, G.M. 1996. Chemical characteristics of migmatites: accessory phase distribution and evidence for fast melt segregation rates. *Contributions to Mineralogy and Petrology* **125**, 100-111.

Weaver B.L.1991. The origin of ocean island basalt end-member compositions: trace element and isotopic constraints. *Earth and Planetary Science Letters*, **104**, 381-397.

Weinberg, R. F. & Podlachikov, Y. Y. 1994. Diapiric ascent of magmas through power law crust and mantle. *Journal of Geophysical Research* **99**, 9543-9559.

Weinberg, R. F. & Searle, M.P. 1999. Volatile-asited intrusion and autometasomatism of leucogranites in the Khumbu Himalaya, Nepal. *The Journal of Geology* **107**, 27-48.

Whalen, J.B, Jenner, G.A., Longstaffe, F.J. & Hegner, E. 1996a. Nature and evolution of the eastern margin of Iapetus: geochemical and isotopic constraints from Siluro-Devonian granitoid plutons in the New Brunswick Appalachians. *Canadian Journal of Earth Sciences* **33**, 140-155.

Whalen, J. B., Jenner, G. A., Hegner, E. Gariepy, C. & Longstaffe, F. J. 1994. Geochemical and isotopic (Nd, O, Pb) constraints on granite sources in the Humber and Dunage zones, Gaspesie, Quebec, and New Brunswick; implications for tectonics and crustal structure. *Canadian Journal of Earth Sciences* **31**(2), 323-340.

White, A. J. R. & Chappell, B. W. 1977. Ultrametamorphism and granitoid genesis. *Experimental petrology related to extreme metamorphism* **43**(1-2), 7-22.

Whithington, A. G. & Treloar, P. J. 2002. Crustal anatexis and its relation to the exhumation of collisional orogenic belts, with particular reference to the Himalaya. *Mineralogical Magazine* **66** (1), 53-91.

Wilson, D. 1975. *Structure and metamorphism of the Ben Wyvis District, Ross-shire.* PhD thesis, Edinburgh University.

Wilson, D. & Shepherd, J. 1979. The Carn Chuinneag granite and its aureole. *In*: Harris, A. L., Holland, C. H. & Leake, B. E. (eds):*The Caledonides of the British Isles – Reviewed.* Geological Society of London, Special Publication **8** 669-675.

Wilson, M. 1989. Igneous petrogenesis. Unwin Hyman, London.

Winchester, J. A. 1985. Major low-angle fault displacement measured by matching amphibolite chemistry; an example from Scotland. *Geology* **13**(9), 604-606.

Zindler, A. & Hart, S. 1986. Chemical geodynamics. *Ann. Rev. Earth Planetary Science Letters* **14**, 493-571.

Appendices

Appendix 1: a) Glossary of lamprophyres with particular respect to the Scottish Caledonides after Rock (1991).

b) Classification of igneous rocks after Le Maitre (1989).

Appendix 2: Geochemical data

Appendix 1

Glossary of lamprophyres with particular respect to the Scottish Caledonides after Rock (1991).

Ach'Uaine hybrid suite. A suite of highly heterogeneous, olivine-hhornblende-biotite-rich rocks forming irregular, pipe-like bodies satellite to Caledonian granitoid plutons in Sutherland, Scotland. Range from ultramafic rocks (e.g. Scyelite) to acidic rocks, with intermediate members formed by hybridisation of the two. Associated with calc-alkaline lamprophyre dykes, and closely related to the Appinite suite. Type locality Achu'aine, Sutherland, Scotland.

Appinite. Originally defined by Bailey & Maufe (1916) as "plutonic equivalents of the hornblende vogesites and spessartites" (see Bailey 1960). Often used to describe unrelated, hornblende-phyric minor intrusions ranging from gabbro to granodiorite. Restricted by Rock (1991) to coarse-grained, K-rich, mafic equivalents of vogesites and spessartites, consisting essentially of abundant stumpy or prismatic hornblende ± clinopyroxene, in a matrix of plagioclase ± alkali feldspar. The type appinites of Appin, Argyll (Scotland) are predominantly gabbroic, but many contain biotite and are more K-rich than normal gabbros.

Appinite suite. Restricted by Rock (1991) to describe pipes and diatremes intimately associated with Caledonian dyke-swarms and granitoids. Covers the rock-types Ach'Uaine hybrid, appinite, kentallinite, scyelite, as well as various hornblende ± biotite-rich ultramafic, monzonitic, granodioritic and syenitic rocks. Excludes the older and variably metamorphosed *microdiorite suite* of D. I. Smith (1979), which in turn excludes the *West Highland appinite suite* of MacGregor & Kennedy (1931).

Calc-alkaline lamprophyres. A group of lamprophyres consisting of the rock-types minette, vogesite, kersantite, spessartite, appinite and kentallinite, which correspond very roughly to andesites but are considerably enriched in volatile elements (H2O, CO2, F, Cl), and in LILE and mafic-ultramafic elements (K, Rb, Ba, Mg, Cr, Ni, etc.). More closely approximated geochemically by some shoshonites and absarokites.

Kentallinite. A K- and Mg-rich rock belonging to the appinite suite; plutonic equivalent to vogesite and spessartite. Type locality Kentallen, Appin, Argyle, Scotland.

Lamprophyre. Term coined by Gümbel (1874) for dyke-rocks from Germany with glistening biotite phenocrysts.

Lamprophyric rock. Group term recommended by the IUGS (Le Maitre 1989) to cover lamprophyres, lamproites and kimberlites.

Minette. A calc-alkaline lamprophyre consisting of phenocrysts of phlogopite-biotite, with or without subordinate calcic or alkali amphibole, forsteritic olivine or diopsidic clinopyroxene, in a groundmass of the same plus alkali feldspar and subordinate plagioclase.

Scyelite. An obscure local term for biotite-hornblende-peridotites of the Ach'Uaine hybrid suite, from Loch Scye, Sutherland Scotland.

Spessartite. A calc-alkaline lamprophyre consisting of phenocrysts of calcic hornblende, with or without subordinate phlogopite-biotite, forsteritic olivine or diopsidic clinopyroxene, in a groundmass of the same plus plagioclase and sub-ordinate K-feldspar. Type locality, Spessart, Germany.

Vogesite. Rare variety of calc-alkaline lamprophyre consisting of phenoccrysts of calcic hornblende, with or without subordinate phlogopite-biotite, forsteritic olivine or diopsidic clinopyroxene, in a groundmass of the same plus K-feldspar and subordinate plagioclase. Type locality, Vosges Mtns., France.

QAPF - M<90%

M<10%="anorthosite"
M>10% & plag>An_{50}="gabbro"
M>10% & plag<An_{50}="diorite"

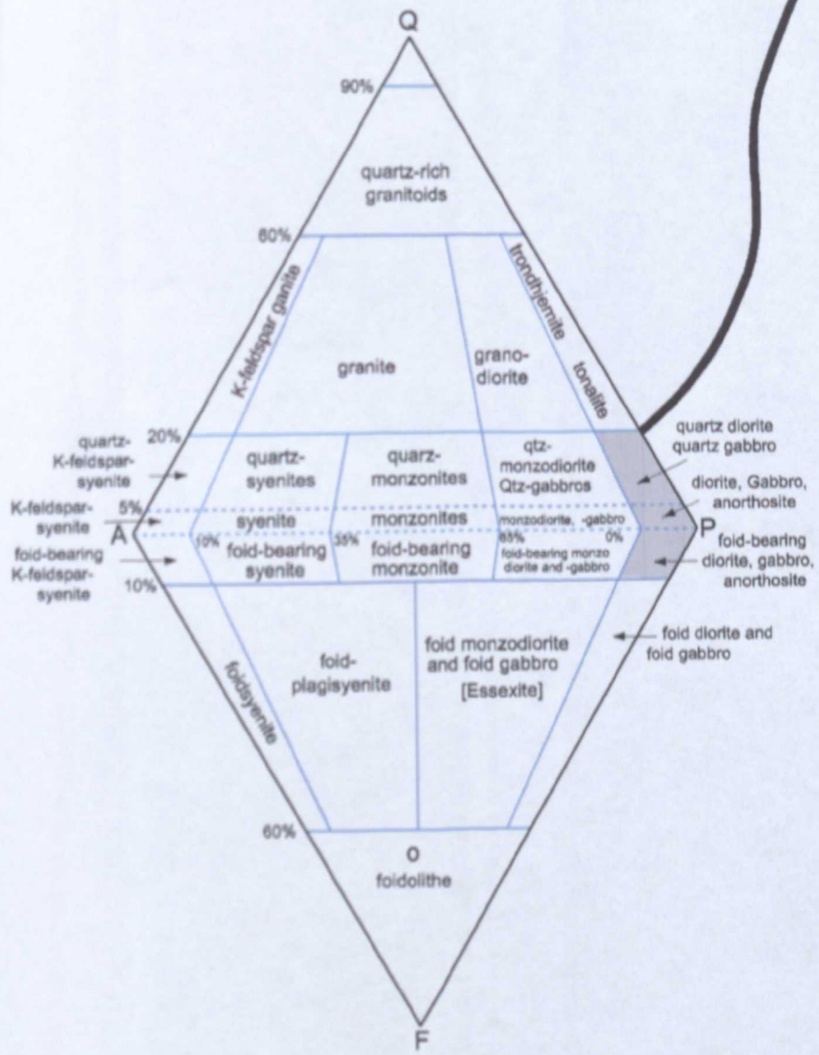

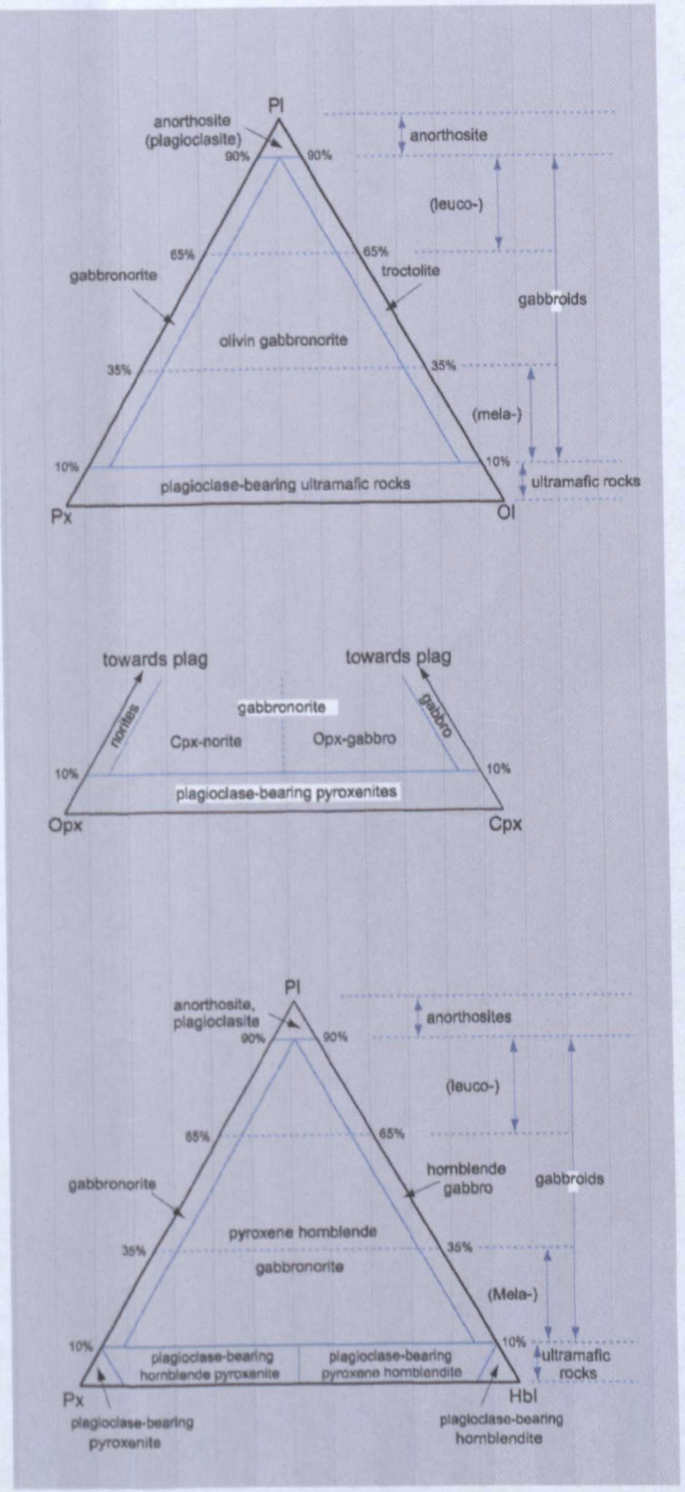

Ultramafic Rocks - M>90%

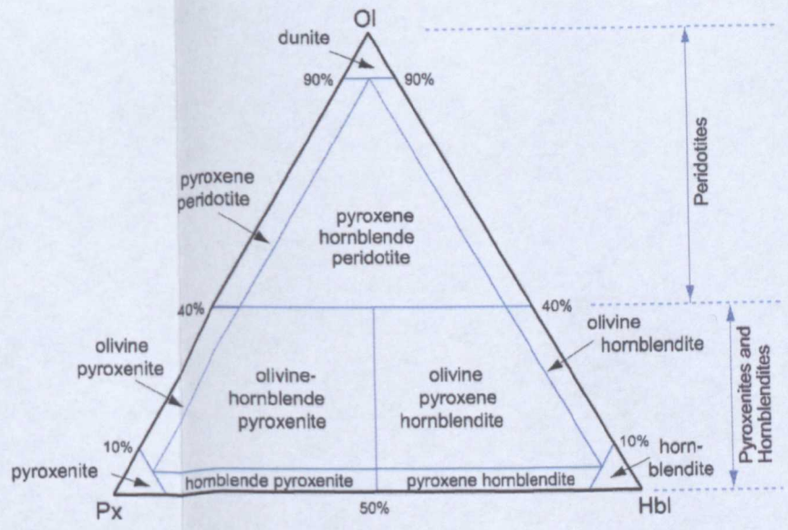

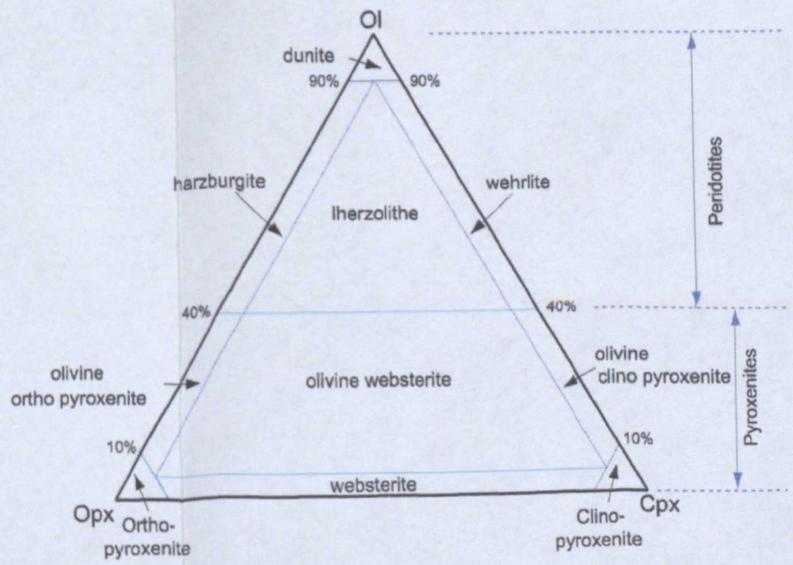

Appendix 1b
Classification of igneous rocks after Le Maitre 1989.

Appendix 2

Sample	1058/1	1058/2	1059	1064	1085	1090/3
lithology	leucogranite	leucogranite	leucogranite	leucogranite	leucogranite	leucogranite
Majors						
SiO2 %	70.22	67.22	64.63	67.21	*	65.7
TiO2 %	0.6	0.88	0.63	0.59	*	0.51
Al2O3 %	14.21	15.56	17.47	16.97	*	18.19
Fe2O3 %	3.4	4.96	3.69	3.3	*	2.54
MnO %	0.07	0.08	0.07	0.05	*	0.05
MgO %	1.75	1.65	2.24	1.55	*	1.28
CaO %	2.13	1.54	2.5	2.4	*	2.92
Na2O %	3.73	3.56	5.47	4.7	*	5.58
K2O %	3.42	4.35	2.83	3.94	*	3.39
P2O5 %	0.22	0.41	0.28	0.24	*	0.18
LOI %	0.54	0.69	0.9	0.61	*	0.75
Total %	100.29	100.9	100.72	101.53	*	101.09
Traces	ppm	ppm	ppm	ppm	ppm	ppm
K	*	*	*	*	*	*
Ba	953	1204	1266	1220	*	829.49
Rb	*	*	*	*	*	*
Sr	663.4	335.9	1285	963.7	*	1240
Ga	*	*	*	*	*	*
P	*	*	*	*	*	*
Nb	*	*	*	*	*	*
Zr	279.74	345.38	234.97	213.9	*	198.26
Ti	*	*	*	*	*	*
Y	22.9	40	4	21.6	*	21.64
Th	*	*	*	*	*	*
U	*	*	*	*	*	*
Cr	53.7	53.55	52.46	26.95	*	31.95
Ni	*	*	*	*	*	*
Sc	*	*	*	*	*	*
V	*	*	*	*	*	*
Cu	*	*	*	*	*	*
Pb	*	*	*	*	*	*
Zn	*	*	*	*	*	*
La	37.2	49.31	78.2	49.9	59.4	74.6
Ce	67.9	95.97	111	85	117	109
Pr	8.14	11.1	11.7	9.77	13.5	13.6
Nd	25.5	38.1	32	37.6	46.1	45.6
Sm	4.23	6.82	3.54	5.45	8.11	7.49
Eu	1.04	1.58	1.03	1.42	1.35	1.83
Gd	4.12	6.21	3.15	4.74	7.18	6.12
Dy	2.89	5.38	1.12	3.46	5.55	3.69
Er	2.47	4.21	1.34	2.42	3.65	2.61
Yb	1.6	3.54	0.48	1.42	2.11	1.71
Lu	0.29	0.6	0.13	0.25	0.37	0.31

Major selected trace elements and REE analyzed by ICP AES at Oxford Brookes University.

* = not analyzed

Rogart

Sample	1108	1145	1146	988	DAL782	L696
lithology	leucogranite	leucogranite	leucogranite	leucogranite	leucogranite	Moine amphibolite gneiss
Majors						
SiO2 %	*	*	*	74.57	64.631	65.46
TiO2 %	*	*	*	0.17	0.6442	0.99
Al2O3 %	*	*	*	15.29	17.392	14.83
Fe2O3 %	*	*	*	0.89	3.481	6.4
MnO %	*	*	*	0.02	0.0506	0.1
MgO %	*	*	*	0.51	1.7979	1.9342
CaO %	*	*	*	1.38	1.8209	2.0669
Na2O %	*	*	*	4.73	5.094	2.6167
K2O %	*	*	*	4.25	3.2595	3.2309
P2O5 %	*	*	*	0.06	0.1786	0.4782
LOI %	*	*	*	0.61	1.21	0.78
Total %	*	*	*	102.48	99.56	98.887
Traces	ppm	ppm	ppm	ppm	ppm	ppm
K	*	*	*	*	27058	26821
Ba	*	*	*	1084	1492.2	642.88
Rb	*	*	*	*	*	*
Sr	*	*	*	1067	1091	283.22
Ga	*	*	*	*	*	*
P	*	*	*	*	778.7	2084.95
Nb	*	*	*	*	*	*
Zr	*	*	*	93.7	226.92	479.52
Ti	*	*	*	*	3862	5935
Y	*	*	*	*	22.509	51.244
Th	*	*	*	*	*	*
U	*	*	*	*	*	*
Cr	*	*	*	10.3	35.893	70.466
Ni	*	*	*	*	*	*
Sc	*	*	*	*	*	*
V	*	*	*	*	*	*
Cu	*	*	*	*	*	*
Pb	*	*	*	*	*	*
Zn	*	*	*	*	*	*
La	61.9	37.5	13.12	10.87	79.3	57.1
Ce	110	63.9	22.94	23.42	99.1	118
Pr	12	7.02	2.93	2.95	11.9	13.8
Nd	35.9	20.5	8.79	9.37	36.3	48.4
Sm	5.33	2.84	1.26	1.49	5.76	8.83
Eu	1.41	0.69	0.48	0.49	1.5	1.66
Gd	4.79	2.63	1.24	1.52	3.824	8.05
Dy	3.7	1.42	0.55	0.82	3.31	6.86
Er	2.94	1.38	0.63	0.88	1.14	5.17
Yb	1.92	0.73	0.24	0.41	1.25	3.72
Lu	0.31	0.15	0.06	0.09	0.216	0.662

Major selected trace elements and REE analyzed by ICP AES at Oxford Brookes University.

* = not analyzed

Rogart

Sample	ps	spg
lithology	Morar psammite	Morar s-pel. Gneiss
Majors		
SiO2 %	*	*
TiO2 %	*	*
Al2O3 %	*	*
Fe2O3 %	*	*
MnO %	*	*
MgO %	*	*
CaO %	*	*
Na2O %	*	*
K2O %	*	*
P2O5 %	*	*
LOI %	*	*
Total %	*	*
Traces	ppm	ppm
K	*	*
Ba	*	*
Rb	*	*
Sr	*	*
Ga	*	*
P	*	*
Nb	*	*
Zr	*	*
Ti	*	*
Y	*	*
Th	*	*
U	*	*
Cr	*	*
Ni	*	*
Sc	*	*
V	*	*
Cu	*	*
Pb	*	*
Zn	*	*
La	12.54	40.83
Ce	27.42	77.3
Pr	3.5	8.86
Nd	12.96	27.7
Sm	2.02	4.67
Eu	0.5	1.09
Gd	2.13	4.19
Dy	1.53	2.98
Er	1.44	2.3
Yb	0.96	1.33
Lu	0.18	0.23

Major selected trace elements and REE analyzed by ICP AES at Oxford Brookes University.
* = not analyzed

Strath Halladale

Sample	SHG 112-A2	SHG 112A1	SHG 131B	SHG 453
lithology	granodiorite / granite	granodiorite / granite	granodiorite / granite	hornblendite
Majors				
SiO2 %	70.571	69.755	69.212	50.227
TiO2 %	0.2889	0.3019	0.2529	1.4061
Al2O3 %	15.79	15.758	16.764	14.985
Fe2O3 %	1.6269	1.71	1.3308	12.022
MnO %	0.0234	0.0279	0.0187	0.1964
MgO %	0.612	0.5601	0.4255	7.5919
CaO %	1.9176	2.1286	1.2257	7.5138
Na2O %	4.9903	4.7571	4.9294	1.8848
K2O %	3.4274	3.1624	4.8857	2.8201
P2O5 %	0.007	0.0029	0.005	0.8946
LOI %	0.45	0.33	0.57	1.13
Total %	99.705	98.494	99.615	100.67
Traces	ppm	ppm	ppm	ppm
K	28452	26252	40558	23410
Ba	1172	1060	1447	453
Rb	77.5	75.6	94.8	11.8
Sr	801.8	796.9	913.8	468.6
Ga	20.5	20.6	17.5	20.1
P	30.52	12.64	21.8	3900.46
Nb	9.8	10.3	4.6	17.5
Zr	179.4	176.7	140.3	131.29
Ti	1732	1810	1516	8430
Y	7.6	7.6	12.5	21.9
Th	20.9	19.5	7	2.1
U	2.1	2.9	2.7	1
Cr	4	10	8	345
Ni	3	1	3	218
Sc	4.3	7.8	4.8	23.4
V	27	21.8	17.5	120.3
Cu	4.3	1	1.6	6.6
Pb	29.3	25.5	24.7	5.6
Zn	34	37	14	105
La	45.6	39.1	48	26.6
Ce	*	*	52.2	23.5
Pr	*	*	6.81	4.24
Nd	22.1	25.6	20.2	16.5
Sm	*	*	3.08	3.92
Eu	*	*	0.728	1.28
Gd	*	*	2.472	5.704
Dy	*	*	2.05	3.72
Er	*	*	0.78	1.165
Yb	*	*	0.74	1.69
Lu	*	*	0.148	0.304

Major elements and REE analyzed by ICP AES at Oxford Brookes University.
Other trace elements analyzed by XRF at Leicester University.
* = not analyzed

Strath Halladale

Sample lithology	SHG 65 Px-bearing hornblendite	SHG 877 granodiorite / granite	SHG 90B granodiorite / granite
Majors			
SiO2 %	48.997	70.614	71.277
TiO2 %	0.6951	0.2314	0.2351
Al2O3 %	7.6901	16.237	16.158
Fe2O3 %	8.3634	1.4453	1.4389
MnO %	0.1842	0.0295	0.0202
MgO %	16.276	0.4284	0.5231
CaO %	12.768	2.2725	2.5221
Na2O %	1.3165	5.2714	5.4531
K2O %	1.4731	2.2776	1.6779
P2O5 %	0.6338	0.005	0.005
LOI %	2.62	0.46	0.49
Total %	101.02	99.267	99.795
Traces	ppm	ppm	ppm
K	12229	18907	13929
Ba	448	875	528
Rb	46.3	71.5	47
Sr	301.4	879.4	944.4
Ga	10.6	18.1	18
P	2763.37	21.8	21.8
Nb	11.7	7.2	4.6
Zr	142.23	153.3	139
Ti	4167	1387	1409
Y	31	12.3	6.3
Th	8.7	7.9	7.9
U	1.4	1	0.8
Cr	1477	11	10
Ni	339	1	3
Sc	37.5	4	4.5
V	121.2	13.7	16.9
Cu	5.1	0.7	1
Pb	2.8	21.1	15.5
Zn	100	18	19
La	48.7	32.5	32.1
Ce	110	47.9	42.8
Pr	14	5.36	4.86
Nd	55.5	18.4	15.3
Sm	9.95	2.42	1.98
Eu	2.42	0.686	0.598
Gd	*	1.728	1.432
Dy	5.15	1.72	1
Er	1.675	0.695	0.435
Yb	2.02	0.79	0.418
Lu	0.343	0.148	0.0935

Major elements and REE analyzed by ICP AES at Oxford Brookes University.
Other trace elements analyzed by XRF at Leicester University.
* = not analyzed

Strath Halladale

Sample lithology	SHG 97 granodiorite / granite	SHG C granodiorite / granite	SHG132 granodiorite / granite	SHG403 quartz diorite
Majors				
SiO2 %	73.046	69.692	71.002	54.774
TiO2 %	0.2092	0.2356	0.2243	1.0453
Al2O3 %	15.202	16.274	14.961	19.28
Fe2O3 %	1.1914	1.496	1.3774	6.3124
MnO %	0.0163	0.0212	0.0322	0.08
MgO %	0.4328	0.4959	0.4614	3.4948
CaO %	1.7559	1.9844	1.8497	5.19
Na2O %	5.0699	4.1726	5.1169	5.1819
K2O %	3.288	3.2995	3.0873	2.9262
P2O5 %	0.005	0.005	0.005	0.4388
LOI %	0.58	0.78	0.44	0.75
Total %	100.79	98.451	98.552	99.473
Traces	ppm	ppm	ppm	ppm
K	27295	27390	25629	24291
Ba	1332	1371	1201	1876
Rb	66.4	72	76.8	76.9
Sr	803.7	747.7	728.6	2024
Ga	16.3	17.6	17.6	24.9
P	21.8	21.8	21.8	1913.17
Nb	3.9	6.1	6.1	10.5
Zr	131.3	141.6	122.5	504
Ti	1254	1412	1345	6267
Y	3.2	7.6	8.2	12.8
Th	11.9	11.2	11.2	12.9
U	0.7	1	1	1
Cr	3	3	5	75
Ni	3	3	3	30
Sc	4.7	5.6	1	14.2
V	16.5	20.8	17.2	120
Cu	4.8	0.7	2.4	20.8
Pb	20.1	21.6	28.4	13.3
Zn	13	25	22	86
La	38.2	36.8	39.9	122
Ce	43.8	52.2	41	168
Pr	5.67	6.28	5.28	17.8
Nd	17.4	18.8	16.7	48.8
Sm	2.22	2.54	2.33	5.68
Eu	0.625	0.661	0.662	1.83
Gd	1.872	2.112	1.848	5.54
Dy	0.973	1.39	1.4	2.53
Er	0.57	0.665	0.59	1.47
Yb	0.333	0.445	0.632	1.07
Lu	0.0965	0.113	0.133	0.268

Major elements and REE analyzed by ICP AES at Oxford Brookes University.
Other trace elements analyzed by XRF at Leicester University.
* = not analyzed

Strath Halladale

Sample	SHG450	PMG	SHG 96B
lithology	Px-bearing hornblendite	aplite	granodiorite / granite
Majors			
SiO2 %	49.8	72.852	71.025
TiO2 %	0.3807	0.0916	0.2092
Al2O3 %	3.9084	14.087	14.92
Fe2O3 %	8.8028	0.6629	1.1808
MnO %	0.1852	0.0067	0.014
MgO %	17.299	0.0615	0.4228
CaO %	14.104	0.1786	1.5418
Na2O %	0.5391	4.6672	4.7445
K2O %	0.6272	5.7031	3.9627
P2O5 %	0.6319	0	0.005
LOI %	2.82	0.33	0.45
Total %	99.098	98.641	98.471
Traces	ppm	ppm	ppm
K	5207	47343	32896
Ba	209	987	1862
Rb	14.7	131.3	71.3
Sr	269.2	200.5	726.1
Ga	6.8	12.6	16.9
P	2755.08	0	21.8
Nb	0.9	6.9	4.1
Zr	73.645	61	126.1
Ti	2282	549	1254
Y	14.1	8.2	4.7
Th	3.8	4.5	9.5
U	2.3	1	1
Cr	1388	5	3
Ni	276	3	3
Sc	61.1	2.3	1.1
V	179.3	10.4	17.9
Cu	11.2	2.8	1.1
Pb	0.2	16.4	23.7
Zn	69	1	15
La	13.9	7.9	25.7
Ce	15.6	*	30.1
Pr	2.4	*	3.41
Nd	12.7	4.2	11.3
Sm	2.54	*	1.35
Eu	0.667	*	0.512
Gd	3	*	1.056
Dy	2.01	*	0.826
Er	0.55	*	0.3345
Yb	0.922	*	0.35
Lu	0.153	*	0.083

Major elements and REE analyzed by ICP AES at Oxford Brookes University.
Other trace elements analyzed by XRF at Leicester University.
* = not analyzed

Reay

Sample	RD 94	RD1	RD2	RD3	RD4	RD80
lithology	quartz diorite	quartz diorite	Bt-amphibolite enclave	Bt-amphibolite enclave	Bt-amphibolite enclave	quartz diorite
Majors						
SiO2 %	58.179	46.66	47.32	48.46	49.29	57.857
TiO2 %	0.8704	1.5	1.71	1.59	1.5	0.7792
Al2O3 %	14.796	19.49	12.54	12.32	12.63	14.922
Fe2O3 %	6.4044	9.28	12.19	11.8	11.27	5.9098
MnO %	0.1103	0.07	0.19	0.21	0.18	0.0906
MgO %	5.8471	3.77	8.77	9.03	8.32	5.6547
CaO %	6.0604	7.03	6.86	5.68	5.96	5.2607
Na2O %	4.2886	3.63	2.12	1.7	2	4.1859
K2O %	2.841	3.34	2.42	3.56	3	3.3194
P2O5 %	0.4479	0.69	1	0.98	0.92	0.3392
LOI %	1.17	2.28	1.26	1.33	1.25	1.34
Total %	101.02	97.74	96.38	96.66	96.32	99.659
Traces	ppm	ppm	ppm	ppm	ppm	ppm
K	23584	27726	20089	29553	24904	27555
Ba	1157	2686	514	908	795	1346
Rb	83.8	97.4	77.1	138.5	107.1	81
Sr	1283.7	3013	593.3	571.8	694.7	1337.8
Ga	19.3	26.4	21.6	21.6	20.7	17.8
P	1952.84	3008.4	4360	4272.8	4011.2	1478.91
Nb	17.9	7.9	18.6	19.6	15.2	13.9
Zr	212	81.5	137.7	123.4	115	227.5
Ti	5218	8993	10251	9532	8993	4671
Y	26.8	18.5	26.4	29.3	30.7	24
Th	16.4	6	4.2	4.8	2.6	15.5
U	2.5	1	1	1	1.9	1.2
Cr	193	14	439	441	410	203
Ni	100	15	226	236	181	102
Sc	19.1	10.8	25.9	22.8	23.6	15.7
V	129.4	264.5	202.7	203.3	192.5	115.2
Cu	11.3	15.2	12.7	22.1	17.2	12.3
Pb	18.3	10.9	11.5	7.8	10.2	21.5
Zn	82	106	133	145	125	71
La	106	58.23	23.08	18.14	18.6	118
Ce	169	106.89	33.32	36.64	35.34	152
Pr	19.4 *	*	*	*		18.3
Nd	64	58.64	21.78	23.07	21.93	58.1
Sm	9.97	9.29	4.73	5.55	4.63	8.87
Eu	2.38	2.77	1.79	1.66	1.68	2.27
Gd	7.656	7.17	5.99	5.66	5.9	7.528
Dy	4.87	3.4	4.44	4.59	4.39	4.41
Er	1.695	1.82	1.9	2.19	2.14	1.535
Yb	1.92 *		1.76	2.23	2.13	1.7
Lu	0.357 *	*	*	*		0.337

Major elements and REE analyzed by ICP AES at Oxford Brookes University.
Other trace elements analyzed by XRF at Leicester University.
* = not analyzed

Sample lithology	HG159As appinitic enclave	HG252 mixed granite	iHG1 adamellite	iHG310 adamellite	iHG317 adamellite	iHG337 adamellite
Majors						
SiO2 %	54.124	73.744	72.265	73.353	72.368	72.262
TiO2 %	0.8507	0.2085	0.3111	0.2806	0.2888	0.3015
Al2O3 %	13.007	13.48	14.494	14.452	14.887	14.971
Fe2O3 %	5.0991	0.9413	1.2578	1.4011	1.4655	1.3416
MnO %	0.1674	0.0004	0.0116	0.0216	0.0331	0.0243
MgO %	3.943	0.0938	0.2829	0.3719	0.5895	0.5036
CaO %	7.408	0.3321	0.6734	0.3131	1.141	1.001
Na2O %	2.456	4.0176	4.2352	4.6559	4.9237	4.9569
K2O %	6.819	4.8888	5.1853	5.134	4.4953	4.5672
P2O5 %	0.3469	0.0476	0	0.0015	0.0092	0.009
LOI %	3.91	0.45	0.63	0.63	0.78	0.92
Total %	98.131	98.204	99.346	100.61	100.98	100.85
Traces	ppm	ppm	ppm	ppm	ppm	ppm
K	56607	40583	43045	42619	37317	37914
Ba	1733	1054	1370	1040	1353	1327
Rb	263.2	215.3	172.3	168.9	193	168.1
Sr	1029.8	288.8	618	336.8	715.4	562.3
Ga	18.6	21.9	20.3	19.6	19.8	19.3
P	1512.48	207.54	0	6.54	40.11	39.24
Nb	23.3	19.6	13.3	13.8	14.4	12.7
Zr	380.3	136.5	173.9	161.9	163.8	168.2
Ti	5100	1250	1865	1682	1731	1807
Y	30.1	6.8	7.6	7.8	7.9	8.6
Th	50.9	29.5	25.3	29.9	17.8	21.6
U	6.8	1	8.3	6.3	3.2	5.1
Cr	189	298	3	6	7	9
Ni	131	3	3	3	3	3
Sc	15.1	3.2	3.2	4.1	4.9	2.9
V	102.9	19.2	24.9	23	26.6	28.1
Cu	7	3.1	9.6	2.9	2.1	2.2
Pb	67.9	29.7	32	22.5	46.6	34.9
Zn	86	1	15	22	32	26
La	190	26.1	35.4	32.9	47.7	46.4
Ce	375	37.3	*	71.7	76.3	77.8
Pr	41.1	4.6	*	7.6	8.42	9.04
Nd	136	15.4	23.6	22	26.6	29.4
Sm	19.7	2.05	*	3.2	3.62	4.04
Eu	4.48	0.453	*	0.732	0.918	0.949
Gd	11.68	1.72	*	2.536	2.272	2.92
Dy	6.89	1.13	*	1.49	1.58	1.71
Er	2.195	0.565	*	0.735	0.605	0.8
Yb	1.61	0.629	*	0.582	0.58	0.556
Lu	0.288	0.141	*	0.139	0.117	0.134

Major elements and REE analyzed by ICP AES at Oxford Brookes University.
Trace elements analyzed by XRF at Leicester University.
* = not analyzed

Helmsdale

Sample	iHG5	iHG807	iHG837	oHG157	oHG159
lithology	adamellite	adamellite	adamellite	porph. granodiorite	porph. granodiorite
Majors					
SiO2 %	73.48	72.736	72.298	72.21	70.045
TiO2 %	0.273	0.2935	0.3142	0.24	0.4056
Al2O3 %	14.009	14.953	15.079	13.49	14.16
Fe2O3 %	1.3098	1.2078	1.5029	1.31	2.2674
MnO %	0.0144	0.0217	0.0272	0.02	0.0499
MgO %	0.3422	0.4296	0.5907	0.47	0.8364
CaO %	0.5756	0.5209	0.6476	1.1	2.2375
Na2O %	4.0168	4.9042	4.8805	3.94	4.2524
K2O %	4.6606	4.9277	4.8268	5.03	4.6328
P2O5 %	0	0.009	0.011	0.08	0.076
LOI %	0.67	0.69	0.8	0.81	1.79
Total %	99.351	100.68	100.98	98.7	100.75
Traces	ppm	ppm	ppm	ppm	ppm
K	38689	40906	40069	41756	38458
Ba	1145	1270	1288	966	1492
Rb	191.5	164.7	157.6	210.6	137.3
Sr	562.2	519.2	541.3	562.1	961.6
Ga	20.6	19.3	20	18.7	18.9
P	0	39.24	47.96	348.8	331.36
Nb	12.3	12.2	10.9	14.3	16.9
Zr	160.3	171.5	179.4	138.5	226.3
Ti	1637	1760	1884	1439	2432
Y	5.3	7.4	8.7	8.8	15.5
Th	26.5	25	27.7	30.8	39.8
U	5	3.4	4.5	4.5	1
Cr	10	4	7	5	30
Ni	3	3	3	3	19
Sc	4.9	2.1	1	1.9	4.8
V	26.5	26.1	28	19.4	40
Cu	1	2.9	3.2	1	3.4
Pb	54.4	42.4	31.9	38.7	41
Zn	22	27	31	19	33
La	15.9	52	60.3	44.8	86.3
Ce	*	73.3	88.5	*	144
Pr	*	8.47	9.62	*	15.9
Nd	12.4	25.4	30.3	29.8	49.5
Sm	*	3.41	3.86	*	6.85
Eu	*	0.819	0.986	*	1.6
Gd	*	2.56	2.344	*	4.696
Dy	*	1.46	1.5	*	2.84
Er	*	0.655	0.545	*	1.185
Yb	*	0.453	0.473	*	0.941
Lu	*	0.112	0.102	*	0.2

Major elements and REE analyzed by ICP AES at Oxford Brookes University.
Trace elements analyzed by XRF at Leicester University.
* = not analyzed

Sample	oHG2	oHG204a	oHG3	oHG810
lithology	porph. granodiorite	porph. granodiorite	porph. granodiorite	porph. granodiorite
Majors				
SiO2 %	64.93	67.549	70.559	73.359
TiO2 %	0.5632	0.5069	0.361	0.2788
Al2O3 %	14.038	14.784	14.395	13.99
Fe2O3 %	2.6958	3.0128	2.0806	1.441
MnO %	0.0648	0.052	0.02	0.0304
MgO %	0.902	1.1869	0.641	0.6286
CaO %	3.6656	2.6858	0.7155	1.2565
Na2O %	4.2968	4.3955	4.1162	4.5079
K2O %	5.0154	4.6672	5.1094	4.5672
P2O5 %	0.0745	0.1445	0.0258	0.0107
LOI %	3.2	1.97	0.76	0.8
Total %	99.446	100.95	98.784	100.87
Traces	ppm	ppm	ppm	ppm
K	41634	38744	42415	37914
Ba	1950	1801	1809	1254
Rb	124.3	144.6	137.9	147.9
Sr	803.9	1293.7	897.2	674.2
Ga	17.8	19.5	19.4	18.6
P	324.82	630.02	112.49	46.65
Nb	19.4	17.4	13.9	14.6
Zr	277.1	254.9	195.5	161.5
Ti	3376	3039	2164	1671
Y	23.1	19.5	12.8	11.7
Th	36.8	37.1	36.4	35.3
U	4.9	6.1	4.1	5.9
Cr	61	49	31	14
Ni	32	34	26	9
Sc	10.4	7.9	5	3
V	58	45.6	39.3	20.8
Cu	3.5	4.3	1.7	1.5
Pb	315	37.7	33.2	38.2
Zn	91	35	39	29
La	114.8	112	76.7	59.5
Ce	*	179	*	94.9
Pr	*	19.4	*	10.2
Nd	81.4	59.8	51.2	30.3
Sm	*	8.11	*	4.11
Eu	*	2.03	*	0.985
Gd	*	4.912	*	2.832
Dy	*	3.36	*	1.87
Er	*	1.16	*	0.755
Yb	*	1.15	*	0.736
Lu	*	0.218	*	0.147

Major elements and REE analyzed by ICP AES at Oxford Brookes University.
Trace elements analyzed by XRF at Leicester University.
* = not analyzed

Sample	SR1	SR2	SR3	SR4
lithology	granodiorite / granite	appinite	granodiorite / granite	granodiorite / granite
Majors				
SiO2 %	62.81	48.34	63.232	63.83
TiO2 %	0.73	1.5	0.7801	0.7561
Al2O3 %	15.46	12.89	15.903	15.942
Fe2O3 %	3.98	8.92	4.2396	3.9943
MnO %	0.06	0.13	0.0655	0.0587
MgO %	2.61	9.97	2.6502	2.4017
CaO %	3.65	8.17	3.7654	4.2029
Na2O %	4.33	2.57	4.7768	4.6846
K2O %	3.74	2.65	2.7859	2.5749
P2O5 %	0.23	0.68	0.2611	0.2342
LOI %	0.61	2.13	0.65	0.57
Total %	98.21	97.95	99.11	99.249
Traces	ppm	ppm	ppm	ppm
K	31047	21998	23127	21375
Ba	1199	776	1114	1043
Rb	62.3	47.5	51.4	59.8
Sr	1168.9	1096.8	1158.4	1084.4
Ga	19.8	19.4	20.9	20.7
P	1002.8	2964.8	1138.4	1021.11
Nb	14.7	13.5	12.1	16.7
Zr	200.1	151.5	188.5	196.5
Ti	4376	8993	4677	4533
Y	17.5	36.4	16.3	18.3
Th	13.7	14.9	10.9	8.5
U	2.2	1	1	2.5
Cr	71	622	63	68
Ni	43	212	40	35
Sc	8.5	33.2	10.6	10
V	70.8	203.9	74.9	70.2
Cu	17	47.4	7.4	11.1
Pb	20.4	10	15.8	13.1
Zn	54	84	54	52
La	59.3	67.9	48.7	48.3
Ce	101	148	80.8	80.1
Pr	11.2	17.4	9.18	9.07
Nd	37.8	67.3	55.8	31.4
Sm	5.46	11.7	5.56	4.75
Eu	1.47	2.96	1.35	1.27
Gd	3.992	7.816	4.208	3.563
Dy	2.88	6.32	3.23	2.96
Er	1.095	1.95	1.39	1.125
Yb	1.13	2.35	1.05	1.29
Lu	0.214	0.388	0.222	0.247

Major elements and REE analyzed by ICP AES at Oxford Brookes University.
Trace elements analyzed by XRF at Leicester University.
* = not analyzed

Cluanie

Sample	CL1	CL2	CL3	CL4	CL5	CL6
lithology	appinite	hybrid	microdiorite	sparsely porph. granodiorite	Bt-rich granite	abundant porph. granodiorite
Majors						
SiO2 %	50.915	59.58	63.63	69.123	68.82	67.86
TiO2 %	1.0958	1.26	0.58	0.3048	0.3226	0.3347
Al2O3 %	11.172	12.94	15.59	16.026	15.287	16.083
Fe2O3 %	8.4048	7.52	3.54	2.3101	2.2701	2.1516
MnO %	0.1608	0.1	0.06	0.0665	0.0478	0.0613
MgO %	12.319	3.69	2.09	0.604	1.1229	0.6098
CaO %	8.5887	4.19	3.58	2.5497	2.1153	2.0052
Na2O %	2.0261	3.21	4.86	6.0728	5.4637	4.8195
K2O %	2.6731	2.64	2.29	2.6788	2.8918	4.7451
P2O5 %	0.6424	0.56	0.19	0.0881	0.0784	0.0669
LOI %	1.94	2.85	1.69	0.26	0.47	0.37
Total %	99.938	98.54	98.1	100.08	98.89	99.107
Traces	ppm	ppm	ppm	ppm	ppm	ppm
K	22190	21915	19010	22238	24006	39390
Ba	947	1000	686	877	1996	2130
Rb	98.1	70	39.1	59.1	45.8	113.5
Sr	1015.8	921.2	761.5	994.7	988.1	861.3
Ga	18.4	22.7	20.3	24.5	21.6	22.9
P	2800.86	2441.6	828.4	384.12	341.82	291.68
Nb	20	66.2	9.3	10.5	7.7	12.6
Zr	209.7	257.1	210.1	177.3	136.9	165.7
Ti	6569	7554	3477	1827	1934	2007
Y	27	46.5	13.7	16.4	12.9	19.2
Th	14.3	14.9	8.1	7.4	4.9	6.1
U	1	3.7	3.9	2	1	2
Cr	779	1	59	4	27	3
Ni	478	4	27	3	10	3
Sc	24.8	15.1	7	1.7	5.5	4.3
V	152.1	124.9	56.3	32.7	38.5	30.9
Cu	6.5	144.7	8.8	1.1	2.9	3
Pb	8.4	6.7	12.3	29.6	23.4	35.3
Zn	155	87	57	54	50	53
La	77.6	74.2	15	24.4	26.1	23.9
Ce	148	150	22.6	36.8	40.8	39.4
Pr	17.1	17.7	3.3	5.32	5.69	5.33
Nd	60	63.1	12.9	19	49.6	20.8
Sm	9.33	10.9	2.06	3.4	4.62	3.66
Eu	2.34	2.48	0.536	0.826	0.889	0.912
Gd	8.24	7.784	1.688	2.76	3.72	2.752
Dy	4.85	7.56	1.38	2.28	2.7	2.57
Er	1.71	2.525	0.575	1.015	1.32	0.995
Yb	1.89	3.46	0.554	1.24	0.874	1.38
Lu	0.342	0.578	0.113	0.255	0.204	0.257

Major elements and REE analyzed by ICP AES at Oxford Brookes University.
Trace elements analyzed by XRF at Leicester University.
* = not analyzed

CL7	CL8	CL9
abundant porph. granodiorite	microdiorite	sparsely porph. granodiorite
68.579	63.19	70.611
0.2904	0.61	0.2188
15.923	15.66	15.915
2.0516	3.54	1.5523
0.0602	0.06	0.0418
0.5767	2.92	0.3688
2.4143	3.31	1.7273
5.7435	5.17	5.9776
2.8871	2.59	3.1284
0.061	0.21	0.0176
0.3	1.27	0.19
98.887	98.53	99.749
ppm	ppm	ppm
23967	21500	25970
1058	1066	1170
71.9	28.5	67.7
931	1412.9	952.4
24.3	22	23.4
265.96	915.6	76.74
11	9	8.7
172.2	216.9	130.1
1741	3657	1312
16.3	14.4	12.2
8.1	10.6	7.1
3.9	1.7	3
3	112	5
3	67	3
4.5	6.4	2.4
27.2	68	19.6
1.9	11.2	0.9
31.2	20	28.4
49	66	41
23.8	44.8	12.6
38.5	79.2	20.1
5.56	9.13	3.29
0	32.3	14.3
4.52	4.79	2.42
0.859	1.27	0.568
3.616	3.704	2.04
2.98	2.55	1.75
1.44	1	0.765
1.26	0.936	0.942
0.276	0.195	0.195

Major elements and REE analyzed by ICP AES at Oxford Brookes University.
Trace elements analyzed by XRF at Leicester University.
* = not analyzed

Sample lithology	bl1 syenite	bl11 syenite	bl4 syenite	bl-se syenite	bl9 syenite
Majors					
SiO2 %	63.6	66.23	64.81	65.06	64.55
TiO2 %	0.51	0.38	0.41	0.37	0.41
Al2O3 %	13.1	15.93	16.57	15.13	16.59
Fe2O3 %	4.83	2.78	2.5	2.58	3.02
MnO %	0.06	0.06	0.08	0.06	0.07
MgO %	3	0.89	1.02	0.83	0.94
CaO %	2.83	1.88	2.15	0.94	1.9
Na2O %	6.32	5.44	6	6.95	6.13
K2O %	5.29	6.76	5.81	6.38	5.86
P2O5 %	0.44	0.19	0.28	0.17	0.31
LOI %	0.1	0.02	0.2	0.42	0.29
Total %	100.08	100.56	99.83	98.89	100.07
Traces	ppm	ppm	ppm	ppm	ppm
K	43914	56117	48231	52962	48646
Ba	3803	*	5658	4681	4632
Rb	84.7	*	84.5	112	88.9
Sr	1081.3	*	2080.4	1338.1	1350.5
Ga	17.7	*	17.7	112	18.3
P	1918.4	828.4	1220.8	741.2	1351.6
Nb	22.3	*	13	26.7	21.6
Zr	499.5	*	186.6	371.1	381.1
Ti	3057	2278	2458	2218	2458
Y	32.5	*	33.9	27.1	30.9
Th	40	*	45.4	50	59.2
U	2.9	*	1	7.1	2.8
Cr	61	*	3	2	3
Ni	65	*	12	9	8
Sc	2.9	*	5.8	3	4.3
V	35.5	*	34.3	33	38.5
Cu	7.1	*	7.3	5	9.3
Pb	48.5	*	38.3	57.3	44.9
Zn	152	*	30	53	48
La	124	215	237	180	211
Ce	247	410	393	231	385
Pr	*	*	*	*	*
Nd	123	159	193	123	179
Sm	18.4	21.4	24.2	16.8	23.3
Eu	4.79	5.32	5.98	4.16	5.56
Gd	13.1	14	15.4	11.1	14.6
Dy	5.52	5.9	6.68	4.68	6.01
Er	2.57	2.98	3.29	2.43	2.99
Yb	1.68	1.54	1.67	1.29	1.47
Lu	*	*	*	*	*

Major elements and REE analyzed by ICP AES at Oxford Brookes University.
Other trace elements analyzed by XRF at Leicester University

Enclosure 1

Simplified structural map of the Rogart area

Henning Kocks 2002

Simplified structural map of the Rogart area

For domain division and lithologies see inset map (above), for detailed explanation see chapter 3. Stereonets are lower hemisphere, equal area projections (Schmid net), symbols as in key. Stereonet of domain 11 is modified after Strachan & Holdsworth 1988; poles to S2 foliation shown as 10%, 5%, 1% contours; dots represent L2 mineral lineations. Crosses on map represent hill tops, closed circles represent settlements or localities. Abbreviations: Ct = Craigton, GR = Grumby Rock, BG = Brora Gorge, CM = Creag Mhór, DB = Dalreavoch Bridge, Sc = Sciberscross, CA = Cnoc Arthur, GC = Glen Cottage, A = Achork, GB = Garvoult Bridge, MR = Marians Rock, AH = Aberscross Hill, BL = Ben Lundi, RS = Rogart Station, DQ = Dalmore Quarry, Mu = Muie, Rha = Rhaoine, LC = Loch Craggie, MD = Meall Dola, ATL = Achatomlinie, CTC = Creagan Tigh na Creige, W-L = West Langwell, E-L = East Langwell, Ct =Collinstown, LG = Lettie's Grave, CB = Creag Bhata, LS = Loch Salachaidh, Re = Reidchalmei. Map scale is 1:25000; National Grid: bottom left hand corner is NC60000-00000, top right hand corner is NC80000-14000.

Domain 1 N = 45

Domain 2 N = 51

Domain 3 N = 70

Domain 5 N = 53

Domain 4 N = 88

Domain 11

Cr Naver Thrust GR BG Sc CTC ATL W-L Lettie River DB Brora River CM CA LC MD Ct E-L GB A GC LG Rha Mu Strath Fleet Fault Strath Fleet LS Rhe DQ CB RS DRIFT MR AH BL Net

MAP

Foliations: Moine 35-50°, 50-70°, 70-89°; Igneous 20-35°, 35-50°, 50-75°

Lineations: Moine (L2), Igneous (Hbl + Plag)

Bt-granite; Quartz-monzodiorite; Morar rocks; Naver nappe rocks

Poles to foliation (S2 & igneous); Lineations (L2 & igneous); Fold axial planes; Fold hinges

1 Naver Thrust 2 3 5 12 15 13 Brora River Central Complex 4 6 14 9 8 10 Strath Fleet Fault 11 7 Strath Fleet ~1km

ORS; Naver Nappe gneisses; Morar Group psammites; Quartz monzodiorite; Granodiorite; Biotite-K-spar granite; Leucogranite injection complexes

1km